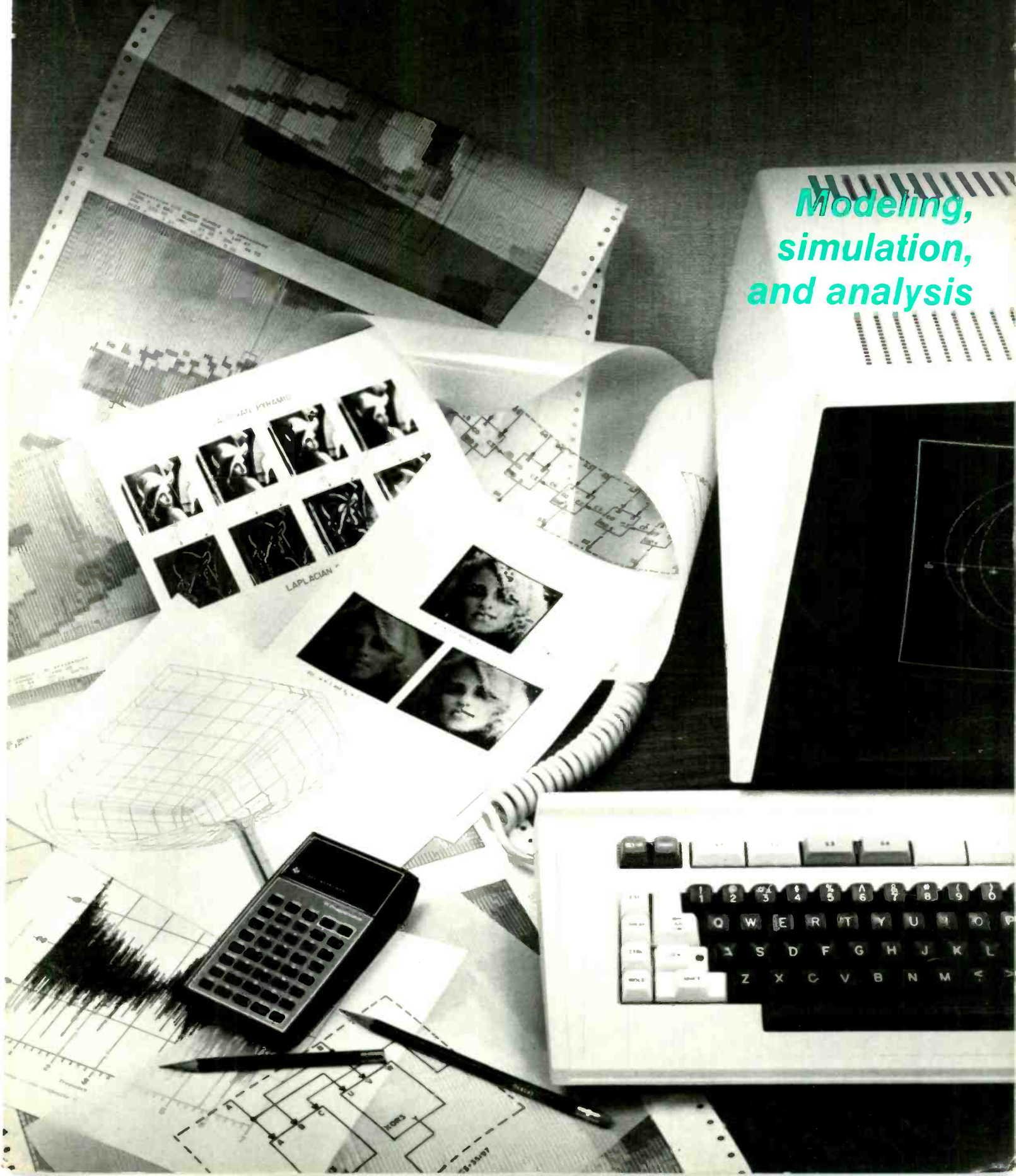


RCA Engineer

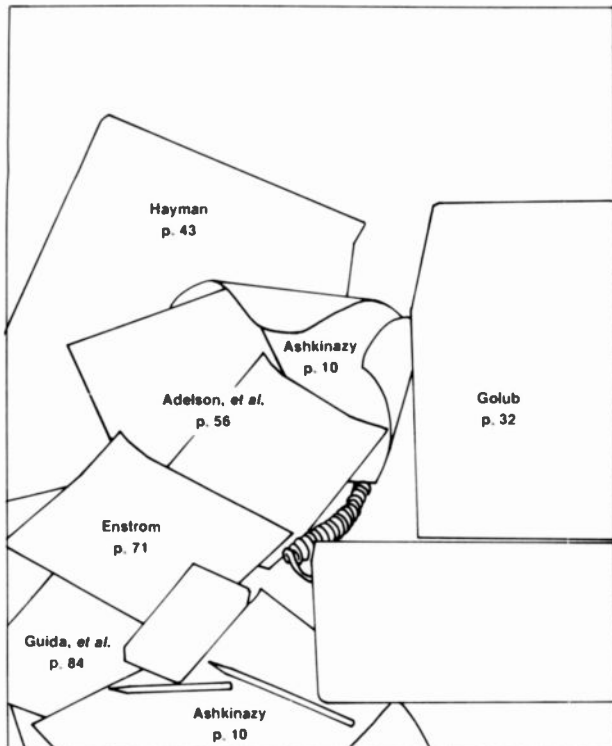
Vol. 27 No. 6

Nov./Dec. 1982

*Modeling,
simulation,
and analysis*



Cover photo: Andy Whiting, MSR, Moorestown



Our cover shows a crisp still life made from outputs generated by authors contributing to this Modeling, Simulation, and Analysis issue (the keyline above shows authors and page numbers). These engineers and scientists are a special breed. They predict how engineered products and systems will act.

Given a jumble of information and outputs, our authors must constantly bestow order and describe gray areas in black and white terms. They can give the green light to a step in an engineering project, or suggest that it go back to the drawing board. More rarely laying hands on costly, time-consuming prototypes and breadboards to try out ideas, our authors today take to their terminals instead, and use increasingly well-developed simulation and modeling programs to tell them whether something will work.

These practitioners, as gurus of the engineering community, establish "photographically accurate" engineering perceptions of the future—based on mathematics, computer analyses, and algorithmically disciplined logic and intuition. Though these professionals may seem to work at their green CRTs and study their green duotoned computer printouts in a silent twilight zone, nevertheless we can see that the stark realism of their work boggles the mind.

—MRS

RCA Engineer

A technical journal published by
RCA Research and Engineering
Bldg. 204-2
Cherry Hill, NJ 08358
TACNET: 222-4254 (609-338-4254)

RCA Engineer Staff

Tom King	Editor
Mike Sweeny	Associate Editor
Louise Carr	Art Editor
Frank Strobl	Contributing Editor
Betty Gutchigian	Composition
Dorothy Berry	Editorial Secretary

Editorial Advisory Board

Jay Brandinger	Division Vice-President and General Manager, "SelectaVision" VideoDisc Operations
John Christopher	Vice-President, Technical Operations, RCA Americom
Hans Jenny	Manager, Engineering Information
Arch Luther	Division Vice-President, Engineering and Product Assurance, Commercial Communications Systems Division
Howie Rosenthal	Staff Vice-President, Engineering
Ed Troy	Director, Operations Planning and Support, Solid State Division
Bill Underwood	Director, Engineering Professional Programs
Bill Webster	Vice-President, Laboratories

Consulting Editors

Ed Burke	Administrator, Marketing Information and Communications, Government Systems Division
Walt Dennen	Manager, Naval Systems Department Communications and Information, Missile and Surface Radar
Charlie Foster	Manager, Systems and Procedures, RCA Laboratories
John Phillips	Manager, Business Development and Planning, RCA Service Company

• To disseminate to RCA engineers technical information of professional value • To publish in an appropriate manner important technical developments at RCA, and the role of the engineer • To serve as a medium of interchange of technical information between various groups at RCA • To create a community of engineering interest within the company by stressing the interrelated nature of all technical contributions • To help publicize engineering achievements in a manner that will promote the interests and reputation of RCA in the engineering field • To provide a convenient means by which the RCA engineer may review his professional work before associates and engineering management • To announce outstanding and unusual achievements of RCA engineers in a manner most likely to enhance their prestige and professional status.



A.H. Teger

Modeling and simulation: Tools for the eighties

Over the last few decades, modeling has had many meanings for different people. When I was a teenager, modeling was something done only by untouchable beauties in sophisticated outfits (or lack of them). As a young graduate engineer in the early sixties, modeling had an overtone of being a last resort when a designer was not able to theoretically analyze, or directly build, his circuit or system. Today the designer often won't begin his task without a selection of these design tools at his disposal.

Modeling and simulation have become integral parts of the design process for a surprisingly wide range of application areas. It will be obvious from scanning this issue of the *RCA Engineer* that the techniques are invaluable for management analyses of new business areas, as well as for technical designs ranging from large multi-satellite communication systems to dc motors to complex integrated circuits. Simulations have become incredible time savers in the design cycle—reducing costs of false starts in fabrication or breadboard, and creating much more flexibility for considering alternate approaches.

Perhaps more important, many of today's technologies cannot be used effectively at all without simulation tools. For example, breadboards alone cannot fully characterize a final integrated circuit; or manual textbook analyses cannot handle the number of variables critical to a large system. In situations such as these, the computer becomes not only an aid, but an essential to the design process.

The usefulness of any of these tools remains critically dependent upon their human interface. How easy is it to input the data, to characterize the parameters, to request different simulations? How are the results reported or displayed? Is it easy to use the results to modify the design or the approach? More and more emphasis is being placed on this interface, and the resulting user-friendliness is largely responsible for the enormous growth in use of modeling and simulation tools.

Despite the recent growth, we have only barely begun to use this aspect of the computer's power. Within ten years, it may well be that every engineer uses computer modeling and simulation to design, test and validate his system long before fabrication.

Alfred H. Teger
Staff Vice-President, Systems Research
RCA Laboratories

RCA Engineer

Vol. 27 | No. 6 Nov. | Dec. 1982

- overview** **4** Simulation in an engineering environment
R.R. Barton | K.A. Pitts
-

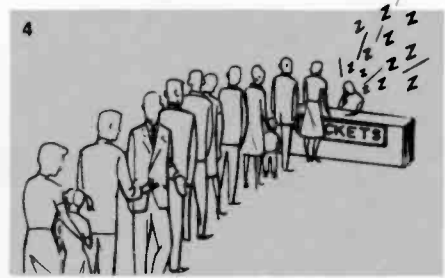
- simulation** **10** The MIMIC logic simulator
A. Ashkinazy
- 18** An HF modem simulation
P.A. De Maria | K.J. Bodzioch
- 24** Dynamic analysis and simulation of mechanically scanned
radar systems
G.M. Sparks | J. Liston
- 32** Discrete-event simulations of complex weapon systems
J. Golub
- 39** Digital interface simulation for large system development
G.W. Suhy
- 43** The Engineer's Notebook: Design and simulation of an intelligent
missile seeker
J. Hayman
- 46** ANA radio-frequency circuit simulation and analysis
S.M. Perlow
-

- modeling** **56** Modeling of the human visual system
E.H. Adelson | C.R. Carlson | A.P. Pica
- 65** Business modeling and the engineer:
An Astro-Electronics application
R. Nigam | S. Hong | S.R. Spence
- 71** Modeling and simulation in mechanical and thermal design
R.E. Enstrom
- 80** Electromechanical motor simulation
R. Browne
- 84** Computer modeling in the RCA Satcom system
A.A. Guida | K. Jonnalagadda | D. Raychaudhuri | L. Schiff
-

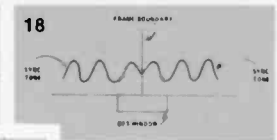
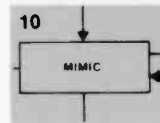
- departments** Patents, **92** | Pen and Podium, **93** | News and Highlights, **97**
Index to Volume 27, **102**

**in this issue ...
modeling, simulation, and analysis**

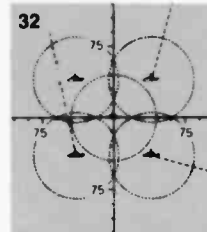
■ **Barton/Pitts:** "We must describe the important questions we want to answer and use these criteria to develop the model."



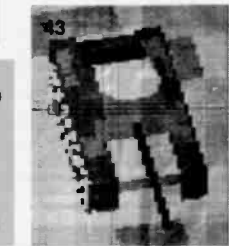
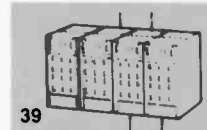
■ **Ashkinazy:** "Due to the complexity of LSI and VLSI chips, computer simulation has essentially replaced the breadboard"



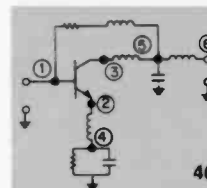
■ **De Maria/Bodzioch:** "The simulation program was written to represent the operation of a specific modem used in HF radio transmission."



■ **Sparks/Liston:** "We have selected a mechanically scanned radar system as an example of a system of moderate complexity, with three distinct areas of concern facing the designer."



■ **Golub:** "Although only weapon systems have been discussed, discrete-event simulations have been widely used for transportation, logistics, and traffic-control problems."

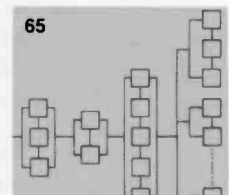


■ **Suhy:** "Thousands of programming errors have been detected, precisely documented, and corrected using such simulations."

■ **Hayman:** "Imaging seekers which utilize considerably more information concerning the target area are now possible."

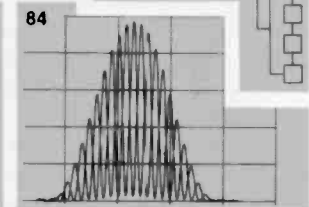
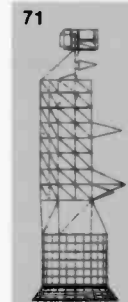
■ **Perlow:** "The circuit and desired outputs can be modified easily by means of a simple conversational mode that does not require editing of data files."

■ **Adelson/Carlson/Pica:** "Indeed, for all of us, seeing seems so direct and effortless that we remain unaware of the complex visual processing that underlies a statement like, 'That's a good picture.'"

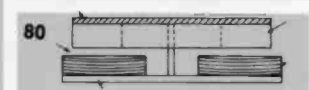


■ **Nigam/Hong/Spence:** "This paper describes a model developed to help Astro-Electronics analyze the business impact of design alternatives of a multisatellite system."

■ **Enstrom:** "Finite-element modeling analysis has been used at RCA in the solution of numerous complex problems."



■ **Browne:** "The model helps design engineers to set manufacturing tolerances by providing estimates of motor-performance variation from these various design parameters."



■ **Guida, et al.:** "The emphasis is on what the models do, not how they do it."

in future issues...

engineering productivity: tools and techniques,
technology transfer/energy,
RCA technology guide

```

*UNPAD [0]
* R=UNPAD MATRIX;TRAIL=LEAD
* J. SOLOMON, 88/12/11/0
* THIS FUNCTION SETS ALL BLANK
* LEADING AND TRAILING COLUMNS
* FROM A CHARACTER-MATRIX.
* TRAIL=[1] \ [2] ' *MATRIX
* LEAD=[1] \ [2] ' *MATRIX
* R=(LEAD*TRAIL) / [2] MATRIX
    
```

I like APL!

Simulation in an engineering environment

Simulation is a powerful tool for solving complex engineering problems. When is it useful?

Abstract: *Simulation—developing a model of a real system—is a powerful tool if used correctly. Concerns in simulation include how to formulate, develop, and verify models; how to use computers effectively; and how to present the results.*

Why simulate? Given that modern science is based on mathematical models that simulate the observed behavior of physical, chemical, and electrical systems, this question, in the broad sense, appears to be rhetorical. The reasons for using models are clear: It may be impractical or costly to manipulate the real system, or one may want to perform experiments on a compressed time scale. We ask the question to focus on the more parochial definition of simulation we're dealing with here. Simulations, though perhaps sophisticated, are usually thought of as modeling by brute force. Rather than solving a system of differential equations to predict circuit behavior or a projectile trajectory, we step through a series of calculations using difference equations and simple arithmetic, recording the approximate voltage or position at each time increment. In this narrower sense, simulation models can be considered as alternatives to analytical models, and the question, "Why simulate?", becomes meaningful.

A frequent reason to simulate is that the system or problem being modeled is too complex to understand any other way. The only way to understand the interaction between parts of a system, to improve the current methods, or to design a new system may be to model the system and simulate reality. For example, we may be

enlarging our production facility. Which machines should we add? How many? Where will our potential bottlenecks be?

Simulation can also be used to identify trouble spots. Suppose a piece of automatic test equipment is a bottleneck. What happens if we increase the speed of the equipment? The quality of incoming material? Another frequent reason to simulate, closely related to the complexity issue, is that the mathematics needed to analyze the system are intractable. In a complex queuing system—such as a production floor, highway-traffic network, or telephone-switching system—the underlying mathematical behavior may not lead to equations that are easy to solve.

Although we usually think of simulation as a problem-solving tool, it does have other uses. Simulation models are frequently used as a training tool—flight simulation is a well-known example. Weapons systems have been simulated, as well as other man-machine interfaces. Another reason to simulate is to check the behavior of a new algorithm, mathematical technique, or model. To answer the question, "Does the algorithm work?", you can construct information you know and understand (historical or randomly generated data), and then examine the algorithm's performance when it is given the known data. This method is frequently used to test mathematical techniques. Recently, statisticians used computer simulations to develop more robust measures than the simple average. The average (arithmetic mean) can give misleading estimates if some of the observations are faulty (misplaced decimal points, bad readings, disasters during the measurement, changes in equipment). Several alternatives to the average have been suggested. These methods have been tested through

simulation: One generates known distributions of numbers, and checks how badly each technique errs when supplied with contaminated data or data from unusual distributions.

Building simulation models

Simulation is a modeling and problem-solving tool. In any modeling situation, each of the following four steps must be used to build good simulation tools: (1) Formulate the problem—What questions do we wish to answer? (2) Develop the model—How do we estimate the parameters? What data and formulas do we need? (3) Verify the model—Does the model work correctly? and (4) Validate the model—Does the model resemble reality closely enough?

Problem formulation

We've said that simulation can tell us the answers to questions we have about our system. Why do we rely on the abstraction? How can we make sure that the information we get is useful and not misleading? To develop a simulation to help us understand our system, we have to decide what portion of the problem we want to study. Good problem formulation is essential. We simply cannot model our current system in all its detail, and then hope to answer questions efficiently or well. Some detail must be lost in the transfer from a real system to a mathematical model of it. We must decide the important questions we want to answer and use those criteria to develop the model.

Keep the following example in mind when we talk about simulation. Consider a production line. Say we have a simple

situation—three process steps to complete, and machines for the three processes, A, B, and C. These processes vary in complexity and time to complete the job. We have incoming raw material, and outgoing finished product. We might want answers to questions like: Where are our bottlenecks? Do we need more type-B machines? Do we need a preventive maintenance program? Do we need a new priority scheme for scheduling work?

Model development

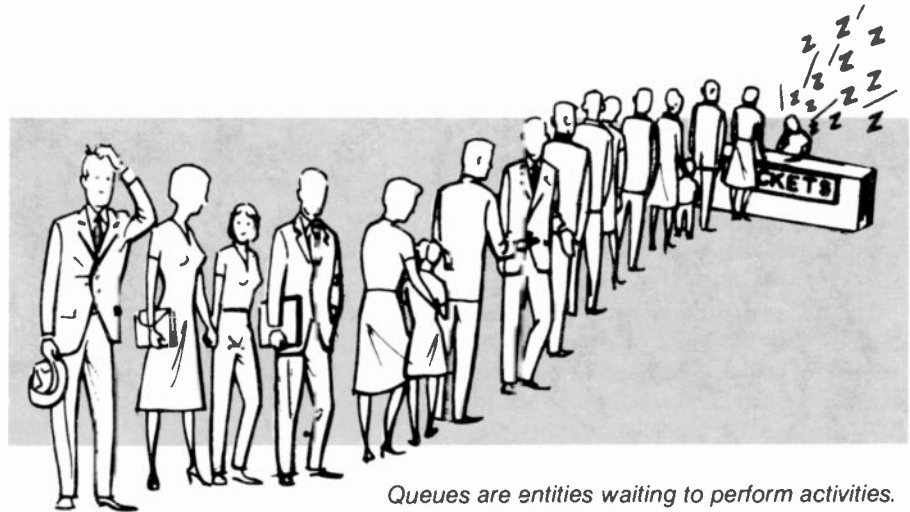
Once we have identified the problems we wish to solve, we must construct the model. Which aspects of our production system must we model in detail to answer these questions? Which parts of our system can be modeled at reduced levels of detail or left out? We will need to collect data from the actual system we are modeling. How long does each process take? What is the variability? How often do orders come in? What probability distribution do the machine failures follow? As we collect the data, we begin to develop the model by making assumptions about the data distribution, the simplifications we want to make, the parameters that are the most important, the variables we will track or control, the ways we will vary them, the ways the variables interact, and so on.

Model development includes implementation. What do we use to build the model? Its parts may be physical, analog, or digital. If it is a digital computer model, we must choose the programming language and the computer on which it will run.

In what form will it provide answers? Tables? Graphs? Will these answers be adequate for our needs? This last point seems common sense, but, incredibly, it is often overlooked until the model is complete. In some cases this oversight means retrofitting the model to provide the right information; in other cases, the consequences are more severe!

Verification and validation

After we have developed the model, we must verify it. The model should work as we planned (debugged). Is the behavior roughly what we expect? Is there something grossly wrong? The final step, one of the most important and also most frequently neglected, is validation. How does our abstraction compare with reality? How well does it do on a different data set? Is it too detailed? Too simplistic? Does it address accurately or precisely the questions of original interest? Can it be extended to



Queues are entities waiting to perform activities.

other questions? At this stage we frequently find problems, and repeat the process of formulation, model development, testing, and verification.

The structure of simulation models

What are the general characteristics of models that simulate systems? We think of a system as being a set of objects with characteristics and some interdependence involved in actions. In simulation jargon, the "objects" are called *entities*, their "characteristics" are *attributes*, and the "actions" are called *activities*. Examples of systems are shown in Table I.

The items listed in Table I for any one system are by no means complete. The items (*entities*, *attributes*, and *activities*) chosen to be included in the model, and the interrelations chosen to be modeled, depend on the purpose the user has in mind. When we *model* a system, we pick such a subset of entities and interrelations. One clear trade-off in model formulation is the level of aggregation. A simple model with many entities aggregated into a few major entities is much easier to program, test, and debug since there are fewer entities and interactions. Of course, the resulting model may generate a poor approximation to the real system. A good strategy is to start

Table I. Examples of systems. Systems are sets of objects, with characteristics and some interdependent actions.

System	Entities	Attributes	Activities
Airline counter	Passengers	With/without ticket With/without baggage Flight Number	Get information Purchase ticket Check in Check baggage
	Agents	Capability (tickets only, baggage only, or both)	Give information Sell ticket Check in Check baggage
Fighter-missile	Fighter	Position Velocity Performance ability	Evasion
	Attack missile	Position Velocity Performance ability	Pursuit
Assembly line	Components	Type Defective/nondefective	Assemble Test
	Assemblers	Type (fast, slow)	Assemble Test
Computer	Programs	Core requirements lan- guage (e.g., FORTRAN) Special libraries Execution time Peripheral devices	Compile Execute Print Plot Store on tape Store data on disk

with simple representations and augment the model later in areas that are found to be too crude.

For the level of detail chosen, the *state* (at time t) of the system is given by a complete description of all entities, attributes, and activities at one point in time, t . We define an *event* to be something which causes the state of the system to change.

The kind of simulation model we choose depends on what kinds of characteristics we try to model. We need to consider whether the structural relationships are to be static or dynamic; and whether the attributes and/or activities are to be deterministic or probabilistic. We might use a static probabilistic simulation to study the strength of a building made with components of randomly varying strength. One could simulate many such buildings being constructed, and simulate stresses, to determine what fraction of such buildings would collapse. To model waiting times at an airline counter, on the other hand, would involve dynamic relations of arrival times and service times. Difference equations or analog computers are often used to perform deterministic simulations of the performance of physical systems.

A broad definition of simulation models includes mathematical models, physical models, and electronic-analog, and digital-electronic models. Each of these implementations can be used to imitate the performance of the real system being studied. Some models such as flight simulators combine physical, electronic-analog, and digital simulation techniques. When we speak of *system simulation* below, we will refer to a narrow meaning—dynamic, probabilistic, digital-electronic (computer) simulation. To give a better understanding of these models, we'll review the important considerations in building and using them.

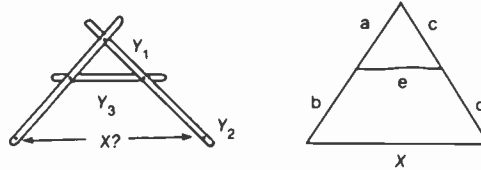
Issues in computer-simulation modeling

Simulation languages

One critical issue in developing a computer model for simulation is whether to program the model with a general-purpose language or to use one of the simulation languages currently available. This decision is based on your access to the language, your ability and desire to program, and the complexity of the system you are simulating. The more complex the system, the more you should seriously consider using a simulation language. There are clear advantages in using a special-purpose simulation language like Simscript, as opposed to

A static, probabilistic computer simulation

For this three-link riveted assembly, what will be the variability in the span (X) given the variability of the inter-hole distances Y_1 , Y_2 , Y_3 ?



$$X = \sqrt{(a+b)^2 + (c+d)^2} - \frac{(a+b)(c+d)}{ac} (a^2 + c^2 - e^2)$$

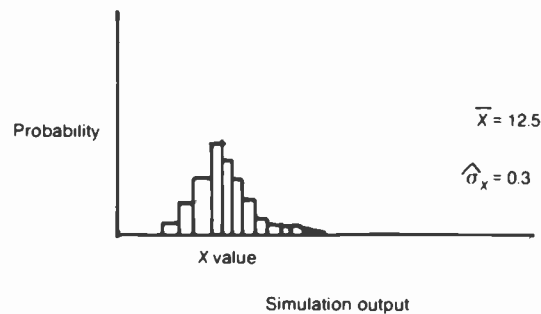
reality \rightarrow trigonometric model

If the random distances a , b , c , d , and e have normal probability distributions, we cannot find the distribution of X analytically. So we simulate the assembly of many parts.

How the computer simulation works:

- Step 1.** Compute random distances for a , c , from distribution 1.
- Step 2.** Compute random distances for b , d , from distribution 2.
- Step 3.** Compute random distances for e from distribution 3.
- Step 4.** Compute X via the model and save the value.

Repeating steps 1 through 4 many times, the computer simulation generates a large set of X values. A histogram of values gives a good representation of the variability that can be expected. The sample variance can be computed from the data as well.

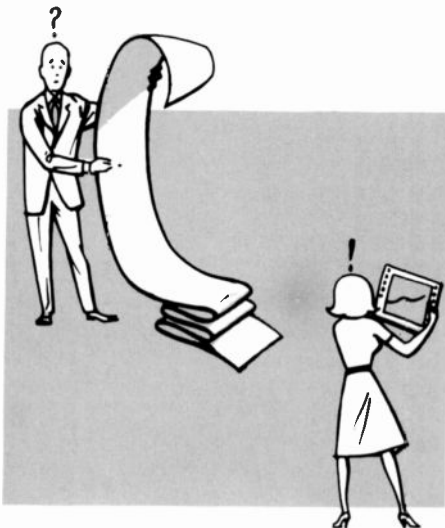


a general-purpose language like FORTRAN. The high-level representation means a shorter, simpler program that takes less time to code and is more likely to pass verification tests for proper operation. On the other hand, the main disadvantages—greater memory and execution-time requirements—can be devastating for a frequently run model. When we use a simulation approach to identify optimal control, or planning strategies, we will need to be able to make many repeat runs quickly, calling the simulation program from within an optimization routine, and modifying its operation via parameters passed from the

optimization program. Fortunately, packages written as a set of general-purpose language subroutines allow the engineer an intermediate approach (see box, page 7).

For complex systems the output of a simulation can be a horrendous pile of numbers. Tables and tables of numbers are difficult to scan for interesting correlations, time trends, or exceptional events. It's of utmost importance to find ways to graphically display the results, so this consideration should weigh heavily in your choice of a simulation language. If you don't find something acceptable, take heart.

Computer-graphics capabilities are changing rapidly, and packages are being continually updated.



Graphical methods increase the usefulness of simulation output.

Modeling a dynamic system

A dynamic system such as the fighter-missile pursuit system is clearly continuous in nature. Position, time of contact, and so on, can vary continuously. For other systems the important events can be considered to occur at discrete points in time. For the assembly-line system, these discrete events are the arrival of components for assembly, completion of assembly, start of test, and so on.

Since dynamic systems evolve over time, some sort of timing scheme must be chosen for the model. For continuous systems, a fixed-increment timing approximation is used for digital simulations. For discrete-event systems, there is no need to examine the system between events. Virtually all modern simulation languages use a *next event scheduling-timing* method.

There are two methods for dynamic discrete-event simulation. One is called *event scheduling*, the other, *process interaction*. In most cases, a simulation language is structured to do one or the other. Simscript II.5 and GASP IV use event scheduling; Simscript II.5, GPSS, and Simula use process interaction. For event scheduling, one models the system by focusing on what events or activities can happen. Typical events are arrival, repair, completion, service interruption, and machine breakdown. Since time lapses between events, one can regard an event scheduling as a string of all events that will happen to the system. Process-interaction provides a separate procedure for each entity in the system. Machine, operator, CPU, I/O-device,

and airplane processes are typical. In the terms we defined earlier, processes are entities/activity sets. In a production-scheduling problem one would model each production process; in event scheduling, each event. Both approaches base their timing routines on a next-event basis. Although the process-interaction approach is often conceptually simpler, there is some loss in programming control. Collecting information about congestion, lengths of queues, and so on, is more difficult.

Modeling random variability

Most simulation models have random variables (service time, interarrival time, component strength, and so on) that one must somehow generate either prior to or during the simulation. Practically speaking, continuous random variables with any kind

of probability distribution can be generated on the computer by transforming a set of random numbers uniformly distributed on the interval $[0, 1]$. The importance of the uniform distribution stems from the fact that if X is a continuous random variable with cumulative distribution function F , then the quantity $F(X)$ has a uniform $[0, 1]$ distribution. Many simulation packages automatically provide random numbers from common distribution families such as the normal, Poisson, or exponential. Some packages also allow one to generate nonstandard distributions.

We often need to model random events that are correlated; for example, assembly time may be correlated with component-interarrival time if the assemblers are fresher after a break. Special multivariate techniques are needed to generate pairs (or triplets, etc.) of correlated random variables.

Some common simulation languages*

Simscript II.5 is a complete high-level programming language with specific structures to make simulation easy. It uses a compiler; has good, well-documented random-number generators; and has good capabilities for handling complex systems. It is, however, a programming language, *not* a software package. You sacrifice ease in getting a model up and running but you gain increased control while it is running. It is available only on large computers.

GPSS is a software package, working with an interpreter rather than a compiler. It is easy to work with, easy for beginners to use. Its defects are clumsy generation of most probability distributions, and difficulties in collecting statistics. In addition, we have not found documentation on its random-number generator. Also, GPSS is no longer supported by IBM. GPSS is available only on large computers.

GASP IV is a collection of FORTRAN IV subroutines to help in simulation. GASP IV provides many of the necessary simulation tools; however, it is necessary to write the programs to handle the data, call the routines, and print the results. Its advantages are that it runs on any system with a FORTRAN compiler. It also does both discrete and continuous simulations.

SIMULA is an algol-based simulation language. It is similar to Simscript in that it is a programming language with all that that implies. (It includes a compiler to decrease computer execution time, but one must still learn a new programming language).

RCAP is a circuit-simulation package that can provide static, dynamic, and frequency-domain simulations of integrated-circuit performance. Arbitrary circuit elements may be supplied as subroutines.

DYNAMO is a language used for modeling large social or industrial systems via a set of interconnected difference equations.

* This list is by no means complete. See Reference 4, page 115-143, for more detail on some of these.

Correlated variables are also useful for improving the precision of the simulation results; we'll talk more about this later.

Verification/validation

What techniques are used to verify and validate simulation models? Some functional checks will be unique to particular models, but there are others that we must make in most situations. The quality of random variates generated for a simulation may require examination. Random-number generators can have several problems—cycling or other serial dependence, wrong distributional form, and so on. Statisticians have developed a battery of tests to check for various kinds of misbehavior. One should plot histograms and perform Kolmogorov-Smirnov tests to check for proper distributional form. An effective check for first-order dependence is to plot generated random variates against time and against one another. Contingency tables (chi-square tests) are also used to check independence.

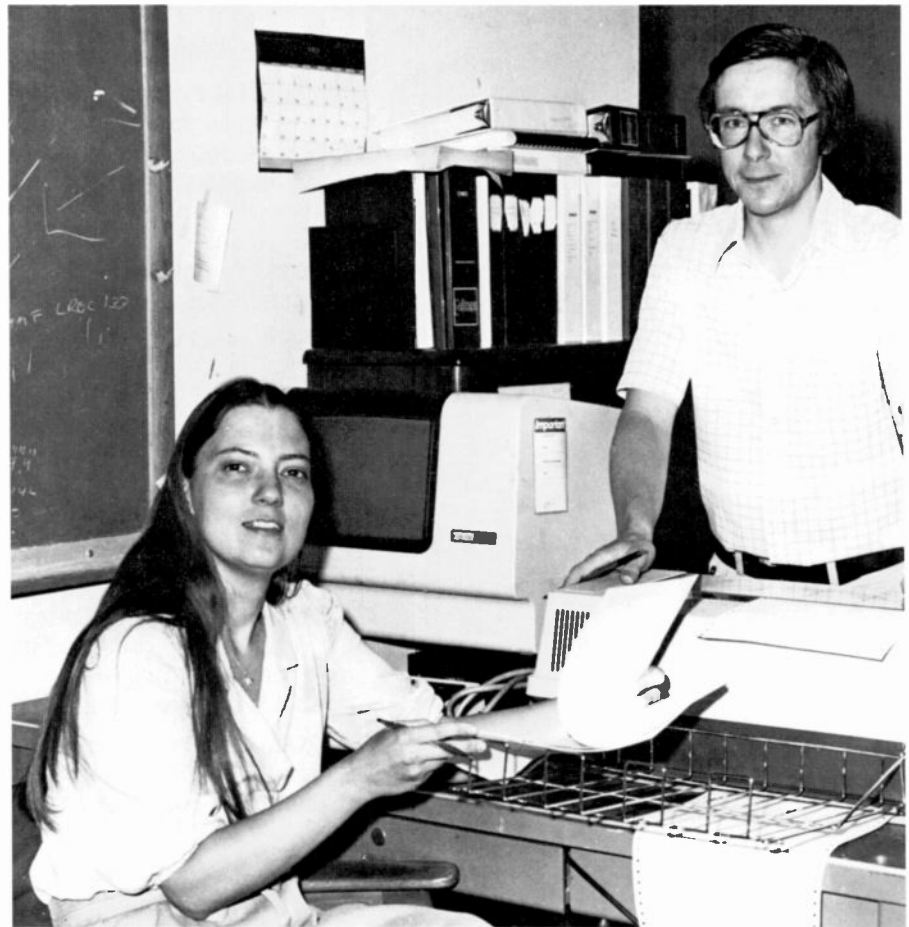
For functional tests, one can often test the model using the following technique: Feed the model by controlled, rather than random, number streams in such a way that the outcome can be clearly predicted. For example, to test the three-link assembly simulation (page 6), one could use values for a , b , c , d , and e that make X easy to check, for example.

$$a = b = c = d = e = 1 \rightarrow X = 2.$$

It is sometimes possible to design an experiment to test a model's faithfulness to reality. This validation technique supplies the same input conditions, or events, to both the real and the simulated systems, comparing the resulting behavior. Typically this is not possible. The most common way to ensure that the simulation is generating a good approximation to reality is to test it on historical data. One of the best methods is to use a random sample of historical data to develop the model, and another sample to verify the model.

Using the model

We have to be careful in deriving information from simulation data, particularly for probabilistic models. In estimating quantities like average backlog, average waiting time, or average throughput, the common statistical techniques assume the observations are random and independent. Clearly for some models, the time it takes the i th item to be completed depends heavily on the completion times for previous items. There are two solutions to this dependence



Authors Pitts (left) and Barton (right) have jointly worked on several projects including a seminar on statistical design of experiments and a recently completed Corporate Engineering Education course on the design of experiments.

Karen Pitts joined RCA Laboratories in 1976 as a Member of the Technical Staff where she has been working as an applied mathematician and statistician. Her simulation background includes electrical circuits, production lines, and scheduling, as well as studying simulation with George Fishman at the University of North Carolina.

Contact her at:
RCA Laboratories
Princeton, N.J.
TACNET: 226-3045

Russell Barton began work at RCA in 1973. He has worked on simulation models for IC fabrication, communication-satellite reliability, and transportation-telecommunication systems. He holds a B.S. in Electrical Engineering, and M.S. and Ph.D. degrees in Operations Research. Dr. Barton is currently active in statistical optimization studies of VideoDisc processes.

Contact him at:
RCA Laboratories
Princeton, N.J.
TACNET: 226-2079

problem. One is based on renewal theory, where you group data into batches, called *epochs*, that are statistically independent. If you study the information for each epoch separately, you then satisfy the independence assumption and can use standard techniques. For example, in the airline-reservation system, with Poisson arrivals and exponential service times, the time between the empty states (no one waiting in the system, no one in service) is independent. In this case, you collect all the

information for times the reservationist is busy and calculate statistics using this data. If it is not possible to identify independent epochs, by renewal theory, another solution is to model the time dependence explicitly. A field of statistics known as time series does this explicit modeling to get valid estimates. Without independent epochs, the estimates may also be biased if they are based on data taken before the system reaches equilibrium. It is usual to start a simulation from an empty and idle

situation; but, most real systems do not start from empty and idle. The simulation system must be given sufficient time to reach conditions matching the real system.

Given a simulation in working order, we can use techniques from experimental design to make efficient use of our computing resources. Suppose we are modeling an eight-step production process, and want to identify the value of adding capacity at each of the eight locations. One-at-a-time modification would not identify any interactions—the effects of improvements at one location on performance at other locations. On the other hand, a full factorial design would require 2^8 , or 256, separate simulation runs. A fractional factorial design, well known in statistics, could provide valuable interaction estimates as well as main effects in perhaps 32 runs.

Statistical techniques can also be used to reduce the variability of estimates derived from the model. One method, called the antithetic variate method, uses uniform [0-1] random numbers U_1, U_2, \dots, U_n for one stream and $(1-U_1), (1-U_2), \dots, (1-U_n)$ for the second stream. Estimates based on sums of these effects will have reduced variance, since the terms are negatively

correlated. This follows from the fact that the variance of a sum is equal to the sum of the variances plus twice the covariance, and the latter term here is a negative number.

When is simulation the right approach?

We have skimmed the surface of several issues in simulation. The question of whether or not to simulate remains unanswered. Simulation is a powerful tool; it also requires effort, time, and extensive runs on a computer. When should we use simulation?

Let's review the costs and practicality of simulation. Are the data for the model readily available? How much will it cost (both in time and effort) to get the data? How complex a model is needed? A simple model will take much less time to develop, verify, and manipulate than a complicated one. How concerned are we about computer time and costs? Simulations are not cheap. How important are the results of the model? If we are designing a production facility and find, through simulation, that the building should be 10 percent longer, the results are very important.

If the model's results are unlikely to be used, think twice before starting to simulate. Finally, can you wait for the answer? The time to develop, run, and verify the model and to analyze the results are non-trivial. Conversely, if you need to simulate, you should plan for the time it will take.

Lest all this seems too negative, let's reiterate that simulation is a powerful tool that solves problems that cannot be solved by other means. For understanding complex systems, for evaluating new techniques, for teaching complex tasks, simulation provides an excellent alternative to inefficient production, invalid algorithms, and expensive mistakes. Simulation, although powerful, is not easy. Simulate, but don't underestimate the complexity of the task.

Bibliography

1. R.L. Launer and G.H. Wilkinson, Editors, *Robustness in Statistics*, Academic Press (1979).
2. Fishman, G.S., *Concepts and Methods in Discrete Event Digital Simulation*, Wiley (1973).
3. Reitman, J., *Computer Simulation Applications*, Wiley (1971).
4. Shannon, R.E., *System Simulation: The Art and Science*, Prentice-Hall (1975).

How may I get a copy of an *RCA Engineer* article?

Call or write to the author

We give authors several reprints of their own articles. Often they order additional copies.

Contact the Technical Publications Administrator (TPA) in the author's business unit

If the author is not available, the TPA often can get the paper. The TPA is ready to assist you, either with a reprint or related material. A current list of TPAs is printed on the inside back cover of the *RCA Engineer*.

Use your RCA Technical Library

The librarian has all back issues of the *RCA Engineer* and can give you photocopied articles.

Buy a back issue of *RCA Engineer*

They can be purchased for \$2.00 a copy from the *RCA Engineer* office in Cherry Hill. Write to Dorothy Berry, Bldg. 204-2, Cherry Hill, NJ 08358, or call TACNET: 222-4254.



The MIMIC logic simulator

MIMIC simulates the behavior of complex digital circuits, and helps engineers do it right the first time.

```

** 10:20:48
** FOR NEW PLA MODEL INFOATION, TYPE 'MIM
** FOR FEB.23,82 MIMIC NEWS, ENTER 'MIMNEW
** BATCH MODE - 90% DISCOUNT
10/12/82 12:38
.. EXECUTE MIMIC PROGRAM ... VERSION 1.7 (6/1/82)
: define file=fa
: get type=full-adder file=fa,lib
N GET NETWORK : FULL-ADDER
* COMPLETED:
NO. PARTS= 5; NO. SIGNALS = 8; NO. INPUTS = 1;
NO. PREPROCESSED NETWORK DESCRIPTION IN FILE FA
file ptest.3= 000 001 010 011 100 101 110 111 0
ply patterns=ptest
n hazard:
t list=carry-in*a,b**sign,carry-out change:
C AB SC
A IA
R GR
R NR
Y

```

Abstract: The author describes the logic simulation program, MIMIC, used at the Solid State Technology Center at Somerville, New Jersey, and gives the benefits (reduction of expensive rework cycles, for example). The needs for logic simulation and an overview of computer-aided design capabilities at Somerville are given. MIMIC is examined in detail by reference to examples, and the network description language, modeling capabilities, and run commands to control the simulation process are covered.

MIMIC is a logic simulation program developed by the Design Automation Group of the Solid State Technology Center at Somerville, New Jersey. Using MIMIC, the engineer can perform logic design verification of large-scale-integrated (LSI) and very-large-scale-integrated (VLSI) circuits in a very cost-effective manner, before mask generation, and reduce or eliminate expensive rework cycles due to design errors. Designers can simulate the actual circuit being implemented, check for races, hazards, or spike conditions, and examine critical timing of various paths in the logic.

©1982 RCA Corporation
 Final manuscript received October 7, 1982.
 Reprint RE-27-6-2

If errors are found, MIMIC contains numerous debugging aids to help the engineer localize problem areas.

Simulation and automated design

Not too long ago, integrated circuits contained less than 100 gates and flip flops per chip. It was then possible for the engineer to perform a paper design of the circuit with reasonable confidence that any design error could be detected and corrected before committing to silicon. The complexity of today's LSI and VLSI circuits, containing thousands of components per chip, precludes a thorough manual analysis. Computer simulation provides the engineer with detailed information about the state of each signal in the circuit that would be difficult or impossible to obtain by hand. Thus, simulation helps the designer get it right the first time and avoid costly and lengthy mask-generation cycles. The Solid State Technology Center in Somerville has an impressive track record in this regard; 21 of the past 22 universal arrays designed by the Tech Center (SOS and Bulk CMOS) worked the first time. All were simulated with MIMIC.

Due to the complexity of LSI and VLSI chips, computer simulation has essentially

replaced the breadboard (which can be viewed as a hardware simulation). Breadboards of complex digital systems are expensive, due to the cost of the hardware, the cost of specialized and sophisticated test equipment for exercising and monitoring the hardware, and the time required to purchase the components and test equipment, assemble the breadboard, and debug the system. Even then, correct operation of the breadboard does not necessarily imply correct operation of the integrated circuit, since the latter's implementation may differ and on-chip delays will certainly differ from those on the breadboard.

On-chip delays can only be determined after the layout has been completed. The Design Automation Group of the Solid State Technology Center is developing the software to close the simulation loop for semi-custom and gate-array designs. These design methodologies use standard cells with fixed geometries, thereby simplifying the tasks of automatic placement and routing (APAR), and extraction of the logical connectivity and wiring capacitance from the computer-generated layout. Standard cell libraries exist, or are being developed, for SOS, CCL, CMOS I, and CMOS II. Figure 1 illustrates the design cycle using this software. The designer (an outside cus-

tomor or an RCA engineer) generates a MIMIC description of the circuit as an interconnection of parts that can ultimately be resolved into standard cells. After generating functional tests, the designer simulates the response of the circuit to the test patterns. If errors are detected, the designer modifies the circuit and/or test patterns, and iterates until the simulation results are correct. From there on, the designer "pushes the button" and everything else is done automatically by RCA software running on RCA-owned computers. These programs generate a finished layout and a simulator-compatible description of the circuit as extracted from the artwork. The designer can then compare the actual circuit description to the one originally simulated, and then simulate the actual circuit using true wiring delays. If there are no errors, masks are made and the chip is manufactured. The sidebar on page 13 details the programs involved.

Structured design

The hierarchical (nested) structure of CADL, MIMIC's circuit description language, allows top-down design and bottom-up verification. In the design phase, the overall circuit with its connections to the outside world is at the highest level. Next, the circuit is partitioned into subfunctions, and blocks representing the subfunctions are interconnected. Then, each subfunctional block is represented as an interconnection of smaller subfunctions, and so on, until the subfunctions at the lowest levels contain only MIMIC primitives (built-in elements; see page 13). Examples of

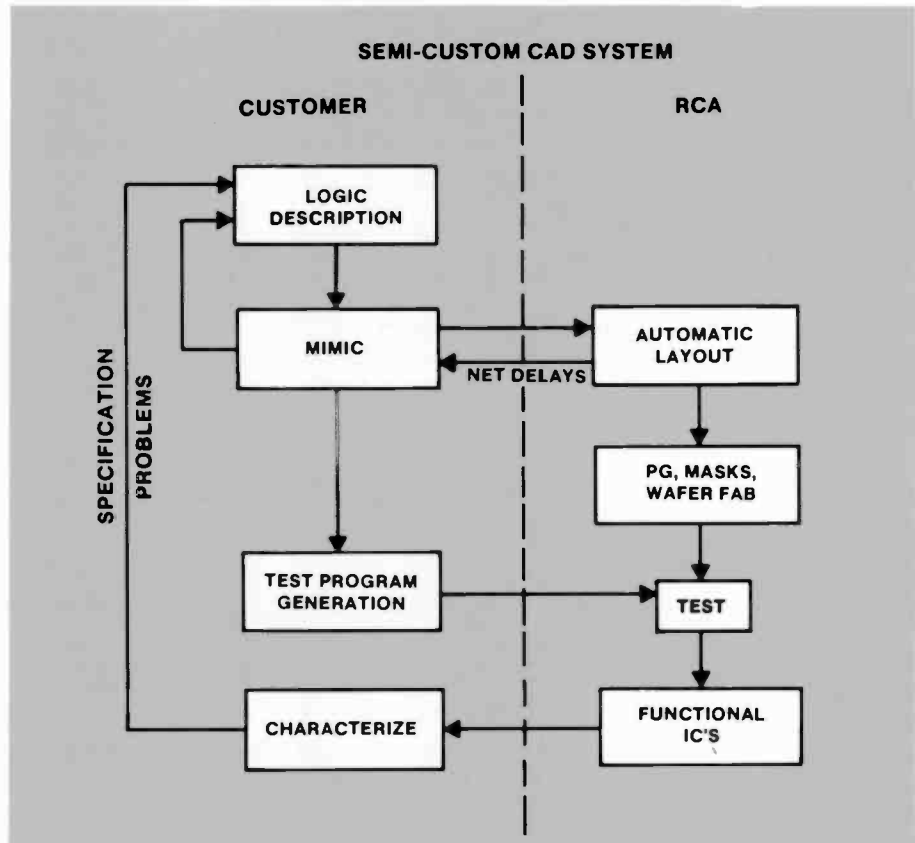


Fig. 1. Semi-custom CAD system. This system consists of a number of computer programs that automate the design cycle from simulation through layout and test-program generation. They help the engineer to minimize errors in all aspects of the design process.

lowest level user-defined subfunctions are the standard cell libraries for semi-custom (APAR) and gate arrays (GUA or AUA). This approach is a top-down design.

In order to debug the circuit, the lowest level subfunctions are simulated, and all

logical errors and timing problems are corrected. Then, the next higher level subfunctions (now containing verified components) are simulated and debugged. This procedure, iterated until the entire circuit is included, is bottom-up verification.

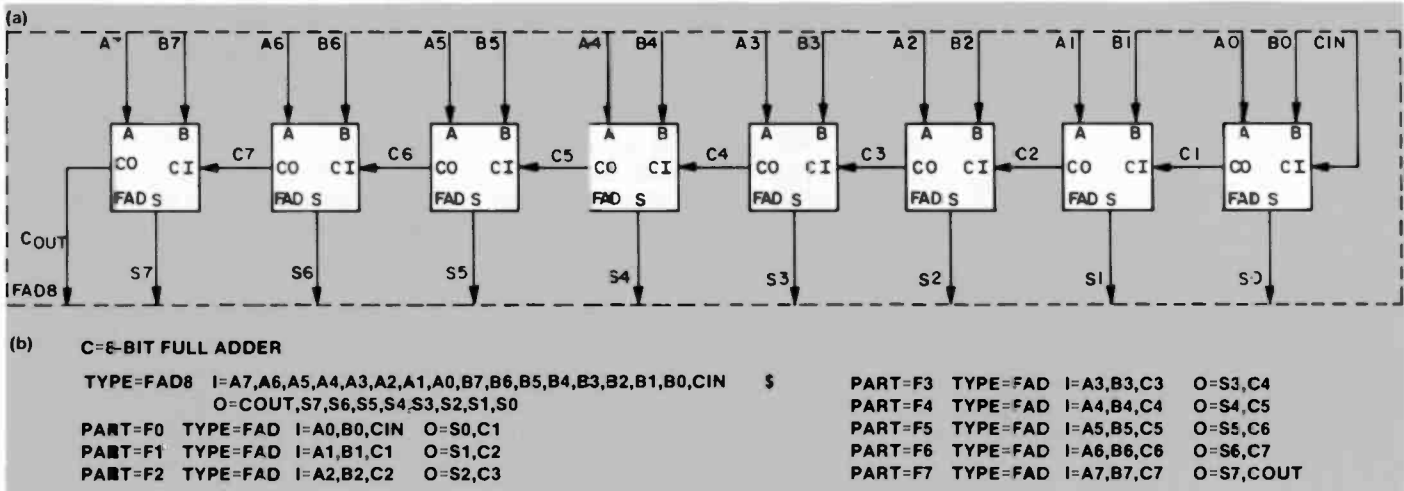


Fig. 2. FAD8 circuit of example #1. (a) Decomposition of FAD8 (eight-bit full adder) as iterative array of eight FAD (one-bit full adder) cells. (b) MIMIC description of FAD8 corresponding to (a). Figures 2 through 5 illustrate the concept of hierarchical design, and the description of this hierarchy to the MIMIC logic simulator.

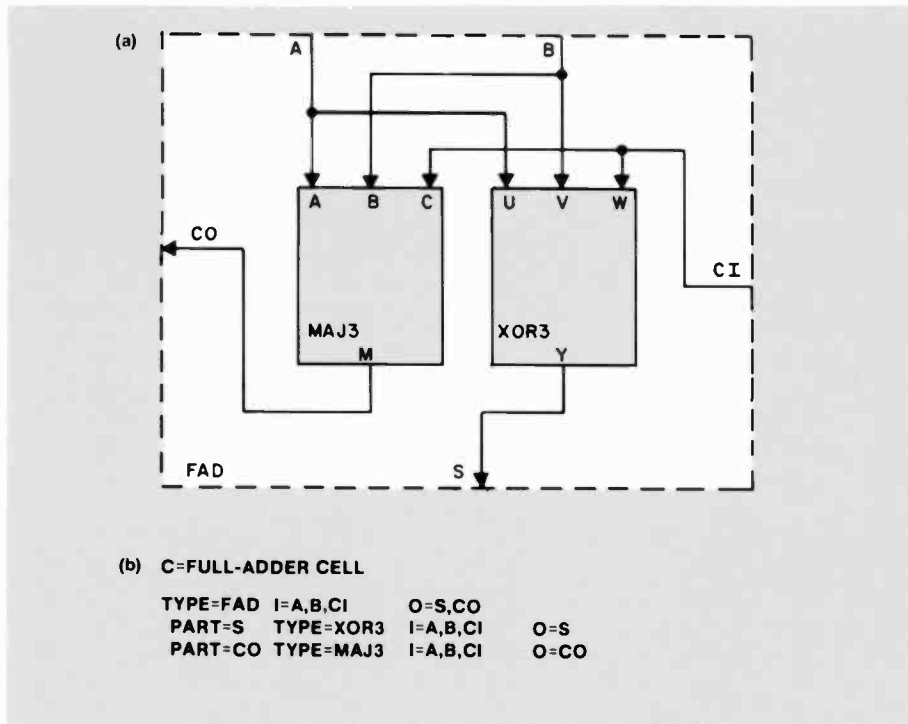


Fig. 3. FAD circuit of Example #1. (a) Decomposition of FAD into sum logic (XOR3) and carry logic (MAJ3). (b) MIMIC description of FAD corresponding to (a).

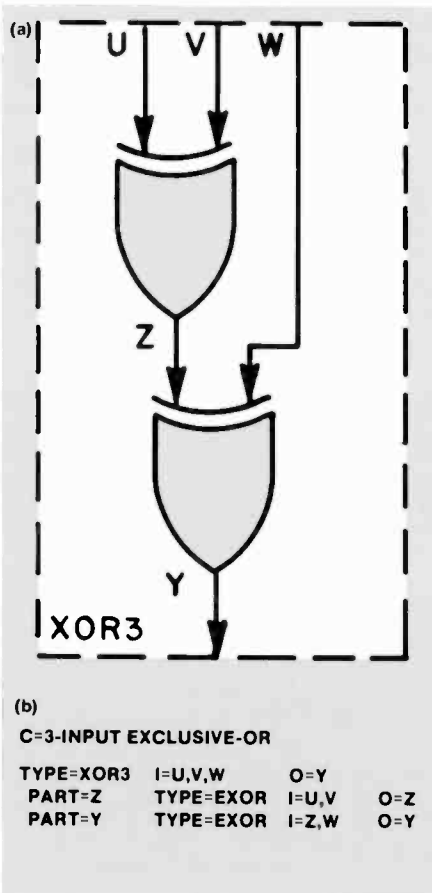


Fig. 4. XOR3 circuit of Example #1. (a) Decomposition of XOR3 into two 2-input exclusive-OR gates. (b) MIMIC description of XOR3 corresponding to (a).

Example #1: Top-down design of an 8-bit ripple-carry adder

The first step in designing an 8-bit full-adder is to decompose it into an array of eight individual 1-bit full-adders. This is shown in Fig. 2(a). At this point, the internal realization of each 1-bit adder is not yet known. The MIMIC description of the circuit at this level is shown in Fig. 2(b). The first statement is a TYPE statement, which declares the beginning of a subnetwork definition. The statement actually spans two lines; the dollar sign at the end of the first line is the MIMIC continuation character. The TYPE statement defines a type of circuit called FAD8 having seventeen inputs (A7-A0,B7-B0,CIN) and nine outputs (COUT,S7-S0). The next eight statements are PART statements that describe the internal components of the FAD8 and their interconnections. Each component happens to be a FAD circuit, as yet undefined. The first FAD circuit, named F0, has three inputs (A0,B0,CIN) and two outputs (S0,C1). The second through eighth PART statements describe the rest of the FAD8 circuit in the identical manner.

The second step in the design procedure is to fill in each 1-bit adder. Figure 3(a) illustrates this next level of design. The S output, representing the modulo-2 sum of A, B, and CI, is the exclusive-or of these three inputs. The CO output, representing the carry-out, is the majority function of

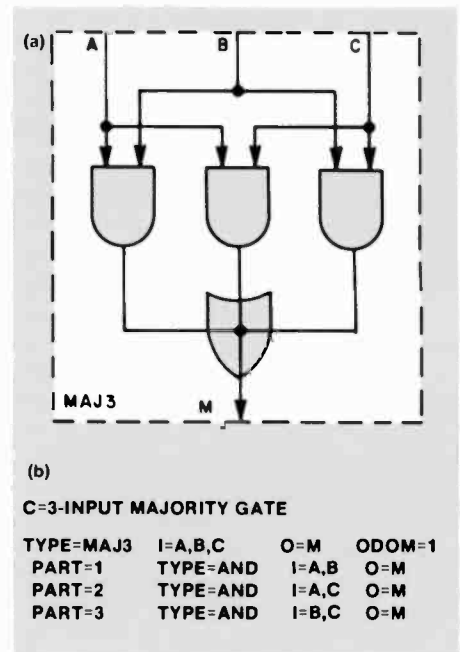


Fig. 5. MAJ3 circuit of Example #1. (a) Implementation of MAJ3. (b) MIMIC description of MAJ3 corresponding to (a).

the three inputs (that is, CO is a logical 1 if two or three inputs are logical 1, and CO is a logical 0 otherwise). Figure 3(b) illustrates the MIMIC description of the 1-bit adder. The TYPE statement defines the FAD cell as having three inputs and two outputs. The next two lines are PART statements that define the two components of the FAD cell as a three-input XOR3 cell (that generates the sum, S) and a three-input MAJ3 cell (that generates the carry-out).

The XOR3 cell and the MAJ3 cell must be filled in next. These cells are shown in Fig. 4 and Fig. 5, respectively. Since all components in these cells are built-in MIMIC primitives, the design is now complete.

The wire-tie in the MAJ3 cell, output signal M, acts as a wired-OR. Delay information has been omitted here, but will be included in the simulation of this circuit in Example #2 below.

MIMIC's simulation capability

MIMIC is a four-state simulator. That is, each signal in the simulated circuit will be in one of four possible states: 0 (logical 0), 1 (logical 1), X (unknown or uninitialized), or HIZ (high impedance or floating). MIMIC models the logical operation of each component, in addition to timing and propagation delays along signal paths of the circuit.

The smallest interval of time in MIMIC

is the time-unit. That is, time is modeled as a sequence of discrete time-units, and all events that occur within the same time-unit are considered to be simultaneous. The user is free to scale time-units according to the technology (for example, equate 1 time-unit to 1 nanosecond).

MIMIC rise and fall delays

All signal delays are expressed in time-units, and the user may specify independent rise and fall delays for each output of each element. Either delay (or both) may be linear functions of loading. Each input of each element may be individually assigned a load value, and the loading on a particular signal is automatically computed as the sum of the load values of the input pins that the signal drives.

MIMIC spikes and pulses

A spike condition in MIMIC is synonymous with an attempt to drive a gate's output faster than it can respond. Here, the gate begins to respond to a new input state, but before the output signal can swing too far, a second input change drives the output back to its original value. This condition is one cause of the ubiquitous "glitch." MIMIC will normally suppress a spike, and the simulated signal will appear clean. Optionally, the user can request propagation of spikes as unknown (X) pulses. In either case, MIMIC will report the occurrence of a spike if the user requests this information.

A pulse condition in MIMIC is the occurrence of a pulse whose width is comparable to the average propagation delay, $(\text{rise} + \text{fall})/2$, of the signal. Narrow pulses on signals are usually unplanned, and an unexpected pulse could cause problems. Pulses could be regarded as spikes that "made it." In many cases, minor variation of element delays could transform pulses into spikes and vice versa. MIMIC reports the occurrence of pulses at the user's option. Example #2 (page 15) illustrates spikes and pulses.

MIMIC built-in models

MIMIC supports a variety of built-in, or primitive, logic elements. In addition to the basic combinational types (for example, inverter, AND, NOR, and so on), MIMIC models a two-input multiplexer, a four-input AND-AND-NOR, and a four-input OR-OR-NAND. It models three basic types of latches and six different edge-trig-

gered flip flops. MIMIC also models several types of tristate input/output pads that are particularly useful for test applications. It models complex functional blocks such as decade counters, ROMs, RAMs, and PLAs. In addition, the bilateral transmission gate (BTG) is a built-in primitive that models two-way signal flow.

Wire-ties and transmission gates

MIMIC automatically handles wire-ties without the user having to insert fictitious elements (as was required in most older simulators). Element ports (for example, the outputs of several AND gates) are tied together by assigning the same name to the signals connected to them. Also, due to the bilateral nature of transmission gates, distinct (differently named) signals could be electrically tied together at times. MIMIC actually supports three types of wire-ties: wired-AND (any 0 dominates), wired-OR (any 1 dominates), and wire-tie-without-dominance (where oppositely-pulling tied signals are recognized and reported as a conflict). Signal M in Fig. 5(b) acts as a wired-OR due to the $\text{ODOM} = 1$ entry in the TYPE statement.

MIMIC's simulation algorithm

MIMIC's simulation algorithm is efficient, since it only performs computation when signals change values (event driven), and only simulates those elements whose inputs have actually changed (selective trace). MIMIC initiates simulation by setting all signals in the network to the unknown (X) state. The user may initialize selected signals to known values, if desired. The first primary input pattern is applied, and the effects of this input state ripple through the circuit being simulated at rates determined by the delays of the changing internal signals. When the circuit reaches a stable state, the second input pattern is applied, and so on, until the simulation is terminated either by exhausting the input patterns or by the occurrence of a user-specified condition. If the input sequence is designed properly, and if the circuit is designed for testability, the number of signals in the unknown (X) state should decrease as the effects of the (known) input patterns propagate through the logic.

MIMIC run commands

MIMIC's run command language allows the user to control the entire simulation process. Run commands may be issued

CAD programs and authors

MIMIC is part of an integrated CAD system used at RCA and illustrated in Fig. 1. The programs and their sequence of use are given below. Program names are capitalized and their authors' names are parenthesized.

After verifying the circuit design using MIMIC, the MIMIC network description is inputted to the CADLM program (David Tsao). The output of this program is then inputted to the MP2D (semi-custom) or the AUA (gate array) program, resulting in a complete circuit layout. This layout can then be inputted to the CONCERT program (Joe Mastroianni) which extracts the logical connectivity from the layout. The FASTRACK system (Fred Heath, Dick Lydick) currently automates the path from MIMIC through CONCERT. This extracted network description can then be compared to the original MIMIC description to verify equivalence (this step is not yet automated). The wiring capacitance can then be added to the extracted network description (this step is not yet automated) and the reconstructed circuit, now containing actual implementation delays, can be simulated by MIMIC.

If no timing problems exist the circuit can optionally be fault simulated by TESTGEN (Henry Hellman) to verify the effectiveness of the test patterns. Finally, the TGEN file created by MIMIC can be inputted to the AFTER program (Mark Turner) to generate the tester (for example, Sentry, Teradyne) program.

from the terminal (interactive session), or may be contained in files that are accessed using the EXECUTE command (interactive or batch). Saving predefined run command sequences in files is extremely useful if these operations are performed repeatedly (in one or more simulation sessions). The following is a brief overview of these commands.

Controlling signal values. The DEFINE command allows the user to define primary input patterns hierarchically. It is

```

ILOGICAL
C=8-BIT FULL ADDER
TYPE=FAD8 I=A7,A6,A5,A4,A3,A2,A1,A0,B7,B6,B5,B4,B3,B2,B1,B0,CIN $
O=COUT,S7,S6,S5,S4,S3,S2,S1,S0
PART=F0 TYPE=FAD I=A0,B0,CIN O=S0,C1
PART=F1 TYPE=FAD I=A1,B1,C1 O=S1,C2
PART=F2 TYPE=FAD I=A2,B2,C2 O=S2,C3
PART=F3 TYPE=FAD I=A3,B3,C3 O=S3,C4
PART=F4 TYPE=FAD I=A4,B4,C4 O=S4,C5
PART=F5 TYPE=FAD I=A5,B5,C5 O=S5,C6
PART=F6 TYPE=FAD I=A6,B6,C6 O=S6,C7
PART=F7 TYPE=FAD I=A7,B7,C7 O=S7,COUT

C=FULL-ADDER CELL
TYPE=FAD I=A,B,C1 O=S,CO
PART=S TYPE=XOR3 I=A,B,C1 O=S
PART=CO TYPE=MAJ3 I=A,B,C1 O=CO

C=3-INPUT EXCLUSIVE-OR
TYPE=XOR3 I=U,V,W O=Y
PART=Z TYPE=EXOR I=U,V O=Z ODEL=DEL1
PART=Y TYPE=EXOR I=Z,W O=Y ODEL=DEL4

C=3-INPUT MAJORITY GATE
TYPE=MAJ3 I=A,B,C O=M ODEL=DEL2 ODOM=1
PART=1 TYPE=AND I=A,B O=M
PART=2 TYPE=AND I=A,C O=M
PART=3 TYPE=AND I=B,C O=M

IDELAY
DELAY=DEL1 RISE=1 FALL=1
DELAY=DEL2 CHANGE=2
DELAY=DEL4 CHANGE=4

```

Fig. 6. MIMIC description of ripple-carry adder (Example #2). Figures 6 through 10 illustrate the use of MIMIC.

```

DEFINE FILE=FAD
GET TYPE=FAD8 FILE:
DEFINE PRIPPLE.17= 00000000 00000000 0 $
00000000 11111111 1
APPLY PATTERNS=PRIPPLE
WARN FILE: HAZARD=COUT,S7,S6,S5,S4,S3,S2,S1,S0
WRITE CHANGE: LIST=A7,A6,A5,A4,A3,A2,A1,A0,*,B7,B6,B5,B4,B3,B2,B1,B0, $
*,CIN,*,COUT,*,S6,S5,S4,S3,S2,S1,S0 FILE:

```

Fig. 7. MIMIC run commands for ripple-carry adder (Example #2).

```

C=          AAAAAAAAA BBBB BBBB C C SSSSSSS
C=          76543210 76543210 I O 76543210
C=          N U
C=          T
0 T 1: 00000000 00000000 0 X XXXXXXXX
2 T 1: 00000000 00000000 0 0 XXXXXXXX
5 T 1: 00000000 00000000 0 0 XXXXXXX0
6 T 1: 00000000 00000000 0 0 00000000
6 T 1: 00000000 00000000 0 0 00000000
0 T 2: 00000000 11111111 1 0 00000000
5 T 2: 00000000 11111111 1 0 11111000
10 T 2: 00000000 11111111 1 0 11110000
12 T 2: 00000000 11111111 1 0 11100000
14 T 2: 00000000 11111111 1 0 11000000
16 T 2: 00000000 11111111 1 1 10000000
18 T 2: 00000000 11111111 1 1 00000000
18 T 2: 00000000 11111111 1 1 00000000

```

Fig. 8. Simulation results of ripple-carry adder generated by MIMIC in response to the WRITE command (in Fig. 7).

also used to establish certain defaults. Example 3 illustrates hierarchical pattern description.

The SET command allows the user to set (initialize) selected signals to specified values (0,1,X,HIZ). These signal values may subsequently change in the course of simulation. The CLAMP command is similar to SET, except that CLAMPed signals remain at their specified values until released by the user.

The RESTORE command allows the user to restore the total state of the circuit to a state that was attained at some previous time, either in the same session or in a previous session. The restored state was saved at that time as a result of MIMIC's SAVE command. The user has total control over which states are saved (if any), and therefore from which states simulation can be resumed.

Observing signal values. The PRINT (to the terminal) and WRITE (to a specified file) commands allow the user to specify the signals whose values are to be listed in the course of simulation. The signal values may optionally be listed whenever any of the selected signals changes state.

The TRACE command allows the user to observe transitions of specified (or all) signals. This command is useful in tracing signal activity leading to spikes and races.

The LOOK command allows the user to observe selected signal values while simulation is suspended. Essentially, the user can probe signal values while the circuit state is frozen in time.

The WARN command allows the user to control reports about questionable circuit operation. Events that are reported include spikes, pulses, wire-tie conflicts, and oscillations. The user may specify signals to be monitored for each type of questionable event.

The TGEN command controls the generation of a file containing the input state and resulting output state for each input pattern. This stimulus/response file is compatible with the output of TESTGEN, RCA's good-logic/fault simulator, and can be used for test program generation in conjunction with the AFTER program. Optionally, the TGEN command may be used to generate a circuit description file that is compatible with TESTGEN, if fault simulation is desired.

Simulation control. The BREAK command allows the user to conditionally interrupt simulation. The user-specified conditions that could interrupt simulation include

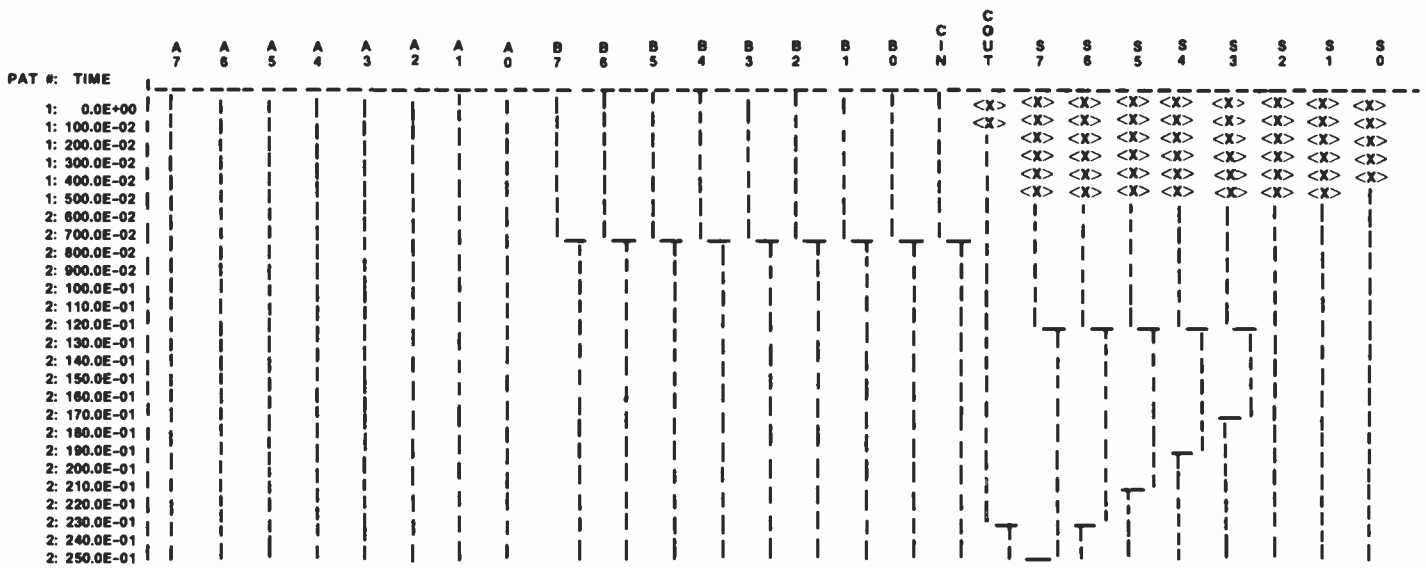


Fig. 9. Simulation results of ripple-carry adder as plotted by MIME program.

(a) a change in value or attainment of a specified value at selected signals, or (b) the occurrence of a spike, pulse, wire-tie conflict, or oscillation at selected signals. Whatever the cause of the interrupt, simulation can always be resumed, if desired.

Example #2. Simulation of the ripple-carry adder

This example illustrates the MIMIC simulation of the 8-bit full adder discussed in Example #1. The MIMIC network description file, shown in Fig. 6, contains all the cell descriptions of Figs. 2 through 5. In addition, delay information has been added to the cells at the lowest levels. For example, the exclusive-or generating $U \oplus V$ in the XOR3 cell has been assigned an output delay (ODEL) DEL1, and the second exclusive-or (generating $U \oplus V \oplus W$) has been assigned an output delay of DEL4. These symbolic delay names reference the delay tables contained in the bottom three lines of Fig. 6. Thus, DEL1 specifies a rise delay of 1 and a fall delay of 1. If the rise and fall delays are identical, the single CHANGE keyword can be used in place of the two keywords RISE and FALL. Thus, DEL4 specifies rise and fall delays of 4, and DEL2 specifies rise and fall delays of 2. Note that the output delay of the MAJ3 has been specified as DEL2, so the carry signal will propagate from stage to stage with a delay of 2 time-units.

The worst-case response time of the ripple carry adder occurs when carry signals propagate through every stage. Thus, if the A-inputs are set to all zeros, the B-inputs are set to all ones, and the carry into the least significant bit (CIN) is set to one, the

```

WARN-ON-SPIKE ... SIGNAL: S0
  TIME: 1. TEST: 2. LEVELS: 0 -> 1 -> 0
WARN-ON-SPIKE ... SIGNAL: S1
  TIME: 2. TEST: 2. LEVELS: 0 -> 1 -> 0
WARN-ON-SPIKE ... SIGNAL: S2
  TIME: 4. TEST: 2. LEVELS: 0 -> 1 -> 0
WARN-ON-PULSE(WIDTH= 1.25) .. SIGNAL: S3
  TIME: 10. TEST: 2. LEVELS: 0 -> 1 -> 0
WARN-ON-PULSE(WIDTH= 1.75) ... SIGNAL: S4
  TIME: 12. TEST: 2. LEVELS: 0 -> 1 -> 0
WARN-ON-PULSE(WIDTH= 2.25) .. SIGNAL: S5
  TIME: 14. TEST: 2. LEVELS: 0 -> 1 -> 0
WARN-ON-PULSE(WIDTH= 2.75) . . SIGNAL: S6
  TIME: 16. TEST: 2. LEVELS: 0 -> 1 -> 0

```

Fig. 10. Spike and pulse WARN messages for ripple-carry adder generated by MIMIC in response to the WARN command (in Fig. 7).

correct output state (COUT = 1, all S-outputs are 0) can only occur after carries have rippled to the most significant bit and the sum, S7, and carryout, COUT, have reacted. Since the carry signals ripple through seven stages, at 2 time-units per stage, and since the XOR3 output signals have a delay of 4 time-units, this will require $7 \times 2 + 4 = 18$ time-units. Meanwhile, transient 1-pulses will appear at the outputs, with longer pulses occurring at the most significant bits.

Figure 7 illustrates the run commands issued to MIMIC, and Fig. 8 shows the simulation results. Referring to Fig. 7, the third run command defines a 17-bit input pattern (called PRIPPLE) consisting of two tests. The first test pattern sets all seventeen inputs to 0 and the second test pattern changes the B-inputs and CIN to all 1's. The WRITE command instructs MIMIC to list all the inputs and outputs whenever any of these signals changes state.

Referring to Fig. 8, time increases vertically downward. Signal A7 is listed first, then A6, and so on, then the B-inputs, then CIN, COUT, and the S-outputs. The output signals (COUT, S7-S0) are initially in the unknown (X) state at the beginning of the first test pattern. As time goes on, known values ultimately reach all these signals. The response to the second test pattern exhibits progressively wider pulses at the S-outputs of higher significance.

Figure 9 illustrates the same waveforms as Fig. 8, formatted as timing diagrams. These plots were generated by the MIME program, which postprocesses MIMIC output files. The pulses on the S-outputs clearly catch the eye in this representation.

Outputs S0 through S2 appear to be constant 0's, but actually they contain spikes. These are shown in Fig. 10, which lists all MIMIC warnings on spikes and pulses for the outputs in response to the WARN run command (see Fig. 7). The

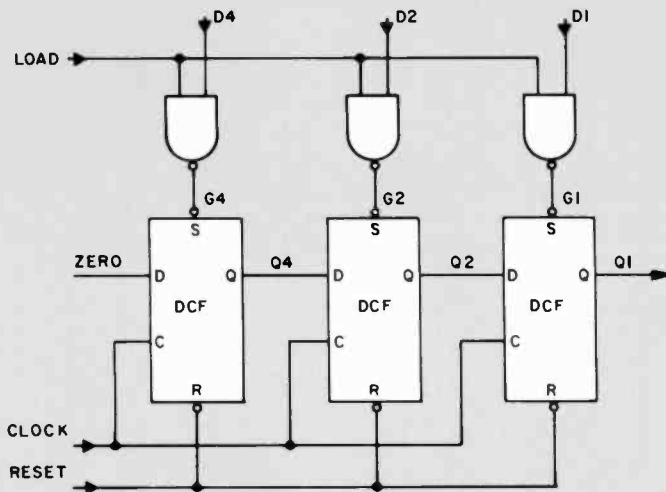


Fig. 11(a). Three-stage shift register of Example #3.

	RESET	CLOCK	LOAD	D4	D2	D1	
(1)	1	1	1	d	d	d	load the value ddd
(2)	1	1	0	0	0	0	disable load control
(3)	1	0	0	0	0	0	
(4)	1	1	0	0	0	0	first clock
(5)	1	0	0	0	0	0	
(6)	1	1	0	0	0	0	second clock edge
(7)	1	0	0	0	0	0	
(8)	1	1	0	0	0	0	third clock edge

Fig. 11(b). Subsequence to test the three-stage shift register.

```

IDELAY
DELAY=GATE-DELAY RISE=2 FALL=1
DELAY=FF-DELAY RISE=(0,1),(3,4) FALL=(2,5),(5,8)

!LOGICAL

!FORMAT PART= TYPE= I= O= ODEL=
TYPE=SHIFTER I=RESET,CLOCK,LOAD,D4,D2,D1 O=Q1
G4 NAND LOAD,D4 G4 GATE-DELAY
G2 NAND LOAD,D2 G2 GATE-DELAY
G1 NAND LOAD,D1 G1 GATE-DELAY
Q4 DCF RESET,G4,CLOCK,ZERO Q4 FF-DELAY
Q2 DCF RESET,G2,CLOCK,Q4 Q2 FF-DELAY
Q1 DCF RESET,G1,CLOCK,Q2 Q1 FF-DELAY

```

Fig. 11(c). MIMIC description of three-stage shift register.

first three WARN messages report spikes at these three signals.

Example #3. Parallel-to-serial converter

The purpose of this example is to illustrate hierarchical input-pattern description. Con-

sider the three-stage shift register shown in Fig. 11(a). This register contains parallel inputs to the three flip-flop-SET terminals (active LOW), and can be operated as a parallel-to-serial converter by using the sequence of eight input patterns (assuming the three flip-flops are initially reset) shown

```

C=DEFINE 65-PATTERN TEST SEQUENCE
'PTEST'
DEFINE PSHIFT.6 = 110000 DO3
(100000 110000)
DEFINE P000.6 = 111000 PSHIFT
DEFINE P001.6 = 111001 PSHIFT
DEFINE P010.6 = 111010 PSHIFT
DEFINE P011.6 = 111011 PSHIFT
DEFINE P100.6 = 111100 PSHIFT
DEFINE P101.6 = 111101 PSHIFT
DEFINE P110.6 = 111110 PSHIFT
DEFINE P111.6 = 111111 PSHIFT
DEFINE PTEST.6 = 010000 P000 P001 P010
P011 P100 P101 P110 P111
C= END OF INPUT PATTERN DEFINITIONS

```

Fig. 12. Hierarchical description of PTEST, the 65 primary input patterns of Example #3.

in Fig. 11(b). Note that the flip-flops are positive-edge triggered and that logical 0 is shifted into the register as the serial data is shifted out.

If the circuit is to be tested exhaustively, all eight combinations of the parallel data inputs must be applied. This requires 8×8 , or 64, input patterns plus an initial resetting pattern. One way to specify these 65 input patterns is to explicitly enumerate them in a DEFINE statement. Due to the repetitive nature of these patterns, they can be hierarchically described as follows:

Let PSHIFT be the last seven patterns of the clocking sequence (patterns two through eight above).

Let P_i be the entire eight-pattern test when the three parallel inputs are in state i (i between zero and seven inclusive).

Let PTEST be the entire 65-pattern test sequence.

Then the ten DEFINE statements shown in Figure 12 completely define the entire test sequence, PTEST.

This example incidentally illustrates several aspects of MIMIC's network description language unrelated to the above. Referring to Fig. 11(c), the delay called FF-DELAY contains independent rise and fall delays based on loading. Each of these delays specifies a pair of points on a straight line representing delay (in time-units) versus loading. Thus, the rise-delay specification contains a delay of 1 for 0 loading, and a delay of 4 for a loading of 3. For any other loading, MIMIC interpolates a value along the line joining these two points.

A second item illustrated in Fig. 11(d) is the !FORMAT statement that specifies

the order of keywords in all subsequent PART statements. MIMIC fills-in each such statement with these ordered keywords. For example, this !FORMAT statement causes the first line after the TYPE statement to be equivalent to:

```
PART = G4 TYPE = NAND
I = LOAD, D4 O = G4
ODEL = GATE-DELAY
```

The !FORMAT statement allows considerable reduction in the amount of typing required to specify the circuit.

Accessing MIMIC

This paper has presented an overview of MIMIC. The MIMIC User Guide contains a complete description of the simulator, and the MIMIC Primer contains good introductory material. Anyone interested in obtaining a copy of the Guide or the Primer, or using MIMIC, should contact Gary Gendel at Somerville (TACNET 325-7399).

Acknowledgments

MIMIC is the result of a team effort. Henry Hellman, the co-author of MIMIC, developed the simulation routines and the

Aaron Ashkinazy joined RCA in 1970, after receiving his Doctor of Engineering Science degree from Columbia University. At that time, he was responsible for investigating and developing algorithms for automatic test generation and fault simulation. In 1974, he joined the Design Automation Department at Somerville, where he developed the first version of AFTER, which generates tester programs from stimulus/response patterns. Having already written a simulation program prior to joining RCA, MIMIC is his second logic simulator. Dr. Ashkinazy is currently responsible for enhancing MIMIC, particularly in the areas of fault simulation and mixed-mode (functional) modeling.

Contact him at:
RCA Solid State Division
Somerville, N.J.
TACNET: 325-6163



bulk of the run-command processor. Chris Davis supervised the project and provided the valuable insight necessary to define and implement MIMIC's capabilities. Shirley Chen has admirably performed the Herculean task of maintaining and extending the MIMIC software. Gary Gendel has done an excellent job of introducing MIMIC to the engineering community and

helping users to model their circuits, interpret MIMIC runs, and utilize MIMIC effectively. He is also the author of MIME. Finally, the author would like to acknowledge the contribution by many MIMIC users, particularly Dick Lydick and Fred Heath, of valuable suggestions and feedback in debugging MIMIC and making it a more useful program.

How many of these *RCA Engineer* issues should you have read?

Order then now.

Back issues and reprints listed here may be ordered from the *RCA Engineer* Editorial Office, 204-2, Cherry Hill.

All back issues are \$2.00 except the *Index*, which is free.

Photocopy this form, include your name, RCA charge number and your internal mailing address.

THEME-RELATED ISSUES

- Consumer Electronics Manufacturing
VOL. 24 NO. 4 Dec 78/Jan 1979
- Microelectronics
VOL. 24 NO. 6 Apr/May 1979
- Microprocessor Applications
VOL. 25 NO. 3 Oct/Nov 1979
- Quality (Do it right the first time)
VOL. 25 NO. 4 Dec 79/Jan 1980
- RCA International
VOL. 25 NO. 5 Feb/Mar 1980
- Color TV Receivers
VOL. 25 NO. 6 Apr/May/June 1980
- 25th Anniversary Issue
VOL. 26 NO. 1 Jul/Aug 1980
- Communications Trends
VOL. 26 NO. 3 Nov/Dec 1980
- Mechanical Engineering
VOL. 26 NO. 4 Jan/Feb 1981
- Increasing Your Effectiveness
VOL. 26 NO. 5 Mar/Apr 1981
- "SelectaVision" VideoDisc, Part II
VOL. 27 NO. 1 Jan/Feb 1982
- Manufacturing Engineering
VOL. 27 NO. 2 Mar/Apr 1982
- Electro-Optics
VOL. 27 NO. 3 May/June 1982

COLLECTIONS OF ARTICLES

- Consumer Electronics
PE-515 1971
- Solid State Technology
PE-552 1972
- COS/MOS Technology
PE-580 1973
- Automotive Electronics
PE-681 1976
- Microprocessor Technology
PE-702 1976
- Electro-Optics
PE-703 1976
- Picture Tube
PE-748 1980

CUMULATIVE INDEX

- 25-Year Index to *RCA Engineer*
Aug 1980

An HF modem simulation

A powerful tool for high-frequency equipment design and evaluation . . . computer simulation and modeling.

Abstract: A modular simulation architecture developed on the VAX 11/780 computer models the transmitter and receiver portions of the AN/USQ-74 multi-tone modem used by the Navy's Anti-Submarine Warfare Operations Center. The program structure is examined, and functional descriptions of the components are given.

With the resurgence of high-frequency (HF) military communications as a backup for satellite communication networks, computer simulation and analysis is becoming a valuable method for evaluating the performance of HF communications equipment. Simulation offers an alternative to the expensive method of evaluating equipment by field testing, and it also provides for a common reference for performance comparison. This is especially true at HF where, due to the dynamic behavior of the media, equipment being compared would need to be tested at the same time, over the same link, so that the widely varying effects of the ionosphere are identical for each test. The computer allows storage of sets of standard ionospheric conditions for regular use when comparing different pieces of equipment.

A result of this interest was a program for modeling and simulating an existing element of an HF radio facility, the AN/USQ-74 multi-tone modem used by the Navy as part of the LINK-11 operations for the Anti-Submarine Warfare Operations Center (ASWOC). Figures 1 and 2 represent the top-level flow for both the transmitter and receiver programs.

©1982 RCA Corporation
 Final manuscript received September 13, 1982.
 Reprint RE-27-6-3

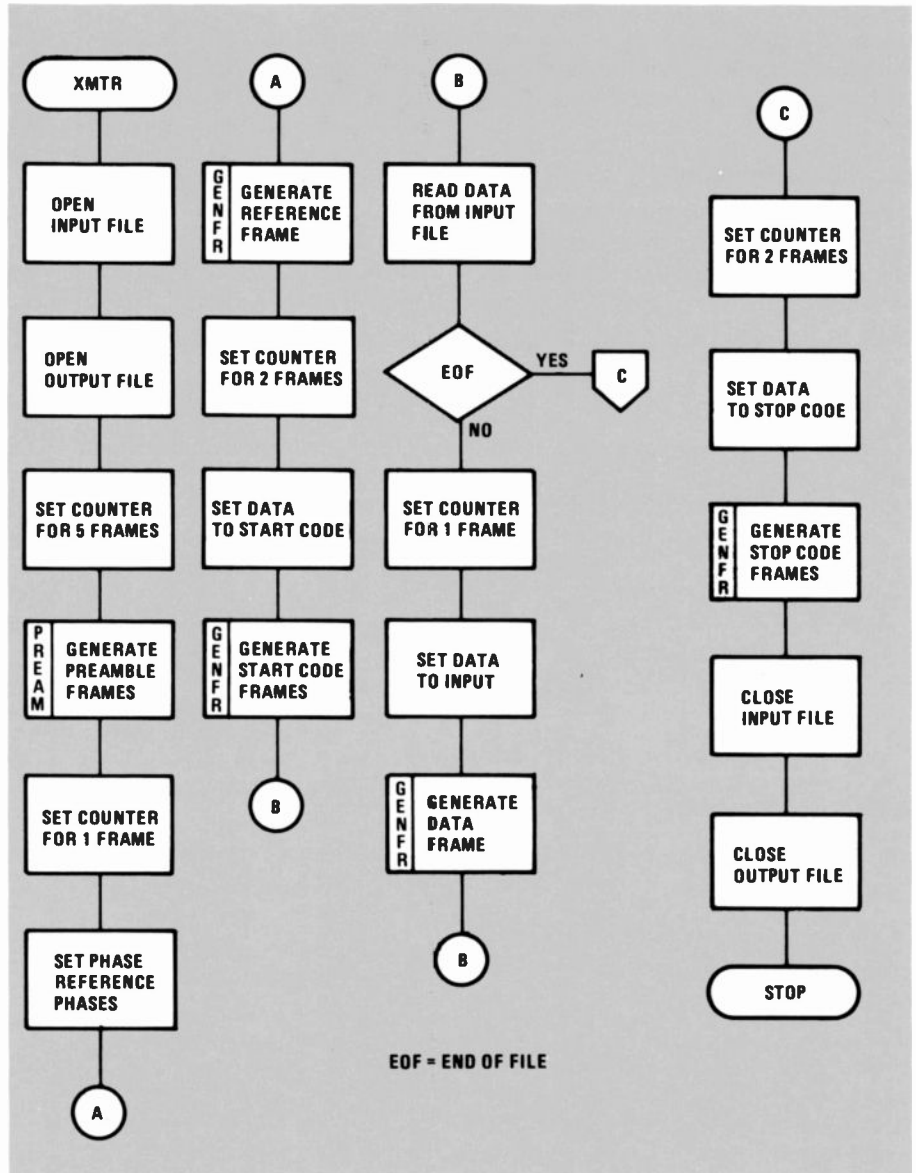


Fig. 1. Top-level flowchart illustrating transmitter functional flow and control code processing.

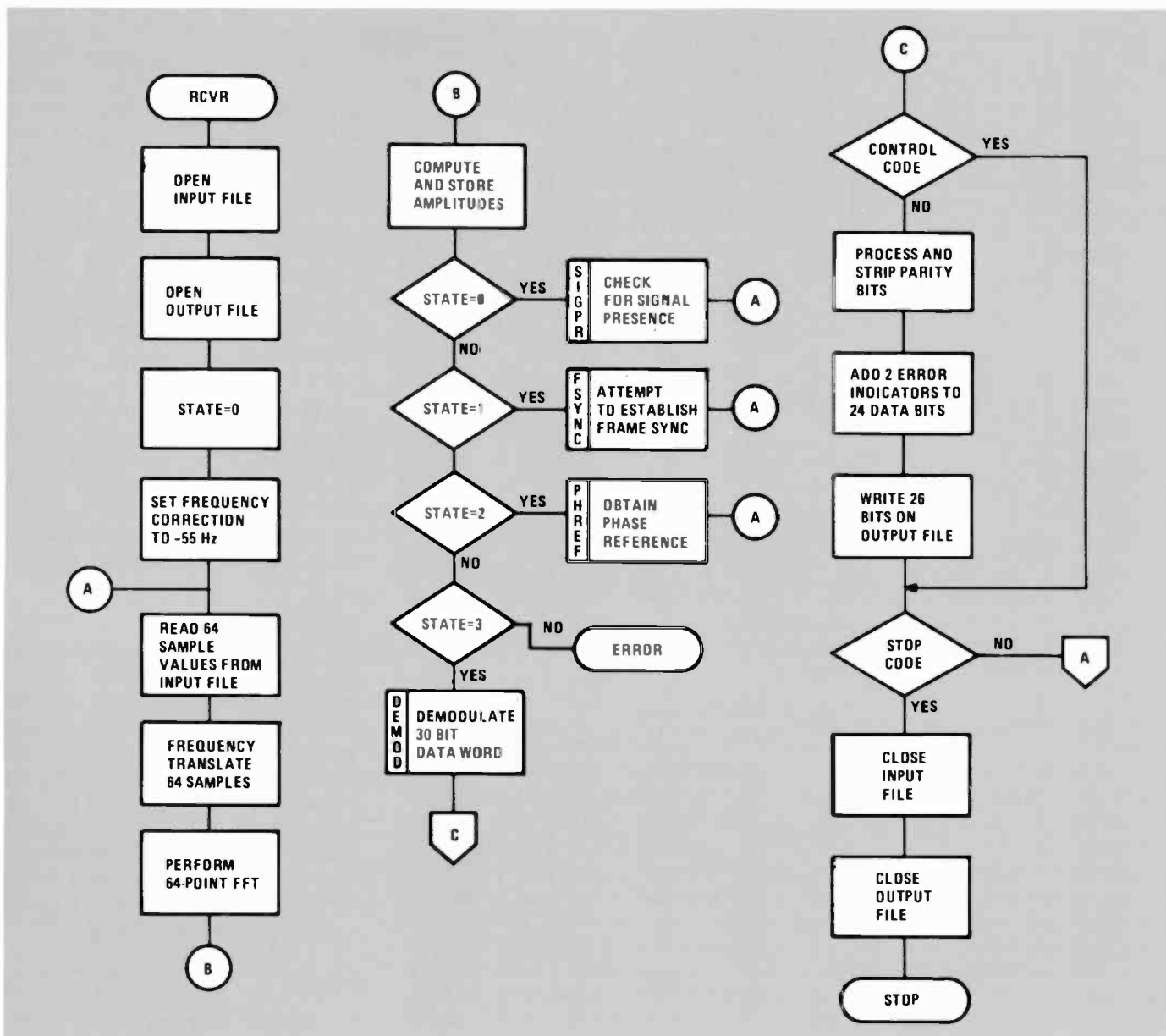


Fig. 2. Top-level flowchart illustrating the receiver's functional flow and control code processing.

The simulation architecture, written in BASIC, was developed on a VAX 11/780 computer as a series of modular subprograms, with each subprogram simulating a major function of the modem. The simulation is divided into two main programs, one performing as the transmitter portion of the modem and the other as the receiver portion.

General description

The USQ-74 can transmit data at two different rates: 75 baud per channel or 45.45 baud per channel. The transmitter has sixteen separate channels: fifteen channels are used for data transmission and one is reserved for the transmission of an unmodu-

lated Doppler reference tone. All sixteen channels are summed to produce a composite waveform, which is sampled by a 12-bit analog-to-digital (A/D) converter. The computer simulation generates a sampled waveform for each channel and these sampled waveforms are summed to produce sampled values of the composite waveform.

Binary data is input to the modem in groups of 24 bits, representing three 8-bit ASCII characters. The modem encodes each 24-bit data word with 6 error-detection/correction (EDAC) bits to produce a 30-bit frame for modulation. The data frames that comprise a message are preceded by header frames, which are pro-

duced by the modem. The header frames include five preamble frames, a phase reference frame, and two start-code frames. The preamble frames contain a Doppler tone used by the receiver for signal detection and a sync tone used to establish frame synchronization.

The start codes are 30-bit sequences that contain no error-detection bits. After the start codes are transmitted, data information is sent in the following frames. The modem encodes each 30-bit data frame by separating it into bit pairs that modulate the fifteen transmitted data tones. Depending on the bit pair, the data tones are modulated in phase by either $\pm 45^\circ$ or $\pm 135^\circ$. The transmitter uses a Quadrature

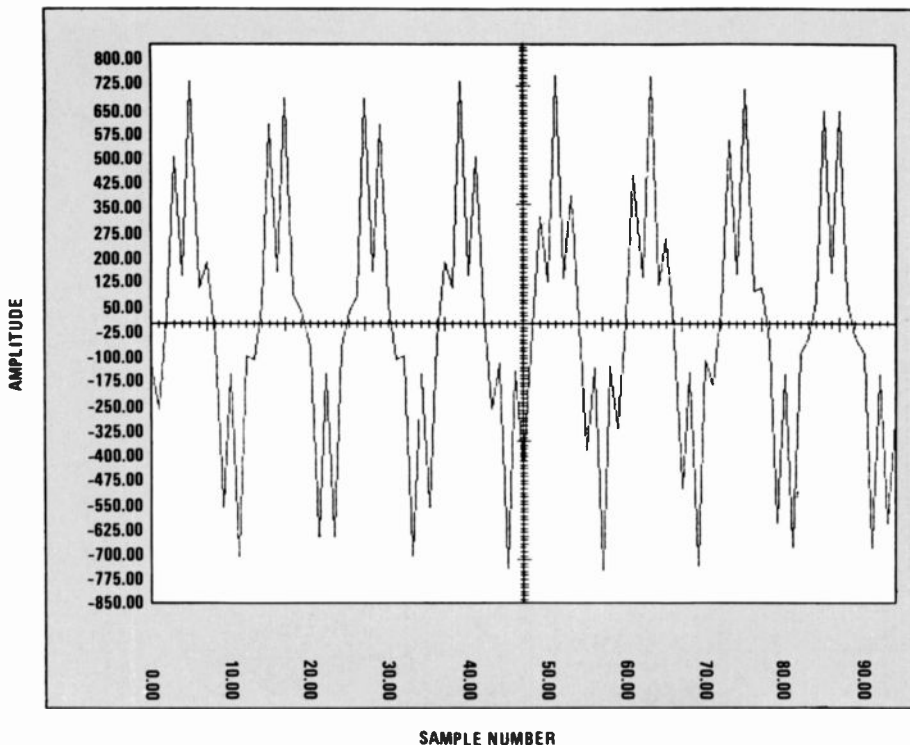


Fig. 3. Plotted sample values generated by the transmitter program for the first frame of the preamble.

Phase Shift Keying (QPSK) modulation scheme to encode the transmitted data on each of sixteen separate channels. Data frames are followed by two stop-code frames used to indicate the end of a message.

The receiver uses the header generated by the transmitter for several functions. The preamble frames are used to determine signal presence and frame synchronization. The phases transmitted in the phase reference are stored by the receiver and used to demodulate the following start-code frames. Both start-code frames must be successfully demodulated for the message processing to continue. The receiver analyzes the transmitted information by performing a Fast Fourier Transform (FFT) on the received frames. The resulting frequency components are examined and their amplitude and phase information are used to accomplish the above functions.

Transmitter subfunctions

The USQ-74 modem simulation uses four subprograms to perform transmitter functions. The subprograms are responsible for computing sample values for each tone, performing EDAC encoding, generating preamble frames, and performing QPSK modulation. The four subprograms used for these functions are called GENTN, PREAM, GENFR, and QPSK.

GENTN

GENTN is the subprogram that generates the sample values for each tone transmitted. The values are produced by executing a table look-up of stored values of a sampled cosine wave. The table contains 128 sample points of one complete cycle of a 55-Hz cosine. The amplitude values of the cosine range over ± 127 . Tones that are multiples of 55 Hz can be reproduced by reading the points from the table in a specified order. By reading every j th point, where j is the harmonic of 55, sample values of the $j \times 55$ Hz tone are produced. For example, to produce a 2200-Hz tone every 40th value would be read from the table. When the index of the table exceeds 128, modulo-128 arithmetic is performed on the index. For this example, sample values corresponding to table entries 40, 80, 120, 12, 52, . . . would be read out.

The phase of the tone is produced in a similar manner. The phase is determined by selecting the appropriate starting point in the table from which the points will be read. Since the wave stored is a cosine, a reading of the points—starting with the first entry in the table—produces a tone at 90° phase. To produce the same tone starting 180° later in phase, the 64th point would be the first point read from the table. Once the starting point is selected to determine the phase, the points are

read out using the algorithm described previously.

In the example of the 2200-Hz tone, to produce that tone at a phase of 135° , the first point read from the table would be 16, then 56, 96, 8, The resulting formula for tone generation can be written as

$$N = (J * M) + P(I)$$

where N is the entry to read from the table; J is the harmonic being generated; $P(I)$ is the starting phase of the I th tone (I equals 1 to 16); and M equals 0 through the number of samples/frame.

As each tone is produced, a running sum of the amplitude values for each sample point is produced. Depending on the rate, either 94 or 155 composite amplitude values will be formed by adding the corresponding sample points for each of the 16 tones. A preamble-frame-waveform generated by this method is shown in Fig. 3.

PREAM

The PREAM subprogram generates the preamble frames that precede each message. The preamble frame consists of two tones, the Doppler tone at 605 Hz and a sync tone at 2915 Hz. The USQ-74 generates five preamble frames for each data transmission. The sync tone is generated using tone 16 so that it is advanced in phase by 180° at the preamble frame boundaries. This phase discontinuity of 180° at each frame boundary allows the receiver to establish frame synchronization.

GENFR

The GENFR subprogram performs two functions. The first function involves encoding the 24-bit data words with six Hamming-code parity bits. The second function involves writing the amplitude values of the composite waveform to the output file.

QPSK

The QPSK subprogram simulates differential phase-shift-keying modulation of the input data. The 30-bit frame from GENFR is broken into 15-bit pairs, each pair corresponding to one of the data tones. The bit pairs are then examined to determine the modulation phase. The modulating phase is then added to each tone's previous phase value, which has indicated the phase of the tone at the end of the last frame. This produces a phase shift at the frame boundary equal to the modulating phase when the tone is generated during the next frame.

Receiver functional description

The receiver portion of the USQ-74 modem can operate in several different modes. It can demodulate either an upper or a lower sideband signal alone or use the two sidebands to form a diversity signal. The receiver demodulates the input signal(s) by performing an FFT on a frame of sample data. The frame is either 94 or 155 samples long, depending on the modem rate (75 or 45.45 baud).

The receiver does not use all of the sample points contained in a frame for demodulation. The abrupt phase changes that occur at frame boundaries make it an undesirable place to look at the signal. Therefore, the receiver examines only the center portion of each frame.

The two frame rates are processed slightly differently. At the fast rate, the central 64 points are used to perform the FFT. This leaves a guard band of 15 points on each side. When the slow rate is being processed, the central 128 points of the 155 sample point frame are used. This leaves a guard band of 13 points at the beginning of the frame, and 14 points at the end. In the slow case, two 64-point FFTs are performed, instead of a 128-point FFT. The first FFT uses the first half of the 128 points; the second FFT, the second half. The results of these two transformations are added together and divided by two to produce a single set of 64 frequency components. These components are then processed in the same manner as in the fast rate.

The receiver performs the following four functions for signal demodulation: (1) it establishes that a signal is present before doing any further processing; (2) it provides frame synchronization; (3) it establishes the proper reference phases; and (4) it decodes the received signal into a binary stream. In addition, the receiver is responsible for various decision-making processes, as well as support processing. Support processing includes performing a Fast Fourier Transform and error-detection-and-correction decoding. The four basic functions have been segmented into subprograms. Each subprogram performs a specific function and passes information back to the main program to be used for further processing.

Signal presence is determined by the SIGPR subprogram. SIGPR uses the Doppler tone present in the preamble frames to determine if a signal is located in the received data. The amplitudes of the frequency components of the signal located about the Doppler tone are compared to

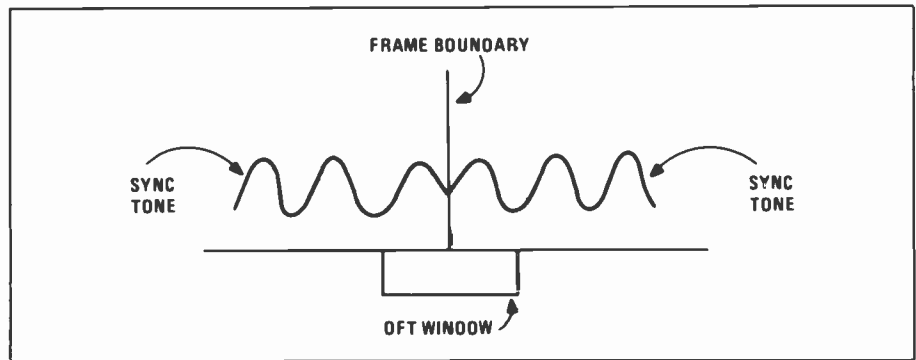


Fig. 4. Window position when a minimum occurs in the DFT value, indicating a frame boundary.

the amplitudes of the frequency components located in the rest of the band. If the power at the Doppler frequency is greater than that in the rest of the band, a signal is assumed to be present.

Once a signal presence is detected, the SIGPR subprogram performs a coarse Doppler-shift calculation. A Doppler shift of the received spectrum may occur if either the radio transmitter or receiver is located on a moving platform (for example, on an aircraft). Instability in any of the frequency devices used in the modulation/demodulation or in frequency translations in receiver and transmitter may also contribute to a frequency shift. This coarse correction is based upon how much energy in the Doppler tone has "spilled over" into adjacent frequency components. The sidelobe with the larger amplitude indicates the direction in which the Doppler shift occurred.

Once signal presence has been detected, the receiver must sync to the incoming signal. The FSYNC subprogram performs this function in addition to calculating a fine Doppler correction. Having stored the frequency components of the Doppler tone, FSYNC computes the phase difference of the Doppler tone in two successive frames. This difference is the amount the phase advanced over 64 sample points or 9.09 milliseconds (64 samples, at 7040 samples/second). The Doppler frequency correction therefore equals the change in phase over the 9.09 milliseconds or

$$f_d = \frac{d\theta}{dt} = (\theta_1 - \theta_2) / (9.09 \times 10^{-3})$$

where θ_1 is the phase of the Doppler in frame 1.

After calculating a fine Doppler correction, FSYNC begins processing to locate the frame boundary. FSYNC uses the 180° phase change of the sync tone between frames in locating the frame boundary. It locates the frame boundary by using a Discrete Fourier Transform (DFT) of the

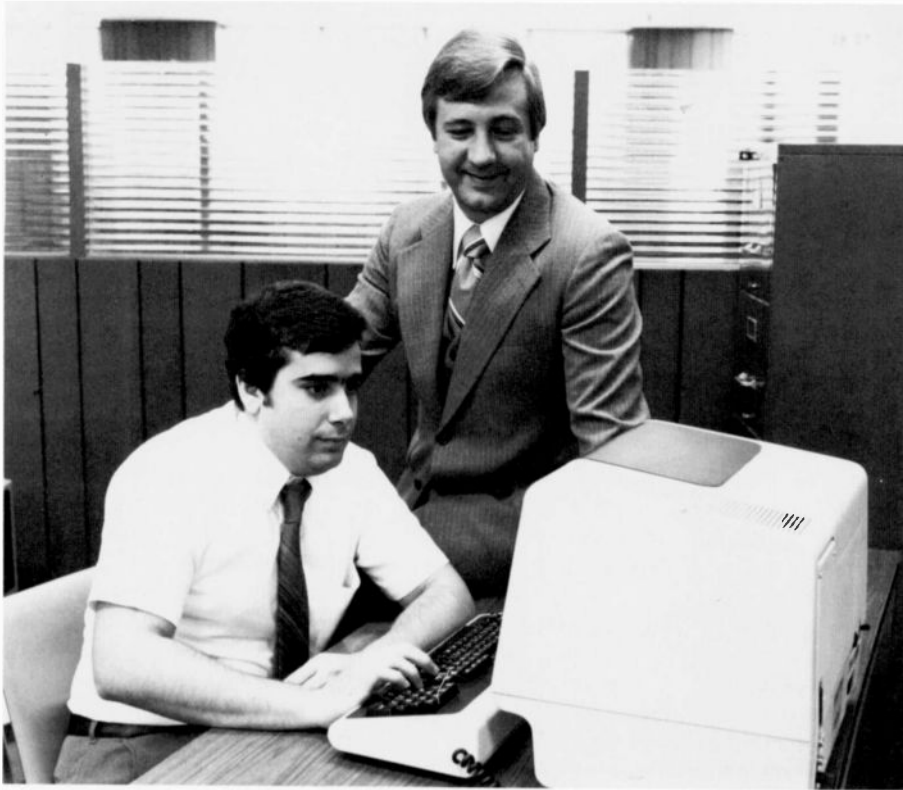
sample points. Because the phase of the sync tone changes by 180°, sample windows of the DFT, which have an equal number of points of the sync tone at 0° phase and 180° phase, will produce a minimum value for the amplitudes of the sync tone. This condition occurs when the DFT window straddles a frame boundary, as shown in Fig. 4. FSYNC, in performing the DFT, slides the sample window one point at a time, using a recursive formula to compute the DFT. By keeping track of the location of the DFT window, and knowing its position when a minimum is produced, the program locates the frame boundary.

The PHREF subprogram is responsible for detecting the phase-reference frame. PHREF also stores the frequency components for each reference vector. These vectors will be compared with the vectors of the next frame. The phase differences between the vectors in successive frames contain the information necessary to allow the decoding of the data tones.

Message decoding

The data information contained in a message can be decoded by the DEMOD subprogram once the phase-reference frame has been found, and the reference vectors stored. Each of the 15 data tones contains two bits of information. The exact bit pair transmitted for each tone is determined by the phase difference between the present data vector and the corresponding vector from the previous frame.

Rather than examining the real and imaginary parts of the frequency components for each tone to determine the phase of each, and then the phase difference between the two, a complex-conjugate vector multiplication is performed between the reference vector and the present data vector. The resultant vector of the multiplication



Paul DeMaria, Communications Systems Engineering, Government Communications Systems, Camden, New Jersey, received his B.E. in Electrical Engineering from City College of the City University of New York in 1979. Mr. DeMaria joined the Systems Engineering group upon graduation. While at RCA, he has been involved in developing packet switching and circuit switching systems. He was also involved in the development of a radio relay network for a forward area tactical operation. He is currently working in the area of the analysis and simulation of communications systems using digital signal-processing techniques. Contact him at:

**Government Communications Systems
Camden, N.J.
TACNET: 222-4634**

Ken Bodzioch, Manager, Digital Communications Systems Engineering, Government Communications Systems, Camden, New Jersey, received a B.S. in Physics from the University of Massachusetts in 1970, and an M.S.E. in Systems Engineering from the University of Pennsylvania in 1977. He has also studied mathematics at the University of Mississippi and the University of Nebraska. Mr. Bodzioch joined RCA in 1974 after four years in the U.S. Air Force as a communications officer. He has been deeply involved in the analysis, design, and implementation of message-, circuit-, and packet-switched communications systems, high-speed signal-processing systems, and classified information-processing systems. Most recently, he has been responsible for the mathematical modeling and simulation of an end-to-end HF communications link and a high-resolution laser-beam recording system. Mr. Bodzioch taught the original microprocessor for logic design course in the RCA After-Hours Study Program.

Contact him at:
**Government Communications Systems
Camden, N.J.
TACNET: 222-3850**

tors $P(k)$ are phase-corrected, using the equation shown below, and stored in the Z array. The equation is

$$Z(k) = P(k) \times e^{j\theta k}$$

where θ is the advance in phase and k is the number of the harmonic of the data tone.

After phase correction, the vectors can be used for decoding the received data. The complex-conjugate multiplication is equivalent to a translation of the axis. It is, therefore, possible to use the resultant vector to determine the phase difference by noting which quadrant the resultant vector lies in. This quadrant of the resultant vector is determined by the sign of its real and imaginary components.

The bit pairs are decoded using the following algorithm. If the real part of the resultant vector is positive, the first bit of the pair is a 1, otherwise it's a 0. If the imaginary part is positive, then the second bit of the pair is a 0, otherwise it's a 1.

The receiver then performs error detection and correction by using the six parity bits at the end of each frame. The Hamming code is capable of double-bit detection and single-bit correction. A two-bit status word, indicating which of the above conditions occurred, is appended to the demodulated word.

Diversity processing

The modem program also simulates the diversity processing of the receiver. The USQ-74 receiver can operate in two diversity modes. One diversity mode forms a coherent combination of the upper and lower sideband signals after they have been individually corrected for Doppler shift. The other diversity mode carries all the signals—upper-sideband, lower-sideband and diversity—through to demodulation. After a frame has been demodulated on all three channels, the receiver determines the frame that will be used as output by examining the error-status bits for each word. The diversity frame is examined first, then the upper-sideband frame and, finally, the lower-sideband frame. If all of the channels are found to have an uncorrectable number of errors, the diversity word is chosen for output.

Summary

The simulation program was written to represent the operation of a specific modem used in HF radio transmission. The simu-

is stored in the P array. This operation is shown in the equation below.

$$P(k) = FO^*(k) \cdot X(k)$$

where $FO^*(k)$ is the complex conjugate of the reference vector; $X(k)$ is the present data vector; and \cdot represents complex multiplication.

Because the phase for each frame is measured several sample points "in" from the beginning of a frame, the phase of the resultant vector of the complex conjugate multiplication must now be corrected by the amount the phase has advanced from the end of one sample window to the beginning of the next. The resultant vec-

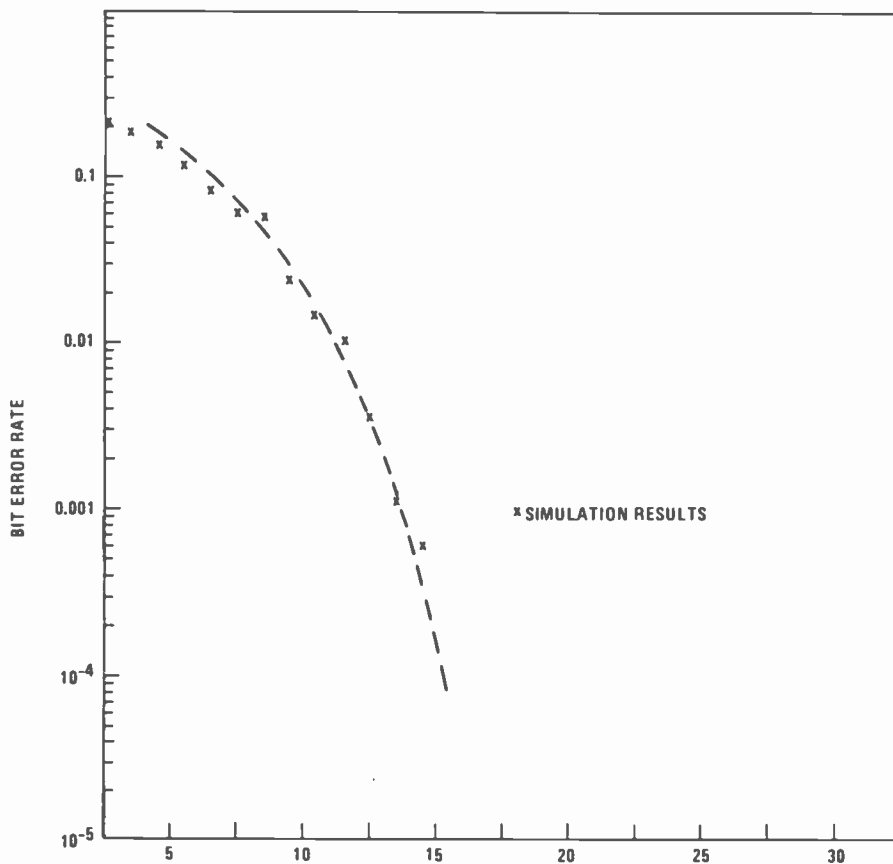


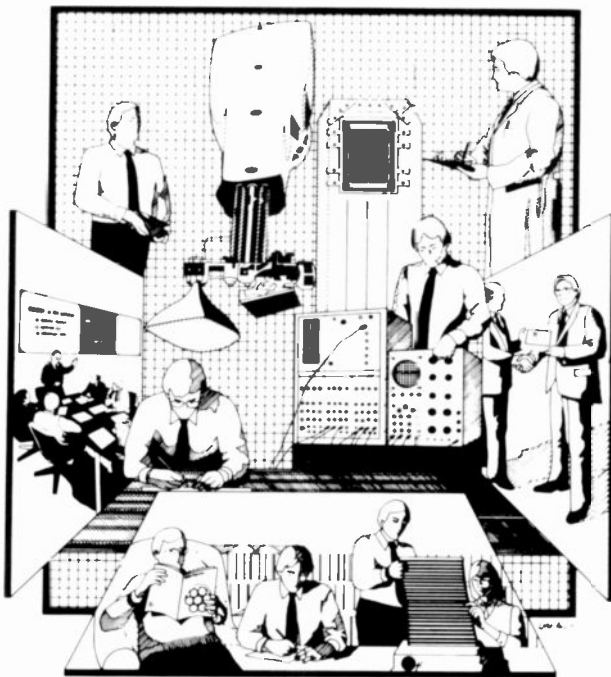
Fig. 5. Simulation results compared with theoretical performance in the presence of Gaussian noise.

lation results correlate well with standard theoretical results. Figure 5 shows the simulation performance when Gaussian noise is added to the simulated signal. The simulation serves three purposes: (1) It offers reduced cost and effort in evaluating modem performance; (2) it can be used as a confidence-building test bed prior to making expensive changes on the existing equipment; and (3) its modular design allows addition or deletion of selected modules to represent performance of other similar Link 11 modems without a major modeling and redesign effort.

Acknowledgment

The authors would like to express their thanks to Dr. T.T.N. Bucher whose help in this project as well as in past efforts has been invaluable.

Have you "given a stroke" to your TEC lately?



Do you know that engineers at RCA are devoting time and effort to help you in establishing and maintaining a satisfying career? They are your Technical Excellence Committee and they attempt to contribute to a stimulating working environment by determining your needs in the areas of technical education, technical information, professional activities and recognition. Once the need is established, they move on to develop and execute supportive activities.

Most of you are somewhat aware of and use the technical excellence activities. But have you paid your dues by expressing your appreciation to your TEC representative? Or even better, do you tell him your views on today's engineering climate and the career needs you perceive?

Engineers are highly skilled professionals, but all too often they keep their thoughts and needs to themselves, perhaps because they are busily engaged solving their problems. Technologies, techniques, and engineering tools—the entire supporting environment is constantly changing and better ways to do engineering work are evolving. Do you take the time to discover and master them? This is where the TEC is attempting to support you—you can help the TEC help you, by sharing your thoughts with the TEC members. Then give them credit for their efforts, every once in a while.

Dynamic analysis and simulation of mechanically scanned radar systems

For complex systems problems with no direct and easily managed solution, digital simulation often affords the only practical analytical approach.

Abstract: *The methods by which mechanically scanned radars are dynamically analyzed through digital computer simulation are summarized. Three distinct areas of concern are addressed as examples: (1) Dynamic modeling of the radar and its antenna drive as the mechanical interaction of a viscous damped spring-mass system; (2) The implementation of digital filters for servo compensation; and (3) Detection analysis as the radar antenna beam scans past a target. The simulation methods that are presented are not restricted to the analysis of radar systems, but can readily be applied to other fields.*

System analysts and designers make extensive use of digital simulation as a means of predicting the dynamic performance of complex systems. These systems are subjected to mechanical and environmental disturbances that, along with design constraints, impose fundamental performance limitations.

Simulation usually is not warranted for relatively simple systems that readily yield a direct mathematical solution for the variables of interest. For complex systems, however, a tractable mathematical solution may not exist, or may be so cumbersome that its utility is compromised. In this situation, digital simulation of the system becomes a virtual necessity; simulation is especially valuable in conserving engineering time and resources.

©1982 RCA Corporation
Final manuscript received September 29, 1982.
Reprint RE-27-6-4



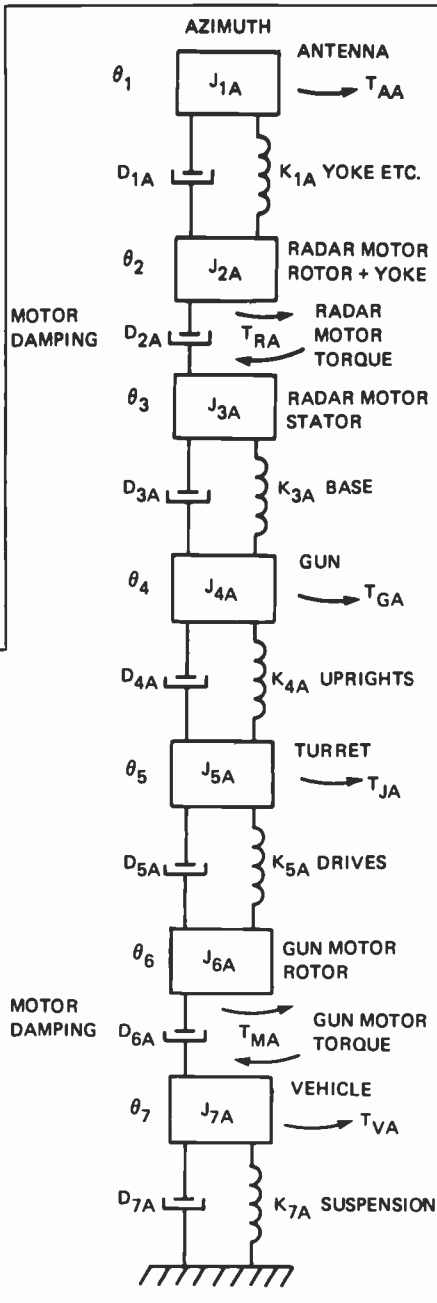
Fig. 1. Mobile radar mounted on a tank (above) and its dynamic model (opposite).

Three areas for simulation

This paper illustrates a number of specific techniques that are useful in simulating the performance of any complex system. We have selected a mechanically scanned radar system as an example of a system of moderate complexity, with three distinct areas of concern facing the designer. Problems in each of the areas cited below have been solved by means of digital computer simulation. The approaches are sufficiently general to be directly applicable to the solution of related problems in other areas.

The first technique is the digital representation of a mechanical system. A com-

plex mechanical body (the radar, antenna, and pedestal) is modeled by springs, masses, and viscous dampers with the objective of simulating the dynamic response as the radar tracks maneuvering targets in noise, clutter, and multipath. The simulation techniques account for the effect of platform motion of the mount to which the radar is attached, and allow for external torque disturbances (for example, wind, gun firing, and vehicle motion) at designated points within the system. These analyses and simulation techniques have been used to identify potential design problems and their solutions early in the design phase



when corrective action can be accomplished with relatively minor schedule and cost penalties.

The second technique is the implementation of digital filters. In modern radar design, many functions previously performed with hardware are now executed with software. One of these functions is the compensation filtering for the servos used to drive the antenna in azimuth and elevation. Two examples are presented that show the importance of using simulation to solve problems that arise during system tests. The simulation model used in these tests precipitated a solution to specific prob-

lems associated with servo-noise transients and also with inherent antenna drive rate and acceleration limits. The simulation allowed these problems to be solved "off-line" during critical periods when the actual system was not available.

The third technique is target detection using a mechanically scanned radar. An important element of radar design is a definition of system parameters that will provide a satisfactory probability of detection. Simulation is a useful tool to estimate the ability of a mechanically scanned radar to detect a target with specified characteristics in a specified environment. Methods are presented that allow this capability.

Dynamic analysis methodology to represent a mechanical system

The first example of simulation as a tool—digital representation of a mechanical system—was used to model a fire control system consisting of a radar mounted on the breech of a gun. The gun and its drive system are mounted on a full-track vehicle. The vehicle, its gun, and the radar are shown in Fig. 1. Each axis of this fire control system is modeled dynamically as a seven-mass system. The elevation-axis model is similar to the azimuth-axis model shown on the right of the figure. Each axis contains both radar and gun-drive subsystems, with external torque disturbances introduced at each mass.

This complex system, with each axis described by seven interacting, second-order

differential equations, can be solved as a set of N simultaneous, linear, constant-coefficient differential equations with M time-varying inputs. The constant coefficients of the differential equations are organized into an $N \times N$ matrix \mathbf{A} , which defines the compliance, inertia, and viscous damping of the system elements.* The M time-varying inputs are represented as an $N \times M$ matrix \mathbf{B} , which defines the manner in which the M -forcing functions are coupled to the system.¹ The resulting differential equations are written in matrix form (see box, equations (1) and (2)).

To simulate this process on a digital computer, we assume the input to be constant over a sample period T . In the resulting equation, the state variables that constitute the vector \mathbf{X} are known at time kT , and the input vector \mathbf{M} is constant within the time interval from time kT to $(k+1)T$. The resulting equation is given in the box as equation (3).

The computational steps in calculating the α and β matrices are rather complex; however, with widely available library routines for matrix operation (solutions for eigenvalues, eigenvectors, and matrix inversion), their implementations in a simulation is straightforward. Also, because their elements are invariant with time, they need only be computed once and stored for use as required. Subsequent iterations of equation (3), which involve only multiplica-

* Matrices and vectors are given in bold face.

Mathematical description of a complex mechanical system

$$\dot{\mathbf{X}}(t) = \mathbf{A}\mathbf{X}(t) + \mathbf{B}\mathbf{u}(t) \quad (1)$$

where:

$$\mathbf{X} = \begin{bmatrix} X_1 \\ X_2 \\ \vdots \\ X_N \end{bmatrix} \quad \mathbf{u} = \begin{bmatrix} u_1 \\ u_2 \\ \vdots \\ u_M \end{bmatrix} \quad \mathbf{A} = \begin{bmatrix} a_{11} & \cdots & a_{1N} \\ \cdot & \cdots & \cdot \\ \cdot & \cdots & \cdot \\ \cdot & \cdots & \cdot \\ a_{N1} & \cdots & a_{NN} \end{bmatrix} \quad \mathbf{B} = \begin{bmatrix} b_{11} & \cdots & b_{1M} \\ \cdot & \cdots & \cdot \\ \cdot & \cdots & \cdot \\ \cdot & \cdots & \cdot \\ b_{N1} & \cdots & b_{NM} \end{bmatrix}$$

The solution to equation (1) is:

$$\mathbf{X}(t) = \exp[\mathbf{A}(t - t_0)] \mathbf{X}(t_0) + \int_{t_0}^t \exp[\mathbf{A}(t - \tau)] \mathbf{B}\mathbf{u}(\tau) d\tau \quad (2)$$

$$\mathbf{X}[(k+1)T] = \alpha \mathbf{X}(kT) + \beta \mathbf{M}(kT) \quad (3)$$

Where $\alpha = \exp(\mathbf{A}T)$, and $N \times M$ is a matrix with constant elements

$\beta = [\alpha - \mathbf{I}] \mathbf{A}^{-1} \mathbf{B}$, and $N \times M$ is a matrix with constant elements

\mathbf{I} is the identity matrix

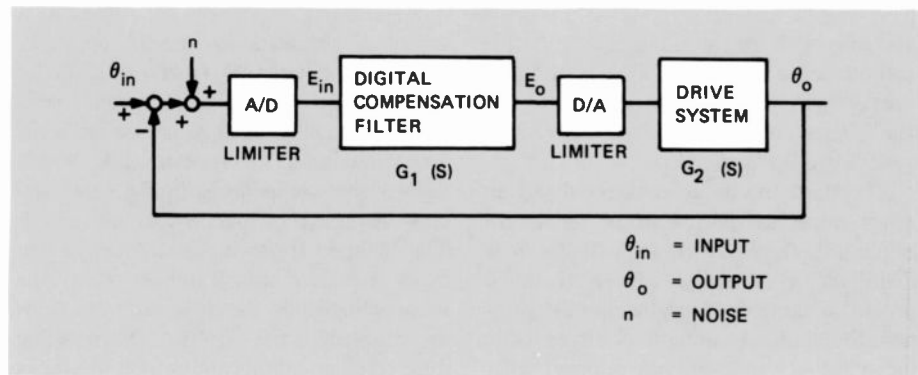


Fig. 2. Block diagram of a digital servo-drive system.

tions and summation, are solved efficiently in a digital computer.

In solving matrix α , the first step involves determining the eigenvalues $\lambda_1, \lambda_2, \dots, \lambda_N$ of the matrix A . Then the N -element eigenvector Z , needs to be determined for each eigenvalue λ_i . The diagonal matrix Λ can then be formed:

$$\Lambda = \begin{bmatrix} e^{\lambda_1 T} & & & 0 \\ & \cdot & & \\ & & \cdot & \\ & & & \cdot \\ 0 & & & & e^{\lambda_N T} \end{bmatrix} \quad (4)$$

The $N \times N$ matrix, F , whose columns are the eigenvectors of A , is formed as:

$$F = [Z_1, Z_2, \dots, Z_N] \quad (5)$$

Finally, $\exp(AT)$ is calculated, using a similarity transformation that involves inverting the F matrix. With successive multiplications,

$$\alpha = \exp(AT) = F \Lambda F^{-1}$$

with α calculated, the matrix β can be determined, as indicated in equation (3). This step requires inverting the A matrix, which must be non-singular.*

These two matrices provide the basis for solving the set of given differential equations for a sequence of time-varying inputs. Once the equations are solved, the system outputs are determined by simple

multiplications from a set of stored coefficients.

Digital implementation of servo compensation filters

A typical digital servo-drive system is represented by the block diagram in Fig. 2. Nonlinear effects occurring in the servo system include signal, rate, and acceleration limiting. Signal limiting occurs in the A/D and D/A converters; rate and acceleration limiting occur in the drive system. Computer simulation is used to determine the effects of such limiting as well as the effects of noise on system performance.

For a second-order (Type II) servo, a compensation filter is required to provide the specified performance and ensure stable operation. The transfer function of this filter is

$$G_1(S) = E_o(S)/E_{in}(S) = K(ST_1 + 1)/S(ST_2 + 1) \quad (7)$$

To implement $G_1(S)$ in a digital computer it is necessary to use a state-variable representation. There is no unique set of state-variable equations for a given transfer function. Discussions of some forms of particular interest are found in references 1, 2, and 3. This paper is concerned with two methods,³ one known as Guillemin's form and another known as Bush's form.† These are shown in Fig. 3 and are, henceforth, referred to as Method 1 and Method 2, respectively.

The integrators in either of the two methods can be digitally implemented by various approaches, the bilinear transformation being a frequently used method.⁴ Each of these two methods were used for two system designs, the HR-76 radar servo and the NIDIR servo; these designs required different state variable representations because of their different requirements and conditions. Specifically, the HR-76 radar was required to provide a means of selecting different servo bandwidths in order to optimize performance in the presence of noise and varying target dynamics. In the case of the NIDIR radar, a single servo bandwidth was specified; however, unlike the HR-76, there was the requirement to accommodate severe antenna-scan-rate and acceleration conditions. Simulation was useful in selecting the best filter design for each system.

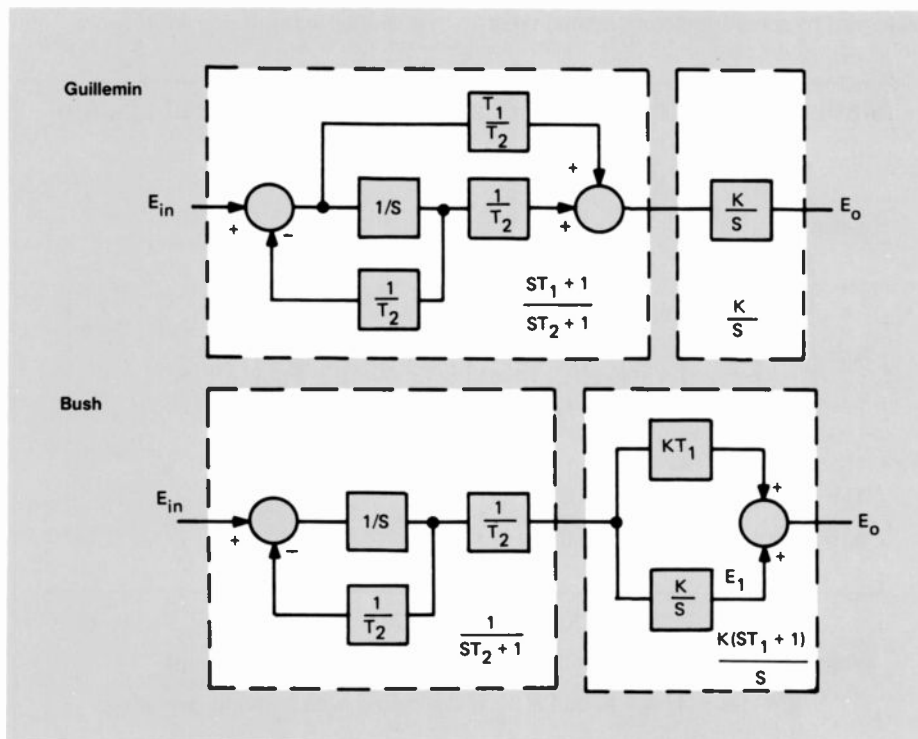


Fig. 3. Alternative methods of implementing digital filters.

* Special techniques exist that can be applied when the A matrix is singular.

† Also referred to as the Standard Controllable form in reference 1.

**HR-76 radar
servo-noise transients**

Method 1 was initially used to implement the compensation filters for the HR-76 radar, which is a system designed and developed at RCA Missile and Surface Radar, Moorestown, New Jersey. During the system tests, a transient error that occurred when switching from a wide to a narrow servo bandwidth was noticed. To determine the cause of this problem, the servo closed-loop system was simulated on the digital computer. The simulated drive-system transfer function was:

$$G_2(S) = 1/S [(S/\omega_o) + 1] \quad (8)$$

The parameters for the compensation filter and the drive system transfer functions, $G_1(S)$ and $G_2(S)$ respectively, are given in Table I.

Table I. Filter and drive-system parameters.

Parameter	BW = 4 Hz	BW = 1 Hz
K	28.8	2.56
T ₁	0.374	1.25
T ₂	0.0064	0.08
ω _o	30	30

With $E_{in} = 0$ (noise input only), the transient effect was reproduced when switching from a 4-Hz to a 1-Hz servo bandwidth. The result is shown in Fig. 4.

The filter implementation in the simulation was changed to Method 2. Using the same input-noise sequence and same system parameters, the bandwidth was again switched from 4 Hz to 1 Hz. This transient error, also shown in Fig. 4, is much smaller than that obtained using Method 1, leading to a design change in the HR-76 system.

Even though these two approaches have identical transfer functions, they do not have identical state equations. At the time the bandwidth is reduced, a non-zero value of E_2 exists. For Method 1, this value immediately after switching is the same as that immediately prior to switching because it is maintained as the initial condition on the integrator. For Method 2, however, the value of E_2 decreases at the switching time because of the reduction of the KT_1 product.

NIDIR designation servo-limiting effects

Another system design that was aided by simulation was the NIDIR-designation ser-

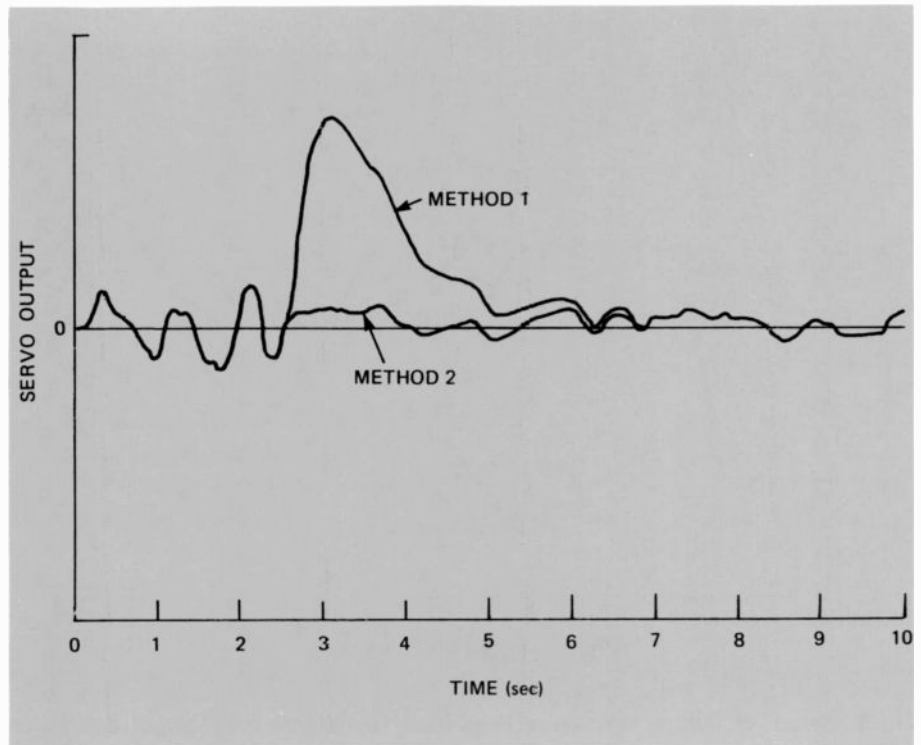


Fig. 4. Servo output with noise only as the input.

vo. This servo did not have a bandwidth-switching requirement but needed to acquire targets under conditions that would reach both system-rate and acceleration limits during the transitional slew to the moving target. In order that the value of E_0 and E_1 in Fig. 3 not reach extremely large values during saturation times, it was necessary to limit the output of the integrator described by K/S to a value equal to the rate limit. Otherwise, the integrator output during saturation periods could reach values, that could cause loss of track. The system of interest had rate, acceleration, and error limits of respectively 0.5 rad/sec, 0.5 rad/sec,² and 0.4 rad. The problem was to acquire a constant velocity crossing target with the conditions given in the inset of Fig. 5.

Systems using both Methods 1 and 2 were simulated and tested, the trajectory being defined as in the inset of Fig. 5. The values of K , T_1 , and T_2 , are, respectively, 4, 1, and 0.0625. Plots of the servo error, as a function of time for each system, are shown in Fig. 5. Note that Method 1 in this case is far superior to Method 2.

For both methods, the output of the integrator, K/S , is limited. In Method 1, the input to the integrator senses the rate of change of the error, E_{in} , and causes the integrator to come out of saturation as soon as the error starts to decrease. In Method 2, however, the integrator input

does not change polarity until the error, E_{in} , changes polarity. The integrator does not come out of saturation until the error changes polarity. This results in a large overshoot.

As discussed, simulation is a valuable analytic tool for selecting design approaches, not only from the two examples presented but for the design requirements that may arise in the future.

Target detection simulation

The process of detecting a radar return as an antenna beam scans past a target can be modeled as illustrated in Fig. 6. In this figure, the radar returns are represented as a time sequence of signal-amplitude samples whose statistics reflect a specific rms signal-to-noise ratio $(S/N)_0$, assuming that the target is located on the peak of the antenna pattern mainlobe. The amplitude of the signal samples vary from pulse to pulse or from scan to scan depending upon the type of target that is modeled. Figure 7 shows a variety of radar-fluctuating target models that are commonly used as a basis for specifying radar detection performance.

Simple algorithms can be used in conjunction with random-number generators to simulate the desired target signal-return fluctuations. Of the models shown in Fig. 7, the amplitude fluctuations from those models that have a suffix I or III are com-

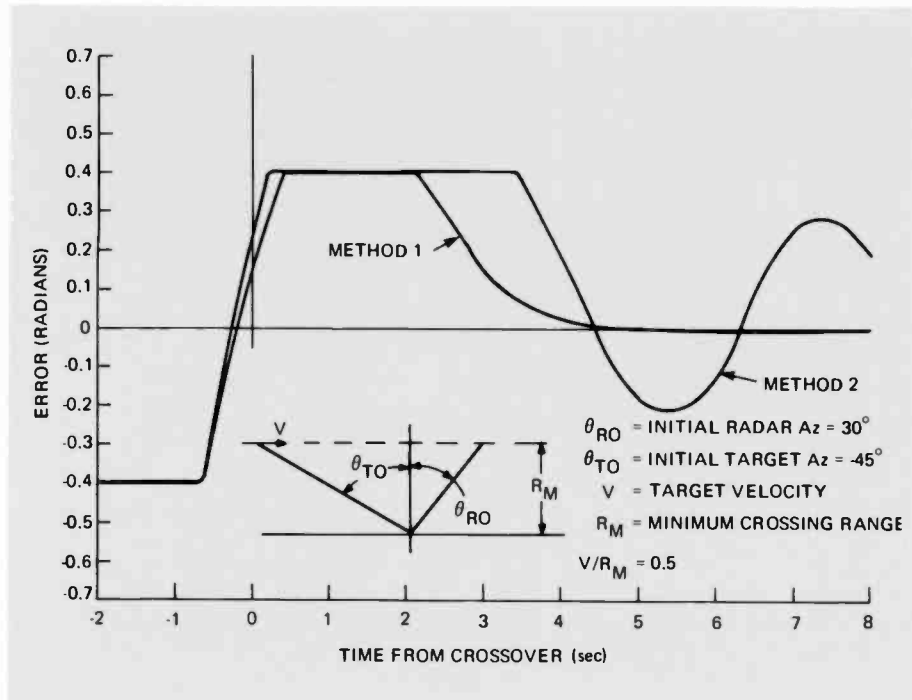


Fig. 5. Servo error as a function of time. Inset represents initial target and radar geometry.

pletely correlated within any given scan and are independent from scan to scan. Those models that have a suffix II or IV result in amplitude fluctuations that are independent from pulse to pulse as well as from scan to scan.

The detection performance, which is achieved with a sequence of N constant rms-amplitude target returns processed with a square-law detector and post-detection integrator (as shown in the shaded blocks of Fig. 6), can be analyzed directly with-

out resorting to Monte-Carlo simulation. In the event a mechanism is present that modulates the level of the target returns, such as the gain pattern of a scanning antenna beam, a rigorous theoretical analysis becomes very cumbersome and Monte-Carlo methods can be presented as a viable alternative.

Figure 8 illustrates the degree to which a simple 2000-trial Monte-Carlo simulation of a detection process, involving the post-detection integration of 4 pulses (exclusive of beam shape modulation effects), approaches the theoretical⁵ detection performance of a 4-pulse integrator. For these cases, the threshold level is analytically calculated using the method of Pachares,⁶ which assumes a square-law detector model of the form:

$$y = (\frac{1}{2})x^2 \quad (9)$$

where x = the input voltage level

y = the output voltage level.

The threshold curves of Fig. 9 show the threshold voltage variation with the number of pulses integrated for different values of false alarm probability. These values are normalized with respect to rms noise and are directly applied to the threshold decision block of Fig. 6.

Detection performance achieved by the entire process outlined in Fig. 6 has been analyzed by means of a 5000-trial Monte-

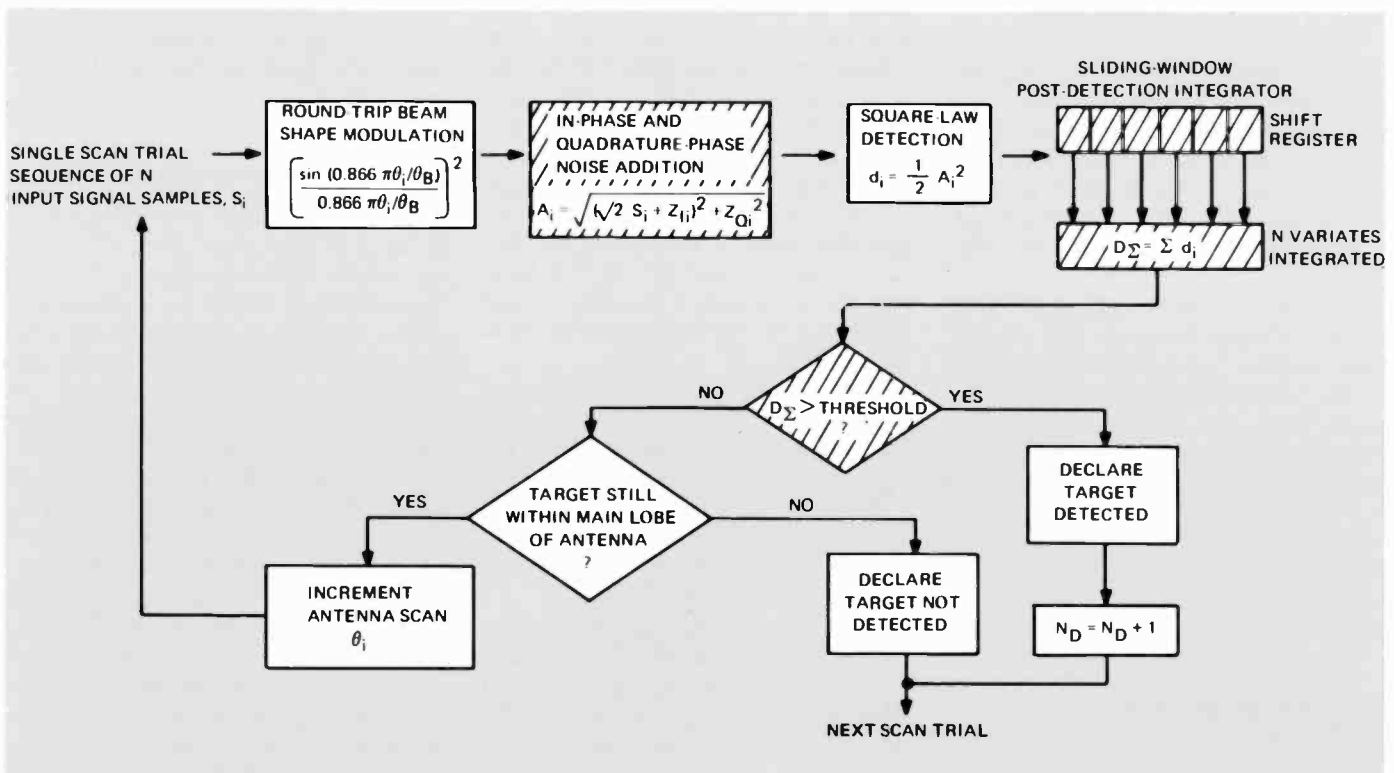


Fig. 6. Radar receiver/signal processor simulation.

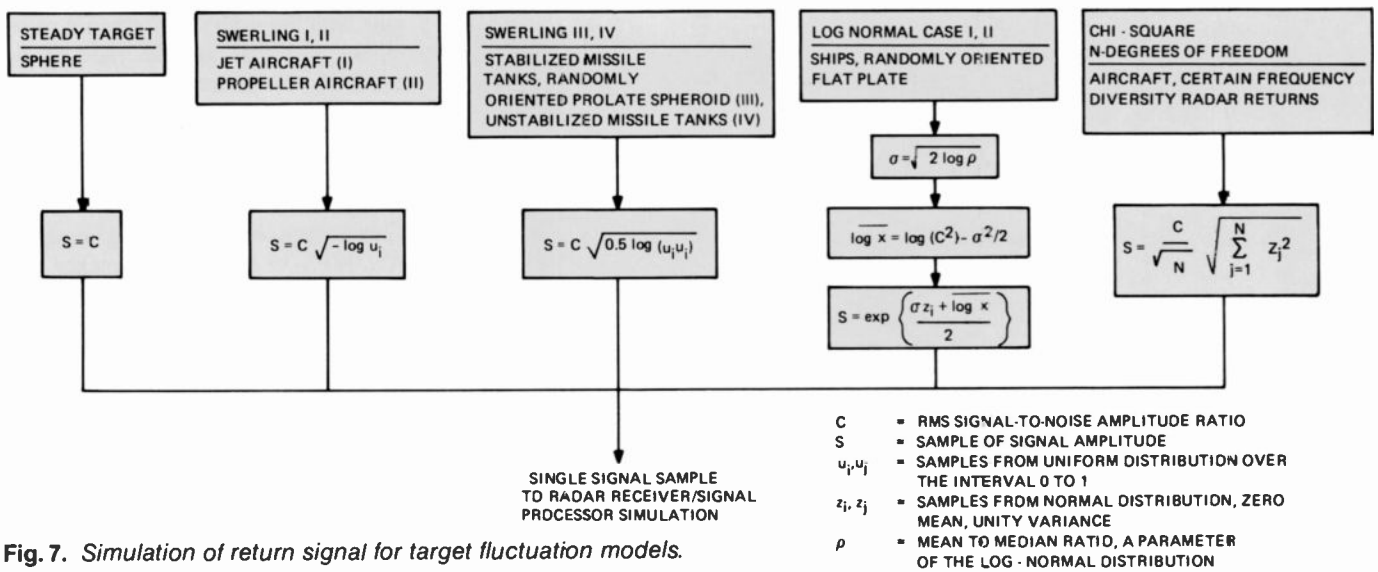


Fig. 7. Simulation of return signal for target fluctuation models.

Carlo simulation, and the results are plotted in Fig. 10. For each trial, the beam (modeled as a $\sin x/x$ one-way amplitude pattern) scans past the target, and eight target returns are integrated in a sliding window integrator. This is a process in which the eight most recent target returns, modulated by the round-trip antenna pattern are: (1) contaminated by in-phase and quadrature-phase components of white Gaussian noise; (2) square-law detected; and (3) accumulated as a summation.

During this process, the beam position and subsequent pattern loss are varied from pulse to pulse to reflect the antenna scan rate. After each target return is received, the summation of the last eight processed returns are tested to see if the detection threshold is exceeded, in which case the Monte-Carlo trial is said to have resulted in a detection and the trial is completed. Otherwise, the beam advances to the next angular position in the sequence, a new return is accepted, and the process is repeated.

In the event no threshold crossing occurs by the time the main lobe of the antenna scans past the target, a missed target declaration is made and the Monte-Carlo trial is completed. For the cases shown in Fig. 10, 5000 trials were carried out for each data point on the curves, with the detection probability calculated as the ratio of detections to Monte-Carlo trials.

Figure 10 also shows the results for an ideal rectangular beam-shape pattern, in which eight pulses are integrated without the influence of an antenna pattern loss. The difference between the curves is the beam-shape loss for a scanning radar, which is seen to be in the neighborhood of 0.7 to 0.9 dB, depending on the SNR and target-

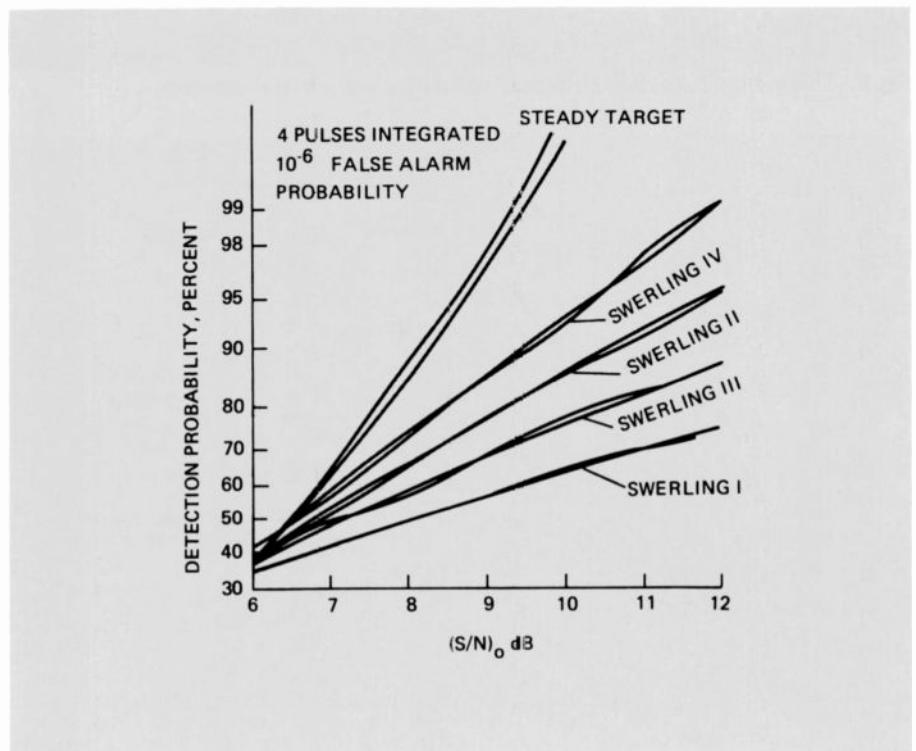


Fig. 8. Comparison of theoretical detection probability values with that obtained from a Monte-Carlo simulation.

fluctuation model. The results presented are based on an antenna-scanning rate such that the sliding-window integrator receives eight pulses as the antenna scans through a sector corresponding to 85 percent of the 3-dB one-way beamwidth.

Blake⁷ and Trunk⁸ show this to be an optimum integration window length in the sense of minimizing the SNR required for a specified detection probability. The results compare with a pattern loss of 1.6 dB, which is frequently cited as a typical beam-shape loss in a scanning radar. The 1.6-dB

value applies strictly to a gate positioned so that the pulses modulated by the antenna pattern are accepted by the gate only within the gated angle centered on the beam maximum 7.

For the cases simulated in this paper, the sliding window (or gate) effectively scans completely through the region of maximum antenna-gain-modulated target returns, thereby affording additional detection opportunities. While the noise component of the post-detection integrated signal-plus-noise variates is highly correlated

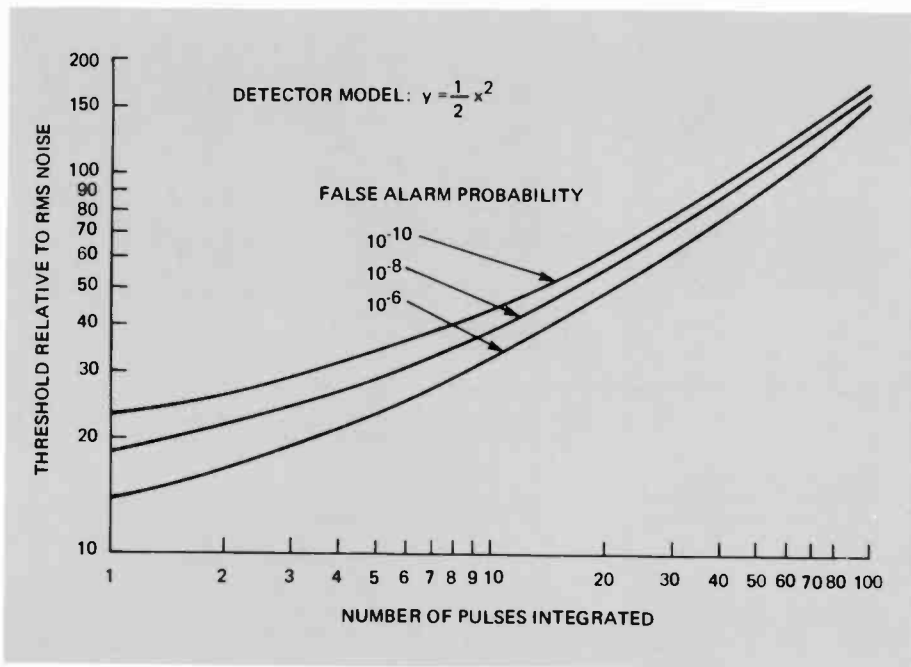


Fig. 9. Theoretical detection threshold values for square-law detector.

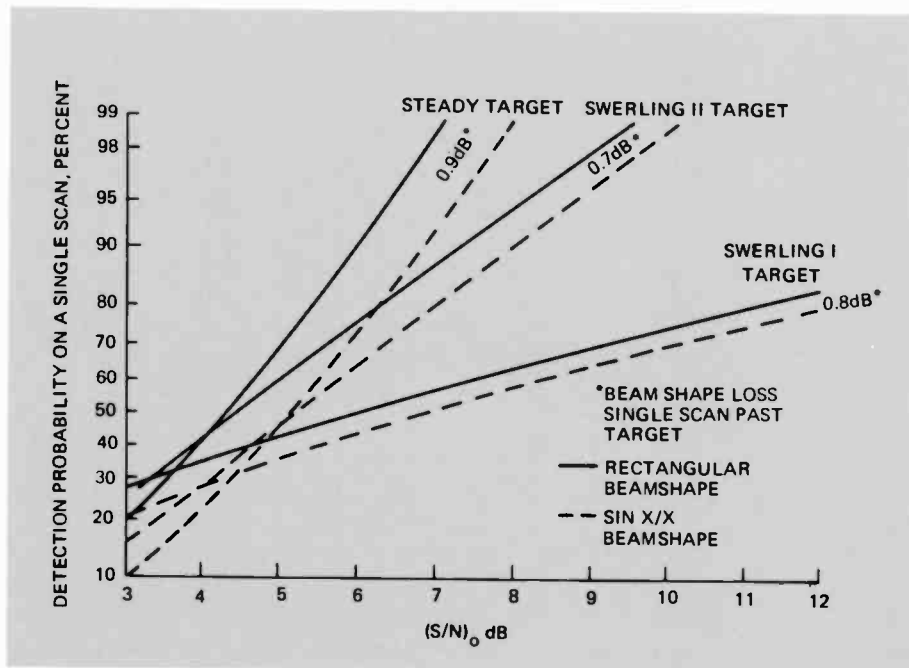


Fig. 10. Monte-Carlo detection analysis of scanning-radar results averaged over 5000 trials. Eight pulses are integrated with a false alarm probability of 10^{-6} . For $\sin x/x$ beam shape, the 8 pulses are integrated within a sliding window that spans 85% of the one-way, 3-dB beamwidth. Uniform weighting is applied within the window.

within the scan, there is still a modest improvement in detectability to account for the reduction in beamshape loss.

Conclusion

In addition to solving these specific problems, computer simulation was used in 1970 to simulate the entire AN/MPS-36

instrumentation radar.^{9, 10} The realism and the modular nature of the simulation enabled a wide variety of experiments and studies as follows:

1. Investigation of the capabilities of the existing radar system to support planned future missions.
2. Isolation of those radar parameters that

may limit the radar's performance capabilities and that are the most likely candidates for future modification.

3. Assessment of the improvements in radar performance that might be achieved from various proposed radar modifications.
4. Comparison of the existing/modified AN/MPS-36 radar's performance and capabilities with the performance that can be achieved with other existing/new tracking systems.
5. Study of the effects of radar location upon the mission-supporting capabilities of the radars.
6. Post-mission data analysis whereby apparent radar breakdowns/problems can be simulated to check on the validity of the analysis results.
7. Integration of the present simulation program as a building block in a larger multi-station, multi-instrument, tracking network. A larger system such as this could be used to determine an optimum tracking configuration for a specific mission.

The simulation of the AN/MPS-36 radar was successful and has been used extensively by the government. These uses have included general studies and investigations of the radar's operation so as to improve understanding of the complex interactions that occur within the complete tracking system (the radar, the target, the environment, and so on).

To summarize, we have presented the solutions to three important problems related to mechanically scanned radar systems. Specific examples have been presented that demonstrate how to use these techniques to solve radar design problems. The approaches to these problems, however, are general and not restricted to radar-related problems.

References

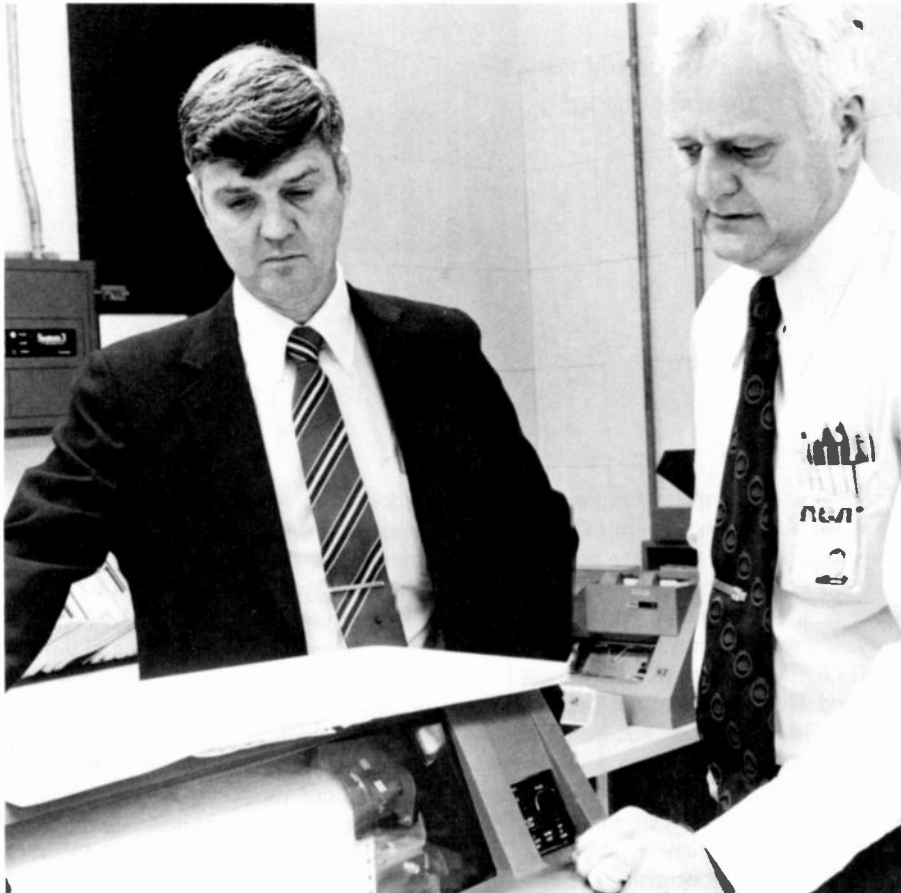
1. M. Athans and D.L. Falb, *Optimal Control*, pp. 173-190, McGraw-Hill Book Co. (1936).
2. C. Chen and J.J. Hass, *Elements of Control System Analysis*, pp. 298-307, Prentice-Hall, Inc. (1968).
3. J.W. Brewer, *Control Systems Analysis Design and Simulation*, Chapter 8, Prentice-Hall, Inc. (1974).
4. W.D. Fryer and W.C. Schultz, "A Survey of Methods of Digital Simulation of Control System," Cornell Aeronautical Laboratory, Inc., Report XA-1681-E-1 (July 1964).
5. R.L. Mitchell and J.F. Walker, "Recursive Methods for Computing Detection Probabilities," *IEEE Transactions on Aerospace and Electronic Systems*, Vol. 7, No. 4 (July 1971).
6. J. Pachares, "A Table of Bias Levels Useful in

Radar Detection Problems," *IRE Transactions on Information Theory*, Vol. 4 (March 1958).

7. L.V. Blake, "The Effective Number of Pulses per Beamwidth for a Scanning Radar," *IRE Proceedings*, Vol. 41 (June 1953) and "Addendum," *IRE Proceedings*, Vol. 41 (December 1953).
8. G.V. Trunk, "Comparison of Two Scanning Radar Detectors: The Moving Window and The Feedback

Integrator," *IEEE Transactions on Aerospace and Electronic Systems* (March 1971).

9. AN/MPS-36 Radar Modeling and Computer Simulation Final Report Contract FO4701-69-C-0131 Subtask 7.3.3 (September 1971).
10. Refinement and Modification of the AN/MPS-36 Radar Computer Simulation Program Contract FO8606-72-C-0031 (June 1974).



Glenn Sparks has been associated with MSR since 1954. During this period he has been engaged in key radar system engineering assignments emphasizing control-system analysis, computer simulation, command and control, and estimation theory.

Contact him at:
RCA Missile and Surface Radar
Moorestown, N.J.
TACNET: 224-3037

Jack Liston has held major systems responsibility for concept design, performance analysis, and design optimization on advanced phased-array radar system developments. Some of the areas of his principal contributions include system computer modeling for cost optimization and performance trade-offs, advanced self-duplexing receiver concepts, and system performance verification through simulation.

Contact him at:
RCA Missile and Surface Radar
Moorestown, N.J.
TACNET: 224-3037

Discrete-event simulations of complex weapon systems

Using proven simulation principles, engineers can easily vary a plethora of parameters and quickly gain information about weapon-system behavior.

Abstract: *Discrete-event simulations model system functions as event subprograms occurring at discrete times. This modeling process yields a structure suited to the representation of complex weapon systems. An elementary example demonstrates the principles. The author describes the initial program developed by the Simulation Group at Missile and Surface Radar, called MEDUSA, and an advanced program derivative. He continues with descriptions of techniques being used to develop a new simulation, and concludes with a note on potential uses in modeling other complex systems such as air-traffic control or transportation planning.*

Modern weapon systems contain many complex components, not the least of which are digital computers that control operations via real-time software. The variables and options available in designing and deploying these systems present a bewildering array of possibilities to systems analysts. Classical analyses cannot provide all the necessary answers in the required time. However, with a well-designed, large-scale digital computer simulation of the weapon system, engineers can readily explore different system designs and deployments.

For the last eight years, the System Simulation group in the Naval Systems Department of Missile and Surface Radar has been designing and developing discrete-event

simulations of complex weapon systems. These simulations, written in FORTRAN, have been applied to many problems in areas such as system performance, algorithm design, evaluation, testing, survivability, and requirements specifications.

MEDUSA (Multi-target Effectiveness Determined Under Simulation for AEGIS), the AEGIS Operations Analysis Simulation, was the initial program developed by the Simulation Group. MEDUSA has been in use for over seven years to aid AEGIS tactical algorithm designers, predict AEGIS Weapon System performance against complex raids, and support tests at the CSED (Combat System Engineering Development) site. MEDUSA is a discrete-event simulation that models significant AEGIS functions—from search, detection, and track through threat evaluation, weapon scheduling, and intercept in defending surface fleets against air attacks. The success of MEDUSA led to the development of discrete-event simulations of other weapon systems. To obtain useful results quickly from these new simulations, their original versions were developed by adding new models to MEDUSA and removing models unnecessary for the new simulations.

SIMATR (Simulation of Integrated Multiple Advanced Tactical Radars), the most successful MEDUSA derivative, models the aspects of Tactical Air Control Systems (TACS) that detect and track hostile aircraft and missiles and that control fighters to intercept these targets. With emphasis on a network of ground radars assisting

airborne interceptors defending Western Europe, SIMATR contributes to the determination of the relative military worth of phased-array and rotator radars.

A current Independent Research and Development (IR&D) program to develop a discrete-event simulation of a naval battle group provides an excellent opportunity to implement the techniques learned and developed from several years experience. Since the scope of this simulation makes it impractical to generate the initial version by modifying MEDUSA, a PROTOTYPE of a Naval Simulation (PROTONS) has been selected as the vehicle to determine development methods, user interfaces, and level of detail for the battle-group simulation.

Elements of discrete-event simulations

A discrete-event digital computer simulation represents a system by event subprograms that model system functions, interactions between the system and its environment, and actions in the environment. The events that model the system are chosen and designed to achieve a sufficient degree of realism without using excessive computer time. Since these events occur at discrete times, the state variables that describe the components and interactions of the system change only at these times and not continuously as they would in the real system.

Computations are performed and logi-

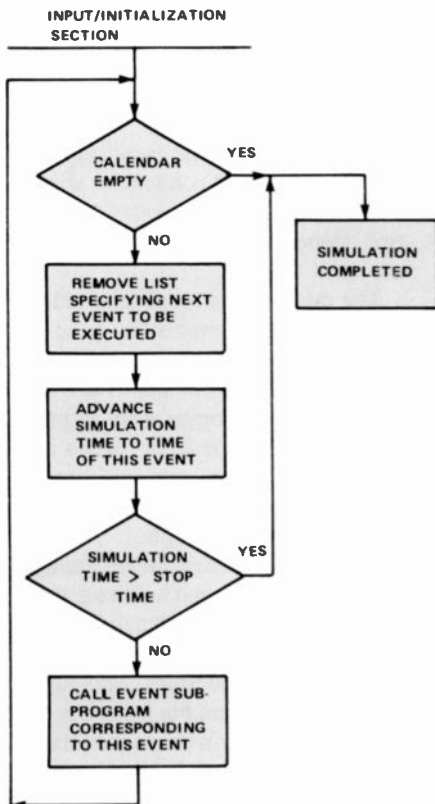


Fig. 1. Operation of the event sequencer, the executive subprogram that controls simulation cycling after initialization.

cal decisions are made when significant events are expected to occur rather than at evenly spaced time intervals. This yields efficient use of computer time as events are executed only when their results are needed. The operation of these event subprograms is controlled by an executive subprogram called the event sequencer that interacts with the event calendar, a time-ordered list of scheduled events.

After the input is read and the initial events are placed on the calendar, control is transferred to the event sequencer, which drives the simulation by the following steps (Fig. 1):

1. Remove the top event from the event calendar.
2. Advance the simulation time to the time of this event.
3. Call the event subprogram corresponding to the removed event.
4. Repeat the above steps until the event calendar is empty or simulation time is greater than a specified simulation stop time.

A hypothetical shipboard antiair missile system (sidebar, pages 34-35) illustrates the above concepts (refer to Fig. 2 for a graphic description of the example).

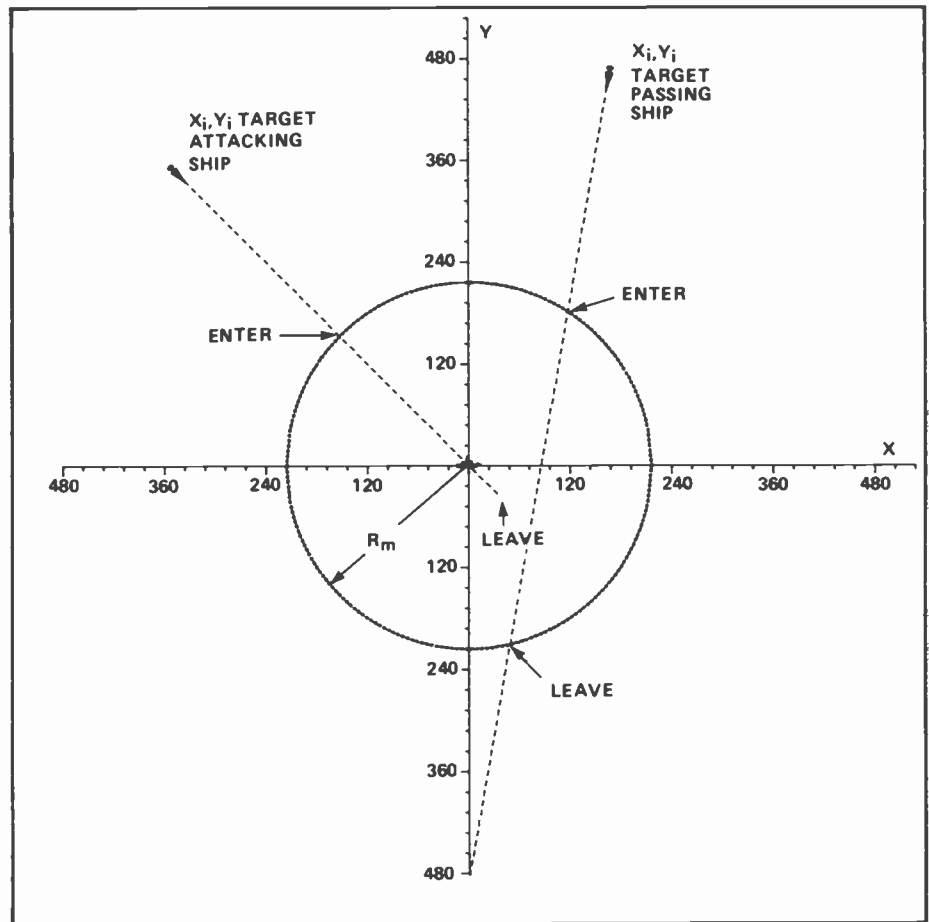


Fig. 2. An aerial view of a surface-to-air missile ship defending an area against two aircraft, one that is attacking the ship and another that is passing through the defended area. The missile coverage zone is represented by the circle, and the points indicate where the two targets enter and leave this coverage. This example was chosen to illustrate discrete-event simulation principles.

MEDUSA, the AEGIS Operations Analysis Simulation

MEDUSA (Multi-target Effectiveness Determined Under Simulation for AEGIS), a discrete-event simulation, was designed and implemented by RCA's AEGIS System Simulation Group to support the development of the AEGIS Weapon System Mark 7, which performs the antiair-warfare functions of the AEGIS Combat System.

The AEGIS Weapon System is composed of nine computer-directed elements that can stand as a fully automatic antiair and antisurface missile system. As part of the Combat System, the AEGIS Weapon System performs the principal air and surface defense functions. The control elements of this group provide track maintenance and threat evaluation, as well as weapon assignment and control for all warfare operations. It is the AEGIS Weapon System that furnishes direction, commands, and automation to the AEGIS Ship Combat System.

Work began on MEDUSA in early 1975 when a simulation was needed to predict the performance of the AEGIS Weapon System against complex multi-target threats. A discrete-event architecture in FORTRAN was chosen because: (1) AEGIS and its interaction with the environment can easily be represented by discrete events; (2) the subroutines described above were available; and (3) discrete-event simulations had been successfully used to model other weapon systems.

The example in the sidebar may be viewed as an extreme simplification of the AEGIS Weapon System and analogously, the sample simulation described is an extremely simplified version of MEDUSA. Some of the important differences between the two simulations indicate the vast disparity in complexity. In MEDUSA, for example, a three-dimensional curved-earth geometry is used; targets are modeled by multi-leg trajectories; radar detection is modeled; the availability of shipboard resources

(Continued on page 36)

Hypothetical antiair missile system example

A ship with a surface-to-air missile system attempts to intercept enemy air targets entering its missile coverage zone but can engage only a single target at a time. The targets fly straight trajectory legs at constant speeds and the ship's missiles fly at an average speed, V_m , over their effective range, R_m . It is assumed that the ship is aware of all targets in its coverage zone. The missile system is controlled by the ship's Combat Direction System (CDS) computer to fire at the closest target. The CDS computer executes a program every 10 seconds to determine the closest target. A missile is launched only if an engagement is not in progress. An engagement lasts from missile firing time to intercept. Missiles are given a 65-percent chance of successful intercept, and a target hitting the ship is given an 80-percent chance of destroying it.

To simplify this example, two-dimensional (x, y) planar geometry will be used. The ship will be stationary and positioned at (0,0). A target trajectory can be specified by:

initial position x_i, y_i
 final position x_f, y_f
 initial time t_i
 speed S

Therefore, its position at any time (t), is computed as:

$$\begin{aligned} x(t) &= x_i + \dot{x}[t - t_i] \\ y(t) &= y_i + \dot{y}[t - t_i] \end{aligned} \quad (1)$$

where \dot{x} is the target velocity in the x direction and \dot{y} is the target velocity in the y direction and S is $(\dot{x}^2 + \dot{y}^2)^{1/2}$.

The position of the target is a continuous function of time, but the simulation will compute the position only at the discrete times when requested by an event subprogram.

The times, $t_{in/out}$, a target enters and leaves the missile coverage zone (a circle of radius R_m) is computed by solving the quadratic equation for the intersection of the straight-line trajectory and the coverage circle (see eqn. 2). The time, t , a missile intercepts a target is computed from the intersection of the missile and target trajectories (see eqn. 3).

Although this system is a simple one, it is a good example to demonstrate the principles of discrete-event simulation, and the seven events described in Table I could be used to model it.

The preceding principles of simulation operation can easily be put into practice if subroutines and techniques exist to:

1. Represent events.
2. Represent a calendar of events.
3. Schedule events on the calendar.
4. Cancel events from the calendar.
5. Access events on the calendar.

Events are represented by five-word blocks of memory called events lists, with words numbered -1, 0, 1, 2, and 3, as shown in Fig. 3.

Word #	
-1	# Words in block (5)
0	Index of next event list
1	Event #
2	Event time
3	Data for event subroutine

Fig. 3. A list representing a simulation event. These lists are linked to the event calendar when the corresponding events are scheduled. They are removed when the event is executed or cancelled.

Words -1, and 0 are for bookkeeping and calendar linkage. Word 1 contains the event number, word 2 contains the event time, and word 3 is available to

pass information to the event subroutine. Word 3 could contain the target number for the *target*, *enter*, *leave*, *at-tack*, *launch* and *intercept* events in the example.

The calendar is a set of time-ordered lists that represent events that have been scheduled but not executed. A package of subroutines that create lists from a dynamic storage array and that schedule, cancel and access events is used to handle simulation bookkeeping functions. Table II shows the event sequencer for the example.

Other available subroutines are useful for maintaining and accessing the internal database that dynamically describes the status of the simulated entities and their relationships. Although these subroutines are not necessary for simulation, they provide an extremely flexible method of maintaining an internal database and they allow the representation of virtually unlimited numbers of entities of different types.

This package of subroutines is written in FORTRAN and is used daily on the MSR DEC 2060 computer.¹ Versions are also available for the IBM 370/168, CDC 6700, Honeywell, and UNIVAC computers. These simulation-management and list-handling subroutines and the techniques for using them are similar to GASP IV,² a simulation language that consists of FORTRAN-callable subroutines. These subroutines were selected at MSR over GASP because of their immediate availability in 1975 and the subsequent success with them.

$$t_{in/out} = t_i - \left[\frac{-(x_i\dot{x} + y_i\dot{y}) \pm \sqrt{(x_i\dot{x} + y_i\dot{y})^2 - S^2(R_i^2 - R_m^2)}}{S^2} \right] \quad (2)$$

where, $R_i = (x_i^2 + y_i^2)^{1/2}$

$$\begin{aligned} t &= \frac{-(x_i\dot{x} + y_i\dot{y}) - \sqrt{(x_i\dot{x} + y_i\dot{y})^2 - (S^2 - V_m^2) R_i^2}}{(S^2 - V_m^2)} \quad | S^2 \neq V_m^2 \\ &= R_i / 2(x_i\dot{x} + y_i\dot{y}) \quad | S^2 = V_m^2 \end{aligned} \quad (3)$$

where x_i, y_i is the target position at launch time, $R_i^2 = x_i^2 + y_i^2$, and V_m is missile average speed.

Table I. Events for hypothetical anti-air missile system example.

Events Name/#	Scheduling conditions	Function
TARGET/1	For each target at the time the target trajectory begins	Computes the time the target enters and leaves missile coverage (eqn. 2) and schedules ENTER and LEAVE events at these times. If a target is within missile coverage at the beginning of its trajectory, ENTER is scheduled at this time. If a target trajectory ends within the missile coverage, a LEAVE event is scheduled at the end of trajectory time. For a target attacking the ship, an ATTACK event is scheduled at the time the target arrives at the ship.
ENTER/2	By TARGET for each target entering missile coverage	Makes the target eligible for engagement by the missile system. The first ENTER event executed schedules CDS, the command and decision event.
LEAVE/3	By TARGET for each target leaving missile coverage	Cancels all events for this target. No further computations will be made for this target.
ATTACK/4	By TARGET when the target arrives at the ship	Assesses the attack by comparing random number (r_A) with 0.80. If $r_A \leq 0.8$, the ship is destroyed and the simulation ends. If $r_A > 0.8$, the attack failed.
CDS/5	The first CDS is scheduled by the first ENTER. Thereafter, CDS schedules itself on a 10-second cycle.	Prioritizes the targets in missile coverage in order of distance from the ship and schedules LAUNCH for the closest target if an engagement is not in progress.
LAUNCH/6	By CDS for each target to be engaged at launch time	Computes intercept time (eqn. 3) and schedules INTERCEPT at this time.
INTERCEPT/7	By LAUNCH at intercept time	Assesses the intercept by comparing a random number (r_i) with 0.65. If $r_i \leq 0.65$, the target is killed and all events for the target are cancelled. If $r_i > 0.65$, the missile missed the target and the target is eligible for re-engagement by CDS.

Table II. Event sequencer to control cycling of simulation of hypothetical anti-air missile system.

FORTTRAN statement	Comment
5 ICAL = 0 CALL GETCAL (ICAL, \$100) CALL CANCEL (ICAL) TIME = Q (ICAL,2)* IF (TIME .GT. TSTOP) GO TO 100 J = Q (ICAL,1)* GO TO (10,20,30,40,50,60,70),J	INITIALIZE GET ICAL, INDEX OF FIRST EVENT, ON CALENDAR REMOVE EVENT LIST FROM CALENDAR UPDATE SIMULATION TIME IS SIMULATION TIME GREATER THAN SPECIFIED STOP TIME? GET EVENT NUMBER GO TO CALL STATEMENT FOR EVENT J
10 CALL TARGET (ICAL) GO TO 5	CALL THE SPECIFIED EVENT AND GET THE NEXT EVENT LIST ON THE CALENDAR.
20 CALL ENTER (ICAL) GO TO 5	
30 CALL LEAVE (ICAL) GO TO 5	
40 CALL ATTACK (ICAL) GO TO 5	
50 CALL CDS (ICAL) GO TO 5	
60 CALL LAUNCH (ICAL) GO TO 5	
70 CALL INTCP (ICAL) GO TO 5	
100 RETURN END	ALL EVENTS HAVE BEEN EXECUTED OR TIME GREATER THAN TSTOP

*Q is the dynamic storage array used to store event lists and other lists that describe system entities.

(Cont. from page 33)

is considered when scheduling targets for intercept; and realistic engageability and missile time-of-flight data are used. Although the two simulations differ in complexity, the discrete-event architecture is suitable for both. The selection from the many AEGIS functions to be used as MEDUSA events was dependent on the intended MEDUSA uses. Some of the events used to model AEGIS Weapon System functions and interactions with the environment are briefly described in Table III. Other MEDUSA events model SPY-1A radar tracking; the Standard Missile launch, mid-course guidance, illumination, and intercept; the Combat Air Patrol target intercept; and the PHALANX close-in weapon system.

Although MEDUSA was developed primarily to demonstrate AEGIS performance against complex raids, the discrete-event architecture permitted a wider range of applications. Some of these are listed below:

1. Evaluation of tactical algorithms for:
 - Standard missile engageability
 - Threat evaluation
 - Missile scheduling
 - Variations in missile salvo doctrine
 - Electronic countermeasures algorithms

2. Evaluation of combat system configurations such as:
 - Casualty modes
 - Alternative illuminator positioning
3. Design of tests at the CSED site and at the production test center
4. Verification of system qualification tests
5. Determination of new missile-system requirements
6. Demonstration of performance of AEGIS derivative systems.

The versatility and portability of these discrete-event simulation techniques is attested to by MEDUSA operation on the UNIVAC SPECTRA 70, IBM 370/168, DEC system 2020, 2040, 2060, and CDC 6700 computers. Naval Surface Weapon Center personnel, who were able to modify and use MEDUSA in less than four months,³ demonstrated that these techniques were easy to learn.

The original version of MEDUSA modeled a limited number of AEGIS functions with nine events. The open-ended nature of the architecture allowed new events to be added easily and quickly as they were required for new analyses and studies. The current version of MEDUSA includes 20 events and the evolutionary nature of the program indicates that more will be added in the near future.

SIMATR (Simulation of Integrated Multiple Advanced Tactical Radars)

In addition to its value to the AEGIS program, MEDUSA has been used as the nucleus for simulations of other weapon systems. These simulations were started by removing events unnecessary to the modeling of the new system and adding events required to model the new system. This technique made it possible to make a working simulation of a subset of the new system operational in a short time.

The most successful MEDUSA derivative is SIMATR,⁴ an air-battle simulation of USAF Tactical Air Control Systems (TACS). SIMATR demonstrates how a network of phased-array ground radars can increase the effectiveness of airborne interceptors in repulsing an enemy air attack. This increased effectiveness is realized in the direct control and designation of each airborne interceptor by extending its effective range to provide the interceptor a standoff shot with an air-to-air missile in the initial engagement phases. RCA needed a TACS air-battle simulation to evaluate the effectiveness of phased-array radars, to assess C³ system loading, and to determine the other resources needed to wage an air battle.

Many of the models required for SIMATR were derived from MEDUSA. Indeed, all of the MEDUSA architectural and simulation management features were

Table III. Selected MEDUSA events that model AEGIS functions and interactions with the environment.

Event	Function modeled	Event operation
DETECT	Response of SPY-1A to the return of a surveillance pulse from a target.	Computes probability of detection (P_D) as a function of radar parameters, target radar cross section, target position, multipath, and the position and power of all simulated jammers. The pseudo-random number r_D is generated from a uniform distribution. If $r_D \leq P_D$, the detection is successful and TRACK is scheduled. If $r_D > P_D$, the target is not detected and DETECT is scheduled to occur one radar scan time in the future.
TEWS	Execution of the threat-evaluation (TV) and weapon-selection algorithms by the AEGIS CDS computer.	Computes TV for all tracks as a function of target identification, position and velocity. The targets are prioritized by TV. Targets beyond a specified range from the AEGIS ship are selected for engagement by Combat Air Patrol and CAPINT events are scheduled at the expected intercept times. An engagement-order transmission is simulated for targets engageable by SM-2 by entering them in the Engagement Order Queue (EOQ). TEWS schedules itself cyclically.
ENGAGE	Execution of the SM-2 scheduling algorithm by the AEGIS WCS computer.	Targets in the EOQ with the highest threat values are placed in the smaller pre-engagement queue (P/Q). A target will be scheduled for SM-2 engagement if a launcher is available within its launch window; an illuminator is available for the homing period; and the maximum allowable missiles in flight will not be exceeded from launch through intercept. To determine the above conditions, there are models to compute earliest and latest launch times (launch window); solve the fire control problem for SM-2; compute the homing interval; maintain periods of launcher and illuminator availability; and determine launcher and illuminator tie-up times. A successful schedule for a target consists of a launcher available for the required tie-up time and an illuminator available for the homing interval. A list of successful scheduled engagements is maintained and ENGAGE schedules LAUNCH, the SM-2 launch event, at the scheduled launch times.

directly applicable to a TACS simulation. In addition, the MEDUSA target-generator, jamming, radar, threat-evaluation, CAP-assignment, and CAP-intercept models fulfilled the corresponding TACS modeling requirements with minor modifications. Thus, after the MEDUSA Standard Missile, PHALANX, and SPY-1 ECM logic models were removed, the MEDUSA architecture and a subset of the MEDUSA models were sufficient for elementary TACS analysis. In order to perform more extensive analyses, models were implemented for surface-to-air missile systems, short-range defense systems, attrition of interceptors, and netted multiple radars.

Although SIMATR models distributed weapon systems and sensors described by analytic algorithms, whereas MEDUSA represents the shipboard AEGIS Weapon System controlled by tactical algorithms, the generality of the discrete-event techniques made it possible to derive the initial version of SIMATR from MEDUSA in less than two months.

Simulation of a naval battle group

In 1982 an IR&D project was undertaken at MSR to develop a digital computer simulation of two opposing naval battle groups. The Operations Analysis and System Simulation groups combined to provide a tool to: determine the effectiveness of new weapon systems in a battle-group environment; perform comparative analyses between existing and new ships; evaluate fleet-level tactics and doctrine; and determine the effects of different types of communications and coordination on battle-group performance. These capabilities will directly support follow-up AEGIS programs.

A survey of existing battle-group simulations developed by government agencies and private industry showed that most of them used a discrete-event architecture. Some used special simulation languages, but most were written in FORTRAN. This confirmed our decision to write the battle-group simulation in FORTRAN using discrete-event architecture.

The battle-group simulation provided an opportunity to apply the techniques developed over the past seven years. The creation of a simulation to accomplish the goals of a complete battle-group simulation is an enormous undertaking, and it is difficult to decide where to begin and how to proceed. A prototype simulation was the vehicle chosen to evaluate development methods, input formats, levels of model

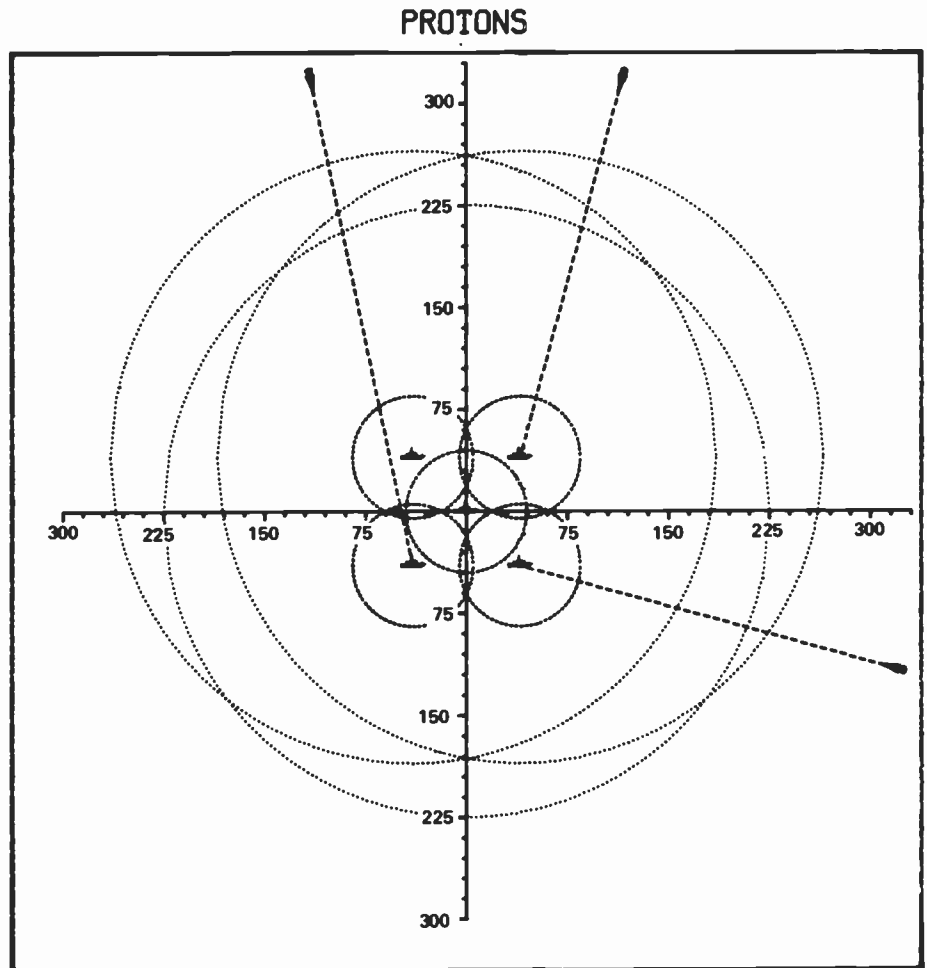


Fig. 4. A sample PROTONS output showing five ships being attacked by three groups of aircraft. The smaller circles represent coverage zones and the larger circles represent radar coverage.

detail, combinations of warfare areas, and output formats.

PROTONS (PROTOTYPE of a Naval Simulation) was initiated in early 1982 and will evolve into a comprehensive battle-group simulation of two opposing battle groups waging air, surface, and subsurface warfare. Extensive models of communication and coordination will be included.

A key simulation technique successfully evaluated with PROTONS was the use of an event-sequencer generator program. The event sequencers used in MEDUSA and SIMATR were created manually and changed manually when events were added and deleted. This approach involves removing or deleting subroutine calls and adding or deleting arrays defining and correlating event names and numbers for internal simulation use. Changes are required in a few subprograms and although it is a direct procedure, it is prone to error as are most manual operations. However, this procedure is ideal for automation via a computer program, GENSIM.

A new PROTONS event sequencer is generated by the GENSIM program whenever an event name is added or deleted from the names of all PROTONS events in a disk file. Although GENSIM was written for PROTONS, it is usable for a simulation of any system and quickly provides an executive subprogram for simulation control.

A program has been developed to create input subroutines from a disk file describing input variables. It allows the addition of input variables and default values to the simulation without programming. This program is applicable to simulations of any system and for any programs that require separate input subroutines.

Other software techniques being evaluated via PROTONS are increased use of graphics for both simulation input and output. The most useful SIMATR and MEDUSA outputs are multicolor plots showing the results of key system events, and area maps showing trajectories and facilities. Figure 4 is the initial PROTONS



Jerry Golub (right) reviews simulation graphics produced by a member of the simulations group.

Jerry Golub is Unit Manager of the System Simulation and Data Reduction group in the Naval Systems Department at Missile and Surface Radar in Moorestown. His group designs and develops simulations of the AEGIS Weapon System and writes data-reduction programs to analyze AEGIS tests. SPECTRM, the AEGIS dynamic simulation, and MEDUSA, the AEGIS operations analysis simulation, have been important system engineering tools throughout the AEGIS Program. Currently, a major group project is the design and development of a battle group simulation. Contact him at:
Missile and Surface Radar
Moorestown, N.J.
TACNET: 224-2426

graphic output showing ship position, radar and missile coverages, and the trajectories of attacking air targets. The battle-group simulation will be the simulation group's first program that will allow users to create input by interacting with data on the screen of a graphic CRT terminal.

PROTONS provides an effective means of evaluating and exercising the simulation techniques learned and developed over the past eight years. The ultimate models to be included in the final version of the battle-group simulation have not been determined, but the discrete-event architecture, and the tools developed to facilitate their use, ensure that this program will easily be developed to meet simulation needs.

Conclusion

Discrete-event simulations of complex weapon systems have been successfully applied to a variety of problems for the past eight years. The discrete-event architecture is well suited to model complex weapon systems that are composed of many elements interacting with the environment and attacking forces. Techniques and software developed by the Naval Systems Department simula-

tion group make initiation of new simulations much easier than previously. Although only weapon systems have been discussed, discrete-event simulations have been widely used for transportation, logistics, and traffic-control problems.

Anyone designing or analyzing complex systems with many elements and interactions can beneficially use the methods discussed in this paper. All of the software discussed is operational on the DEC 2060 computer system, and the calendar management and list-handling subroutines have operated on the RCA IBM 370/168. Moreover, since all programs are written in FORTRAN, their conversion to other systems would not be difficult. MEDUSA has been operational on UNIVAC, IBM, and CDC computers, and SIMATR has been converted to operate on UNIVAC, CDC, and Honeywell computers.

Discrete-event simulations of complex weapon systems have been successfully used for system design, algorithm design, test design, test analysis, predicting system performance, evaluation, requirements specification, operations analysis, mission analysis and education. Without simulation, the myriad weapon-system parameters that

were varied for these analyses would have required many more years of engineering manpower.

Acknowledgment

Many people have contributed to the success of the simulations described in this paper. Of all these, Beryl Levy is the one most responsible for converting the ideas presented here into concrete, usable programs.

References

1. J. Golub, "FORTRAN Simulation with Dynamic Lists," *Record of Proceedings of the Seventh Annual Simulation Symposium*, Tampa, Florida (March 1974).
2. A. Alan and B. Pritsker, *The GASP IV Simulation Language*, John Wiley & Sons (1974).
3. J. A. Clancy and J. Golub, "Dual Development of a Simulation," 1979 Summer Computer Conference Proceedings, Toronto, Ontario (July 1979).
4. J. Golub, D.M. Greeley, and B.B. Levy, "SIMATR, an Air Battle Simulation of the USAF Tactical Air Control System (TACS) with Advanced Tactical Radars," 1981 Summer Computer Simulation Conference Proceedings, Washington, D.C. (July 1981).

Digital interface simulation for large system development

Techniques used to simulate critical hardware-software interfaces are essential to cost-effective development and test of very large real-time systems.

Abstract: *Digital real-time interface simulation has become an important tool in developing large military systems, particularly those incorporating embedded computer subsystems. This paper discusses the application of interface simulation as a means of reducing programming errors, improving the technical quality of developmental systems, and significantly cutting the cost and complexity of system testing.*

The in-process testing of incremental base-lines has always been a vital part of the development process for large electronic systems. As these systems have made increasing use of embedded computer subsystems, the testing technology to support them has also become increasingly computer-based. This condition has led to the application of digital interface simulation as a significant element of large system development.

At RCA Missile and Surface Radar, the extensive use of real-time interface simulation technology has become an integral part of the engineering development process for the U.S. Navy's AEGIS Combat System as well as for a range of other advanced, highly computer-based radar systems. This paper describes the application of interface simulation to this type of project, with particular emphasis on the AEGIS System because of its large size and the diversity of technical issues involved.

© 1982 RCA Corporation
 Final manuscript received October 22, 1982
 Reprint RE-27-6-6

AEGIS Combat System application

The *Ticonderoga* (CG 47) class of guided-missile cruisers armed with the AEGIS Combat System, is the primary protection for the Navy's aircraft carrier battle groups. Armed to provide anti-air, anti-surface, and anti-submarine protection, *Ticonderoga* and her AEGIS Combat System create an "envelope of defense" for the battle group,

providing protection that ranges from below the surface to the stratosphere. The quick reaction and the high firepower of AEGIS repel missiles and aircraft attacking from very low and very high altitudes. The ship can counter a saturation missile attack, making her one of the most survivable cruisers ever built. Figure 1 is an overview of the AEGIS Combat System.

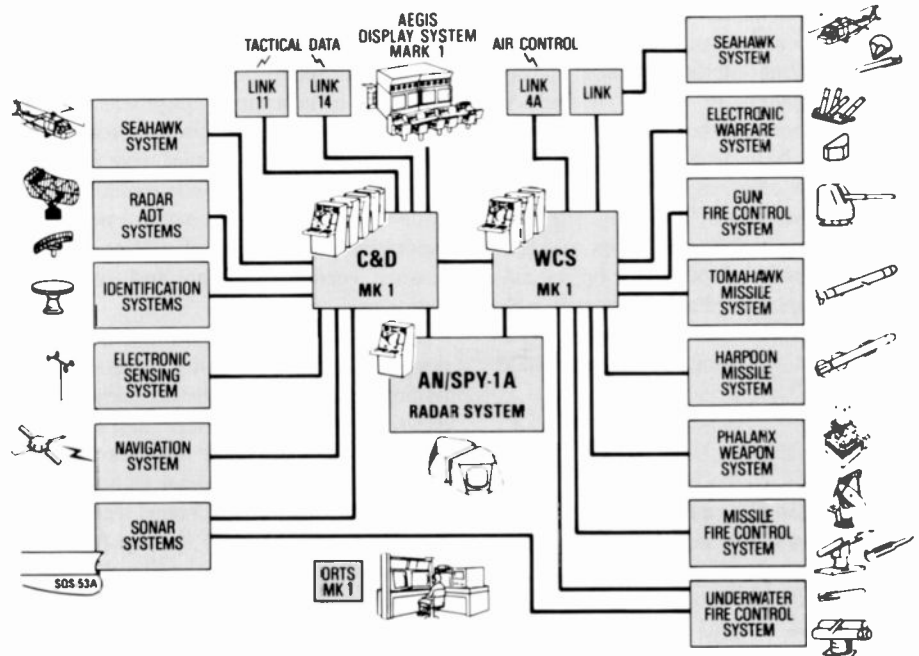


Fig. 1. *Elements of the AEGIS Combat System. The AEGIS system includes a wide range of sensor and weapons subsystems under computer control, all of which must be extensively simulated prior to ship delivery.*

Development of the many computer programs required is a major part of the AEGIS shipbuilding program. Hundreds of thousands of lines of source code are needed to control and process sensor information, control the weapons systems, monitor equipment status, and provide the crew with a powerful and flexible command and control capability. Major computer programs must be developed and tested before the equipment with which they interface is fully available; frequent, and sometimes major, design changes occur after the equipment becomes available; and the entire development process involves large numbers of subcontractors, all with different approaches to equipment and computer-program development.²

Tens of thousands of detailed test items must be demonstrated in acceptance procedures; the cost of personnel, aircraft, missiles, and targets is prohibitive for all but the final stages of testing. In this environment, the AEGIS Interface Simulator System filled a need for an affordable, highly versatile test bed for the development of the tactical computer programs.

Requirements

The general requirement for the AEGIS Interface Simulator System (ISS) is to provide for each major computer-program element (or group of elements) a real-time interface simulation sufficiently realistic to test each of the functions of that element (or group of elements) over its entire range of operating conditions. In addition to providing a realistic interface at each channel of the computers in which the tactical programs operate, other requirements are that the ISS be reconfigurable for a wide range of test cases using the same basic programs, that it provide monitoring and data recording at these interfaces, and that it have a minimal dependence on special-purpose equipment (that is, it must be able to operate in an off-site computer laboratory without requiring special shipboard equipment).¹

Design

The computer programs that control the ship equipment are organized into three major groups, or tactical elements: AN/SPY-1A (radar), Command and Decision Mark 1 (C&D), and Weapons Control System Mark 1 (WCS). Three ISS configurations were developed to support testing of each of these elements individually (Fig. 2). Other configurations were then

Table 1. Principal and derivative ISS configurations.

Configuration	Purpose	Number of computers
AN/SPY-1A	Stand-alone testing of AN/SPY-1A tactical element	2
C&D	Stand-alone testing of C&D tactical element	3
WCS	Stand-alone testing of WCS tactical element	3
CDS	Testing of combined C&D and WCS tactical elements	3
System	Testing of all three tactical elements	5
SPY/VLS	Testing of AN/SPY-1A tactical elements, modified for vertical launching system*	2
CDV	Testing of combined C&D and WCS, modified for VLS	3
System/VLS	Testing of all three elements, modified for VLS	5
ORTS	Testing of the Operational Readiness and Test System	2
GDC	Testing of the Gyro Data Converter	2
ADG	Testing of the special display system	1
ADG/MAC	ADG ISS reconfigured to operate in MAC maintenance computer	1
Scenario generator	(See text)	1

* VLS is a missile launching system to be used in later AEGIS ships.

derived for combinations of these groups and for special functions, as shown in Table 1. The ISS consists of approximately 320,000 lines of source code in the CMS-2 language and operates on one to five Univac AN/UYK-7 computers, depending on configuration.

In addition to meeting its functional requirements, the design of the Interface Simulator System had to resolve a number of other computer-program engineering issues such as cost, host equipment characteristics, precision, communications, and maintainability. These issues were resolved in the form of two fundamental design trade-offs: cost and processing time versus modularity, and degree of off-line preprocessing versus precision and real-time resources.

In the first relationship, there are strong design and maintainability advantages in writing a set of functionally decoupled modules (or subprograms) rather than one very large program. Separate modules are easier to design, and it is easier to isolate the source of a system problem when each module performs only a specific function. As module sizes become smaller, however, the total number of modules increases, as do the computer time and memory overhead for inter-module communications, configuration control, and maintenance. Furthermore, as retroactive design changes are made throughout the system's later life,

the number of modules that must be modified for each change also increases. The nature of this relationship is shown in Fig. 3. The optimum modular partitioning for ISS was one module for each equipment subsystem to be simulated; one module for each group of equipment subsystems would have been the next higher step, and one module for each function of each subsystem, the next lower. This resulted in 80 modules with an average module size of about 4,000 lines of source code.

The second relationship, on-line versus off-line processing, is somewhat more complex. Many of the phenomena being simulated (such as radar reflections from multiple targets in an electronic countermeasures environment) occur very quickly, on the order of several microseconds, and the tactical programs expect to receive these signals at very high data rates. However, the analytical solution of these complex electromagnetic phenomena by a simulator requires computer time that is several orders of magnitude greater than that required by the tactical programs to measure and process these signals. Furthermore, many of these external electromagnetic events cause the simultaneous reporting of signals by sensors having widely different characteristics; as a result, the simulator must synchronize events precisely.

The use of very-high-speed computers and special-purpose analog simulators to

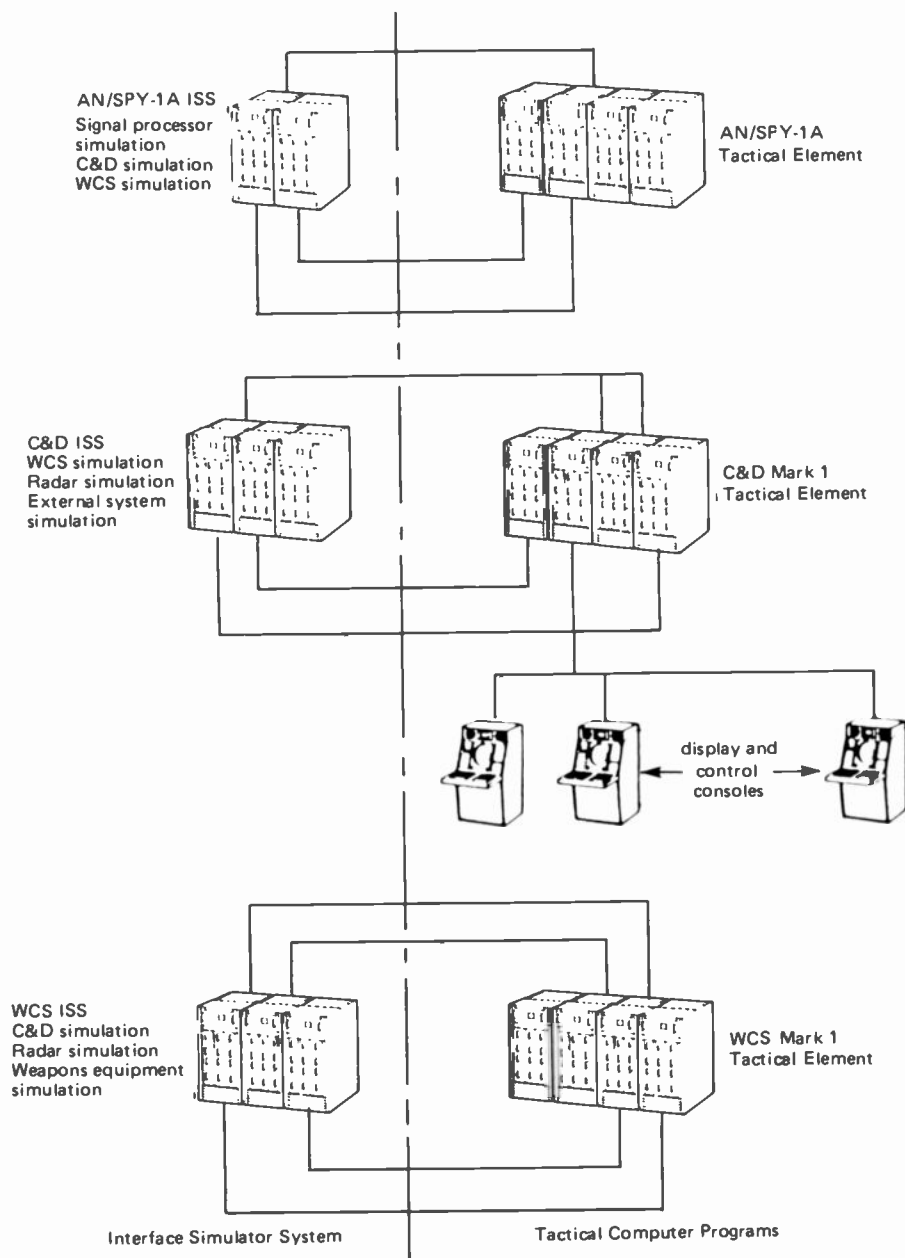


Fig. 2. Principal configurations in the AEGIS Interface Simulator System. The ISS is designed to be reconfigurable to support the AEGIS system at various stages of development.

solve the computational loading and multi-sensor synchronization problems was not economically feasible. The general approach to solving these problems within available resources required that the simulation process operate on standard Navy computers and be divided into a real-time phase and an off-line preprocessing phase. During the preprocessing phase, all external events are analyzed in terms of the effects they would have on all possible sensors. This information is re-computed in discrete steps across both the range of normal operating conditions and the length of the test case, and

then stored to a high-speed disk file.

During the real-time phase, this data is read back from the disk, corrected for factors not predictable in advance, and transmitted to the tactical computer programs. Examples of the types of corrections performed in real-time are: suppression of signals for sensors that are not enabled; interpolation of the data to the value of the real-time clock; response to human operator actions; and generation of flight data for manually initiated missile launches.

A roughly inverse relationship exists between the sizes and other cost factors of

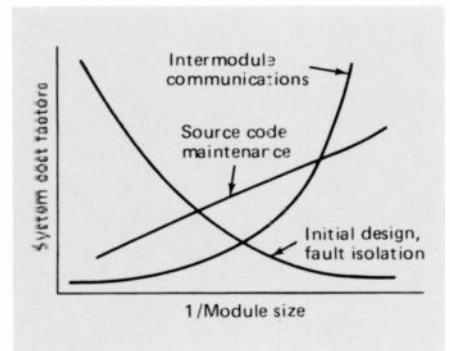


Fig. 3. Program modularity trade-offs. Optimum subprogram module size depends on communications and maintenance costs as well as functional partitioning.

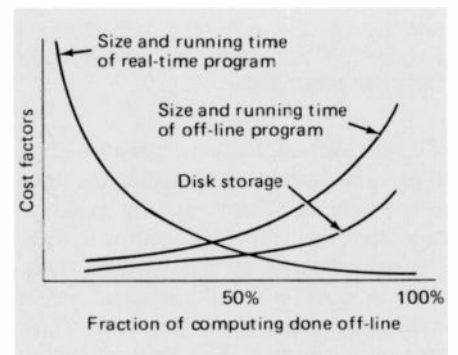


Fig. 4. Real-time/off-line trade-offs for a single configuration. For an interface simulator, cost savings can be achieved by preprocessing functions that use an off-line program.

the real-time and off-line programs, as shown in Fig. 4. The size of the real-time program tends to decrease in a linear fashion (down to some absolute minimum) as functions are transferred to the off-line program. The size of the off-line program increases linearly with the increase of precision and the addition of relatively uncoupled functions. A point is reached, however, where the further transfer of real-time functions to the off-line process requires a high degree of anticipation and the compounding of interrelated conditions. At this point, the size of the off-line program increases much more rapidly.

If the interpolation required in real-time were halved, the size of a target trajectory file produced off-line would double. However, transference of the responses to operator actions from the real-time program would require the anticipation of all possible operator actions and would increase both size and computing time by far more than a proportional amount. In manually initiated missile launches, for example, the computation of a missile trajectory is affected by firing doctrine, launch time, type

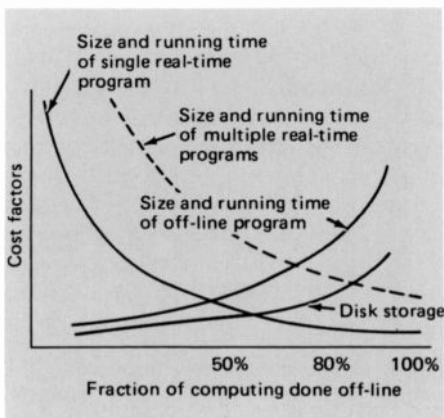


Fig. 5. Real-time/off-line trade-offs using a common off-line program with multiple real-time programs. Additional cost savings can be achieved by sharing a general off-line program with several real-time programs.

of missile selected, and the cumulative effect of previous launches. In addition, the flight path is altered in real-time by guidance data from the Weapons Control System. The anticipation of all possible flight paths, even with real-time interpolation, would involve the generation of hundreds of distinct trajectory files. This kind of nonlinearity determines the optimum trade-off point between real-time and off-line processing.

Within the functional requirements and equipment characteristics of the AEGIS ISS, the optimum fraction of total processing for a given configuration to be performed off-line was 50 to 60 percent. However, an additional economy was realized due to the inherent similarity among the data files used by different sensor simulations. For example, although the AN/SPY-1A phased-array radar, the RDP (Remote Digital Plotter) radars (Fig. 1), and the AN/UPX-29 IFF (identification, friend or foe) radars have different ranges, data rates and interface formats, they have substantial overlap in the targets that they can detect simultaneously. By modifying the off-line program to produce a disk file (or "scenario") general enough to be used by all sensors and by adding simple discrimination logic to each of the real-time programs to suppress inapplicable data, it was possible to have one off-line program driving several real-time programs.

When seen in this light (that is, the cost of one off-line program versus the total cost of several real-time programs), the trade-off point shifts considerably in the direction of a more sophisticated off-line program (Fig. 5). In the case of the ISS, the trade-off point was approximately 80

percent. An additional advantage in this common-data-file approach is the considerable simplification of intersensor synchronization processing in the real-time programs. The use of several files would have required compensation logic for the timing differences between the different disk drives.

Development

Once the overall design of the Interface Simulator System was completed, a number of detailed development policies were established to assure the technical integrity and timely availability of the ISS to the overall AEGIS Program. With the large number of programmers participating in the development of the ISS and the number of tactical programs (peak levels of 30 and 150, respectively), it was necessary to assure that the two efforts did not drift apart. A parallel development plan was established wherein both projects were governed by the same set of formal interface design specifications and supported by the same system engineering team under similar, concurrent schedules.

Because of the large size of the Interface Simulator System (approximately 320,000 lines) and the contract requirements, special attention was given to a formal development methodology. Use of CMS-2 (a structured, higher-order Navy computer language) was specified, as were formal documentation and coding standards, and approval of both the initial designs and the subsequent changes by external review teams. High productivity levels were supported with the extensive use of programming tools such as a text editor, source-code indenter, automatic flowcharter, file management system, and module-level test drivers. Additional cost and reliability advantages were achieved by using the same types of computers, the same operating systems (one for real-time and one for off-line operation), and the same configuration control and quality assurances services as those used by the tactical programming team.

With *Ticonderoga* due to commission early in 1983, the role of a sophisticated interface simulation facility in reducing costs and assuring technical integrity is well established. Throughout the AEGIS engineering development process, the Interface Simulator System provided a number of valuable functions:

- A controlled and repeatable means for meeting thousands of detailed formal test requirements;

- An effective bridge between system-level test engineers and software developers;
- Early identification of the specification conflicts;
- A basis for long-term "regression testing";
- A basis for testing otherwise untestable "worst-case" tactical scenarios;
- Reduced dependence on equipment-availability schedules; and
- A major system-performance and configuration-control mechanism.

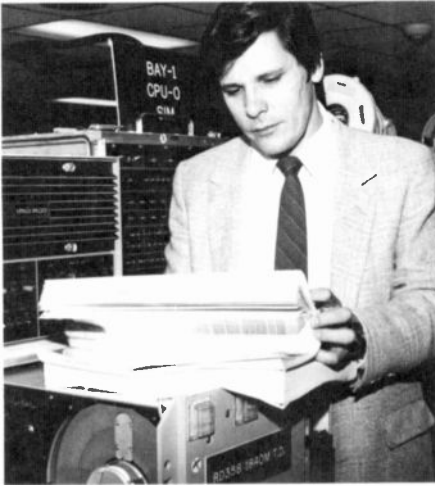
The Interface Simulator System will continue to be used to support the production of subsequent *Ticonderoga*-class ships and will be used at the Naval Surface Weapons Center, Dahlgren, Virginia, to reproduce, investigate, and correct problems encountered in ships at sea as well as to support any computer-program retrofitting of future ships.

Related applications

Interface simulation techniques have been applied to the development of a wide range of systems such as conventional and phased-array radars and also for such non-radar applications as communications, electronic countermeasures, navigation and fire control. The best candidates for interface simulation are systems having an embedded control computer (or distributed system of computers) and well-defined digital interfaces to peripheral equipment. The most economically advantageous applications of interface simulation have been for real-time target generation, particularly for coordinated multiple-sensor systems.

Another benefit has been the resolution of hardware/software specification conflicts. Since an interface simulator, although itself a computer program, is usually derived from the specifications of the external equipment being simulated, the operation of the embedded computer against the simulator can often reveal specification errors or ambiguities that, although minor in a technical sense, can be very costly to isolate and correct at a later stage.

In several projects in the early stages of design, simulators are being used to replace some equipment subsystems and are being operated with the embedded control computer to optimize computer timing as well as overall system performance. This is being done at an early enough stage to allow modifications in both the hardware and software designs. In other systems, analyti-



George Suhy is Unit Manager, Simulator Systems, in the Software Design and Development Activity at Moorestown; he is currently responsible for the AEGIS Interface Simulator System. After joining RCA in 1973 he worked on a variety of system software projects before his current assignment on the AEGIS Program. He received the BSEE degree (1970) and the MS in Systems Engineering (1975) from the University of Pennsylvania. He is active in the Computer Society of the IEEE and the Association of Old Crows.

Contact him at:
RCA Missile and Surface Radar
Moorestown, N.J.
TACNET: 224-2542

Summary

The use of digital real-time interface simulation has repeatedly demonstrated both technical and economic benefits in the development of large system projects. Thousands of programming errors have been detected, precisely documented, and corrected using such simulations. It also has enhanced flexibility of project scheduling, has improved technical quality by providing precise and reproducible external conditions, and has greatly reduced many of the costs associated with full-system testing. As the size and complexity of modern electronic systems continue to grow, interface simulation will be a required engineering tool for large system development.

References

1. F.G. Adams, "Putting AEGIS to Sea," *RCA Engineer*, Vol. 26, No. 7, p. 40 (July/August 1981).
2. C.N. Falcon, "Testing of Systems Developed by the Incremental Build Method," *Proceedings of the Workshop on Software Testing and Test Documentation*, Ft. Lauderdale, Florida (December 1978).
3. G.W. Suhy, "Real-Time Simulation as a Tool for System Development," Ninth Annual Modeling and Simulation Conference *Proceedings*, University of Pittsburgh (April 1978).

cal simulators, which are much larger and usually do not operate at real-time speeds, are used to develop detailed critical test cases. These test cases then are reprogrammed as input data to interface simulators, thereby combining the analytical power of a large computer with the real-time characteristics of an interface simulator.

Although many of the early applications of interface simulation were developed with Independent Research and Development funding, this approach is gaining increasing acceptance and many newer system projects now require the use of interface simulation for development and acceptance testing as part of the development contract.

The Engineer's Notebook

Design and simulation of an intelligent missile seeker

Julius Hayman

RCA Government Systems Division
Cherry Hill, N.J.

An intelligent tracking algorithm for an infrared (IR) imaging missile seeker and a method of evaluating its performance in simulated flight is described in this paper. The missile is a fire-and-forget, shoulder-launched, anti-tank weapon that lofts to an altitude of approximately 150 meters and then homes toward the target using proportional guidance. A gyro-stabilized seeker is precessed to the target by pointing commands. These pointing commands are developed from an imaging sensor by a new tracking algorithm that performs well in a highly cluttered background.

Both the tracking algorithm design and its evaluation in missile flights were accomplished using a digital computer simulation called HUGGER. This program includes a 6-degree-of-free-

dom missile simulation, a detailed seeker model, a three-dimensional model of the target, a two-dimensional background model, and the intelligent tracking algorithm.

Sensor images of the target as seen from the missile are formed on a 64×128 pixel IR-charge-coupled-device (CCD) array. The algorithm uses three features within the image: intensity, spatial frequency, and internal gradients. A multithresholding technique is also described which enhances target discrimination.

Tactical missiles of today have definite operational limitations because seekers are apt to lose track of targets against highly cluttered backgrounds. Such scenarios may be attacks on tanks against a background of roads, foliage, rocks, and so on; attacks on aircraft against a varied cloud background; or attacks from above on aircraft against a terrain background.

The next generation of tactical missiles may use imaging

© 1982 RCA Corporation
Final manuscript received October 7, 1982
Reprint RE-27-6-Technical Note

trackers because of the large amount of information in the image that can be utilized by an intelligent tracking algorithm. The algorithm is used to separate (or segment) the target from a cluttered background, and then track this target. With the advent of small, solid-state CCD arrays and high-speed microprocessors, it is now practical to utilize imaging seekers with intelligent tracking algorithms. Two recent developments by RCA initiated this study. These are the ATMAC microprocessor developed by the Advanced Technology Laboratory,¹ and the Schottky-barrier IR-CCD array developed by the David Sarnoff Laboratories^{2, 3, 4, 5}. The latter is a 64×128 element staring array that operates in the 3- to 5-micrometer wavelength band with excellent uniformity, sensitivity, and dynamic range. Since it uses silicon technology, its potential production economy appears very attractive.

Computer simulation work verifies successful operation of a missile system containing the IR-CCD array and tracking algorithm. Both the tracking algorithm design and its evaluation in missile flights were accomplished using program HUGGER whose scenario is illustrated in Fig. 1. Simulated sensor images of the target as seen from the missile are displayed with the tracking gates superimposed to assist in the algorithm development. HUGGER also provides each corresponding segmented image so that the algorithm's discrimination capability can be evaluated.

The intelligent tracking algorithm encloses the target with an adaptive gate and uses multifeature and multithreshold techniques to achieve superior image segmentation. A rectangular adaptive gate is servoed to enclose only the target vicinity, thereby eliminating most of the extraneous background clutter within the field of view. A background gate is located around the perimeter of the centroid gate. There are three features extracted from the image: intensity, spatial frequency, and internal gradients. Each of these features is thresholded using the multi-threshold technique where up to four thresholds are automati-

cally employed, allowing target pixels to be identified if they are above, below, or in between background value bands. Enhancement is accomplished by changing the intensity value of a pixel if either the spatial frequency or the gradient value is over its respective threshold. The enhanced intensity feature is then finally thresholded to provide the segmented image. Adaptive gate size, seeker pointing commands, as well as missile guidance signals, are all derived from this segmented image.

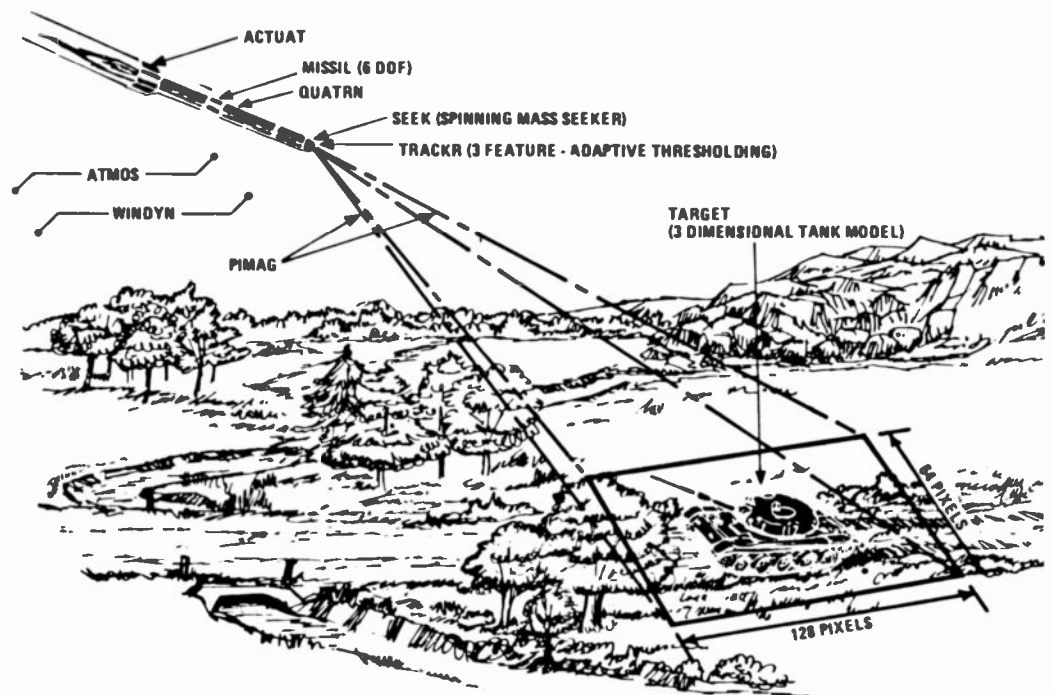
During terminal navigation, when the target fills the entire field-of-view, the adaptive gate tracker is replaced by a centrally weighted correlation tracker. Correlation is performed along a horizontal strip for yaw and a vertical strip for pitch. These two strips form a cross at the center of the field-of-view. Because of the high rate of range closure and the high-line-of sight rates during terminal flight, correlation must be done on a frame-to-frame basis. Drift due to the range closure effect is minimized by centrally weighting each correlation strip. This low-drift algorithm is used until impact.

The simulations showed that the 64×128 CCD array, with the intelligent algorithm, would track targets in high clutter and could be made to consistently impact the upper surface of a tank where armor is at a minimum. Program HUGGER was an excellent tool for evaluating algorithm modifications during development. Algorithms can be compared over the same trajectory, with the same target intensity and background statistics. It would be impossible to do this otherwise, even with actual hardware. HUGGER also allows target tracking with realistic line-of-sight rates and accelerations, range closure, and a changing aspect angle.

Program HUGGER

Program HUGGER is a modularized FORTRAN program consisting of 18 subroutines. Output data is provided in the follow-

Fig. 1. Program HUGGER is a simulation of a missile-target system in which a seeker forms images on a 64×128 CCD array. The missile is guided by a processing of these images with an intelligent tracking algorithm.



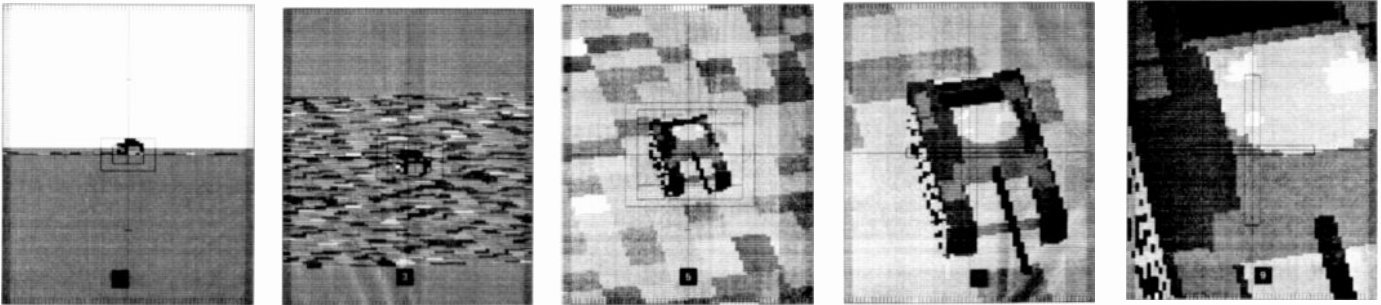


Fig. 2. Simulated images of a tank are formed by Program HUGGER with the tracking gates superimposed. These images are formed every 1/60 second and are processed to obtain missile guidance commands.

ing formats:

- Printed data, where 56 variables are printed.
- Stripplot, where up to 10 variables are plotted against time.
- Segmented image plots, indicating target/nontarget pixels as determined by the intelligent algorithm.
- Image plots (Fig. 2), where images formed on a 64×128 IR-CCD array are plotted using a gray scale.

Considerable detail is modeled in HUGGER so that many parts of the missile system can be studied during flight. To eliminate excessive execution time, the following options are provided:

- A detailed gyro-stabilized seeker with gimbal friction, magnetic torques and input errors, or a simplified seeker model.
- A three-dimensional target model, the tracking algorithm and image forming, or a simple point target.
- An optical point-spread function, or a simple one-ray-per-pixel projection.
- Image plots, or no image plots.
- Steady or gusty wind or both, or no wind.
- A moving or a static target.

Conclusion

Recent military events have vividly shown that precision guided missiles are so effective they have changed concepts of modern warfare. With the advent of small, high-speed microprocessors and solid-state staring arrays, this trend will continue. Imaging seekers which utilize considerably more information concerning

the target area are now possible. The recently-developed Schottky-barrier IR-CCD sensor array has the potential for being economically produced since it is fabricated using conventional silicon technology. Intelligent tracking algorithms can be implemented economically with software using presently available digital processors.

Development of intelligent algorithms can be accomplished efficiently by using computer simulations of the entire missile-target system. All the variables of the algorithm and missile are observable, and both the target intensity and the background statistics are controllable.

References

1. W.A. Helbig, W.J. Davis, and A.D. Feigenbaum, "ATMAC Microprocessor," *RCA Engineer*, Vol. 23, No. 1, pp. 36-39 (June/July 1977).
2. W.F. Kosonocky, H. Elabd, *et al.*, RCA Laboratories, Princeton, N.J.; and M.J. Cantella, *et al.*, RCA Automated Systems, Burlington, Mass., "Design and Performance of a 64×128 -Element PtSi Schottky-Barrier IR-CCD Focal Plane Array," SPIE Technical Symposium East, 1982, Arlington, Va (May 3-7, 1982).
3. R.W. Taylor, I. Skolnik, *et al.*, "Improved Platinum Silicide IRCCD Focal Plane," SPIE Technical Symposium, Advances in Focal Plane Technology, Los Angeles, Calif., 217, 103 (February 4-5, 1980).
4. F.D. Shephard, R.W. Taylor, *et al.*, "Schottky IRCCD Thermal Imaging," *Advances in Electronics and Electron Physics*, Vol. 52, p. 495, 7th Symposium on Photo-Electronic Image Devices, (1979).
5. J.A. Tegnelia, "DARPA Unveils Staring Focal Plane Array," *Defense Electronics*, Vol. 12, 101 (1980).

Contact:

J. Hayman

TACNET: 222-5944

ANA radio-frequency circuit simulation and analysis

Computer-aided circuit simulation permits the development and adjustment of circuit elements without costly construction of a laboratory model.

Abstract: *Computer-aided design enables the radio-frequency (RF) or microwave circuit designer to design a circuit and modify element placement quickly and cost effectively. The ANA program, designed primarily for minicomputers, is an extremely simple approach to computer-aided design of linear RF circuits. With it, coding of elements and their placement is in the form of easily remembered English acronyms. The simulator circuit can be modified by use of an on-line conversational mode.*

Computer-aided design provides the modern radio-frequency (RF) circuit designer with a tool that allows initial circuit element and topology design and adjustment before a laboratory model is constructed. In addition to providing a means for producing designs quickly and at a relatively low cost, computer simulation allows the creation of circuits that may have been impossible to design otherwise.

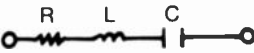
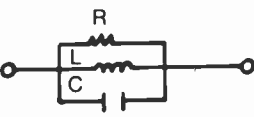
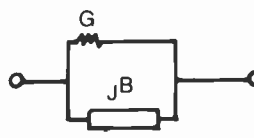
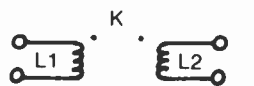
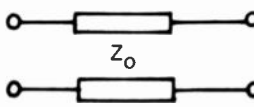
The circuit analysis program, ANA, can be used to design and model RF circuits. It is easy to use because it requires only a simple description of elements and circuit topology. The circuit and desired outputs can be modified easily by means of a simple conversational mode that does not require editing of data files. Data, or complete circuits, may be written to or from disks or magnetic-tape-based libraries. This program was expected to be used on a continuous, daily basis; it was, therefore, written to be run on a minicomputer rather than a large, time-shared mainframe com-

puter with prohibitive running costs. ANA is presently installed on HP1000 computers at RCA Laboratories, Princeton; Astro-Electronics (AE), Princeton; Missile and Surface Radar (MSR), Moorestown; Consumer Electronics Division (CED), Indianapolis; RCA Laboratories Limited, Zurich; and Advanced Technology Laboratories (ATL), Camden.

Describing the circuit elements

Circuit elements may be divided into three categories, as shown in Tables I, II, and III. The coding for each element type consists of either a simple acronym or, as in the case of impedance and admittance, the symbol conventionally used in texts. The simple two-port elements shown in Table I have fixed parameter values.

Table I. Two-port element descriptors.

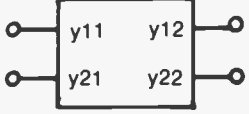
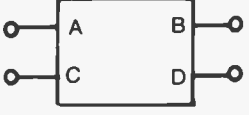
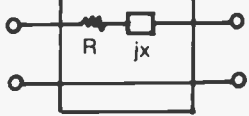
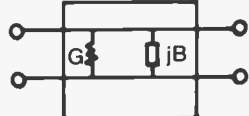
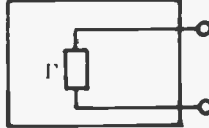
Element type	Coding*	Parameters
 Series RLC	SRLC	$R(\Omega)$, $L(\text{nH})$, $C(\text{pF})$
 Parallel RLC	PRLC	$R(\Omega)$, $L(\text{nH})$, $C(\text{pF})$
 Impedance	Z	$Z_0(\Omega)$, R/Z_0 , X/Z_0
 Admittance	Y	$Y_0(\Omega)$, G/Y_0 , B/Y_0
 Coupled coils	CC†	K, $L1(\text{nH})$, $L2(\text{nH})$
 Transmission line	TL	$F(\text{GHz})$, $\text{ATT}(\text{dB}/\lambda)$, $Z_0(\Omega)$, $L(\text{deg})$

* Only the first two characters for SRLC and PRLC are needed.

† For ideal transformer, use $K = 1$ and then $L1:L2$ is square of turns ratio.

© 1982 RCA Corporation
Final manuscript received September 29, 1982
Reprint RE-27-6-8

Table II. Tabulated element descriptors.

Element type	Coding	Parameters
	Scattering parameters SPara	S11, S21, S12, S22 (MAG, ANGLE)
	Y-parameters YPara	Y11, Y21, Y12, Y22 [MAG (mmhos), ANGLE]
	ABCD-parameters ABcd	A, B, C, D (REAL, IMAGINARY)
	Tabulated impedance TZ	$Z_o(\Omega)$, R/Z_o , X/Z_o
	Tabulated admittance TY	$Y_o(\Omega)$, G/Y_o , B/Y_o
	Reflection coefficient GAMMA	(MAG, ANGLE)

The tabulated elements of Table II consist of parameters that must be tabulated for each frequency specified in the analysis. The impedance and admittance elements may also be tabulated for each frequency by specifying TZ or TY, instead of Z or Y. This feature is useful if the impedance or admittance of an element is known as a function of frequency, but is difficult to synthesize as R, L, and C values.

The multiports of Table III cannot be connected as two ports, but must always be connected in a nodal configuration. This is discussed in the next section.

Describing the circuit topology

A complete circuit description requires specification of how its elements are connected and what its input and output are. This may be accomplished by using standard, two-port connections such as cascades, branches, and paths, or by specifying nodes to which the elements are connected.

Two-port connections

Two-port connections are preferred over nodal connections because they are computationally more efficient. A designer accustomed to two-port connections can usually generate a complete circuit mentally, because node numbers do not have to be remembered.

Cascade connections. Cascade of elements is easily accomplished by specifying that the element is connected as either a *series element* (SE) or a *parallel element* (PE), as shown in Fig. 1.

Branch connections. Branch connections are used if more complex networks are connected in series or parallel with the main signal path. A *series branch* is initiated by the symbol SB, while a *parallel branch* is initiated by the symbol PB. All topology and element entries following these symbols are considered part of the branch until the symbol EB, indicating the *end of branch*,

is used. Entries following EB are considered to be main-path entries. A second branch may not be imbedded in a branch. Branch connections are shown in Fig. 2.

Path connections. Path connections indicate circuit elements that depart from the main path, but eventually return (unlike branches that just terminate). The symbol PP indicates the beginning of a *parallel path*. All entries following this symbol are considered part of the first path until either another PP or an SP for *series path* is entered. The second path symbol indicates the end of the first path and the beginning of the second. All entries following the second path symbol are considered part of this second path until a third path symbol is entered. This third symbol indicates the end of the second path and the rejoining of both paths into a single or main path. Note that the first- and second-path symbols do not have to be the same. For example, the main path can break into two parallel paths, initialized by PP. The two paths can then be reconnected in a series path rather than a parallel connection, in which case the second- and third-path entries are SP. The second- and third-path entries must agree because they are the same conditions. The four possible path combinations are shown in Fig. 3.

An incomplete path will cause the terminal to show an error message when an analysis is performed.

Structure connections. *Series structures* (SS) and *parallel structures* (PS) are identical to the path connections, except for name and symbol. The change in nomenclature is to allow imbedding a structure within a path, or vice versa, without ambiguity. For example, if a series path were to be imbedded (or nested) within a parallel path, initiation of the parallel path would be PP. Initiation of the imbedded series path would be SP. Unfortunately, the use of SP as the second-path entry indicates the conclusion of the original parallel path in a

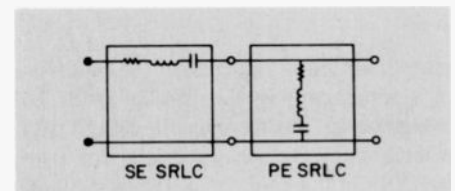
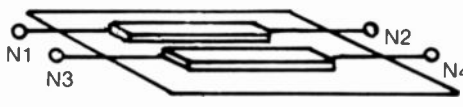
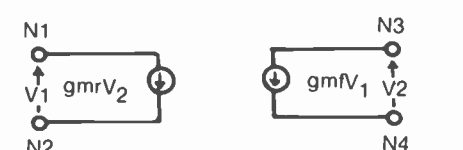


Fig. 1. Cascade connections of two ports provide the simplest interconnection of elements. The interconnection consists of a single main path.

Table III. Multiport element descriptors.

Element type			
Coupled transmission lines		N1,N2 N3,N4 CL	F(GHz), ELE LGTH(DEG), ATT(dB/λ) Line Between Nodes N1 and N2: YOO(MMHO), YOE(MMHO) Line Between Nodes N3 and N4: YOO(MMHO), YOE(MMHO)
			
Inhomogeneous coupled lines*		N1,N2 N3,N4 ICL	F(GHz), C MODE: LGTH(DEG), ATT(dB/λ), RC PI MODE: LGTH(DEG), ATT(dB/λ), RPI Line Between Nodes N1 and N2: YC(MMHO), YPI(MMHO) Line Between Nodes N3 and N4: YC(MMHO), YPI(MMHO)
Dependent current generator		N1,N2 N3,N4 GM	GMF(MMHO,DEG), GMR(MMHO,DEG)
			

* C and PI modes are as defined in the paper by V.K. Tripathi, "Asymmetric Coupled Transmission Lines in an Inhomogeneous Medium," *IEEE Trans. Microwave Theory & Techniques*, Vol. MTT-23, No. 9, pp. 734-739 (September 1975). Determination of these parameters can be made using ELOP, as described by F.J. Campbell in PTR-2649, "An Electron Optics Computer Program for the RCA Spectra, 70/45-55" (February 12, 1969).

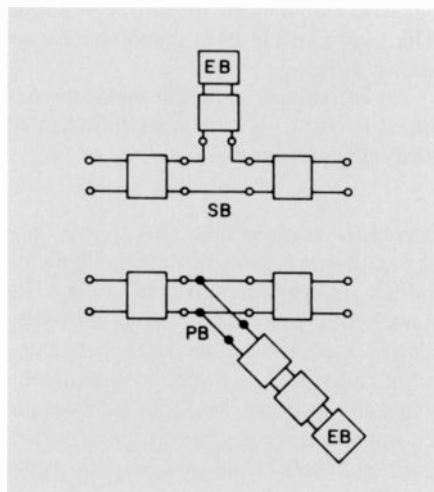


Fig. 2. Branch connections represent simple departures from the main path. A series branch (SB) is connected in series with the main path. A parallel branch (PB) is connected across the main path.

series connection rather than the initiation of a series path in the parallel path. To overcome this shortcoming, the second path is initiated by the use of the *structure symbol* (SS). In this case, the next two symbols must be structures to complete the nested path, followed by two path symbols to complete the outer paths.

Up to five paths or structures may be

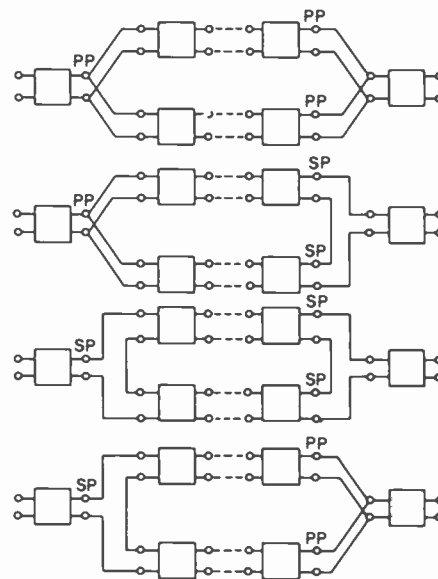


Fig. 3. Path connections represent the breaking of the main path into two sub-paths. The junctions of these paths may be connected in parallel (PB) or in series (SB).

nested. If this number is exceeded, an error message appears on the terminal when the analysis is performed. A summary of all two-port connections is presented in Table IV.

Nodal connections

Many circuits cannot be represented by the preceding two-port connections. To allow for these networks, nodal descriptors may be used in place of the two-port topology connections.

Circuit nodes may be arbitrarily numbered by integers used in any sequence. Entry of nodal connections into ANA is accomplished by simply replacing the topological descriptor, SE or PE, with two integers representing the nodes to which the element is connected. A series RLC element, connected between nodes 5 and 11, is designated as: 5, 11 SRLC. Nodal connections may be imbedded in any of the two-port branches, paths, or structures. ANA automatically sets up the following conditions:

- Input nodes are always 1 and 0.
- Reference node is always 0.

The following two rules must be adhered to:

- An integer cannot be skipped.
- The last nodal entry must define the output nodes. It must be: N1, N2 OUT where N1 and N2 represent the two output nodes. Note that the reference node does not have to be an output node, even though it is an input node.

Table IV. Two-port connections.

Connection type	Coding
Series element	SE
Parallel element	PE
Series branch	SB
Parallel branch	PB
End branch	EB
Series path	SP
Parallel path	PP
Series structure	SS
Parallel structure	PS

Notes on elements connected by nodes

Some of the elements shown in Table I are restricted by the use of two-port connections. For example, *coupled coils* (CC) are restricted to a common lead between input and output when SE or PE is used as the topological connection. This restriction is unnecessary when nodal connections are employed. A four-terminal device can be connected to four different nodes.

The multiport elements of Table III cannot be used with two-port connections because they have more than three terminals. The way in which the nodal descriptors are used for these elements is shown in Table V.

Modeling coupled transmission-line arrays

In many microwave circuits, coupled transmission-line arrays are required. Modeling

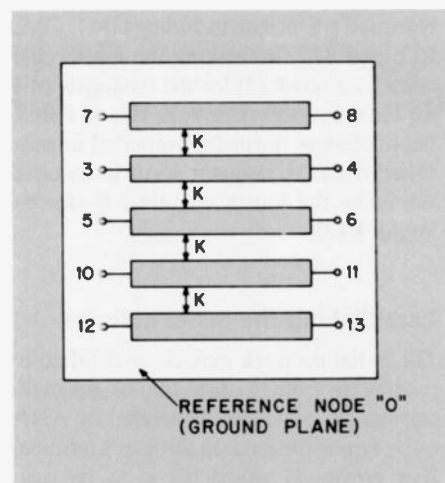


Fig. 4. Coupled lines can be arranged to form arrays of coupled lines, which are used to analyze microwave filters and couplers.

Table V. Nodal descriptors.

Element type	Nodal descriptors	Comments
SRLC	N1,N2 SRLC	
PRLC	N1,N2 PRLC	
Z	N1,N2 Z	
Y	N1,N2 Y	
TZ	N1,N2 TZ	
TY	N1,N2 TY	
TL	N1,N2 N3,N2 TL	First pair: input nodes
SP	N1,N2 N3,N2 SP	Second pair: output nodes
YP	N1,N2 N3,N2 YP	Note: repetition of N2
AB	N1,N2 N3,N2 AB	
CC	N1,N2 N3,N4 CC	
GM	N1,N2 N3,N4 GM	
CL*	N1,N2 N3,N4 CL	First pair: first trans line
ICL*	N1,N2 N3,N4 ICL	Second pair: second trans line

* Multiple coupled lines are accommodated by repeating N3,N4 of a preceding set of coupled lines as N1,N2 of a new set.

comb-line and interdigitated structures requires the coupling of more than two lines together. ANA allows complicated line structures to be constructed very easily.

The first two nodes of a *coupled line* (CL) designate the first transmission line, and the second two nodes designate the second transmission line. Simply repeating either set of these nodes for another CL element couples the line represented by these nodes to a third line. To illustrate this construction technique,

3,4	5,6	CL
3,4	7,8	CL
5,6	10,11	CL
10,11	12,13	CL

represents the structure shown in Fig. 4. The order is purposely scrambled to show that it is of no importance to the analysis. These lines can also be represented in a more orderly fashion:

7,8	3,4	CL
3,4	5,6	CL
5,6	10,11	CL
10,11	12,13	CL

In repeating the line nodes, ANA assumes that the repeated line is only one line and not two lines in parallel. Some models require that lines really be connected in parallel. In those cases, it is important not to make the mistake of repeating the same set of nodes in the CL designations.

Generator and load topological descriptions

ANA automatically assumes a 50-ohm source or generator impedance and a 50-ohm load impedance. If any other source or load impedance is required, the descriptors, GEN for *generator* and LOAD for *load*, must be used. The function of GEN and LOAD is to set the topological reference plane of the source and load in the analysis routine. Any network followed by the entry GEN indicates that the program should calculate the output impedance of the network preceding the GEN and use that as the source impedance. Likewise, the entry LOAD followed by any network indicates that the input impedance of the network following LOAD must be used as the load impedance. These networks may contain nodally described subnetworks, but GEN and LOAD cannot be imbedded in a nodal network. This is consistent with the fact that GEN and LOAD are themselves topological descriptors and cannot have other topological descriptors.

If the first or last element is series connected (SE), and GEN or LOAD is specified, ANA will automatically assume that the off-common lead is returned to common through a short circuit (in the case of GEN, the Thevenin equivalent voltage source representation). Similarly, if the first or last element is a parallel-connected element, PE, the off-common lead will be left floating (Norton's equivalent). The GEN and LOAD elements may be moved about

Table VI. Output options.

GAIN	GAIN (AVAILABLE POWER GAIN)
VOLT	VOLTAGE GAIN
CURR	CURRENT GAIN
ZIN(N)	INPUT IMPEDANCE (NORM TO 50 OHMS)
ZOU(N)	OUTPUT IMPEDANCE (NORM TO 50 OHMS)
YIN(N)	INPUT ADMITTANCE-MMHOS (NORM TO .02 MHO)
YOU(N)	OUTPUT ADMITTANCE-MMHO (NORM TO .02 MHO)
ZS(N)	SOURCE IMPEDANCE (NORM TO 50 OHMS)
ZL(N)	LOAD IMPEDANCE (NORM TO 50 OHMS)
ISOL	ISOLATION (REVERSE GAIN)
STAB	STAB FACTOR (ROLLET'S-K) AND GMAX(dB)
FLAT	GAIN FLATNESS (MAX, MIN, AND ACCUMULATIVE)
GM1	SOURCE REFL COEF REQUIRED FOR GMAX
GM2	LOAD REFL COEFFICIENT REQUIRED FOR GMAX
GA1	INPUT REFLECTION COEFFICIENT — GAMMA
GA2	OUTPUT REFLECTION COEFFICIENT — GAMMA
GAS	SOURCE REFLECTION COEFFICIENT (ZO = 50 OHMS)
GAL	LOAD REFLECTION COEFFICIENT (ZO = 50 OHMS)
DELY	DELAY (GROUP AND PHASE)
VSWR	VOLTAGE STANDING WAVE RATIO
RLOS	RETURN LOSS
TLOS	TRANSMISSION LOSS
PE1	PARALLEL RC EQUIVALENT OF INPUT IMPEDANCE
PE2	PARALLEL RC EQUIVALENT OF OUTPUT IMPEDANCE

Two-port parameters available: -S- -Y-
-Z- -H- -ABCD-; ask for desired parameter (that is, S11, H21, and so on).

Note 1: If GEN and/or LOAD REF plane are not specified, SOURCE and/or LOAD are assumed to be 50 ohms.

Note 2: CONJ of any REFL COEF—make 4th character *.

Note 3: Reciprocal of any REFL COEF—make 4th character R.

Note 4: Y, Z, H, and ABCD are in polar form. RECT form is obtained by making last character an I. Example: Y22I,AI

to find various input and output parameters throughout the circuit.

Output options

At present, there are over 70 different output options. These outputs may be obtained in tabulated form with as many as five different quantities printed during any single analysis. In addition to the tabulated output, a graphics display can be obtained for any output on a Hewlett-Packard graphics terminal. All outputs, with the exception of reflection coefficients, are plotted on rectilinear coordinates, automatically scaled to fit the data plotted. The scales are segmented into decimal divisions. Reflection coefficients are plotted on a computer-generated Smith chart. Table VI provides a summary of output options.

The desired outputs are calculated by assuming that all the elements preceding the GEN element form the generator or source impedance. All elements after the LOAD element establish the load impedance. If the GEN element is missing, the source impedance is assumed to consist of a simple 50-ohm resistance. Similarly a miss-

ing LOAD element means that the load is a pure 50-ohm resistance.

The GEN and LOAD elements also establish the reference plane for network input and output. The input impedance, or admittance, is the impedance or admittance looking into the network at the plane of GEN. The input of the network, if GEN is missing, is taken to be the input of the first element.

Voltage gain, VOLT, is calculated by placing a voltage source at the input terminals of the network and calculating the voltage at the output terminals. This makes the voltage gain independent of source impedance. This is also true for current gain, CURR.

The input and output reflection coefficients, GA1 and GA2, are referenced to the real part of the source and load impedances, respectively. However, the source and load reflection coefficients, GAS and GAL, are referenced to 50 ohms.

The two-port parameters (S, Y, Z, H, or ABCD) are independent of source and load impedance because they are defined for specific terminating conditions. The characteristic terminating resistance for S-parameters is 50 ohms.

A very useful application results from the different reference impedances for the reflection coefficients GA1, GA2 and S11, S22. A network can be designed by use of GA1 and GA2 to match between a complex source and load. The outputs can then simply be switched to S11 and S22 so that the calculated network can be compared to the real network, as measured on a network analyzer, without reconstructing or eliminating the complex source and load impedances.

The output, STAB, prints Rollets' stability factor in column one and the maximum gain in column two, if the stability factor is greater than unity. GM1 and GM2 provide the source and load reflection coefficients that produce the maximum gain. If the stability factor is less than unity, GM1 and GM2 are undefined and the printout contains zeros. These three outputs are particularly useful in designing networks that are nonreciprocal and active, such as two-port amplifiers.

VSWR, RLOS, and TLOS are all calculated from the reflection coefficients GA1 and GA2. The VSWR is one plus the magnitude of the reflection coefficient, divided by one minus the magnitude of the reflection coefficient. The *return loss*, RLOS, is the reflected power in dB and is calculated as the magnitude of the reflection coefficient squared. *Transmission loss*, TLOS, is one minus the squared magnitude of the reflection coefficient expressed in dB. The first column for all three of these outputs represents the values at the input of the network, while the second column represents the values at the output.

In many design situations, the conjugates or reciprocals of a reflection coefficient are required. These are easily obtained for any reflection coefficient, including GM1, GM2, S11, and S22, by making the fourth character an asterisk (*) for the conjugate or R for the reciprocal. The Y, Z, H, and ABCD parameters are normally outputted in polar form. If the rectangular form is required, we make the fourth character I—for example Y12I.

Establishing the initial network

The initial network may be established by reading it from a disk file or magnetic cassette file previously generated by ANA, or by typing the data on the user's terminal. If a previously saved file is to be used, ANA will prompt for the name of the disk file or the number of the magnetic cassette file and retrieve the data.

If the terminal is used to initially estab-

lish a network, ANA prompts the user with the following statements:

TITLE:

FREQS. (MHz) =

OUTPUT #1:

OUTPUT #2:

OUTPUT #3:

OUTPUT #4:

OUTPUT #5:

ELE NO 1: CONN, TYPE =

•
•
•

ELE NO 99: CONN, TYPE =

ANALYZE? CHANGES? WRITE?

The response to *TITLE* is any group of characters limited to a maximum of 44. It is used as a personal means of identifying the analysis.

The FREQS. (MHz) may be inputted as discrete values in the start, stop, step fashion, or in any combination of these methods. For example, an entry of the form,

1.35,1.76 2,10,2 10.15 20,100,10

results in an analysis at the frequencies,

1.35,1.76,2,4,6,8,10,10.15,
2,10,2
20,30,40,50,60,70,80,90,100
20,100,10

The maximum number of frequencies is limited to 21 at any one time. If this number is exceeded, a message is issued indicating that more than 21 frequencies were asked for and that the frequency list was terminated after the 21st. The frequency list may be modified later.

The outputs are then selected. If less than five outputs are desired, a simple space return will leave the output blank. The output may also be changed after the initial data has been inputted.

The final stage of the input phase consists of establishing the elements. After each element is specified by the user's response to connection CONN, TYPE, the program prompts with the parameters required to completely define the element. By typing END in response to the *ELE NO XX: CONN, TYPE =* question, the input phase is completed, and ANA responds with:

ANALYZE?, CHANGES?, WRITE?

This is the prompt that ANA returns to after each task is completed.

Table VII. Replies.

Replies to "ANALYZE?, CHANGES?, WRITE?" are:

ADD	ADD MORE ELEMENTS
DELETE	DELETE ELEMENTS
ANALYZE	ANALYZE
CONVERT	CONVERTS Z AND Y ELEMENTS TO SRLC AND PRLC
EL #	ELEMENT CHANGE
FREQ	FREQUENCY CHANGE
GEN	GENERATOR REFERENCE PLANE CAN BE MOVED
LOAD	LOAD REFERENCE PLANE CAN BE MOVED
HELP	LISTS PROGRAM PARAMETERS
INTERPOLATE	INTERPOLATES TABULATED ELEMENT DATA
OUTPUT	OUTPUT PARAMETER CHANGE
START	RESTARTS PROGRAM
TITLE	TITLE CHANGE
TERMINAL	TERMINAL CHANGE
WRITE	WRITES DATA FILE TO TERMINAL, DISK, OR MAG TAPE
PURGE	PURGES DISC DATA FILES CREATED BY ANA
DATA	WRITES DATA TO TERMINAL ONLY
TABULATED	WRITES TABULATED DATA TO TERMINAL
OFF END	TERMINATES PROGRAM
??	GIVES PARAMETERS FOR SINGLE ELEMENT IN DATA FILE
REACTANCE	CALC L&C FOR X(F1) AND X(F2)
TUNE	ALLOWS TUNING OF ELEMENTS
TT	TUNE TABLE LISTING
PLOT	PLOTTING ON VERSATEC
VID	PLOTTING ON VIDEO MONITOR
ERAS	STOPS VIDEO PLOTTING

Note 1: Only the first two letters of each reply are needed.

Note 2: The reply "FREQ" automatically interpolates tab data.

Reply options

Most of the replies to the prompt, summarized in Table VII, are self-explanatory. The reply ANALYZE obviously results in an analysis of the modeled network. Since ANA responds to the first two characters of a reply, only two are required. An unrecognized reply is ignored.

The reply DATA produces a list of the network elements and parameters on the user's terminal. It does not produce a listing of the actual parameters of the tabulated data, such as S-parameters. They may be obtained by replying TAB.

Any element connection, type, or parameter may be changed by replying ELEMENT XX, or simply EL XX. If the connection and type are to remain the same, a space return is all that is required. Any of the parameters may be kept the same by commas used to preserve the correct order. For example, if element 11 is a series-connected, series RLC, and the inductance is to be changed, we can write

ANALYZE?, CHANGES?, WRITE? EL 11
ELE NO 11: CONN, TYPE = (Space Return)
R, L(NH), C(PF) = ,120
ELE NO = 0

ANALYZE?, CHANGES?, WRITE?

Note that after the first element is changed, ANA responds by asking for an additional element number. This continues until answered with a zero. The addition of a new element is achieved using the ADD reply. Any element may be completely eliminated from the network using DELETE.

The generator and load reference planes may be moved about by using the replies GEN or LOAD. This reply will result in ANA's requesting:

ANALYZE?, CHANGES?, WRITE?, GEN
MOVE FROM ELE#A TO AFTER ELE#B
... A, B =

If element A does not contain the element GEN, the question is repeated. A generator or load can be created by making A equal to zero.

Any element that is not tabulated, or coupled lines, may be tuned by setting it up in the tune table. The tune table defines which elements and parameters are to be varied during the analysis phase of ANA. When analysis is performed, the variable elements and their parameter values are printed out just before the calculated output quantities. To create the tune table,

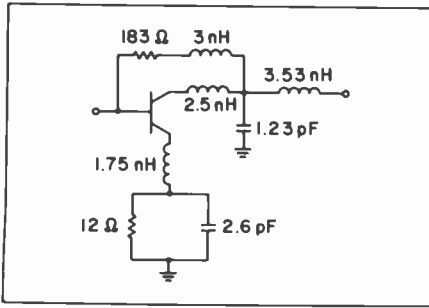


Fig. 5. Schematic of wideband amplifier used in Example 1. Shunt and series feedback are used, along with high-frequency peaking, to obtain flat gain and good input and output VSWR characteristics.

reply TUNE. To check on the variable elements, a printout of the tune table may be obtained by replying with TT. Up to four element parameters may be tuned at one time. After the analysis is complete, the element values are reset to their values before tune was initiated.

The title, frequencies, and outputs may be changed by simply replying with TITLE, FREQ, or OUT. Video plotting on the HP graphics terminal is accomplished by the reply VIDEO, followed by the output and column numbers associated with the desired output. The command, ERASE, stops the plotting.

Two very helpful replies that can be used when designing circuits are CONVERT and REACTANCE. CONVERT automat-

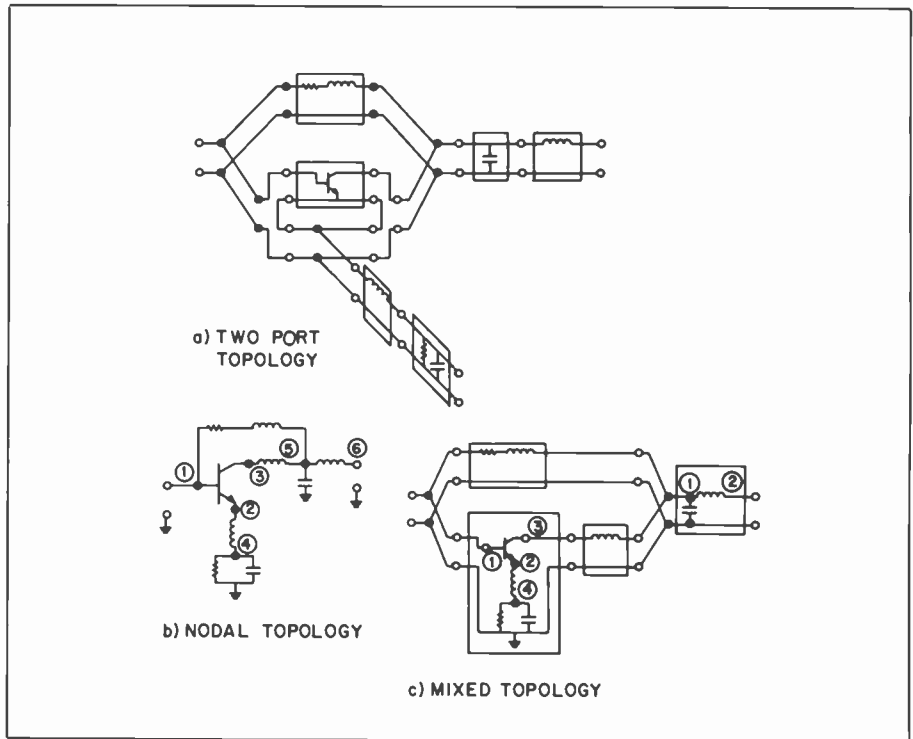
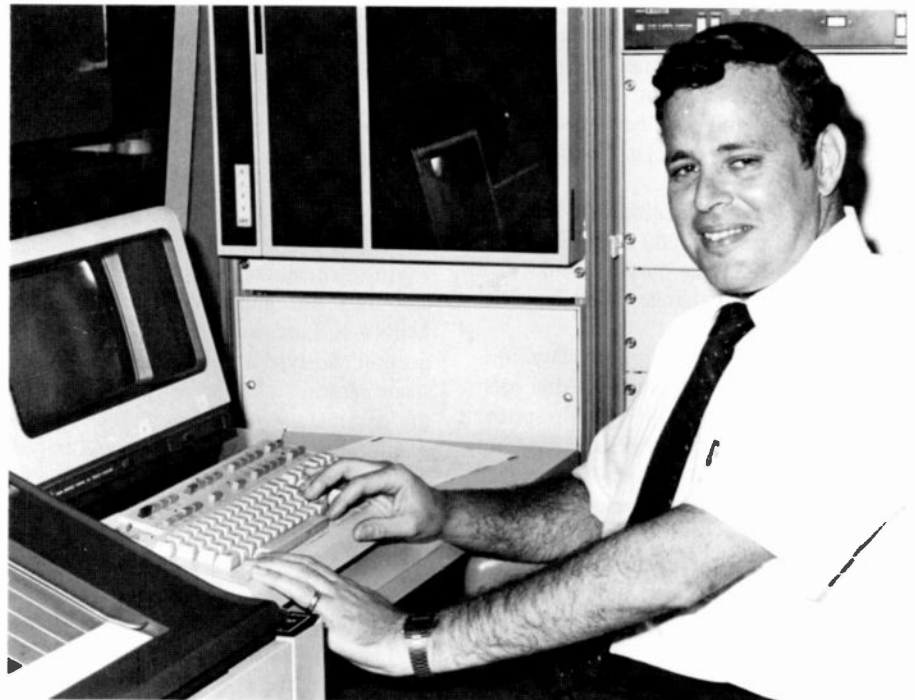


Fig. 6. Circuit topologies used in analyzing the wideband amplifier of Fig. 5. (a) two-port topology; (b) nodal topology; and (c) mixed topology consisting of both two-port and nodal topology.

ically converts all Z and Y elements in the network to equivalent SRLC or PRLC elements. REACTANCE provides the L and C values required to obtain a specified impedance or admittance at two different frequencies.

The reply HELP allows listing of the most recent tables of elements, connections, outputs, replies, and limitations. START allows restarting ANA so that a new disk file may be read. END or OFF terminates execution of ANA.

Stewart Perlow, Member of the Technical Staff, RCA Laboratories, received his BEE from City College of New York and MSEE from the Polytechnic Institute of Brooklyn. His nineteen years of professional experience include RF and microwave component development, contributions to studies of distortion relationships in RF signal processors, and computer-aided design and measurements. Mr. Perlow is presently with the Consumer Electronics Research Laboratory, where he is involved in development of low-cost front ends for 13-GHz direct broadcast satellite receivers, and computer-aided design. He received an individual RCA Laboratories Outstanding Achievement Award in 1980. Mr. Perlow is a member of Eta Kappa Nu and the IEEE. Contact him at:
RCA Laboratories
Princeton, N.J.
TACNET: 226-3168



ANA
IF LATEST INFO ON ANA IS REQUIRED TYPE 'HELP' <REV. 0.3>

TITLE:WIDEBAND AMPLIFIER 0.1-2.0 GHZ
DATA INPUT-TERM,DISC,MAG TAPE?TERM
FREQS.(MHZ)=100,2000,100
OUTPUT # 1:GAIN
OUTPUT # 2:GA1
OUTPUT # 3:GA2
OUTPUT # 4:VSWR
OUTPUT # 5:STAB
ELE NO 1:CONN,TYPE=PP
ELE NO 2:CONN,TYPE=SE SRLC
R,L(NH),C(PF)=183,3,1E6
ELE NO 3:CONN,TYPE=PP
ELE NO 4:CONN,TYPE=SS
ELE NO 5:CONN,TYPE=SE SPAR
TABULATED DATA FROM TERMINAL?,DISC?,MAG TAPE?DISC
DISC FILE NAME=SPS
NO. OF FIRST DATA LINE=48
ELE NO 6:CONN,TYPE=SE SRLC
R,L(NH),C(PF)=0,2,5,1E6
ELE NO 7:CONN,TYPE=SS
ELE NO 8:CONN,TYPE=PB
ELE NO 9:CONN,TYPE=SE SRLC
R,L(NH),C(PF)=0,1,75,1E6
ELE NO 10:CONN,TYPE=PE PRLC
R,L(NH),C(PF)=12,1E6,2.6
ELE NO 11:CONN,TYPE=EB
ELE NO 12:CONN,TYPE=SS
ELE NO 13:CONN,TYPE=PP
ELE NO 14:CONN,TYPE=PE SRLC
R,L(NH),C(PF)=0,0,1,23
ELE NO 15:CONN,TYPE=SE SRLC
R,L(NH),C(PF)=0,3,526,1E6
ELE NO 16:CONN,TYPE=END

ANALYZE?,CHANGES?,WRITE?DATA
TITLE: WIDEBAND AMPLIFIER 0.1-2.0 GHZ

	100.000	2000.000	100.000		
GAIN					
GA1					
GA2					
VSWR					
STAB					
1 PP					
2 SE	SR	183.000	3.000	1000000.000	
3 PP					
4 SS					
5 SE	SP				
6 SE	SR	0.000	2.500	1000000.000	
7 SS					
8 PB					
9 SE	SR	0.000	1.750	1000000.000	
10 PE	PR	12.000	1000000.000	2.600	
11 EB					
12 SS					
13 PP					
14 PE	SR	0.000	0.000	1.230	
15 SE	SR	0.000	3.526	1000000.000	
16 EN	D				

ANALYZE?,CHANGES?,WRITE?ANA
9:20 AM THU., 9 SEPT, 1982
TITLE: WIDEBAND AMPLIFIER 0.1-2.0 GHZ

FREQ	DB	DEG	MAG	DEG	MAG	DEG	IN	OUT	K	GMAX
100.00	7.9012	168.7	0.1632	-60.9	0.05153	42.51	1.0331	1.109	1.1997	7.914
200.00	8.0203	158.2	0.3004	-94.3	0.08821	55.37	1.0619	1.193	1.1925	8.057
300.00	8.1068	147.9	0.4392	-106.	0.12573	53.26	1.0918	1.288	1.1796	8.182
400.00	8.1273	137.6	0.5601	-114.	0.16155	47.41	1.1186	1.385	1.1690	8.254
500.00	8.2287	127.4	0.6626	-118.	0.19374	39.95	1.1419	1.481	1.1521	8.415
600.00	8.1796	117.4	0.7610	-127.	0.21531	32.06	1.1647	1.549	1.1465	8.416
700.00	8.0844	107.8	0.8748	-134.	0.23026	23.73	1.1917	1.598	1.1423	8.361
800.00	8.1170	98.08	0.9894	-140.	0.24158	14.58	1.2196	1.637	1.1324	8.430
900.00	8.1983	88.45	1.0829	-146.	0.24906	4.463	1.2428	1.663	1.1157	8.553
1000.0	8.2038	79.17	1.1750	-156.	0.24824	-6.08	1.2663	1.660	1.1015	8.597
1100.0	8.3248	69.14	1.2478	-161.	0.24216	-18.8	1.2851	1.639	1.0837	8.745
1200.0	8.3358	59.50	1.3610	-171.	0.23090	-32.3	1.3150	1.600	1.0674	8.814
1300.0	8.3885	50.06	1.4229	-178.	0.21494	-47.9	1.3317	1.548	1.0500	8.933
1400.0	8.4128	40.18	1.5580	-171.0	0.19709	-68.0	1.3690	1.491	1.0284	9.134
1500.0	8.4320	30.48	1.6631	-160.8	0.19211	-91.2	1.3989	1.476	1.0028	9.695
1600.0	8.4776	19.26	1.7465	-155.6	0.20703	-119.	1.4232	1.522	0.97357	0.000
1700.0	8.4004	9.282	1.8145	-145.3	0.23397	-143.	1.4433	1.611	0.94698	0.000
1800.0	8.2070	-1.01	1.8659	-138.1	0.27146	-164.	1.4587	1.745	0.92281	0.000
1900.0	7.9212	-11.1	1.8901	-128.2	0.31268	-176.8	1.4661	1.910	0.90204	0.000
2000.0	7.6705	-22.2	1.8843	-121.3	0.36456	-160.1	1.4643	2.147	0.87510	0.000

ANALYZE?,CHANGES?,WRITE?EL 1
ELE NO 1:CONN,TYPE=1,5 SRLC
R,L(NH),C(PF)=183,3,1E6
ELE NO=2

ELE NO 2:CONN,TYPE=1,2 3,2 SP
TABULATED DATA FROM TERMINAL?,DISC?,MAG TAPE?DI
DISC FILE NAME=SPS
NO. OF FIRST DATA LINE=48
ELE NO=3
ELE NO 3:CONN,TYPE=2,4 SRLC
R,L(NH),C(PF)=0,1,75,1E6
ELE NO=4
ELE NO 4:CONN,TYPE=4,0 PRLC
R,L(NH),C(PF)=12,1E6,2.6
ELE NO=5
ELE NO 5:CONN,TYPE=3,5 SRLC
R,L(NH),C(PF)=0,2,5,1E6
ELE NO=6
ELE NO 6:CONN,TYPE=5,0 SRLC
R,L(NH),C(PF)=0,0,1,23
ELE NO=7
ELE NO 7:CONN,TYPE=5,6 SRLC
R,L(NH),C(PF)=0,3,526,1E6
ELE NO=8
ELE NO 8:CONN,TYPE=6,0 OUT
ELE NO=9
ELE NO 9:CONN,TYPE=END
ELE NO=0
ANALYZE?,CHANGES?,WRITE?

ANALYZE?,CHANGES?,WRITE?DATA
TITLE: WIDEBAND AMPLIFIER 0.1-2.0 GHZ

	100.000	2000.000	100.000		
GAIN					
GA1					
GA2					
VSWR					
STAB					
1 1, 5	SR	183.000	3.000	1000000.000	
2 1, 2 3, 2 SP					
3 2, 4	SR	0.000	1.750	1000000.000	
4 4, 0	PR	12.000	1000000.000	2.600	
5 3, 5	SR	0.000	2.500	1000000.000	
6 5, 0	SR	0.000	0.000	1.230	
7 5, 6	SR	0.000	3.526	1000000.000	
8 6, 0	OU				
9 EN	D				

ANALYZE?,CHANGES?,WRITE?AN
9:27 AM THU., 9 SEPT, 1982
TITLE: WIDEBAND AMPLIFIER 0.1-2.0 GHZ

FREQ	DB	DEG	MAG	DEG	MAG	DEG	IN	OUT	K	GMAX
100.00	7.9012	168.7	0.1632	-60.9	0.05153	42.51	1.0331	1.109	1.1997	7.914
200.00	8.0203	158.2	0.3004	-94.3	0.08821	55.37	1.0619	1.193	1.1925	8.057
300.00	8.1068	147.9	0.4392	-106.	0.12573	53.26	1.0918	1.288	1.1796	8.182
400.00	8.1273	137.6	0.5601	-114.	0.16155	47.41	1.1186	1.385	1.1690	8.254
500.00	8.2287	127.4	0.6626	-118.	0.19374	39.95	1.1419	1.481	1.1521	8.415
600.00	8.1796	117.4	0.7610	-127.	0.21531	32.06	1.1647	1.549	1.1465	8.416
700.00	8.0844	107.8	0.8748	-134.	0.23026	23.73	1.1917	1.598	1.1423	8.361
800.00	8.1170	98.08	0.9894	-140.	0.24158	14.58	1.2196	1.637	1.1324	8.430
900.00	8.1983	88.45	1.0829	-146.	0.24906	4.463	1.2428	1.663	1.1157	8.553
1000.0	8.2038	79.17	1.1750	-156.	0.24824	-6.08	1.2663	1.660	1.1015	8.597
1100.0	8.3248	69.14	1.2478	-161.	0.24216	-18.8	1.2851	1.639	1.0837	8.745
1200.0	8.3358	59.50	1.3610	-171.	0.23090	-32.3	1.3150	1.600	1.0674	8.814
1300.0	8.3885	50.06	1.4229	-178.	0.21494	-47.9	1.3317	1.548	1.0500	8.933
1400.0	8.4128	40.18	1.5579	-171.0	0.19709	-68.0	1.3690	1.491	1.0284	9.134
1500.0	8.4320	30.48	1.6631	-160.8	0.19211	-91.2	1.3989	1.476	1.0028	9.695
1600.0	8.4776	19.26	1.7465	-155.6	0.20703	-119.	1.4232	1.522	0.97357	0.000
1700.0	8.4004	9.282	1.8145	-145.3	0.23397	-143.	1.4433	1.611	0.94698	0.000
1800.0	8.2070	-1.01	1.8659	-138.1	0.27146	-164.	1.4587	1.745	0.92281	0.000
1900.0	7.9212	-11.1	1.8901	-128.2	0.31268	-176.8	1.4661	1.910	0.90204	0.000
2000.0	7.6705	-22.2	1.8843	-121.3	0.36456	-160.1	1.4643	2.147	0.87510	0.000

ANALYZE?,CHANGES?,WRITE?

ANALYZE?,CHANGES?,WRITE?DATA
TITLE: WIDEBAND AMPLIFIER 0.1-2.0 GHZ

	100.000	2000.000	100.000		
GAIN					
GA1					
GA2					
VSWR					
STAB					
1 PP					
2 SE	SR	183.000	3.000	1000000.000	
3 PP					
4 1, 2 3, 2 SP					
5 2, 4	SR	0.000	1.750	1000000.000	
6 4, 0	PR	12.000	1000000.000	2.600	
7 3, 0	OU				
8 SE	SR	0.000	2.500	1000000.000	
9 PP					
10 1, 0	SR	0.000	0.000	1.230	
11 1, 2	SR	0.000	3.526	1000000.000	
12 2, 0	OU				
13 EN	D				

ANALYZE?,CHANGES?,WRITE?

Program-size limitations

The present version of ANA is limited to a maximum of 100 elements. The maximum node designator is 30, which means that any network or subnetwork can have a maximum of 30 nodes. If, however, there are several nodal subnetworks, each may have up to 30 nodes. The nodal numbers for each subnetwork are completely unrelated to those of the other subnetworks.

The maximum number of frequencies for any analysis is 21. The product of frequencies and tabulated elements (the number of total lines in the TAB data file) is limited to 84. If all 21 frequencies are used for an analysis, this value limits the number of transistors to four. However, reducing the number of frequencies to 10 allows the use of eight transistors.

The maximum number of coupled lines, or unhomogeneous coupled lines, is limited

to 20 pairs. If any of these limits are exceeded, ANA informs the user of the violation.

Example: Wideband amplifier, Figure 5

The following analysis is done in three different ways. The first method uses a pure, two-port analysis. It is shown here as an example of a parallel branch within a series structure that is within a parallel path. The topology is shown in Fig. 6a.

All the program prompts and the user responses are shown. The initialization of the input data ends at element 16 by responding with END. The input data is then visually verified by using DATA, and an analysis is performed with the AN command.

The elements are then changed by using the EL XX command so that the second method of analysis, purely nodal topo-

graphy, is used. This configuration is shown in Fig. 6b.

The third method of analysis uses both two-port and two-nodal subnetworks, as shown in Fig. 6c. The data listing is shown (page 53), but the actual changing of elements and analyses has been left out.

In this particular case, it is evident that the nodal configuration is far simpler than the two-port; this is not true in general. This complex case is included here to indicate ANA's versatility in analyzing circuit topology.

Acknowledgment

The writer wishes to thank the users of ANA for the many helpful suggestions incorporated into the program. His special acknowledgments go to R.M. Evans, A. Presser, B.S. Perlman, and G.E. Theriault for their continuous flow of ideas.

RCA Review available now

The two most recent issues (June 1982 and September 1982) of the *RCA Review* are now available. For additional information, contact Ralph Ciafone, Editor, RCA Laboratories, TACNET: 226-3222.

Contents Page, June 1982

An Optical Communication Link in the 2.0-6.0 GHz Band
Daniel W. Bechtle and Stefan A. Siegel

Fluorescent Tracers—Powerful Tools for Studying Corrosion Phenomena and Defects in Dielectrics
Werner Kern, Robert B. Comizzoli, and George L. Schnable

Simplified Analysis of Kinescope Electron Guns
D. A. deWolf

Miniature Beryllia Circuits—A New Technology for Microwave Power Amplifiers
F.N. Sechi, R. Brown, H. Johnson, E. Belohoubek, E. Mykiety, and M. Oz

Interpreting the Beta Versus Collector Current and Temperature Characteristics of a Transistor
Robert Amantea

Positive and Negative Tone Near-Contact Printing of Contact Hole Maskings
Lawrence K. White

Contents Page, September 1982

Chemically Vapor-Deposited Borophosphosilicate Glasses for Silicon Device Applications
Werner Kern and George L. Schnable

A Radiation Hardened 256×4 Bulk CMOS RAM
L.S. Napoli, R.K. Smeltzer, R. Donnelly, and J. Yeh

Single Sideband, Amplitude Modulated, Satellite Voice Communication System Having 6000 Channels per Transponder
Krishnamurthy Jonnalagadda

Broadband Microwave Power Amplifiers Using Lumped-Element Matching and Distributed Combining Techniques
R.L. Camisa and A. Mikelsons

Offset Near-Field Gregorian Antenna Scanning Beam Analysis
Eugene C. Ngai

A Simplified Real Frequency Technique for Broadband Matching a Complex Generator to a Complex Load
B.S. Yarman

The Photoresponse of Thin-Film PtSi Schottky-Barrier Detectors with Optical Cavity
Hammam Elabd and Walter F. Kosonocky

Theory of Large-Angle Deflection of Electrons in the Magnetic Field Inside a Television Tube
Basab B. Dasgupta

Online Literature Searching

Did you know that the following databases are available to you for online searching?

Conference Papers Index, 1973 to present—provides access to records of more than 100,000 scientific and technical papers presented at over 1,000 major regional, national and international meetings each year.

RCA TAD (Technical Abstracts Database), 1968 to present—provides access to records of more than 18,000 RCA technical documents, including technical reports, engineering memoranda, unpublished manuscripts, patents, and technical notes.

Your RCA librarian will be pleased to assist you in searching these databases. . . and many others, too.

Modeling the human visual system

High-quality television pictures are the goal, but what constitutes quality? What kind of image processing produces the best visual effect? To find out, these RCA researchers are trying to quantify psychological and physiological aspects of the human visual system.

Abstract: *Considerable progress has been made recently in understanding certain aspects of early information processing in the human visual system. For example, there is good evidence that the visual system is sensitive to information localized in both space and spatial frequency. Using this and other results, we now can build models applicable to several interesting image-quality and image-processing problems. Examples discussed include the prediction of visible changes in image sharpness and the development of efficient algorithms for image encoding.*

The final test of a television picture comes when a viewer looks at it and says, "That's a good picture." For the viewer, this judgment is simple and requires no understanding of operations of the eye and brain. Indeed for all of us, seeing seems so direct and effortless that we remain unaware of the complex visual processing that underlies a statement like, "That's a good picture." Coming to understand some of that processing is part of the function of the Image Quality and Human Perception Group at RCA Laboratories.

RCA has a long tradition of vision research. In the 1940s, Al Rose introduced noise analysis into models of vision, establishing a law that bears his name (the Rose-DeVries law) and a conceptual framework that is now basic to much work in visual discrimination. And in the 1950s, Otto Schade showed how we could consider the eye as part of an overall optical

system, and applied the techniques of linear systems analysis to characterize its performance. Schade's work laid the foundations for much of our current thinking about both biological and nonbiological optical systems: A symposium in Schade's honor was held at this year's convention of the Optical Society of America.

The contrast-sensitivity function

Schade's approach was to quantify human visual sensitivity by using gratings with sinusoidal luminance profiles—the same inputs he had used for studying optical and electro-optical systems.¹ A sinusoidal grating is illustrated in Fig. 1. By varying the spatial frequency, and then measuring the

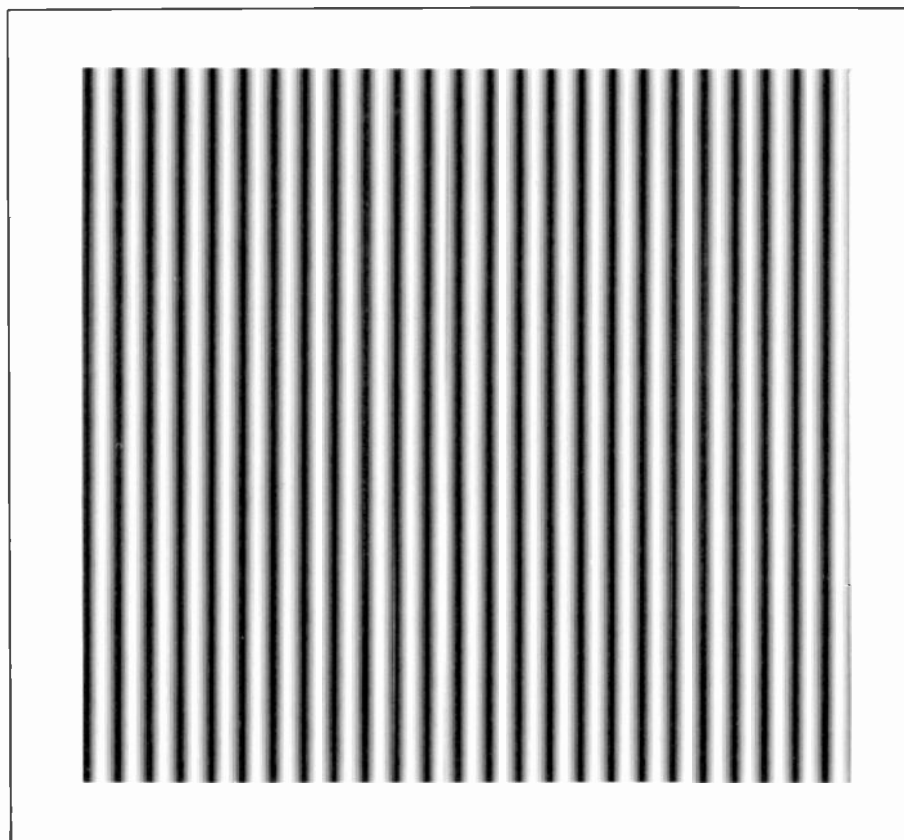


Fig. 1. Patch of a one-dimensional luminance sine-wave grating. At a viewing distance of 18 inches, its frequency is approximately 3 cycles/degree.

©1982 RCA Corporation
Final manuscript received October 8, 1982.
Reprint RE-27-6-9

minimum contrast necessary for detection, Schade derived what is now known as the "contrast-sensitivity function" (CSF), which is closely related to the "modulation-transfer function" (MTF) familiar to engineers. Figure 2 shows a typical contrast-sensitivity function.² Note that sensitivity peaks at about 3 cycles/degree, and drops at both higher and lower spatial frequencies.

You can visualize your own CSF by looking at Fig. 3, which shows a sinusoidal grating whose frequency is swept logarithmically along the abscissa, and whose contrast is swept logarithmically along the ordinate. You should see an inverted, U-shaped envelope in which gratings are visible. This envelope is not present in the picture, but only in your perception of it. Move the page either closer or farther from you, and the peak will shift.

The CSF is a natural quantity to measure if one conceives of the visual system as containing a single, broadly tuned, linear filter, followed by a detector stage with a fixed threshold. But the visual system is more complicated than that; more complicated measurements must be made if one is to model the eye effectively. The current view, pioneered by Campbell and Robson and others around 1968, is that the visual system contains a bank of spatial-frequency-tuned channels, which function more or less independently of each other.³

In this model, the overall CSF of the eye is the outer envelope of the CSFs of the individual channels; Fig. 4a illustrates the idea. Support for this scheme comes from adaptation experiments, in which one "fatigues" the channels' responses to a given spatial frequency by having a subject stare at a sinusoidal grating for a long time. After such adaptation, it is found that a notch has been cut in the CSF, as shown in Fig. 4b. This indicates that the channels sensitive to the adapting stimulus have had their sensitivities reduced.⁴

You can convince yourself of the adaptation effect by staring at the grating of Fig. 1, and then examining Fig. 3. Adaptation takes about one minute, and your eyes should be constantly moving during adaptation to avoid build-up of a static after-image. When you look at the swept sine-wave pattern, a flattening or a dip should be visible near 3 cycles/degree. The subset of filters tuned to around 3 cycles/degree have been fatigued by the adaptation, and so they respond less strongly than before.

To understand how the filtering comes about, we must begin at the retina, which consists of an array of about 100 million

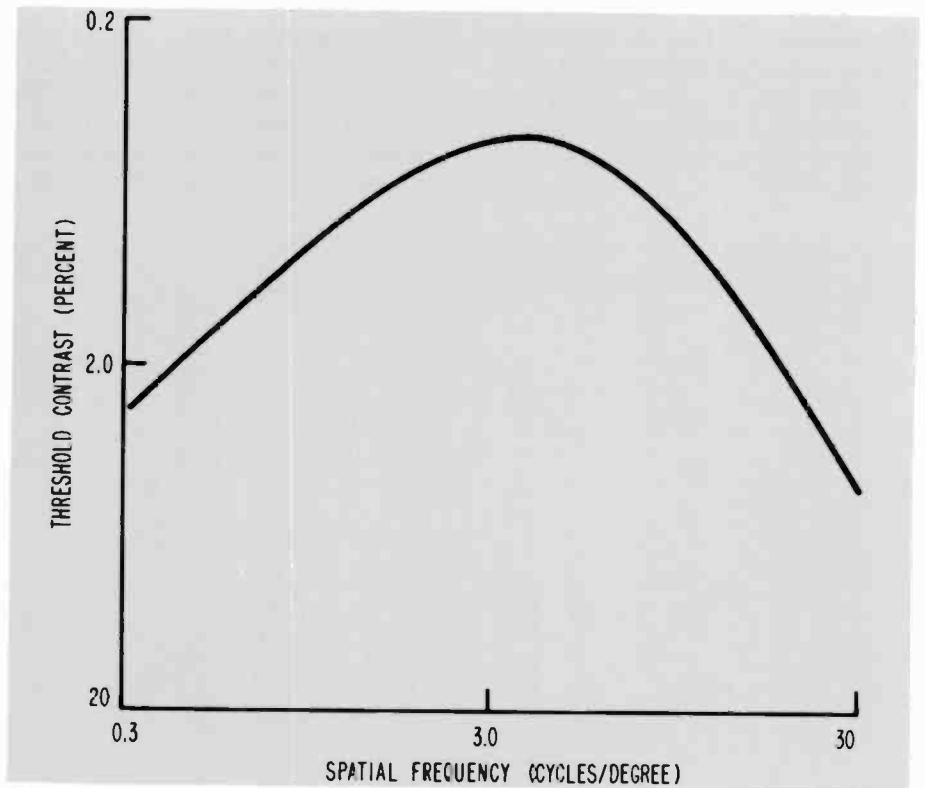


Fig. 2. Contrast-sensitivity thresholds for the human eye for high-luminance displays (that is, above 30 fL). The ordinate is the threshold contrast necessary for detection of a sine-wave grating.

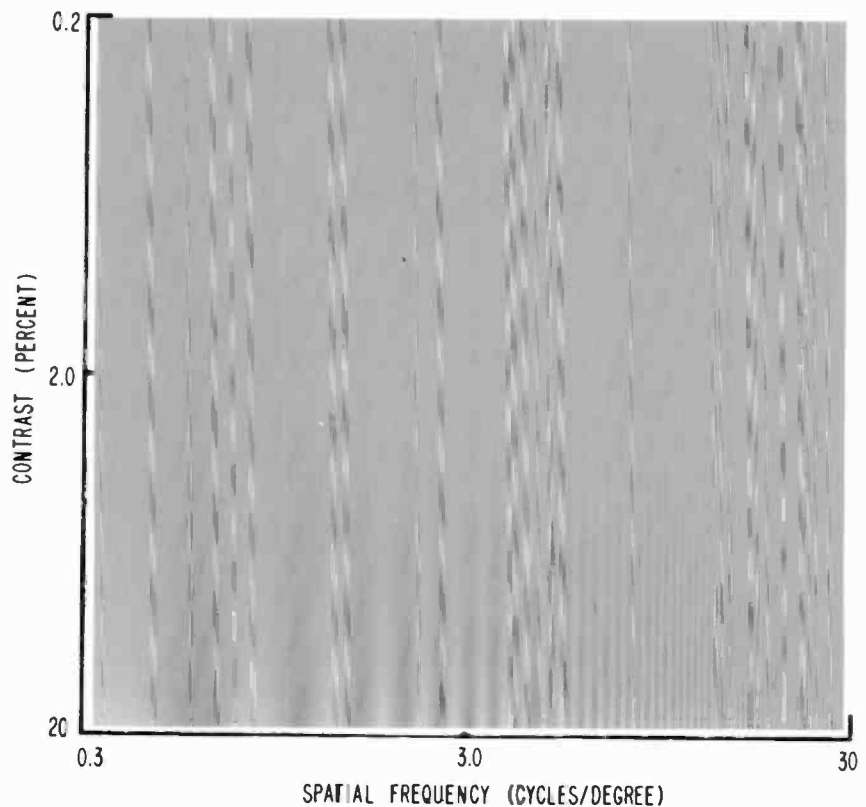


Fig. 3. Plot of a sinusoidal grating whose frequency is swept logarithmically along the abscissa and whose contrast is swept logarithmically along the ordinate. Using this plot, you can see your own contrast-sensitivity function, which should be similar to that given in Fig. 2. The units of the abscissa are valid when the figure is viewed from a distance of 18 inches.

photoreceptor cells. Each photoreceptor responds to the light at one point in the visual field. Next, the outputs of many photoreceptors in a small patch of retina are combined into a new set of signals within the eye.

These signals are passed from the eye to the brain through the optic nerve, which is a bundle of about 1-million nerve fibers. Each fiber corresponds to a local region on the retina,⁵ and thus to a local region in visual space. The output of a fiber repre-

sents, in effect, a weighted sum over space, which is called its "receptive field." Receptive fields of neighboring fibers overlap. The weighting functions have both positive and negative parts; a typical cell's receptive field will resemble a "difference-of-Gaussians" shape, sometimes known as a "Mexican-hat function." Such a function is shown in Fig. 5.

The difference-of-Gaussians function serves as a simple bandpass filter, selecting out information in a certain spatial-frequency range. A large array of fibers, whose receptive fields cover the visual scene on the retina, can represent a bandpassed and sampled version of the scene. Of course, to fully represent the scene, all regions of the spectrum must be represented, which is to say that there must be cells with receptive fields of all sizes. This is true in the eye; it is also true in the brain, where cells are similarly found to be tuned for specific bands of spatial frequencies, localized within finite regions of visual space.⁵

Applications

Building on the concept of receptive fields, solutions to a number of interesting problems can be obtained. For example, it has been found that when the outputs of the receptive fields are combined over space according to a simple summation rule, that the threshold visibility of arbitrary luminance patterns can be accurately predicted.^{6,12}

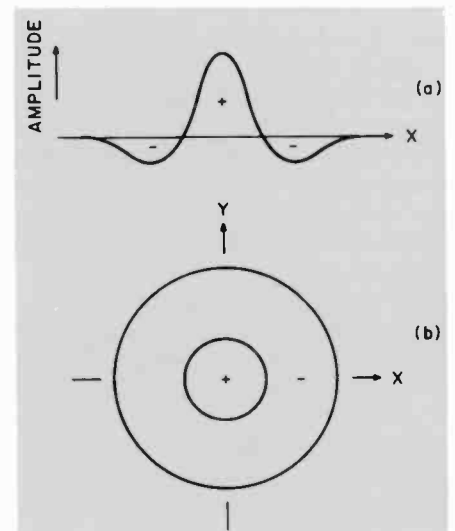


Fig. 5. A receptive field. Figure 5a shows the relative response of the receptive field through its midline. Figure 5b shows the receptive field response from above. In the center of the field, the receptive field's response is positive. In a ring surrounding the center, the receptive field's response is negative.

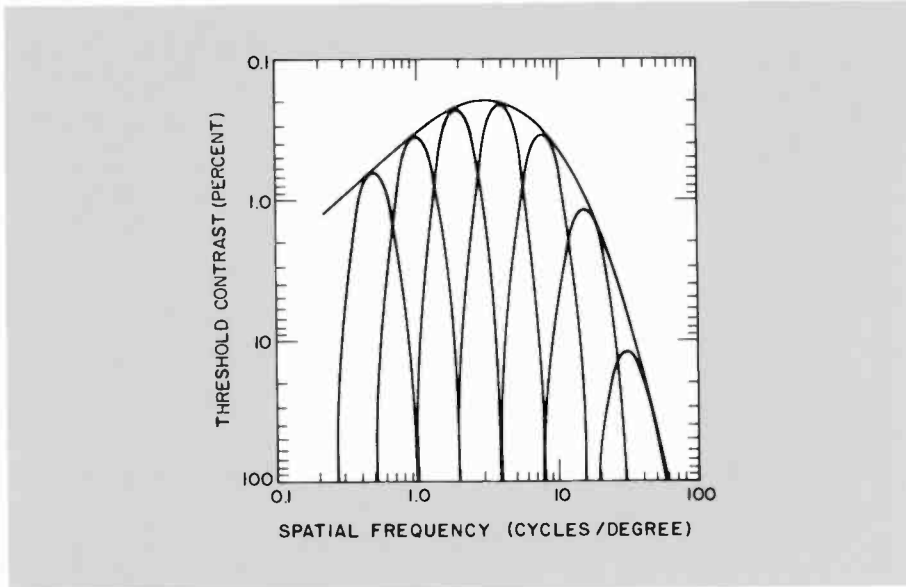


Fig. 4a. A bank of spatial-frequency filters in the human visual system. Overall response determines the contrast-sensitivity function of Fig. 2.

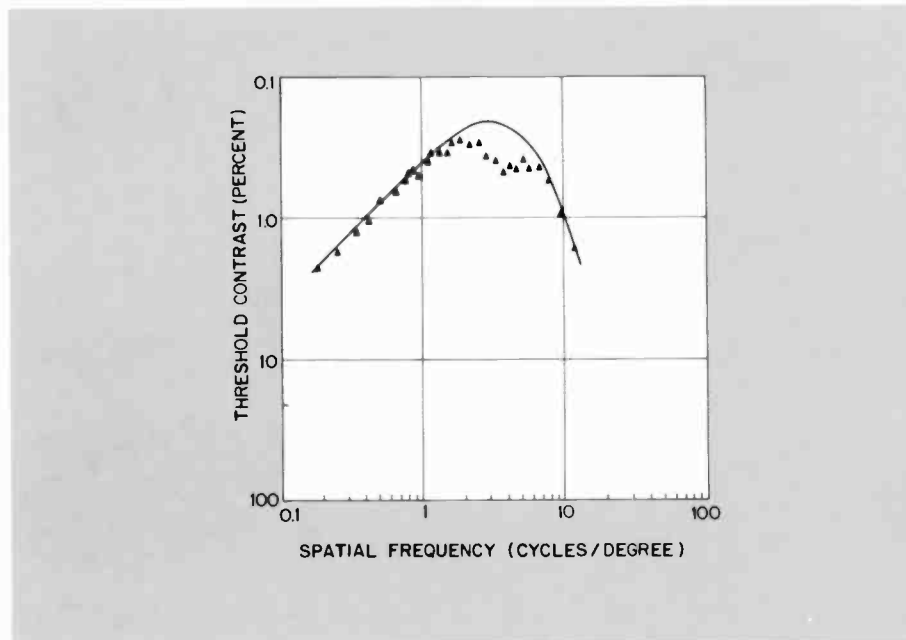


Fig. 4b. Measured results from an adaptation experiment that support the representation indicated in Fig. 4a. In this experiment, an observer's contrast-sensitivity function was first measured, as indicated by the solid line. Next, the observer viewed a high-contrast, 6.4-cycle/degree "adapting" grating for an extended period before again having his contrast-sensitivity function remeasured, as indicated by the data points. It may be seen that only near the adapting frequency is the observer's threshold sensitivity reduced. That is, the adaptation effect was frequency specific, supporting the idea that spatial-frequency information is processed by the human visual system in relatively narrow spatial-frequency bands, as indicated in Fig. 4a. These data are from reference 19, after reference 4.



(a) Original



(b) $\Delta J = -3$ jnd's



(c) $\Delta J = -10$ jnd's

Fig. 6. Examples of images that differ in their image sharpness by roughly 3 and 10 jnd's. When viewed from about 18 inches, there is a 3-jnd difference between Fig. 5a and Fig. 5b, and a 10-jnd difference between Fig. 5a and Fig. 5c.

In the two examples given below, the receptive field concept is used differently. In the first example, where noticeable differences in image sharpness are predicted, it is assumed that the outputs of the receptive fields are combined over space in a way that suggests the visual system performs a Fourier-like decomposition of spatially complex scenes. This simplification allows a large number of problems to be solved analytically with reasonable precision.^{7, 8}

In the second example, where image processing is achieved by use of a pyramid structure, an image transform is constructed that contains features of the receptive field structure of the human visual system.^{9, 10} Image transforms of this type have some interesting advantages when compared to more conventional approaches.

Predicting just-noticeable differences in image sharpness

One of the principles of display design is that the performance of a display should match the perceptual requirements of the observers. One aspect of this principle is that information that cannot be seen should not be transmitted. Thus, a basic display-design issue is knowing when a change in a display variable will result in a perceivable change in display performance. In this section we describe a simple signal-detection model for the visual system that predicts answers to questions of this type. We will illustrate the application of the model by applying it to the problem of predicting noticeable differences in displayed image sharpness.

Since the work of Schade, researchers

have known that the overall spatial-frequency response of a display determines its perceived image sharpness.¹¹ One aspect of a display's frequency response is given by its modulation-transfer function (MTF), which specifies the ratio of the displayed contrast of sine-wave gratings divided by their input contrasts. Phase variations are not included in the modulation-transfer function.

When will a change in a display MTF result in a perceivable change in displayed image sharpness? The type of analysis required to answer this question is called just-noticeable-difference (jnd) analysis. One jnd is defined as the change in a stimulus necessary for a viewer to see that change 75 percent of the time. Perceptually, one jnd is obviously a small unit. But a 3-jnd change can be seen 99 percent of the time and a 10-jnd change, or more, represents very significant perceptual effects. Exam-

ples of images that differ by roughly 3 and 10 jnd's are shown in Fig. 6.

Fig. 7 shows a schematic of a signal-detection model for the visual system that accurately predicts when changes in display MTF can be seen.^{7, 8} There are five elements in the model. The first element is a bank of spatial-frequency filters (or channels) as is suggested by Fig. 4a. These act to decompose an arbitrary scene into relatively narrow, contiguous bands of spatial-frequency information. Each channel is centered about a retinal frequency ν , given in cycles/degree, and has a bandwidth $\Delta\nu$. We assume that luminance information falling within a channel is processed independently of information falling within any other channel. We also assume that the channel bandwidths, for frequencies above 1.5 cycles/degree, are an octave wide: that is, $\Delta\nu/\nu$ equals 2/3. This estimate is in agreement with much psychophysical evi-

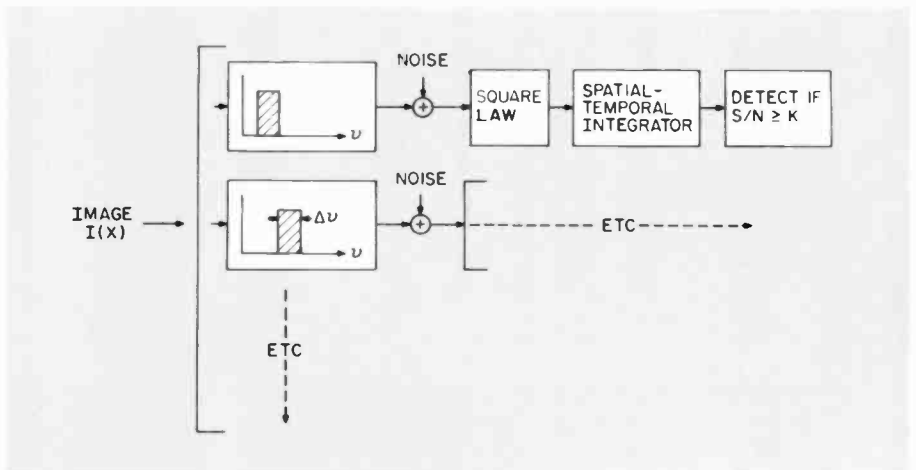


Fig. 7. The visual signal-detection model.

dence.¹² In making these assumptions we have, in effect, taken the large number of receptive fields that exist over visual space and combined them into a relatively small number of frequency-specific channels. This simplification allows us to develop an analytic model for visual processing that is easily applicable to a wide range of problems and is still reasonably accurate. The second element within each channel is the addition of several sources of visual noise that interfere with the perception of a signal. The third element is a square-law nonlinearity. The motivation for the nonlinearity is provided by our interpretation of basic contrast-detection experiments. Although the explanation of these experiments requires a nonlinear stage, the actual choice of a square law is motivated in part by its mathematical simplicity. The fourth element of the model is a spatial-temporal integrator to smooth the squared output from each channel. The fifth and final element is a detection stage, which specifies the probability of detecting a signal change occurring within the channel.

Whether a change in display MTF will result in a perceived change in image sharpness obviously depends on the scenes being displayed. We have found that for pictorial scenes a very good test image is a one-dimensional luminance edge transition.⁷ Observers are usually very sensitive to small changes in display MTF when looking at edges, and edges are often the most important feature in pictorial scenes. Other important display variables that determine whether a noticeable change in image sharpness will occur are the display brightness and display signal-to-noise ratio. We will assume

here high-brightness displays (that is, above 30-foot lamberts) with high signal-to-noise ratios.

Once a scene has been selected, the signal-detection model (Fig. 7) can be used to predict when a change in display MTF will result in a perceivable change in displayed image sharpness. The operation of the model is straightforward, since changes in display MTF will result in changes in the signals existing within the appropriate frequency-specific channels. The model simply converts these signal changes within each channel to the appropriate number of perceived jnd's.

To facilitate the application of the signal-detection model, we have developed a graphical representation of it called a jnd diagram.¹¹ A jnd diagram is shown in Fig. 8a, where the quantity $m(\nu)R(\nu)$ is plotted as a function of retinal frequency ν , in cycles/degree. Retinal frequency is given by

$$\nu = \pi r f / 180,$$

where r is the viewing distance in inches and where f is the display frequency in cycles/inch. As before, $R(\nu)$ represents the display MTF; the quantity $m(\nu)$ is a function that represents the scene being viewed. For a one-dimensional edge transition, with edge height ΔI and mean luminance \bar{I} , $m(\nu)$ can be shown to be given by

$$m(\nu) = (1/14\pi^2)(\Delta I/\bar{I})^2(\Delta\nu/\nu),$$

where $\Delta\nu$ is the bandwidth of a frequency-specific channel and where ν is the center frequency of the channel.⁷ If, as stated earlier, we let $\Delta\nu/\nu$ equal 2/3, and take a 100-percent contrast edge (that is, $\Delta I/\bar{I} = 2.0$) then $m(\nu) = 0.14$.

Returning now to the jnd diagram, each vertical line, located at the key frequencies of 0.5, 1.5, 3.0, 6.0, 12, 24, and 48 cycles/degree, defines the center of a frequency-specific channel in the human visual system (as indicated in Fig. 4a). On each vertical line the distances between the small tic marks indicate the change in $m(\nu)R(\nu)$ necessary over that channel for an observer to perceive a 1-jnd change in displayed image sharpness. When jnd changes occur over more than one channel, the total perceived change, to a first approximation, can be obtained by simply adding the jnd's occurring over each frequency-specific channel.⁷

Figure 8b illustrates two examples of the application of the jnd diagrams. This figure is identical to Fig. 8a except for the four curves, which represent different values of $m(\nu)R(\nu)$. In all the cases, we have assumed a 100-percent contrast-edge transition as our image, so that $m(\nu)$ equals 0.14. Thus, the differences between the curves are only due to differences between the MTFs, $R(\nu)$.

Figure 8b, case A, represents the MTF of an extremely good display for which there exists only one full jnd (at 24 cycles/degree) in image sharpness between this display and the perfect display where $R(\nu)$ equals 1.0. Or, said differently, if the bandwidth of this display were increased infinitely, an improvement of only one jnd in the sharpness of the image would be realized. Case B is more typical of television viewed at normal viewing distances. For this situation the increase in display bandwidth, defined where $R(\nu)$ equals 1/2, necessary to produce one additional jnd in

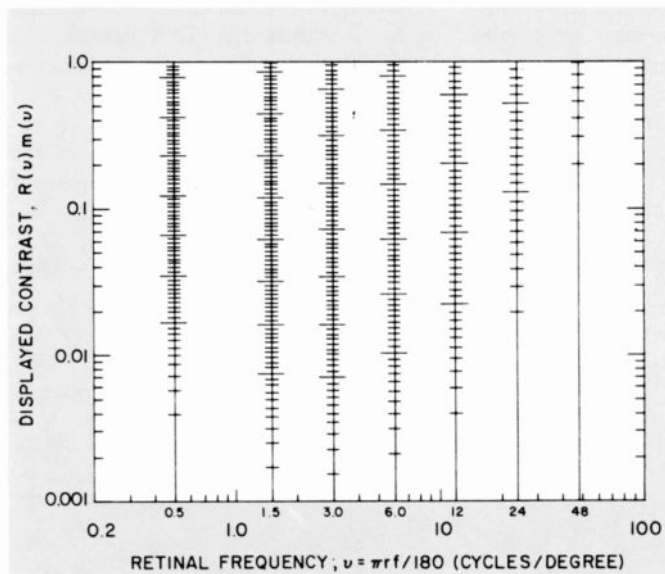


Fig. 8a. Jnd diagram appropriate for high-luminance displays.

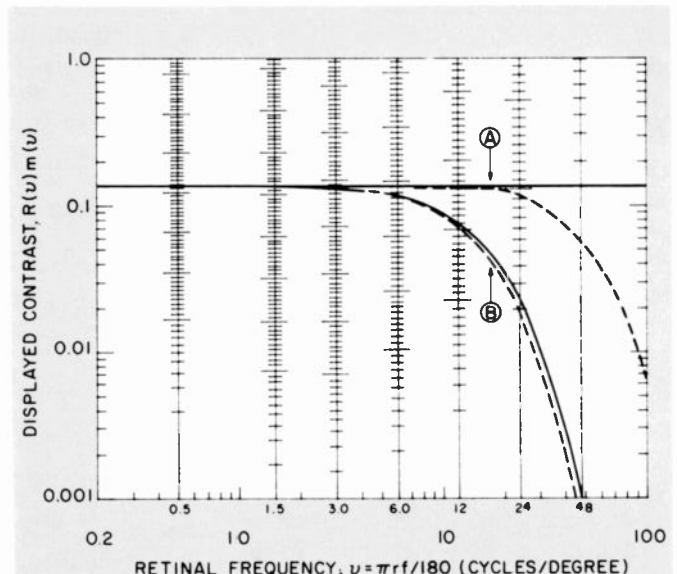


Fig. 8b. Two applications of the jnd diagram shown in Fig. 8a.

image structure is only about 0.7 cycles/degree. This example indicates that, for practical displays, perceivable increases in image sharpness can result from relatively small changes in display MTF.

Figure 9 shows the results of actual experiments with pictorial scenes and MTFs similar to those shown in Fig. 8b.⁷ The solid line in Fig. 9 shows the predictions from Fig. 8b, assuming that the pictorial images are approximated by a 100-percent contrast-edge transition. It may be seen that the predictions of the model, as summarized in the jnd diagram, correspond to the measured values obtained with pictorial scenes.

In conclusion, this example has shown that it is possible to incorporate a number of important visual properties into a relatively simple model that accurately predicts when a change in display MTF will be seen. A large number of other applications have also been computed, including the perceptual effects resulting from either sampled or raster displays.^{7, 8}

Image processing based on the visual system

By understanding the visual system, we can also develop techniques for the efficient digital encoding of images. The goal is to represent images in a way that emphasizes image information that is important to the eye, at the expense of information that is redundant or visually insignificant. Digitized images are normally represented in terms of the intensities of individual pixels. A popular alternative is to store a transform representation in which the coefficients of, say, the Fourier transform of the image are stored and the image is later reconstructed via the inverse transform. In an interesting variant on the transform coding theme, we can generate a representation in which the basis functions resemble the receptive fields in the human visual system. The image is then represented in terms of the responses of many receptive fields of many sizes, located at many positions.

The basis functions in such a scheme are not orthogonal, which leads to some complexities in generating and inverting image representations. However, Peter Burt of Rensselaer Polytechnic Institute has developed a convenient computational structure for manipulating this kind of encoding scheme.⁹ We have been collaborating with Burt in applying the scheme to the efficient encoding and decoding of images.¹⁰

The basic idea is shown in Fig. 10. A 256×256 pixel image is blurred by a Gaussian blur function in successive stages.

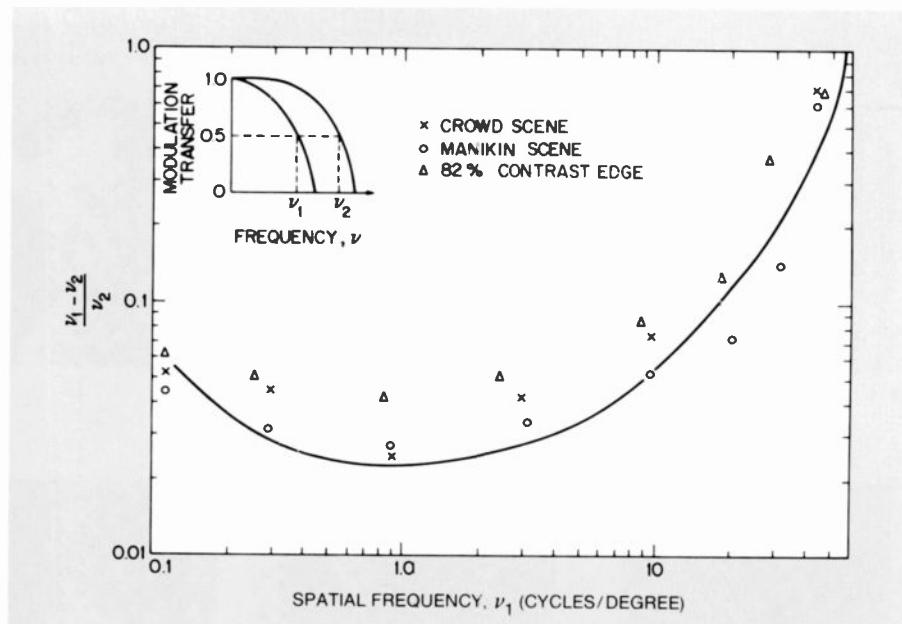


Fig. 9. Measured data for the change in display bandwidth, from ν_1 to ν_2 , necessary to produce a 1-jnd difference in image sharpness as a function of the initial display bandwidth ν_1 . The bandwidths are all defined where $R(\nu)$ equals 1/2. Different symbols represent different scenes. The solid line is the predicted result from Fig. 8b obtained when the change in any one channel was 1 jnd.

At each step, the effective size of the Gaussian blur function is doubled. At the same time, the linear sampling density is halved (so the number of samples per image area is quartered). Next, difference-of-Gaussians images are formed by subtracting the values of adjacent blurred images. The result is a sequence of images representing different spatial frequency bands. Information within each image is localized in both space and spatial-frequency. The bands are spaced logarithmically in frequency, since each image represents frequencies an octave below that of its predecessor. And the sampling density becomes sparse as the frequency becomes lower.

The resulting representation is called a "pyramid," because each image is computed from the one below and because there is a 4-to-1 convergence of pixels from one level to the next. The number of samples in the highest frequency bandpass image (that is, the image at the bottom, left, of Fig. 10d) is the same as the number in the original image. The next-lower level has 1/4 as many, the next has 1/16 as many, and so on. Thus, the image is represented by $1 + 1/4 + 1/16 + \dots$, or 4/3 times as many samples as were in the original image. But note that 75 percent of these samples represent the high frequencies, and only 25 percent represent the medium and low frequencies.

The high-frequency image is densely sampled, but its sample values can be coarsely

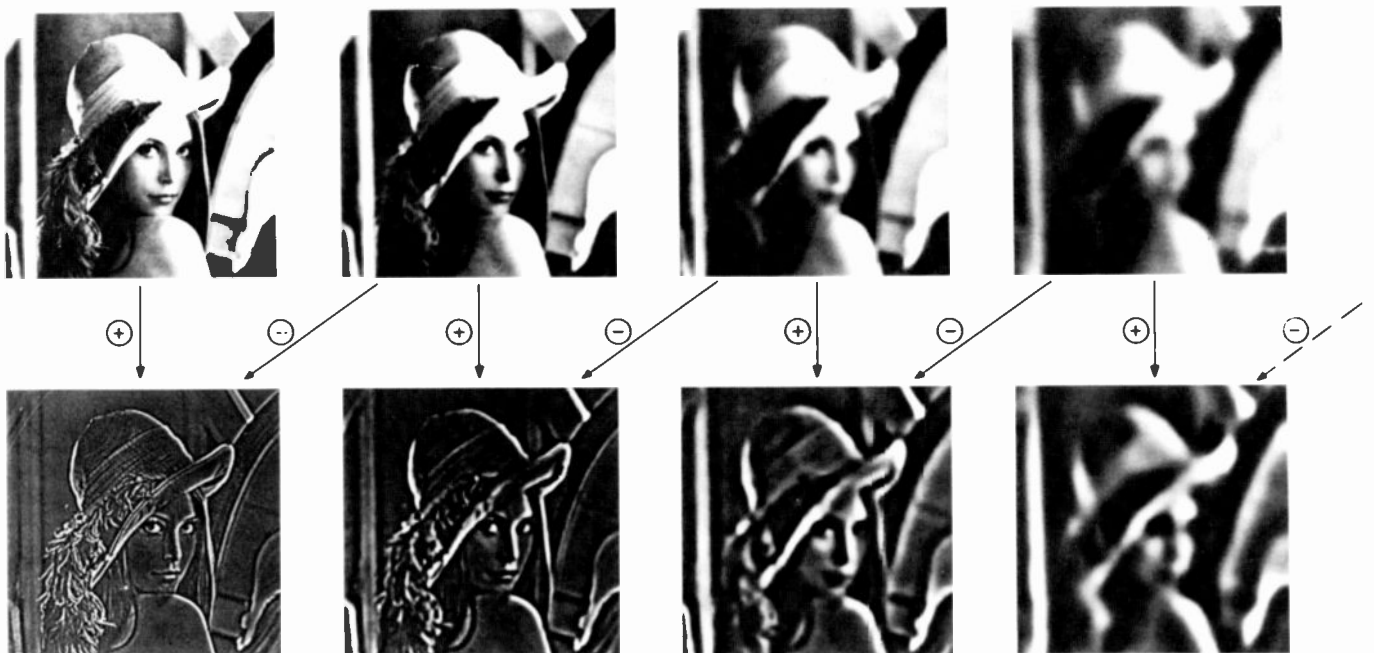
quantized. That is, in digitizing the sample values, one can use a small number of bits. There are two reasons for this. First, there is relatively little high-frequency energy in most scenes, so that the intensity values in the high-frequency image tend to be small, clustering around zero. Thus, the dynamic range and the entropy are small to begin with. Second, the eye is fairly insensitive to contrast errors in the high frequencies, and so the errors due to coarse quantization tend not to be noticed.

The medium- and low-spatial-frequency images require finer quantization. There is relatively more energy in these frequency bands, and the visual system is more sensitive to the errors. However, these images are sampled more sparsely. Only 25 percent of the samples in the image code correspond to the medium and low frequencies. Thus, the high-frequency image is densely sampled but coarsely quantized, while the other images are sparsely sampled but finely quantized. The result is an efficient encoding that puts the information where it is needed.

This encoding scheme may be used in concert with other techniques to store or transmit an image at a rate of about 1.5 bits/pixel, which is considerably lower than the standard rate of 8 bits/pixel. An example is shown in Fig. 11.

The pyramid encoding is also quite convenient for a procedure called "progressive transmission." Suppose that an image is

GAUSSIAN PYRAMID



LAPLACIAN PYRAMID

Fig. 10. The sequence of steps by which the pyramid representation is built. In the top row, the image is convolved with a sequence of Gaussian blur functions, leading to a sequence of low-passed images. In the bottom row, "difference-of-Gaussians" images are generated by subtracting adjacent

low-pass images. The resulting images represent information within a given spatial-frequency band, and the band center drops by one octave from one image to the next. Low-frequency images require fewer samples, in proportion to the square of their band center.

being transmitted over a low-bandwidth channel, such as a phone or teletext line. It may take as much as a full minute to transmit the fully detailed image, during which time the viewer patiently (or impatiently) waits. In progressive transmission, a spatially coarse version of the image is sent initially, and finer and finer details are provided as time progresses.^{14, 15} Thus, the viewer quickly gets a sense of what the image is. He can wait longer to see it in full detail or, if he prefers, he can skip to a new image as soon as he sees what the current one is. Figure 12 shows how the pyramid representation can be used in transmitting a progressive sequence of images. The information in the low frequencies is sent first, followed by successively higher octaves of frequency. In the example shown here, additional data-compression techniques were used and the blur functions used were somewhat different from the difference-of-Gaussians. The numbers below the images indicate the number of bits/pixel required for each stage of the progressive transmission. Even at 0.1 bits/pixel, we can get a good sense of what the pic-

ture portrays. The lady can be recognized at 0.31 bits/pixel; most of the details are available at 0.81 bits/pixel; and the last details are filled in at 1.58 bits/pixel. The

pyramid appears to be well suited for a variety of other image-processing tasks, including preprocessing for pattern recognition and image enhancement.



Fig. 11a. The original image before encoding. It is represented as a 256 by 256 array of pixels, with 8 bits/pixel. Figure 11b is the same image reconstructed from an encoded representation, based on the pyramid structure of Fig. 10. High-frequency information is coarsely quantized but finely sampled; low- and medium-frequency information is finely quantized but coarsely sampled. The result is an encoding requiring only 1.5 bits/pixel, which remains faithful to the original.



Fig. 12. Progressive transmission of an image by means of the pyramid scheme. The low-frequency information is sent first, and high frequencies are sent as time goes on. One can get a good impression of the final image content quite

quickly, without waiting for all the bits to be transmitted. The number beneath each picture indicates the accumulated number of bits/pixel required at that stage of transmission.

Conclusions

A central concept in much of current vision research is that the visual system performs an early decomposition of images by the use of receptive fields, which are filters selectively responsive to limited ranges of spatial frequency and space. The outputs

of filters are further limited by inherent noise before they are sent to a detector stage, which combines their outputs over space and spatial frequency. Although these general properties of the receptive fields are established, the specific properties of the receptive fields remain areas of active

research in our laboratory and in many others.

As the two examples outlined here demonstrate, however, we now have sufficient understanding of the receptive field properties to realize some interesting results. These ideas have also been applied to a



Authors Edward Adelson, Albert Pica, and Curtis Carlson.

Edward Adelson is a Phi Beta Kappa graduate of Yale University, where he majored in Physics and Philosophy. He received his Ph.D. in experimental psychology at the University of Michigan and performed postdoctoral research at New York University. His research areas have been in vision, visual perception, and image encoding. Currently, Ted is a member of the Image Quality and Human

Perception Research Group at RCA Laboratories, where he is involved in developing models for human motion perception and in developing image-processing algorithms based on aspects of the human visual system.

Contact him at:
RCA Laboratories
Princeton, N.J.
TACNET: 226-3036

Curtis Carlson is a Tau Beta Pi graduate from Worcester Polytechnic Institute, where he received his B.S. degree in Physics in 1967. He received his M.S. and Ph.D. degrees from Rutgers University in 1969 and 1973, respectively. Since joining the technical staff of RCA Laboratories in 1973, Curt has been involved in the general areas of imaging devices, image analysis, and human perception. He is a member of the SMPTE Vision Committee on High Definition Television and was recently a Special Editor of an issue of the SID Proceedings on "Advances in Visual Information Processing." In 1979, he received an RCA Individual Outstanding Achievement Award. Curt is currently Head of Image Quality and Human Perception Research at RCA Laboratories.

Contact him at:
RCA Laboratories
Princeton, N.J.
TACNET: 226-2436

Albert Pica joined RCA Laboratories in 1977. He received his B.S. in Physics from the City College of New York in 1974, and his Masters from Rutgers University in 1976. Since joining RCA he has worked on the CED VideoDisc System helping to build a digital scanning capacitance microscope that measures disc-stylus capacitance variations. He has also performed research in visual perception. Albert is presently working in the Image Quality and Human Perception Research Group, where he specializes in computer and image processing systems as well as computer simulations of human visual performance.

Contact him at:
RCA Laboratories
Princeton, N.J.
TACNET: 226-2859

number of other television problems, such as predicting the required signal-to-noise ratio of different displays¹⁶; determining the number of phosphor-stripe triads required to produce a high-quality color-television image¹⁷; and establishing the convergence requirements for color television.¹⁸

One future objective is to use some of these ideas to perform image enhancement within commercial receivers. As the cost of digital memory comes down, more image processing within the receiver will become practical. The basic question is then: What kind of image processing will produce the best visual effects? Since representations like the pyramid structure described earlier incorporate the receptive field concept of the visual system, they promise to be useful in answering this question.

Acknowledgments

We wish to express our warm appreciation to our colleagues, C.H. Anderson, P.J. Burt, R. Klopfenstein, and R.Sverdlove, for their many contributions to this research.

We also give special thanks to E. Cuomo and G. Zak for making Figs. 1 and 3.

References

1. O.H. Schade, Sr., "Optical and Photoelectric Analog of the Eye," *J. Opt. Soc. Amer.*, Vol. 46, p. 721 (1956).
2. F.L. VanNess and M.A. Bowman, "Spatial Modulation Transfer in the Human Eye," *J. Opt. Soc. Amer.*, Vol. 57, p. 401 (1967).
3. F.W. Campbell and J.G. Robson, "Application of Fourier Analysis to the Visibility of Gratings," *J. Physiol. (London)*, Vol. 197, p. 551 (1968).
4. C. Blakemore and F.W. Campbell, "On the Existence of Neurones in the Human Visual System Selectively Sensitive to the Orientation and Size of Retinal Images," *J. Physiol. (London)*, Vol. 203, p. 237 (1969).
5. F.C. Carterette and M.P. Friedman, *Handbook of Perception*, Vol. V: Seeing. Academic Press, New York, N.Y. (1975).
6. C.S. Harris, Ed., *Visual Coding and Adaptability*. Laurence Erlbaum Ass., Inc., Hillsdale, N.J. (1980).
7. C.R. Carlson and R.W. Cohen, "Visibility of Displayed Information," *Technical Report to the Office of Naval Research*, Cont. No. N0014-74-C-0184 (July 1978).
8. C.R. Carlson and R.W. Cohen, "A Simple Psychophysical Model for Predicting the Visibility of Displayed Information," *Proc. Soc. Infor. Display*, Vol. 21, p. 229 (1980).
9. P.J. Burt, "Fast Filter Transforms for Image Processing," *Comp. Graphics and Image Proc.*, Vol. 16, p. 10 (1981).
10. P.J. Burt and E.H. Adelson, "The Laplacian Pyramid as a Compact Image Code," Rensselaer Polytechnic Institute I.P.L. Report No. 25 (March 1982).
11. O.H. Schade, Sr., *Image Quality*. RCA Laboratories, Princeton, N.J. (1975).
12. H.R. Wilson and J.R. Bergen, "A Four Mechanism Model for Threshold Spatial Vision," *Vision Res.*, Vol. 19, p. 19 (1979).
13. C.R. Carlson and A.P. Pica, "Predicting Just Noticeable Differences in Image Sharpness: The Universal JND Diagrams," Private Communication.
14. V.R. Sloan, Jr. and S.L. Tanimoto, "Progressive Refinement of Raster Scan Images," *IEEE Trans. Comput.*, Vol. C-28, p. 871 (1979).
15. K. Knowlton, "Progressive Transmission of Gray-Scale and Binary Pictures by Simple, Efficient, and Lossless Encoding Schemes," *Proc. IEEE*, Vol. 7, p. 885 (1980).
16. R.W. Cohen, "Applying Psychophysics to Display Design," *Phot. Sci. Eng. J.*, Vol. 22, p. 56 (1978).
17. C.R. Carlson, "Application of Psychophysics to Display Evaluation," *Proc. of the 1982 Int. Display Res. Conf.*, Cherry Hill, N.J. (October 1982).
18. C.R. Carlson, "Convergence Requirements for Color Television," Private Communication.
19. R.W. Cohen, C.R. Carlson, and G.D. Cody, "Image Descriptions for Displays," Office of Naval Research Tech. Report No. N00014-74-C-0184 (May 1976).

Schade's book available from RCA

Image Quality—A Comparison of Photographic and Television Systems, by Otto H. Schade, Sr., gives a technical overview of the concepts developed by the author, and now in universal use, that permit a quantitative evaluation of image quality. Dr. Schade describes in some detail the three basic parameters that determine image quality: the intensity-transfer function, which is a measure of the gray scale; the modulation-transfer function, which is a measure of sharpness and definition; and the particle or quantum density that can be stored in the sensor of the camera, which is a measure of granularity, or noise.

A unique feature of the book is a series of 54 unusually high-quality reproductions of photographic and television images that dramatically illustrate the effects of various parameters on image quality. For example, the same subject is shown as reproduced by television systems having 525 lines, 4.25 MHz; 625 lines, 5 MHz; 525 lines, 7 MHz; 625 lines, 9 MHz; and 1760 lines, 60 MHz. Another set of reproductions shows photographic images of a subject made with films of different speeds and with formats

requiring different magnifications. The story told by these illustrations will be readily perceived by the expert and the layman alike.

Most of the reproductions measure 8½ by 6¼ inches. Some have appeared in various of Dr. Schade's papers scattered throughout the technical literature (although usually in a much smaller format and with less detail) and others have not been published before. Here, for the first time, they are brought together in a single volume.

Otto Schade has been active in the field of television for more than thirty-five years. His pioneering work in the 1940s and 1950s led to the concept of Modulation Transfer Functions and Noise Equivalent Pass Bands, which can be applied equally to amplifiers, lenses, and the human eye. He made the first measurements on the human visual system in terms of these parameters. Dr. Schade's work has received worldwide acclaim.

For your copy send \$20.00 (U.S.A.) or \$22.50 (elsewhere) to:

Scientific Publications
RCA Laboratories
Princeton, New Jersey 08540

Business modeling in an engineering context: An Astro-Electronics application

Operations Research developed a successful model to analyze complex mission requirements. The focus was on business issues, while technical underpinnings were retained.

Abstract: *This paper describes a model that has been developed to assist Astro-Electronics in analyzing the business impact of design alternatives of a multi-satellite system. The model simulates the aggregate-level technical, systems and business requirements—satellite design, orbital placement, launch timing, and spares policy. To ensure that the business aspects are reflected well, the model also captures the technical microstructure—the details as they relate to operation, reliability, and cost. The model demonstrates how engineering and business aspects can be blended together to produce a total perspective for decision making.*

The primary use of the model is to test and refine various alternatives until a balance is struck among cost, risk, and availability requirements. Results from the model can then be used in setting initial bidding prices on contracts and in production scheduling. This model was used for the conceptual design study of the National Oceanic Satellite System (NOSS)—a proposal in the 700-million-dollar range—and the Defense Meteorological Satellite Program (DMSP) Block 5-D satellites.

RCA Astro-Electronics designs, develops, and manufactures satellites on a contractual basis. It has been doing so since the early 1960s and has successfully partici-

pated in TIROS, ITOS, Satcom and numerous other satellite systems ranging from meteorological and communications to defense-related systems. Astro-Electronics is currently experiencing the largest backlog of work in its history.

The contracts are awarded on a very competitive basis. Hence, a key element in the success of Astro's business is the ability to design a satellite system that meets the customer's mission requirements—overall operational and reliability requirements—in a very cost effective manner. A conceptual design is a necessary first step in the process of bidding for satellite systems.

In a given design, alternatives can differ in the number, configuration, and reliability of the satellites built, in the schedule of building and launching the satellites, and in the replacement policy of failed satellites. Other operational policies considered are the use of standby satellites and satellite retrieval by the space shuttle. This paper describes a model developed to help Astro-Electronics analyze the business impact of design alternatives of a multisatellite system. The model simulates aggregate-level technical, systems, and business requirements. For a given alternative, the model determines the system availability by trying to meet the operational requirements with the specified resources and calculates the time-phased costs. The model can be used iteratively to arrive at the best balance among cost, risk, and availability requirements.

Complexity of the situation

The primary concern in any contractual arrangement is the mission objectives, and there are numerous ways in which they can be satisfied. Before proceeding further, some definitions are necessary. A satellite consists of essential bus systems (for example, power, attitude control) and sensor systems (for example, atmospheric temperature-profile measurement). Each of these systems has several identical subsystems (for redundancy) performing the function. Figure 1 gives a simplified schematic of a satellite's systems. To meet the mission objectives, Astro-Electronics has to answer questions relating to the number and type of satellites to be used, their overall design, and general performance and lifetime characteristics at an aggregate level. At a finer level, trade-offs between redundancy in sensor and bus systems, and trade-offs between redundancies and satellite lifetime, among others, have to be resolved. At a still finer level, issues of which specific components should be chosen, their lifetime and reliability characteristics, costs and learning curves, all have to be addressed. It thus involves looking at the entire spectrum—from the business issues, to the satellite system issues, to the technical issues of component reliabilities and redundancies.

Increasingly, a customer's requirements must be or are best satisfied with multiple satellites, operating simultaneously and/or consecutively. The number of satellites that must be operating simultaneously are usu-

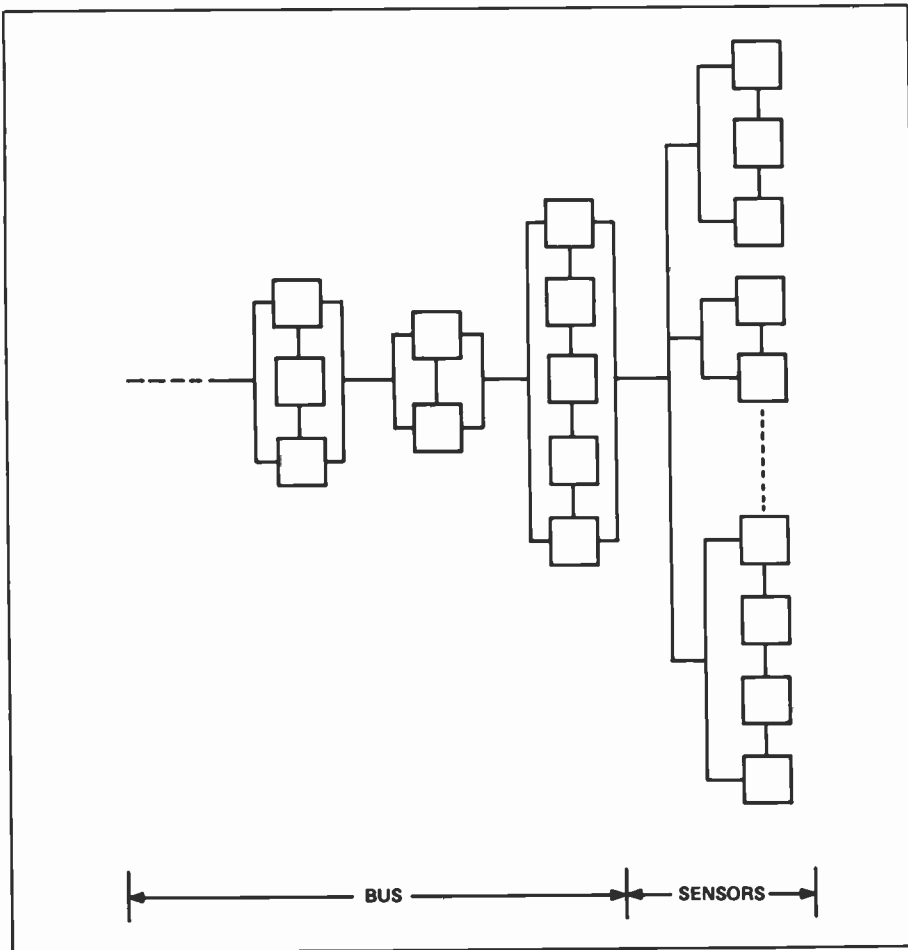


Fig. 1. This satellite schematic shows redundancies in bus and sensor systems. The satellite model consists of systems in series (the bus) and the sensor systems in parallel. Each of the systems has a number of identical subsystems in parallel. Subsystems may be redundant in either active or standby mode.

ally determined from the satellite system's capacity or coverage requirements. For example, a meteorological satellite has a limited payload of instruments and can monitor only selected areas of the earth. Consecutive launch and operation of satellites may be necessary to maintain the system during its life.

With a multiple satellite system, the number of system designs is greatly increased. Alternative designs can differ in the number, configuration, and reliability of the satellites built; in the schedule of building and launching the satellites; and in the replacement policy of failed satellites. With the advent of the space shuttle, which allows the retrieval of satellites and the use of in-orbit standby satellites, planners are faced with the increasingly difficult task of assessing many possible system configurations.

Compounding the complexity of these issues is the fact that the performance of satellite systems is subject to a multitude of uncertainties. For example, the orbital placement of an individual satellite involves some

elements of chance. These chance events are usually addressed by adding redundant components to each individual satellite and by including entire redundant satellites in the system. Therefore, the difficulties involved in making cost-effective design choices are amplified in order to reduce uncertainty. However, competitive bidding procedures dictate that such choices be made.

New approach

Over the last twenty-five years, satellite technology has made major advances so that it is indeed a different world now. This period has seen growth from small-satellite/single-objective missions to multi-functional satellites with mission definitions spanning several years. Over the years, Astro-Electronics had developed rather sophisticated computer programs to assist them in designing satellites. But the performance of an individual satellite does not address the complexity inherent in a

more complex mission objective. To address this situation, Astro's Engineering management asked the Corporate Operations Research group, whose charter is to promote the use of quantitative methods in management, to assist them.

The approach we took was to explicitly shift the focus to the business issues, while retaining the technical underpinnings. It was more of a top-down approach. The business issues played a vital role in the development of the model.

Business issues

As mentioned earlier, a satellite design is judged only in the context of a mission or system requirement. A typical mission requirement may be gathering certain information (cloud pictures, infrared images, temperature profiles, and so on) over a period of several years. In responding to this requirement, Astro has the following alternatives:

- It can build inexpensive short-lived satellites that will be replaced again and again over time, or it can build more costly long-lived satellites (even up to the life of the mission).
- It can put all the sensor systems in all the satellites (but with a reduced reliability because of weight limitations), or equip certain satellites with certain sensor systems, thereby spreading the load to several satellites.
- To ensure that a certain minimum coverage will be provided, Astro-Electronics can allow for an in-orbit spare (an orbiting satellite that will be fully activated when a satellite failure occurs), or it can reduce the risk of not meeting the mission requirements over an extended period of time by having satellite inventory on the ground.
- Astro-Electronics can provide for different levels of on-ground satellite inventory. The basic decision is how many satellites of each type should be in inventory. The inventory costs are traded off against satellite system availability.
- Now that the shuttle is operational (or nearly so), the question of what to do with satellites that have catastrophic failures is one that adds to the decision complexity. The satellite can be brought back, repaired, refurbished and launched again. There are costs and risks in this procedure but there are also savings to be achieved.

Note that in dealing with these broader mission issues, the underlying technical issues of reliability and redundancy cannot be ignored. In fact, several of these mission objectives have become possible only because of the technological advances in subsystem weights, costs, and reliabilities. As a result, the mission can be accomplished in many technically feasible ways, and thus choosing the best alternative is a dominating business issue. In the past, the technical issue was itself the business issue. The challenge to Astro-Electronics is to find the satellite system designs that are cost effective and will stand the challenge of competition.

These business issues were explored in great detail with Engineering management; it took several rounds to define the scope of the problem. The Operations Research group then responded by developing a Monte-Carlo-based computer-simulation model called the Life Cycle Cost model (or, LCC, for short).

The Life Cycle Cost model

For a proposed satellite system design, LCC generates the availability of the satellite system, the spacecraft reliability, and the cost data from a number of trials, each one of which represents a possible history of the satellite system. The model uses Monte-Carlo simulation—a technique for studying the performance of systems involving random variables—to accomplish this. The model has the flexibility to simulate diverse satellite systems—systems that differ in the number, configurations, and reliabilities of the satellites built; in the schedule of building and launching the satellites; and in the replacement policy of failed satellites. For a given systems design, the model simulates in detail the satellite-launch operation, satellite performance, and necessary satellite-replacement operations, and it produces reports on the system performance and on all costs incurred.

To evaluate any alternatives, the satellites are considered in detail from the point of view of reliability and cost. Each satellite is modeled as a number of support systems in series (the bus) and a number of sensor systems in parallel. Each bus or sensor system is composed of a number of identical subsystems in parallel (Fig. 1). Some of the subsystems may be redundant, either in active or standby mode. More specifically, the user specifies—for each system—the total number of subsystems installed, the number of these subsystems desired to be active, and the min-

imum number of active subsystems required for the system as a whole to be still called operational. Also specified is the number of subsystems that should be active when the satellite is an in-orbit standby.

The life of an active subsystem is determined by its reliability function, such as an exponential decay with normal wear-out or a probability distribution table, obtained through an independent analysis. When the subsystem is in standby, its life is determined by a scaled reliability distribution of the active case. Standby subsystems are automatically activated, with a specified probability of success, to replace failed subsystems that were active. Reliability and cost distributions are specified at the subsystem level.

Because of the series/parallel structure, satellite failure is caused by the failure of either a bus system or all the sensor systems. When an active satellite fails, an in-

orbit standby satellite is activated if available, and a new launch may be scheduled. Here, the policy governing the number and usage of standby satellites and launch schedules is controlled by the user input.

The launch sequence is a function of the satellite inventory arrival times and sensor requirements and will vary in each trial in response to the different failure patterns that occur. When a particular satellite has to be launched, the model schedules the earliest possible launch. The simulation of the launch process, the insertion into the right orbit, the turn-on of subsystems, all determine the initial state of the satellite in the sky. These events successfully occur according to user-specified probabilities, based on prior design experience.

The model captures the time cycle of the manufacture of satellites in considerable detail. The model progresses on a month-to-month basis, while getting all the com-

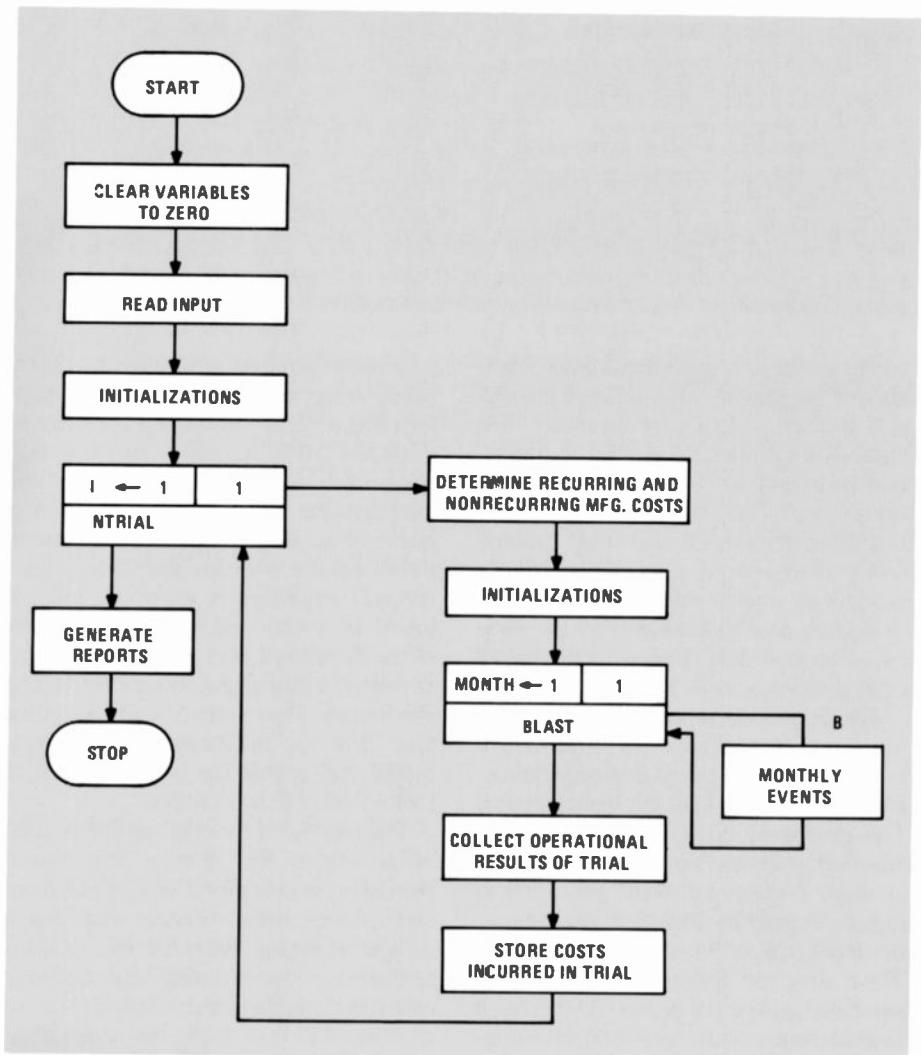


Fig. 2. This simplified system-level flowchart of LCC shows the two primary loops: one for the trial number and the other for the launch month. This structure is common to many simulation models.

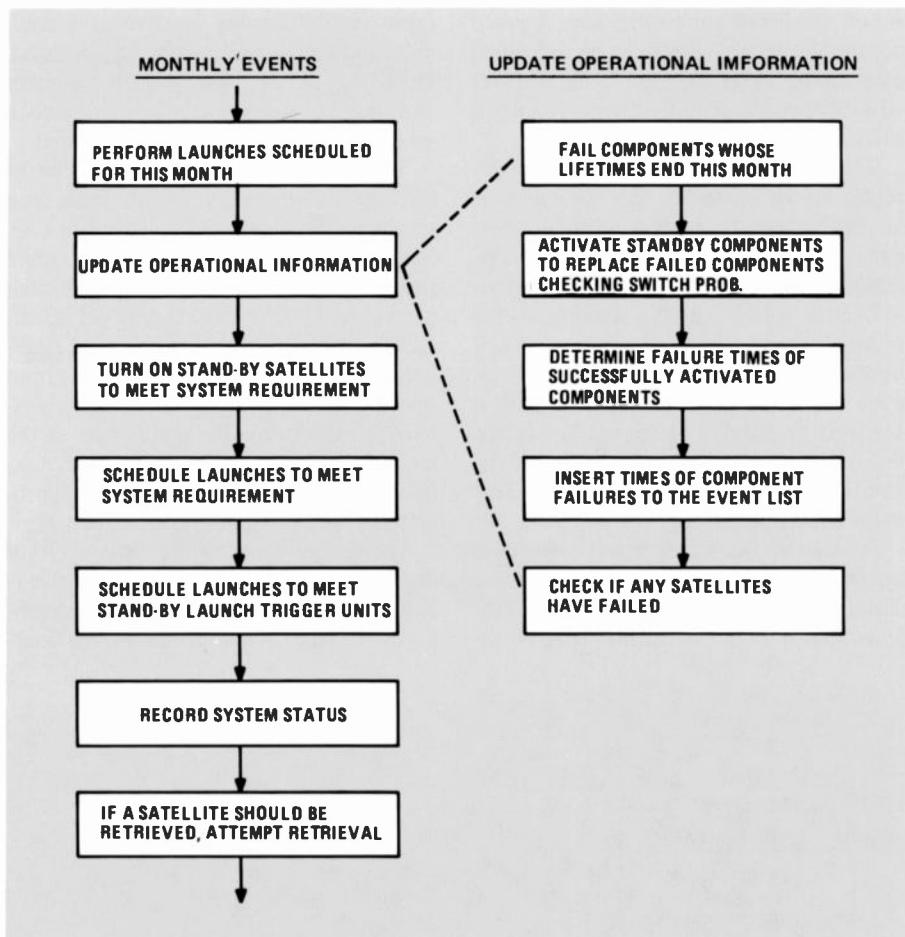


Fig. 3. Every month in the simulation, LCC checks the status of subsystems, systems, and satellites and schedules launches to determine the required actions.

ponents (and incurring related costs), starting satellite assembly, and putting it through tests before it is ready for inventory. The number of satellites, the satellite configuration built, and the lead time to complete the task are all controlled via user inputs.

The model keeps a tab on the bus and sensor subsystem failures and also records whether or not they are still operational. From this, after looking over all the satellites, one can determine whether overall mission objectives are being met or not.

The costs in the model are of two types. The nonrecurring costs for a subsystem capture the development cost required before a subsystem may be manufactured. This cost is incurred once and may be allocated over consecutive quarters. The recurring costs in the model are meant to include subsystem manufacturing, launch, inventory, refurbishment, and repair costs. These costs are incurred every time the associated operation occurs. The cost of manufacturing every subsystem is considered to be probabilistic, and the mean cost is adjusted downward as the number of previously manufactured components of the

same type increases, according to a learning-curve rate input by the users. The manufacturing costs of components are also correlated to reflect the reality that improvements in the design or manufacture of one subsystem may spill over in the cost improvements of another subsystem. All costs in the model are normally distributed. Since the cost expenditures occur at different times, the means and standard deviations of the discounted costs are also calculated to provide a meaningful comparison among alternatives. The standard deviations of the cost allow for an assessment of the risk profile and enable the largest sources of cost variation to be identified.

The input to the model consists of a set of parameters that describe the mission objectives for operational sensors as a function of time, the subsystem and launch vehicle reliability, the mean and standard deviation of nonrecurring and recurring costs, the number and configuration of each satellite type built, the schedule of building the satellites, the launch vehicle used for each satellite type as a function of time, the prespecified launches of each satel-

lite type, and the replacement policy of failed satellites.

Model logic

A flowchart of the program's logic is shown in Figs. 2 and 3. The time increment in the simulation is one month. First, LCC simulates all launches scheduled for the current month. This launch may have been prescheduled by the user or dynamically scheduled by the model. When a launch is attempted, the launch vehicle may fail or the final orbital placement may be unsuccessful. To take advantage of the possibilities offered by the shuttle, recovery of the satellite can be attempted where applicable. If recovery is successful, the satellite is refurbished and returned to the satellite inventory.

After all scheduled launches for the current month have been simulated, LCC checks the status of the entire system. If, due to bus or sensor-system failures, system demands are not satisfied, the model will activate available in-orbit standby satellites that contribute to meeting the mission requirements. A satellite is activated by switching on enough of its standby components to bring it up to its active configuration. Successfully activated systems are given a new lifetime from their unscaled lifetime distribution. If mission demands are still unsatisfied, one or more replacement satellite(s) may be scheduled for launch. The model selects the satellite(s) from inventory whose type will satisfy the largest number of unmet demands (as determined by the different sensor systems aboard an available satellite).

Finally, the standby satellite requirements are checked, and additional launches are scheduled if necessary. The model allows for launch preparation time when it schedules the launches in the simulation. The current model logic reacts to unsatisfied mission demands only as they occur rather than anticipating wear-out failures. Because of this, it is meant to be used in an iterative mode. For a given scenario, if the achievement of mission objectives is unsatisfactory (as in Fig. 6), then this indicates that the replacement policy needs to be changed by the addition of a standby satellite or a prescheduled launch to avoid a drop in availability. The model would then be rerun to test the revised replacement policy.

Model outputs and uses

After completing the specified number of trials, usually around one hundred, the

CAUSE OF SATELLITE FAILURE		
	SAT ONE	SAT TWO
ADACS	0.03	0.0
PWR	0.29	0.0
THERM	0.0	0.0
SOLAR	0.21	0.0
TLM	0.02	0.0
COMM	0.0	0.0
CC	0.30	0.0
DLS	0.07	0.0
ADACS2	0.0	0.05
PWR2	0.0	0.27
THERM2	0.0	0.0
SOLAR2	0.0	0.22
TLM2	0.0	0.02
COMM2	0.0	0.00
CC2	0.0	0.24
DLS2	0.0	0.12
SENSORS	0.0	0.0
AT LAUNCH	0.08	0.07

Fig. 4. For each satellite type, the fraction of the satellite failures caused by the failure of each bus system is shown. Also listed is the fraction of satellite failures caused by the failure of all the sensors or by an unsuccessful launch.

program computes descriptive statistics (mean and standard deviation) on the events (launches, retrievals, satellite failures, demand failures, and the like) that have been observed. The output reports produced by the model fall into the following major categories:

- Reports on the technical features have to do with the bus/sensor failures, the number of bus/sensor subsystems in the active and standby mode every month by each satellite configuration, the causes of satellite failure, the lifetime of satellites failed, and so on. A sample report is shown in Fig. 4.
- Reports on the system features show the number of launch attempts each month, the number of active and in-orbit standby satellites, the number of satellites in ground inventory, and the number of satellites ordered by each satellite configuration type, the shuttle launches and refurbishments invoked, and so on. A typical report is shown in Fig. 5.
- Reports on measures that relate to the overall business/mission performance in-

clude the mission objectives achieved every month by each sensor type, the degree and type of shortfall, if any, the overall performance over the entire mission duration, and the nonrecurring and recurring costs expended over the life of the system. In addition to these reports presented in a tabular form, graphical outputs are used to enhance understanding. Figure 6 shows a sample graph of the probability of meeting the mission objectives over time.

The primary use of the model has been to test and refine various alternatives until a balance is struck among the cost, risk, and availability requirements. Results from the model can then be used in setting initial bidding prices on contracts and in production scheduling.

In spite of all this flexibility in handling the tremendous diversity of satellite systems, this model, written in FORTRAN, requires only 1 megabyte of core, and a 100-iteration simulation costs only \$20 in the batch mode. This low cost of running the model and evaluating the scenarios plays an important role in its use.

The model was developed by the Operations Research group and then turned over to Astro-Electronics. Because they were

MEAN AND ST. DEV. OF LAUNCH MONTH AND PROB. OF LAUNCH OF THE 1ST, 2ND, 3RD, . . . LAUNCH OF EACH SATELLIE TYPE

	SAT ONE	SAT TWO
1	1.00 0.0 1.0000	6.00 0.0 1.0000
2	14.25 2.49 1.0000	48.53 14.29 1.0000
3	39.91 14.64 1.0000	87.54 22.77 1.0000
4	55.64 12.68 1.0000	97.02 22.23 0.4100
5	78.33 21.01 1.0000	0.0 0.0 0.0

Fig. 5. The pattern of the launches is shown in this report. The first launch of each satellite type was prespecified so that the standard deviation of the launch month is zero. The other launches were dynamically scheduled by the model. This shows that a fifth satellite of the second type will not be required.

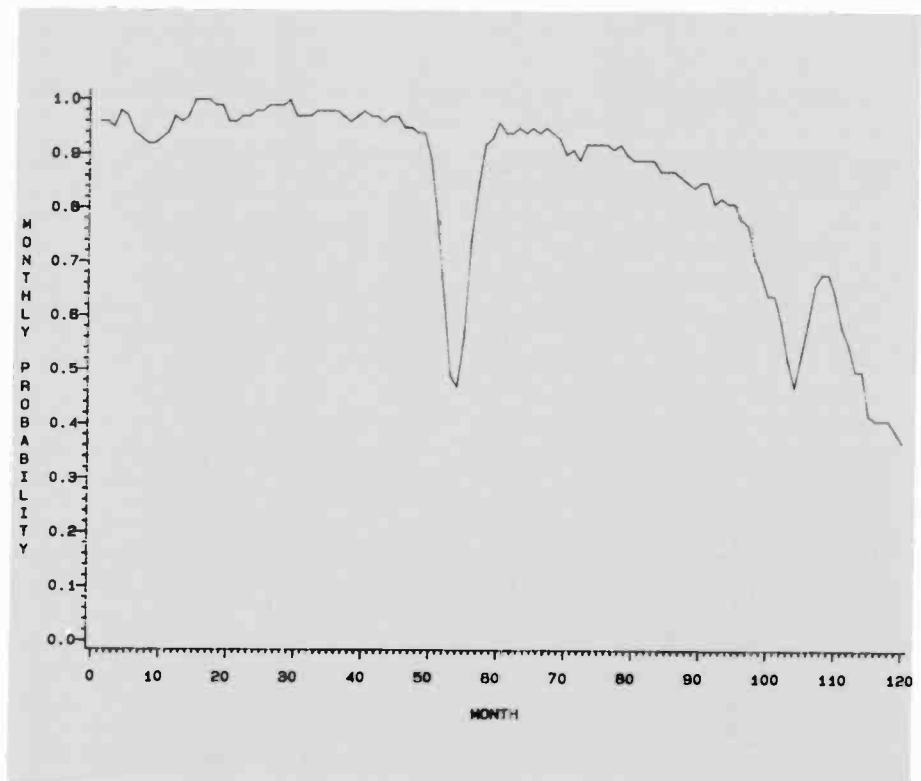
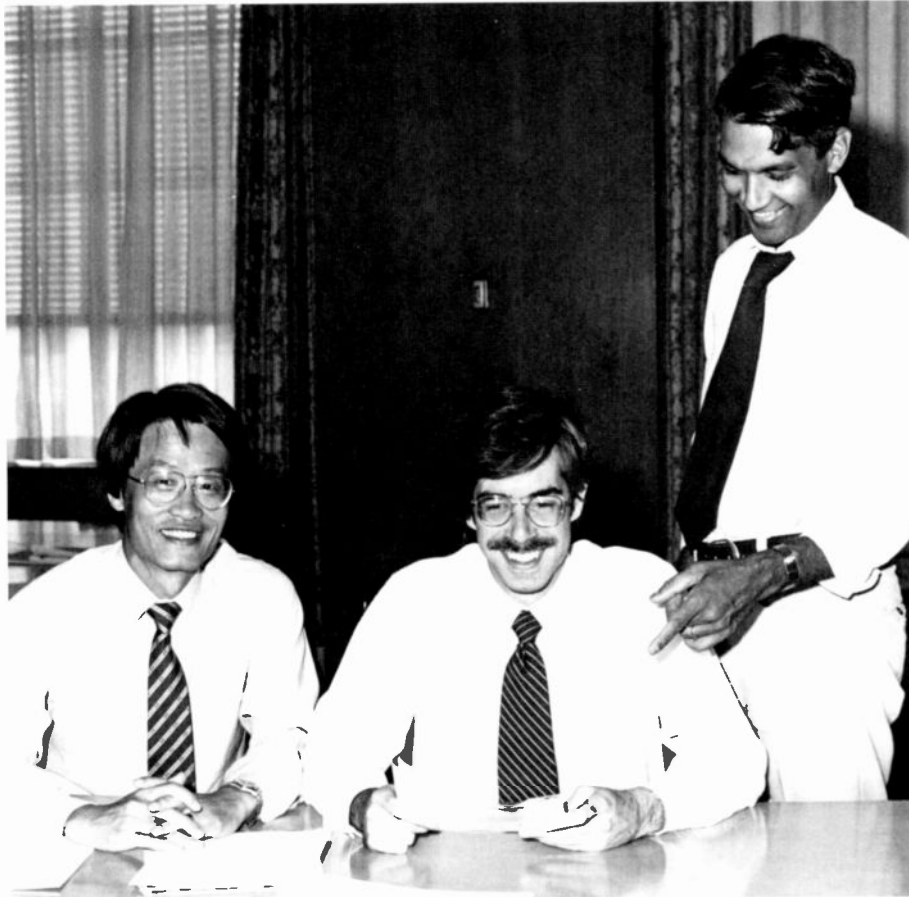


Fig. 6. This graph shows the fraction of the time the system requirements are met in each month—the monthly probability of mission success. The graph indicates that a satellite launch should be scheduled near month 50 in a subsequent scenario to avoid a dip in the availability curve.



Authors (left to right) Hong, Spence, and Nigam.

Raj Nigam is currently Operations Research Scientist with the Corporate Operations Research group. He joined RCA in 1970 and has worked with practically all RCA MOUs and Corporate Staff. He has been applying quantitative tools—modeling and data analysis—to aid in business decision making. His current interests include performance and productivity measurement, strategic analysis, and the application of fuzzy logic.

Contact him at:

**RCA Corporate Operations Research
Princeton, N.J.**

TACNET: 254-9629

Saman Hong is Manager of Operations Research at the Corporate Operations Research group. He joined RCA in 1978, and has since been working on the analytical approaches to business problems for the Corporate Staff and divisional management.

Contact him at:

**RCA Corporate Operations Research
Princeton, N.J.**

TACNET: 254-9616

Stephen Spence joined the RCA Business Systems and Analysis Career Program in 1980. He is currently employed as an analyst in the Corporate Operations Research group. He has completed projects for Service Company, Records, Hertz, and Corporate Staff.

Contact him at:

**RCA Corporate Operations Research
Princeton, N.J.**

TACNET: 254-9690

constantly involved in outlining the scope of the model and in the development process, the Engineering group at Astro had little difficulty in using the model. Soon thereafter they were making inputs and, more importantly, analyzing outputs and developing alternatives for sensitivity analyses on their own. The transfer of the model has been so successful that the role of Operations Research has now been reduced to general maintenance and minor enhancements.

Business evaluations

This model was successfully used by Astro-Electronics in studies of the National Oceanic Satellite System (NOSS)—a system whose overall cost was publicly acknowledged as being in the 700-million-dollar range—and in the DMSP Block 5-D program. It helped in analyzing several alternatives of satellite configurations, bus/sensor subsystem reliabilities and redundancies, in-orbit standby and ground-inventory policies, shuttle retrieval-and-refurbishment

issues, among others. It proved its worth in shifting the emphasis to the business/mission objectives while retaining the proper emphasis on the technical underpinnings.

Acknowledgment

The authors thank Dr. Warren Manger of Astro-Electronics, for his assistance, support and encouragement throughout this project.

Modeling and simulation in mechanical and thermal design

Finite-element computer-modeling programs have been used to accurately predict the response of engineering structures to complex mechanical and thermal loads.

Abstract: *Finite-element methods are reviewed and applications within RCA Corporation are discussed. The computer-modeling programs based on these methods have been used to solve complex engineering problems related to mechanical design and thermal analysis. In most cases, solutions could not have been achieved by other means because of the complexity of the structure, loads, or boundary conditions. Finite-element modeling is extremely useful both in the design of new structures and in the analysis of those that have failed or that need improvement.*

Finite-element modeling is a powerful method for the simulation of heat transfer and mechanical stresses in various structural bodies. The power of the finite-element method lies in the *a priori* prediction of the response to a complex mechanical, thermal, electrical, or fluid load from a blueprint of the structure and its physical properties. In this way, design changes can be made before molds are produced or construction is begun. A number of finite-element methods available to RCA scientists and engineers are being used in projects throughout RCA to solve otherwise hopelessly complex mechanical-design and thermal-analysis problems.

©1982 RCA Corporation
Final manuscript received September 17, 1982.
Reprint RE-27-6-11

Finite-element modeling theory and procedures

In this method, a complex solid continuum is divided up into a series of discrete blocks—finite elements—that have preprogrammed mathematical descriptions for their behavior. The number and locations of discrete blocks chosen to describe the structure influence the accuracy of the final solution and the cost. Therefore, a finer mesh is used in a rapidly varying stress or temperature regime, and a coarser mesh is used in other regions to minimize computer costs.

The elements are geometrically described by their node points. For the case of two dimensional structures, this is generally done as 3 or 4 node points per element; for solid structures, this is 8 nodes per element (or up to 20 nodes for some elements, including the 8 corners and the centers of the 12 edges). The node-point spatial locations (discretization) can be readily digitized from a blueprint of the structure with the aid of commercial finite-element programs or with the aid of RCA-developed software programs^{1, 2} used in conjunction with a Tektronix graphics terminal and digitizing tablet.

A force acting on a node causes a displacement, much like that described by Hooke's law. For all the nodes of an element, this response is described by the element stiffness equation³:

$$\{F\} = [K] \{u\}$$

Here the components of $\{F\}$ and $\{u\}$ are

the nodal force and displacement vectors, and $[K]$ is the element-stiffness matrix. Included in $\{F\}$ are the vectors for applied nodal loads, pressures, temperature gradients, accelerations, plastic strains, creep, swelling, large displacements, and so on. The node points locate the displacements in structural analyses and temperatures in thermal analyses. Each node point has one degree of freedom in a thermal analysis since it is a scalar function of position, and up to 6 degrees of freedom (3 translational and 3 rotational) since displacement is a vector quantity. The analogy between the mechanics and thermodynamics of structures is used to extend finite-element methods to heat-transfer problems, and the resulting matrix equation is similar:

$$\{Q\} = [\bar{K}] \{T\}$$

where $\{Q\}$ is the heat-flow vector, $[\bar{K}]$ is the thermal conductivity matrix, and $\{T\}$ is the vector of node-point temperatures.

The matrices for the individual elements are next combined to form a complete set of matrix equations (global) for all the elements in the continuum with the additional constraints of equilibrium, boundary conditions, and continuity of nodal displacement conditions. There are as many simultaneous equations as degrees of freedom, and this can range up to 10,000 or more for large or complex structures. The general solution for the displacement $\{u\}$ or temperature $\{T\}$ in the global equation is achieved by sophisticated wave-front meth-

ods that can be thought of symbolically as inverting the matrix. Stresses in each element are obtained from the displacements calculated for each element.¹

Time-dependent parameters such as the natural frequency and shape of the vibrating structure can be determined as well as transient dynamic and transient heat-transfer properties. For these calculations, the damping (C), mass (M), velocity (\dot{u}), acceleration (\ddot{u}), specific heat (\bar{C}), internal heat-generation rate (\bar{q}), film coefficients (h_f), and the emissivity (ϵ) must be known. The basic matrix equations then include additional terms as follows:

$$\begin{aligned} \{F\} &= [K] \{u\} + [C] \{\dot{u}\} + [M] \{\ddot{u}\} \\ \{Q\} &= [\bar{K}] \{T\} + [\bar{C}] \{\dot{T}\} \end{aligned}$$

From a procedural point of view, one type of element is used for stress analysis, and up to three other elements for conduction, convection, and radiation are used for the heat-transfer solution. If both a structural analysis and a thermal analysis are to be performed on the same structure, the same discretization (that is, assembly of node points described by their Cartesian, cylindrical, or spherical coordinates) can be used for both analyses. Thus, the thermal analysis can be performed first to determine the heat transfer and temperature distribution, and then the structural analysis can be conducted to determine the stresses generated by the induced temperature distribution.

The properties of the materials constituting the structure are needed as input data for the finite-element solution because stresses and deformations induced and the heat transferred are a function of the materials properties. The mechanical properties required are the modulus of elasticity, Poisson's ratio (which is a measure of the lateral contraction when a material is extended in the axial direction), the coefficient of thermal expansion, and the density. For special analyses involving creep, swelling, plasticity, and damping, these values will also have to be input as material properties. The heat-transfer properties required for solutions include the heat capacity, the heat-transfer coefficients (as a function of temperature, if necessary) for convection, conduction, and radiation. For radiation problems, the radiation area is required and this can be calculated from the viewing angles and the geometry of the structure. This tedious procedure can be facilitated using a program developed at Astro-Electronics, entitled RVFAC.³

Once the structure has been discretized and the materials properties added, then

the structures can be analyzed for stresses, thermal heat transfer, and so on, by using a general-purpose finite-element computer program. These programs include ANSYS, MARC, STRUDL, NASTRAN, DYNA-3, TVTOWER, and PLAFOM. Some of these programs have been developed within RCA in response to specific needs: DYNA-3 for dynamic analyses²; TVTOWER for guyed broadcast-tower analyses⁵; and PLAFOM for modeling of metal-forming processes.^{6, 7} The other programs have been developed by commercial software houses and are continuously maintained, upgraded, and documented.

A new feature is to incorporate finite-element modeling with mechanical design so that one can both design the structure and do a computer analysis for stress, displacements, frequencies of vibration, heat transferred and temperature gradients, using the same descriptor for the structure. This is then a powerful method of both designing the structure and calculating the response of the structure to the externally applied factors of force, pressure, and ther-

mal gradients. In turn, the structure can then be readily redesigned to reduce critical values of the induced parameters of stress, deformation, heat transferred, and so on. Computervision is one of a number of systems that are particularly useful for this type of application. Here, the structure is developed locally on the built-in minicomputer and then the finite-element structure with the appropriate materials properties and job-control cards is sent to a large-scale scientific computer for execution of the solution run using a general-purpose program such as NASTRAN.

Other trends in finite-element modeling include the tendency to model structures interactively from a video terminal rather than by batch processing, the use of large-scale minicomputers such as Prime or DEC VAX rather than a large mainframe computer, and the increasing use of graphics to display the analytical results rather than pages of numerical output.

Finite-element modeling analysis has been used at RCA in the solution of numerous complex problems. In the following

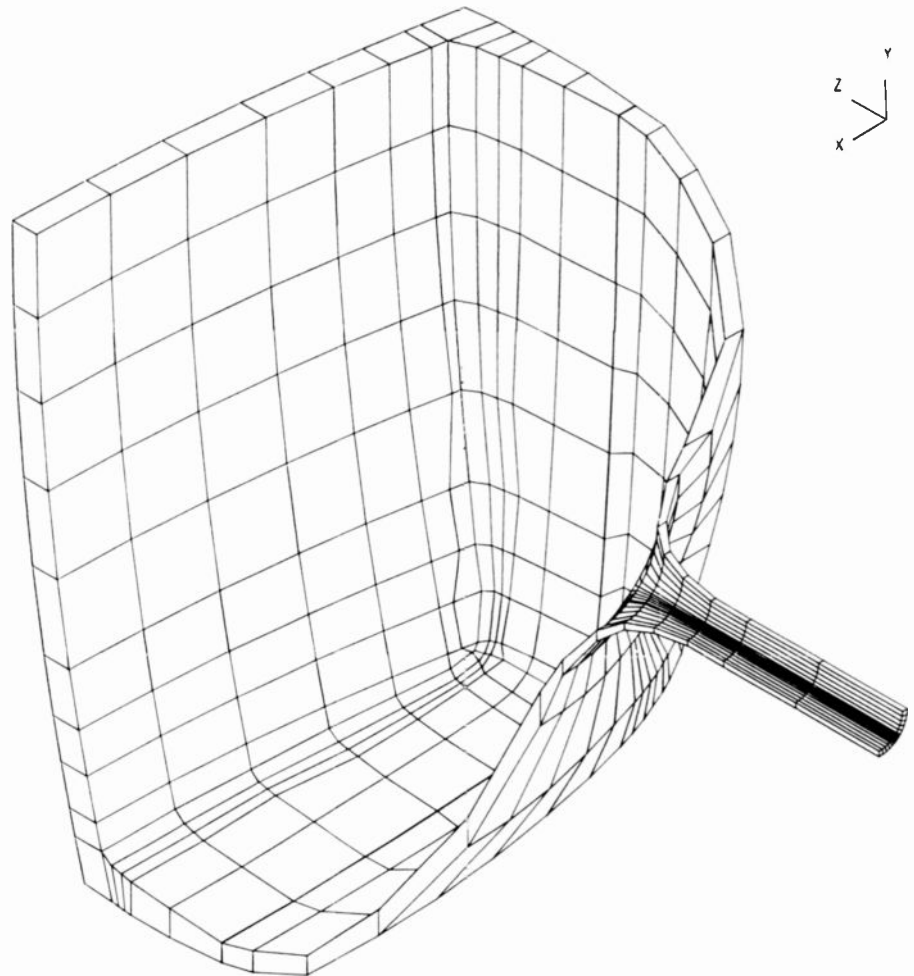


Fig. 1. View of a 25V100° bulb from the electron-gun end and looking toward the viewing surface. The structure is modeled in quarter symmetry.

sections, specific applications of the finite-element method to a few of these mechanical and thermal problems are described and discussed.

Mechanical modeling

Mechanical modeling includes the response of a structure to applied pressure, applied forces, gravitational forces, wind loads, and temperature gradients. These externally applied loads can induce stresses, change shapes, and cause buckling, plastic deformation, and vibration. All of these external forces can cause the structure to fail; indeed, finite-element analysis can determine the effect of various external parameters on the response of the structure. In the case of a failed part, a systematic investigation will thereby show the principal malefactor causing the failure. Thus, finite-element analysis can be used both for designing new structures to avoid failure and for the analysis of existing structures that may have failed. It should be emphasized that finite-element modeling does not provide remedies to a breakage problem; alternative designs must be created by the human mind. Rather, it does facilitate the investigation of these alternate designs and quantifies the results.

In modeling the structure, the finite-element mesh can very closely resemble the structure (TV picture tube) or lumped mass elements can be used with a resulting loss of visual similarity to the structure to reduce the complexity and computer computational costs (satellite); examples will be shown of both approaches. Many structures are symmetrical about a plane or an axis so that $\frac{1}{2}$ or $\frac{1}{4}$ of the structure can be modeled, by employing appropriate boundary conditions at the edges of the model, without any loss in accuracy but with an appreciable savings in computer cost.

Model of a TV tube

The finite-element model of a TV tube is shown in Fig. 1. Here, the model closely resembles an actual 25-inch diagonal tube. With this model, it is possible to predict the stresses and displacements induced by evacuation of the bulb. Further, this can be done for a variety of geometry variations to investigate the effect of funnel and panel design, manufacturing tolerances, application of implosion protection bands, and temperature gradients on the stresses.⁸ The stress distributions calculated over the viewing face of the kinescope and along its sides were found to agree with subsequent

strain-gage measurements within about 10 percent. In this way, a much more detailed stress and distortion distribution can be determined than could be done experimentally.

Model of a spacecraft

The finite-element model of a spacecraft is created somewhat differently than that shown for the TV kinescope. For the TIROS-N spacecraft, the model was constructed from equivalent masses and stiffnesses to describe the mechanical behavior of the structure even though it does not necessarily resemble the actual spacecraft; the structure and the equivalent finite-element model⁹ are shown in Fig. 2. After tests of the TIROS-N spacecraft were completed, the predicted and corresponding actual test results could be compared; excellent agreement was found between the predicted and observed natural frequencies of vibration for the various parts of the spacecraft. Finite-element modeling for the Advanced TIROS-N spacecraft is now complete and the experimental vibration tests are in progress. In this case, the finite-element model more closely resembles the actual spacecraft as shown in Fig. 3a; Fig. 3b is the spacecraft second lateral mode of natural vibration at 38 Hz.¹⁰ To help develop the finite-element model, a CDC program called UNISTRUC was employed

to generate both the Cartesian description for the node-point locations and the element connectivity. In this way, much time can be saved developing the model compared to manual methods. UNISTRUC is also being used for the latest Astro communications satellites, GSTAR and SPACE-NET, which are being built for GTE and Southern Pacific, respectively.¹⁰

Model of a hardened-steel press part

Engineers encountered a problem, at one point, in the press used for RCA's Video-Disc manufacture. One of the steel parts that creates the center hole during compression molding of the disc would break prematurely. The part is steam heated and water cooled during the pressing cycle and was found to fail by cracking after a relatively short time. In this case, the part is cylindrical, and is modeled as an axisymmetric solid so that only half of the structure is discretized. The program rotates the structure around its axis to mathematically approximate the entire structure, so that a 2-dimensional representation of a 3-dimensional structure is obtained.

To try to understand the effect of the various process parameters on the stress induced in the part during the pressing operation, the parameters were applied one at a time, and the stress distribution was calculated.¹¹ It was found that the internal

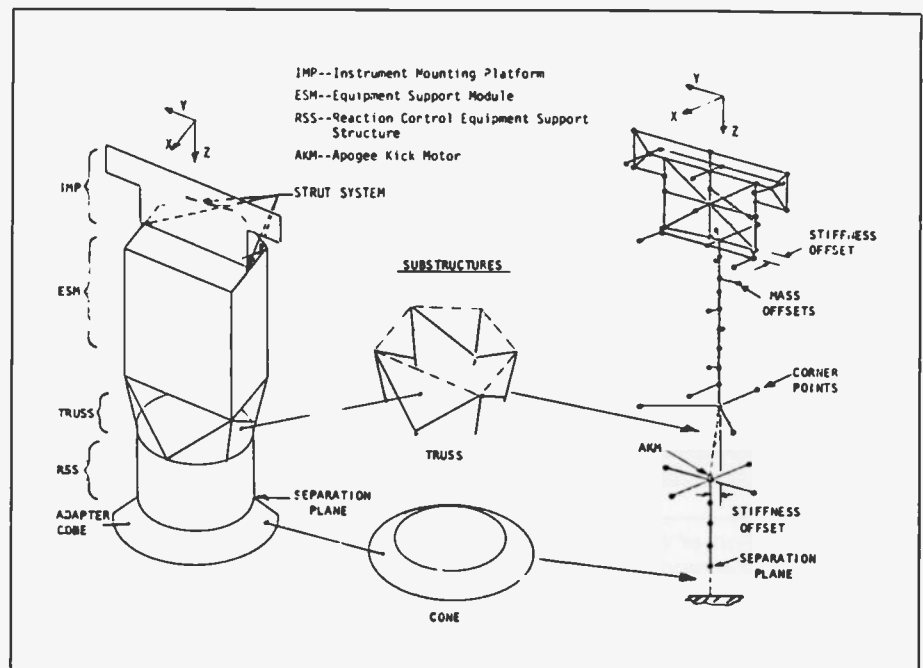


Fig. 2. TIROS-N spacecraft, dynamic, finite-element model showing the relationship between the actual structure and the lumped-mass finite-element model. Here point masses are used to represent the spacecraft rather than a detailed representational model.

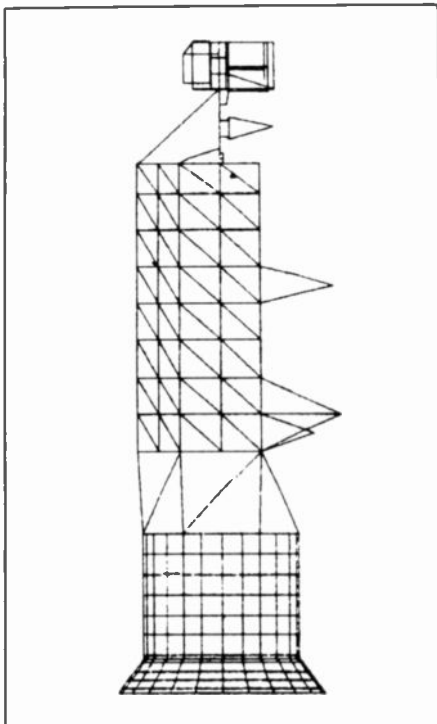


Fig. 3a. Finite-element model of the Advanced TIROS-N spacecraft.

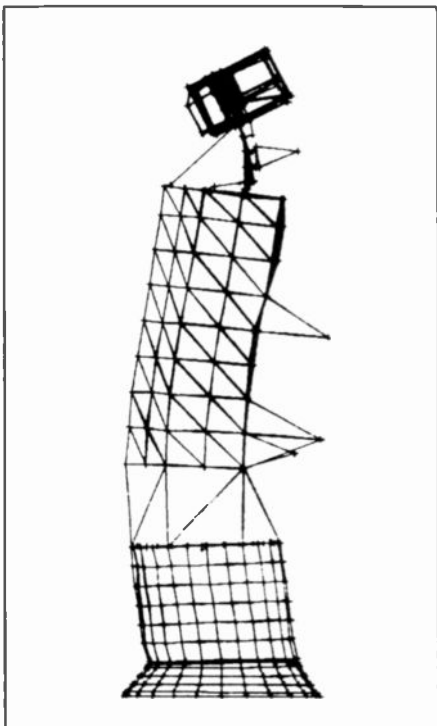


Fig. 3b. Distortion of the spacecraft in the second lateral mode of vibration.

steam pressure and the axial load create insufficient stress to cause fracture of the hardened steel part. However, the calculations showed that thermally induced stresses caused by the impingement of the cold water on the heated surface could create

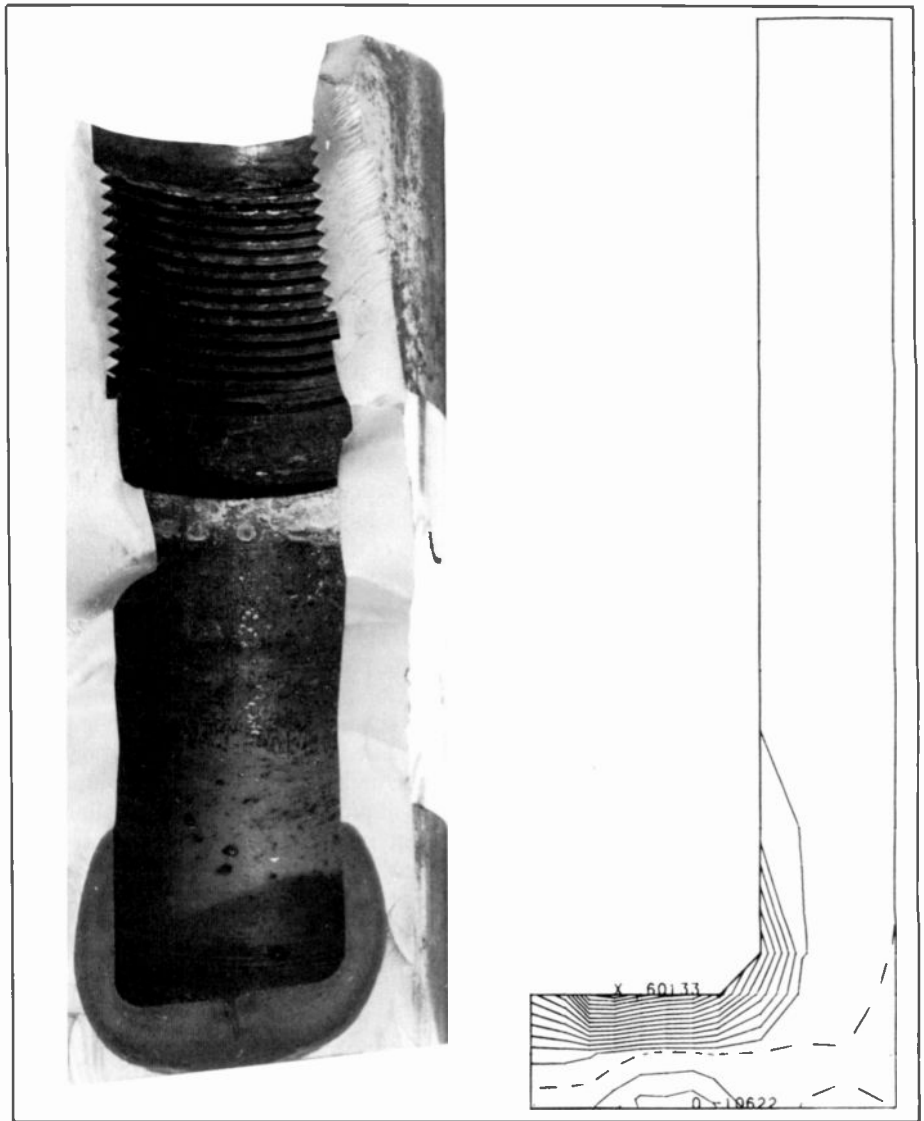


Fig. 4. Cross section through a press part exposing the internal crack generated during disc pressing. The dark area represents the cracked region. The stress contour lines are shown in the accompanying finite-element model plot, where lines spaced closer together represent a steeper stress gradient.

tensile stresses on the order of 60,000 psi and that the presence of a crack nucleus could increase this stress to about 75,000 psi tensile. Here, both the magnitude of the stress and the tensile nature are important in causing failure. Further, the stress distribution calculated for the thermally induced stress corresponded very well with the crack geometry observed in the failed part, as may be seen by comparing Figs. 4a and 4b. The back pressure created by the plastic pushing up against the bottom of the part was also found to be an important parameter inducing tensile stresses, especially when combined with the thermally induced stresses. Fracture was therefore postulated to arise from the induced tensile stresses, the flexing of the part during the various portions of the process cycle.

and the corrosion of the inside surface under the influence of the tensile stresses.

Model of a VideoDisc caddy

Another VideoDisc-related finite-element modeling problem involved the caddy that the disc comes in. In this case, it was desired to determine the force needed to contact the video play area of the disc as might be done by a consumer when squeezing the caddy between his fingers during normal handling. Figure 5 shows the finite-element model of the disc, spine, and caddy in half symmetry.¹¹ The calculations show that the force is about 2 pounds, and subsequent experimental measurements are in virtual agreement with this value. Now that the model has been developed, it is

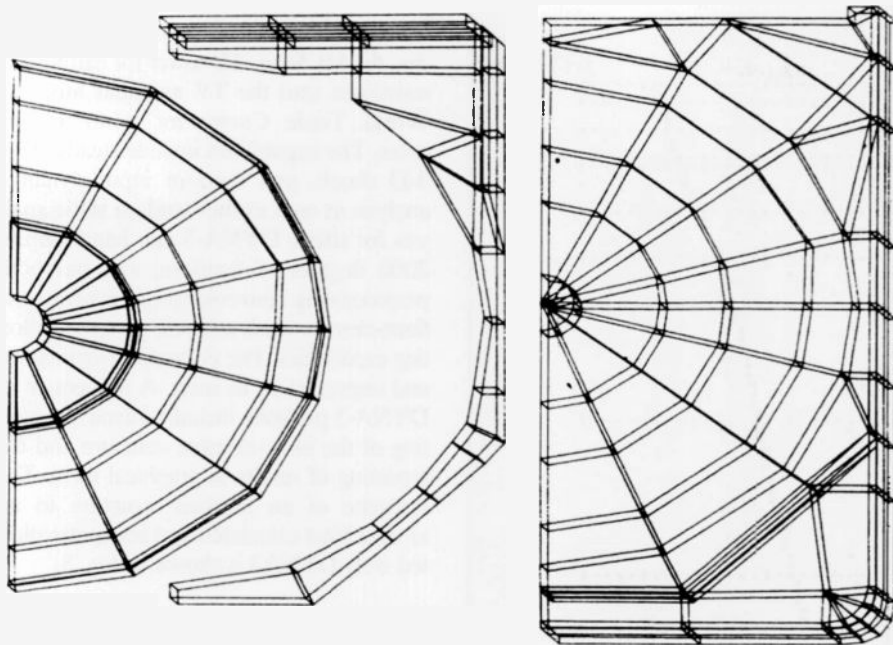


Fig. 5. Finite-element model of a VideoDisc record, spine, and caddy shown in half symmetry.

possible to investigate the effects of geometry changes, material changes, and external static and dynamic loading on the response of the caddy structure. In this particular model, a new feature was introduced, namely the presence of three separate parts. The three parts have to be mathematically connected to achieve a solution. This is done by having gap elements joining opposite nodes in the structure. The gap elements are nonlinear elements, though, so that a number of iterations have to be performed to arrive at the correct solution, and convergence may be difficult to achieve if the problem is not defined correctly.

Model of silicon wafer strength

Silicon wafer breakage concerns semiconductor manufacturers because it is an important component of device yield and cost. To understand differences in silicon wafer strength that could affect breakage, it was necessary to determine first the elastic properties of perfect wafers, free of defects. In this way the deflection of wafers subject to a central point load could be established as a function of the value of the load, and experimental values could be compared with this theoretical curve. The mechanical properties had to be carefully chosen since Young's elastic modulus and Poisson's ratio are a function of direction for a (100)-oriented wafer.

The finite-element model and the stress at the bottom of the wafer¹² are shown in

Fig. 6. Since the wafer is a flat circle, it could be modeled with 14 axisymmetric conical shell elements to describe the complete wafer. As shown in the accompanying plot, the stress rises very rapidly, going from the edge toward the center of the wafer. It was further found that the agreement was quite good between the calculated and experimentally determined curves for deflection as a function of the load, and for the relative relationship of the curves for the (100)- and (111)-oriented wafers.

Model of a plastic-packaged device

Another semiconductor-related finite-element study involved the plastic package for a power device. In this case, electrical leads had been breaking for unexplained reasons and the reliability was not as high as desired. A finite-element model of the package and leads was developed.¹¹ The package consists of a hard silicone plastic case and a soft rubber compound that surrounds the chip to protect it.

It was postulated that high stresses could develop as the package cools from the encapsulation temperature to room temperature. Thus, differential thermal contraction between the various components—silicon, silicone, rubber, and metal—could be important. This possibility was investigated and was found to develop high stresses in the electrical lead. A different geometry for the lead was investigated and calculations

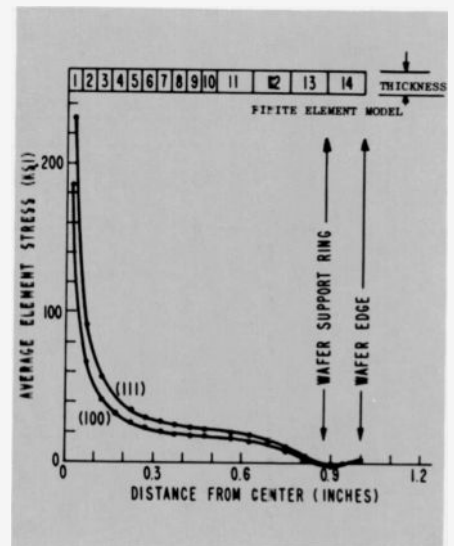


Fig. 6. Finite-element model and stress distribution across a silicon wafer. The wafer is supported near the rim and a point load is applied at the center. The deformation at the center as a function of the applied load is also calculated and can be compared with experiment.

incorporating the different lead geometries showed a reduced stress level. Experiments verified the desirability of the modified geometry, and the package incorporating these changes was put into production with good results and higher reliability.

Model of towers

The need to predict the response of over-the-horizon radar antennas in any wind directions or tall TV masts to comply with Electronic Industries Association or American Institute of Steel Construction specifications led to the development of a finite-element program entitled TVTWR⁵ by R.J. Pschunder at Moorestown. It is used to calculate deflections and stresses as well as the first and some higher natural frequencies of vibration for both guyed and free-standing structures. In a wind loading, the tower deflects until the horizontal guy and tower reactions equal the wind load. The analysis is highly nonlinear and requires iteration to achieve a final solution; here the criteria are obtaining all the calculated tower levels within 0.010 inches of their true position. A plot of tower deflection as a function of height is given in Fig. 7.

Model of ship structures

Another program that has been developed by R.J. Pschunder is DYNA-3.² This finite-element program has been used to analyze ship structures for the AEGIS pro-

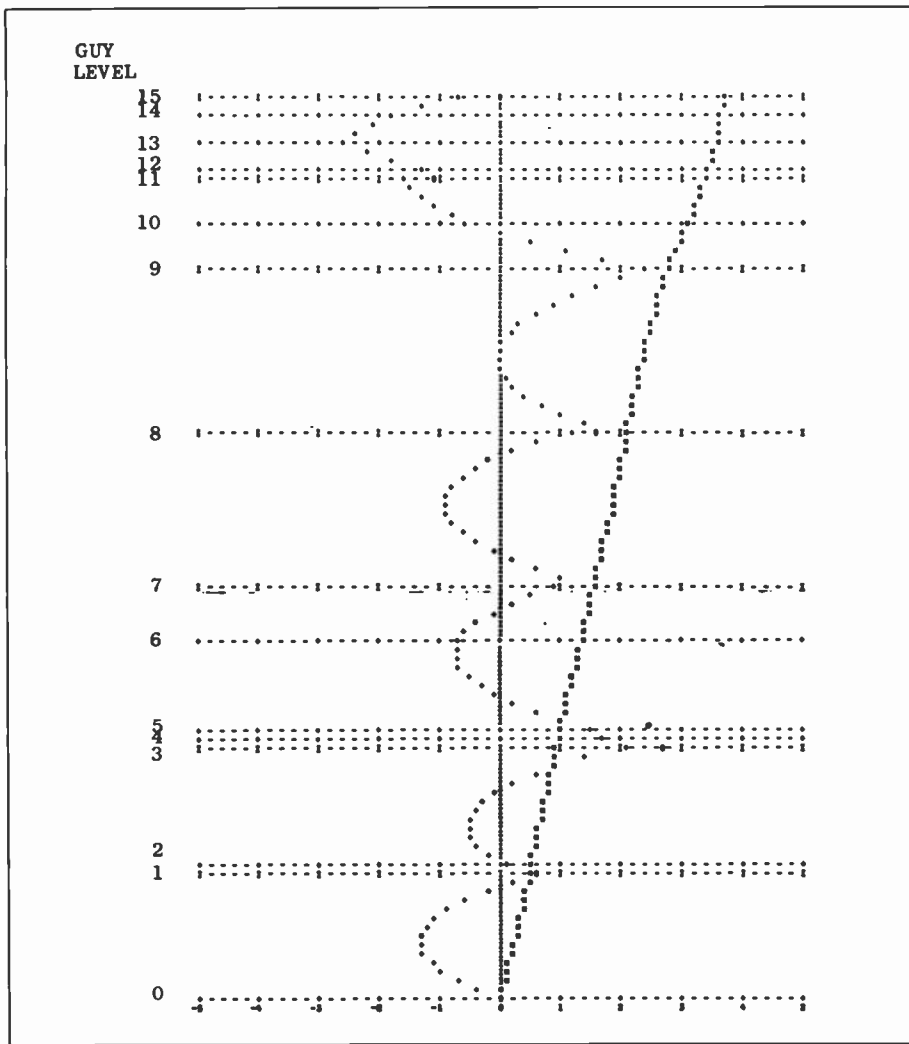


Fig. 7. Broadcast-tower deflection calculated with the TVTWR finite-element program.

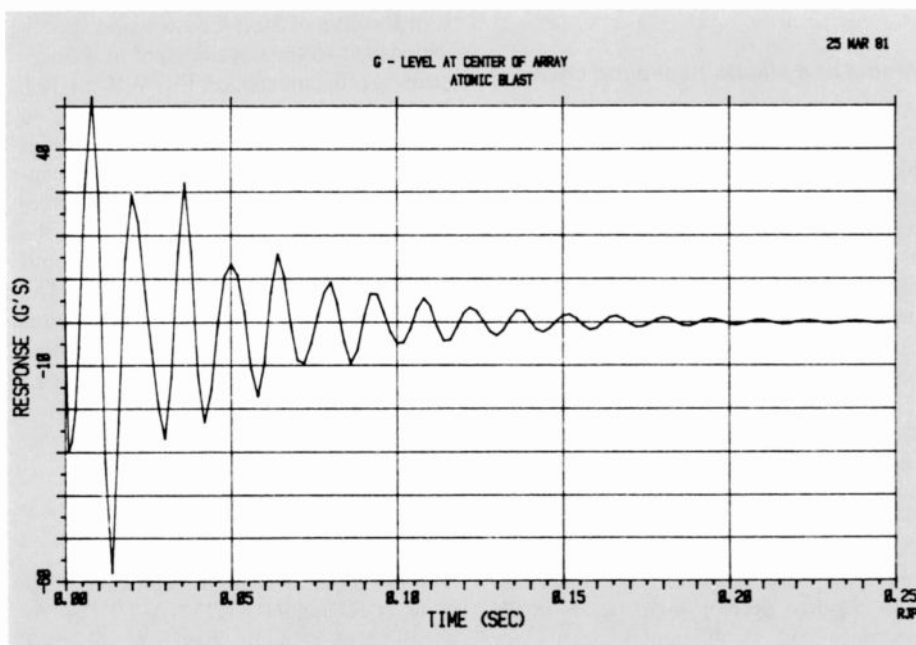


Fig. 8. Response of an antenna structure to atomic blast.

gram, a high-power laser pedestal, the antennas for the Mars and moon-landing vehicles, the Mt. Sutro TV tower for earthquake resistance, and the TV antennas atop the World Trade Center for wind-induced stress. The capabilities include steady-state, 3-D shock, and random input dynamic analysis as well as the standard static analysis for stress. DYNA-3 can handle up to 2000 degrees of freedom, and has both preprocessing conveniences to generate the finite-element mesh and post-processing plotting capabilities. The program is maintained and improved by its users. A refinement of DYNA-3 presently includes interactive plotting of the finite-element structure and the reporting of results in graphical form. The response of an antenna structure to an atomic blast calculated and computer plotted with DYNA3 is shown in Fig. 8.

Model of metal-forming processes

A finite-element program has been developed by C.C. Chen^{6, 7} for the analysis of metal forming of non-steady-state axisymmetric or plain strain metal-forming processes, such as deep drawing, coining, forging, or stretch forming. Here the material at its forming temperature is more like a fluid (specifically a rigid-plastic) rather than an elastic solid material considered in all the finite-element programs and problems described above. The finite-element discretization produces a set of nonlinear equations in terms of nodal and elemental velocities as well as hydrostatic pressure. The program calculates geometry changes, velocity, stress, strain, punch load, and die-pressure distributions.

Because of the material characteristics and the nature of the forming processes, the calculations must be iterated to achieve a solution and the finite-element mesh is updated at each step of the forming operation to accommodate the large deformation changes. The input data include: nodal coordinates, boundary conditions, die geometries, coefficients of friction and velocities, material properties, and an initial assumption of the velocity field. Several examples have been compared with literature results and the agreement has been excellent.⁷ A punch-stretching operation is depicted in Fig. 9. It is expected that this finite-element program will have extensive application at RCA Lancaster, where many parts must be formed for electron guns and other components.

Thermal modeling

Thermal problems have been modeled in structures ranging from the electron gun in

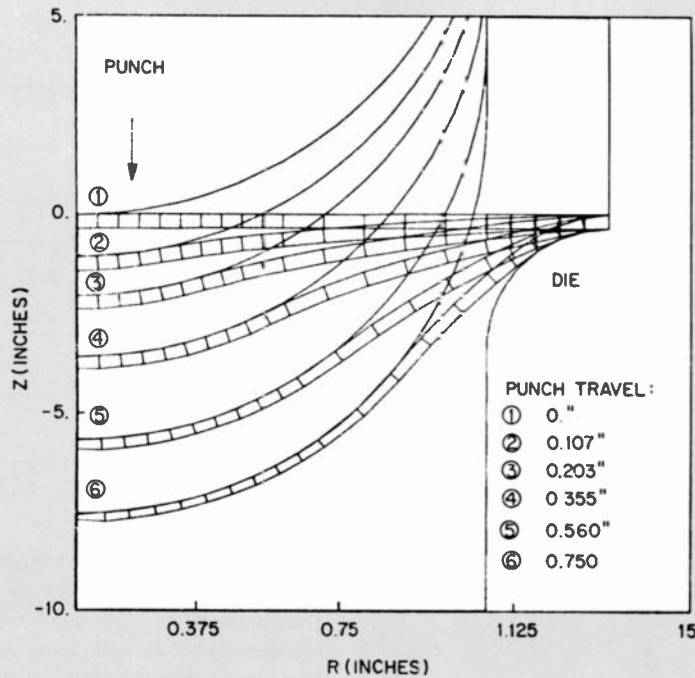


Fig. 9. Finite-element model and deformation of a metal blank in a punch-stretching operation.

a 25V color TV kinescope to a 25-megawatt power tube used for the nuclear-fusion test reactor. The finite-element method of analysis is useful for the solution of transient and steady-state thermal and thermal-stress problems, especially since any nonlinear material properties or heat transfer coefficients can be readily expressed as a function of temperature or heat flux.¹⁴

Model of power-tube anode

A 25-megawatt power tube and an 8-megawatt ion beam heat sink¹⁵ to be incorporated into the Tokamak Fusion Test Reactor (TFTR) at the Princeton University Plasma Physics Laboratory were designed with the aid of finite-element analysis.¹⁴ The 25-megawatt power tube is used to switch an ion beam that, after neutralization, ignites the tritium plasma. The anode of this tube must dissipate up to 2 megawatts of power. Two alternative designs were considered: a water-cooled, low-temperature copper anode section having a low thermal inertia and lag, shown in Fig. 10a, and a high-temperature, solid-molybdenum, high-thermal-inertia integrator with a lower cooling-water requirement.

For each design, it was necessary to predict the transient temperature profile at the surface and in the interior, the cyclic thermally induced stress that might induce fatigue failure, the transient heat flow across

the coolant boundary, and the effect of material and manufacturing tolerances. For these calculations, the ANSYS finite-element general-purpose program was used because it easily handles transient thermal and thermal stress problems, and because it can express the material properties as a function of temperature and can give convection coefficients as a function of wall

temperature. The copper design reaches a maximum temperature of 234°C, as shown in Fig. 10b, and the molybdenum design reaches 1390°C. These temperatures reflect the differing thermal conductivities of the copper and molybdenum, and the proximity of the cooling water to the incident beam.

The copper anode reaches steady state in 0.4 second while the molybdenum takes more than 15 seconds to reach equilibrium (peak heat flow occurs about 2 seconds after the 1-second pulse is input). Temperature gradients produce stresses up to 8860 psi tensile in the copper design and up to 19,000 psi compressive in the molybdenum design.

Model of circuit board

Porcelain-enameled-steel printed-circuit boards have been developed at RCA Laboratories that have attractive features for use in electronic applications.¹⁶ The partially devitrified glass porcelain can be re-fired at temperatures as high as 950°C after application of thick-film patterns and can withstand high voltages because it incorporates alkali-free materials. ANSYS finite-element calculations were initiated to determine the stresses resulting from firing, applied loads, and the geometry of the hole region; and to determine the thermal flow resulting from thick-film resistor Joule heating.¹⁷

Porcelain materials are weak in tension but strong in compression; therefore, the relative expansion coefficients have to be

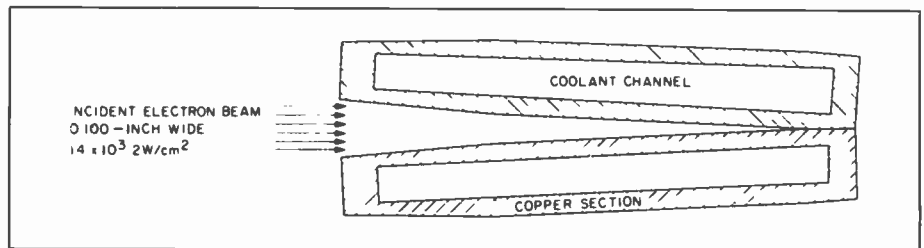


Fig. 10a. Power tube copper anode sections using a thin-wall high-coolant flow design.

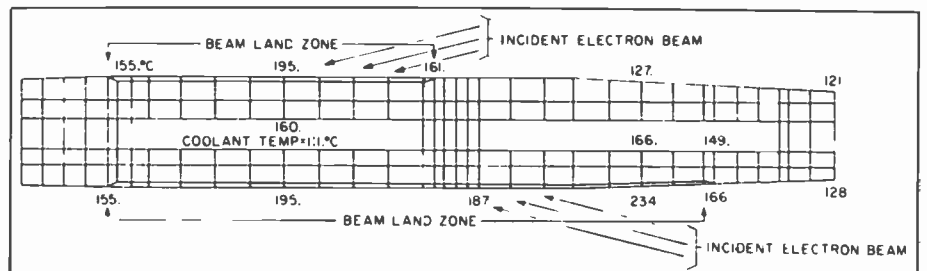


Fig. 10b. Finite-element model of a thin-wall copper anode section showing the temperature distribution resulting from an incident electron beam flux.

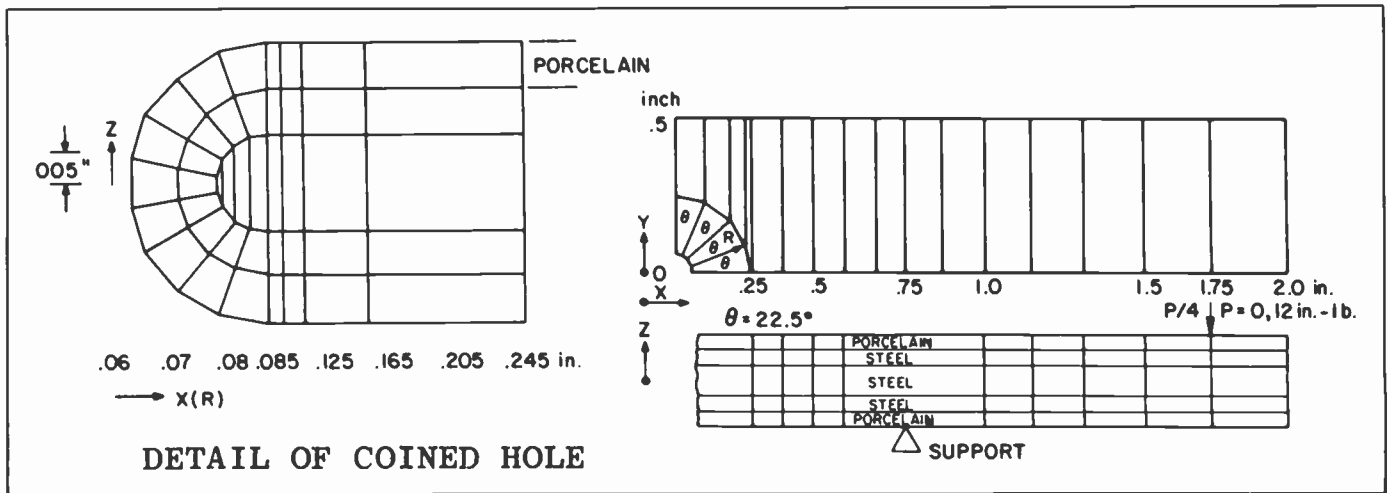


Fig. 11. Finite-element model of one quadrant of the porcelainized steel substrate having a well-rounded (coined) hole.

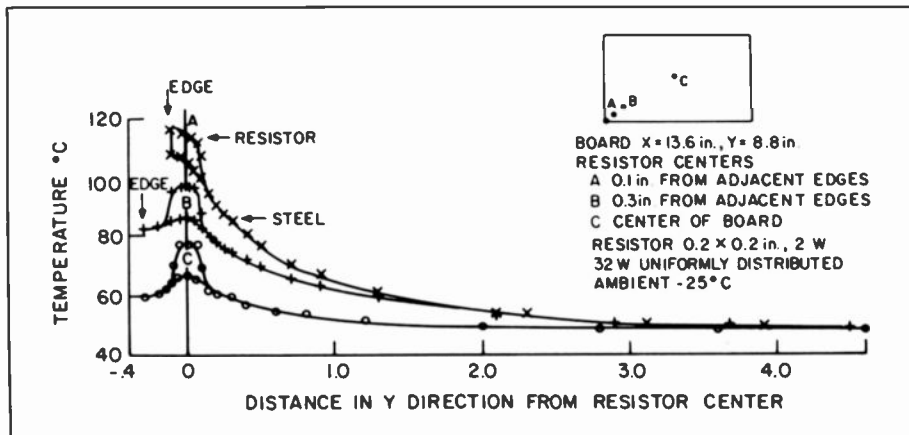


Fig. 12. Finite-element calculation of the thermal distribution for a resistor located at several different regions on a large substrate. The resistor contributes 50 W per square inch of localized heating while the background general heating is 0.25 W per square inch.

adjusted to a difference of about 1.4×10^{-6} per $^{\circ}\text{C}$ to achieve compression in the porcelain with the porcelain coefficient being lower. In this way, the steel is stressed to below its yield point and the porcelain can be bent without cracking. The finite-element model of the board and an expanded view of the hole region for a well-rounded hole are shown in Fig. 11.

Less-well-rounded and nonrounded holes were also investigated; the computer results showed that maximum roundness of the hole is desired. Another finite-element model was constructed for a board 13.6 inches long by 8.8 inches wide having resistors placed 0.1 or 0.3 inch from the edge of the board or at the center of the board. The results of the finite-element calculation are shown in Fig. 12. Note that, as the 2-watt resistor is placed farther away from the corner of the substrate, the temperature decreases substantially (going from

case A to C), suggesting that the resistor should be at least 0.3 inch from any edge. Further, up to 16 uniformly spaced 2-watt resistors should be tolerated without appreciable heat build up since the results in Fig. 12 show that the temperature is quite low at a distance of 2 to 3 inches from the resistor. In many applications, therefore, the porcelainized steel substrates should be thermally superior to alumina. The high thermal conductivity of the steel, the high emissivity of porcelain, and the thinness of the porcelain are favorable to thick-film resistors operating at high thermal densities.

Model of a cathode

The thermal characteristics of cathodes in a kinescope electron gun have been investigated by finite-element methods. Since the structure is centrosymmetric, an axisymmetric finite element can be used to

describe it. The finite-element model is shown in Fig. 13, and has been used to predict the effect of material and geometry changes on the cathode temperature as the heater power is changed.¹⁸ These calculations are important in the design of cathodes that have improved thermal and mechanical stability.

References

1. K.W. Coffey and R.E. Enstrom, "Interactive Digitizing and Graphics for Analysis of Random Lines, Surfaces, and Solids," RCA internal report.
2. R. Pschunder, "DYNA-3," presented at RCA Finite-Element Symposium, *DYNA-3 User's Manual*, Vol. 1—General Description; Vol. II—Program Description (November 1979).
3. R.H. Gallagher, "Finite-Element Analysis Fundamentals," Prentice-Hall, Englewood Cliffs, N.J. (1975). Also, O.C. Zienkiewicz, "The Finite-Element Method," McGraw-Hill, London, 3rd edition (1977).
4. F.W. Gorman, private communication.
5. R.J. Pschunder, "TVTOWER," presented at RCA Finite-Element Symposium.
6. C.C. Chen, "Computer-Aided Design of Metal-Forming Processes," *RCA Engineer*, Vol. 27, No. 2, pp. 45-49 (March/April 1982).
7. C.C. Chen, "PLAFOM2D-A Two Dimensional Axisymmetric Finite-Element Program for Metal Forming Analysis," RCA internal report.
8. R.E. Enstrom, R.S. Stepleman, and J.R. Appert, "Application of Finite-Element Methods to the Analysis of Stress in Television Picture Tubes," *RCA Review*, Vol. 39, pp. 665-698 (1978).
9. G.R. Niederoest, "Finite-Element Methods in Spacecraft Dynamic Analysis," *RCA Review*, Vol. 39, pp. 632-647 (1978).
10. G.R. Niederoest, private communication.
11. R.E. Enstrom, RCA internal memos.
12. R.E. Enstrom and D.A. Doane, "A Finite-Element Solution for Stress and Deflection in a Centrally-Loaded Silicon Wafer," RCA internal report, published in *Semiconductor Characterization Techniques*, edited by P.A. Barnes and G.A. Rozgonyi, *Proceedings*, Vol. 78, No. 3, The Electrochemical Society, Princeton, N.J., pp. 413-422 (1978).

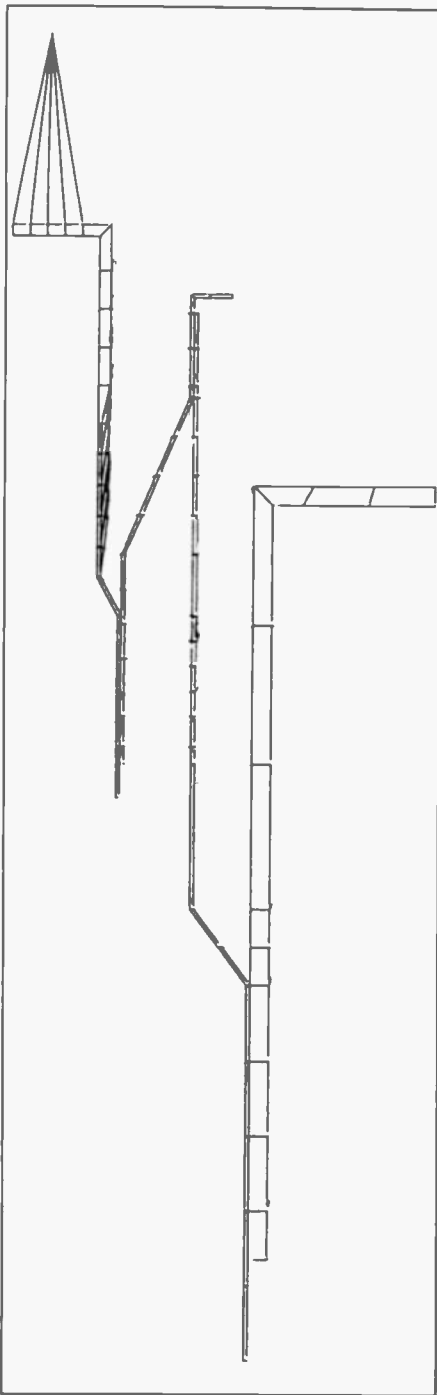
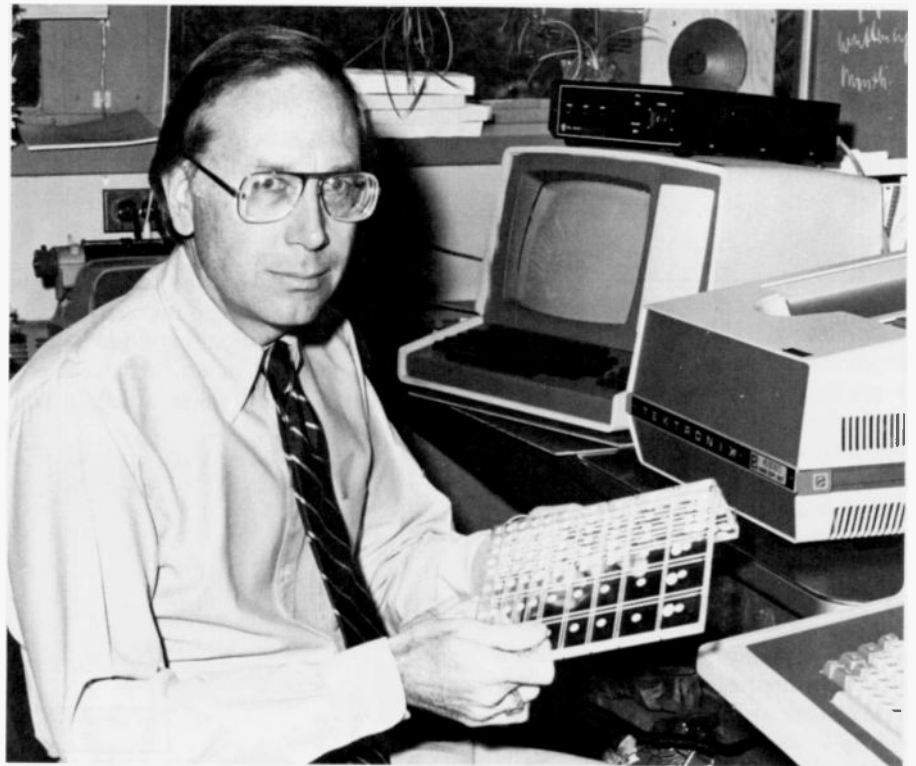


Fig. 13. Finite-element model of the gun structure of a 25V kinescope. Emission is from the front of the cathode; the other parts hold the cathode in place.

13. R.C. Bauder and R.E. Enstrom, RCA internal memos.
14. R.C. Bauder, "Finite-Element Analysis of a Twenty-Five Megawatt Power Tube and a High-Energy Water-Cooled Heat Sink for Fusion Research," *RCA Review*, Vol. 39, pp. 699-717 (1978).
15. W.E. Harbaugh, "The Development of a High-Energy Density Heat Sink," presented at the 8th Symposium on Engineering Problems of Fusion Research, San Francisco, Calif. (November 3, 1979).
16. K. Hang, J. Andrus, and W.M. Anderson, "High-Temperature Porcelain-Coated Steel Substrates—Composition and Properties," *RCA Review*, Vol. 42, pp. 159-177 (1981).
17. J.H. McCusker, "Finite-Element Analysis of Stresses and Thermal Flow in Porcelain-Enamelled Steel PC Boards," *RCA Review*, Vol. 42, pp. 281-297 (1981).
18. R.C. Bauder, S. Opresko, and R.E. Enstrom, RCA internal memos.



Ron Enstrom received the S.B., S.M., and Sc.D. degrees from M.I.T. in 1957, 1962, and 1963 respectively. All degrees were awarded in the field of metallurgy. He joined RCA Laboratories in 1963 where his research has included superconducting materials and devices, silicon and III-V compound semiconducting materials and devices, glass technology, polymer processing and high-conductivity polymers, metallurgy, and finite-element

computer modeling of semiconductor, VideoDisc, and kinescope-related problems. His research has resulted in two RCA Laboratories Outstanding Achievement Awards, in 1965 and 1972, and a David Sarnoff Award for Outstanding Technical Achievement in 1967.

Contact him at:
RCA Laboratories
Princeton, N.J.
TACNET: 226-2309

Electromechanical motor modeling

Computer modeling aids calculation of the start-up torque of a novel motor design, intended for use in various high-performance systems, including high-reliability space applications and consumer electronics.

Abstract: *The primary purpose of computer modeling of electromechanical motor design is to estimate allowable tolerances in mechanical design parameters. Input parameters such as coil-rotor gap spacing and radial coil positioning are easily varied in the model, permitting estimation of the sensitivity of motor performance to those parameters. Start-up torques and forces are the primary output of the model. They are related to start-up time and running performance of the motor. The geometric shape of the motor coils and their relative positioning are variable inputs to the model, along with the permanent magnetic field of the rotor. The model divides the coil into individual current elements; the program then analyzes the interaction of each current element with the magnetic field of the rotor.*

Computer modeling of electromechanical motor design aids the manufacturing design engineer. By selectively changing the design parameters entered as inputs into the model calculations, the effects of manufacturing tolerance variations upon motor-performance characteristics may be estimated. In particular, one very important performance characteristic is the maximum possible torque output. The torque delivered during the start-up period is directly related to the time necessary to reach the required operating rotational velocity.

The result of an effort to develop a

model that calculates the start-up torque of a novel motor design is described here. The motor in question is a brushless, ironless two-phase dc motor. It consists of a stationary set of ironless armature coils

mounted below a rotating ferrite permanent magnetic field structure as shown in Fig. 1. The rotor was magnetized into eight evenly spaced salient poles. Instead of brushes, Hall-effect field sensors are used

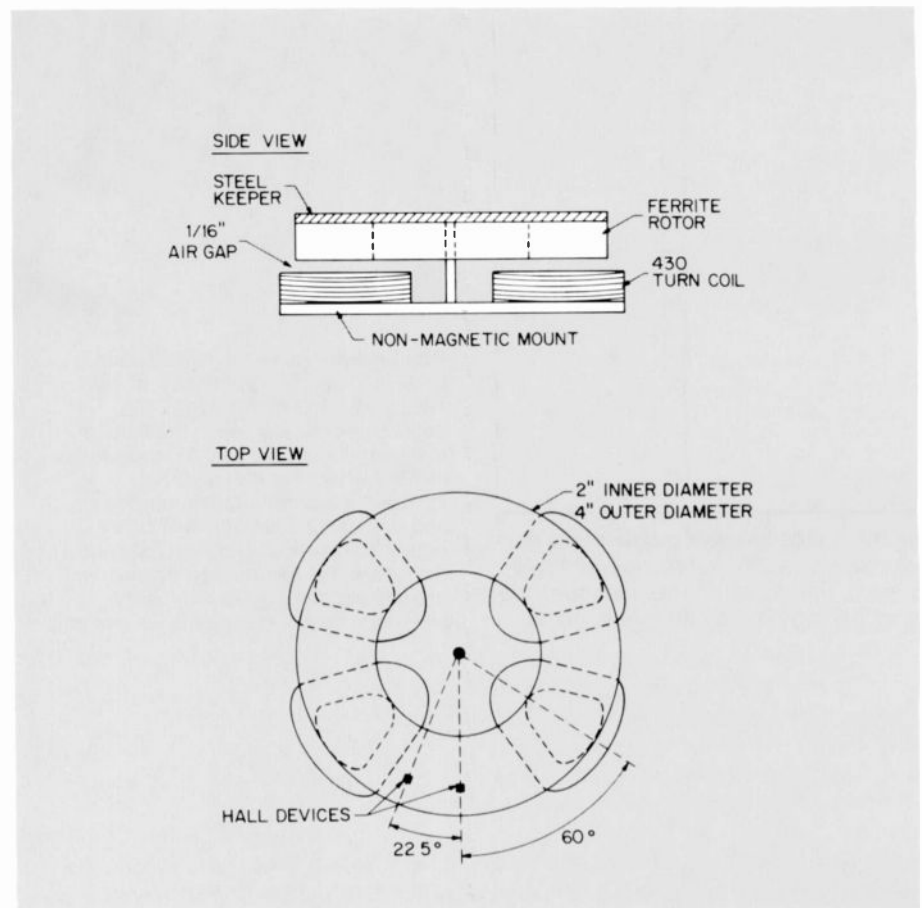


Fig. 1. Two views of a brushless, ironless motor.

© 1982 RCA Corporation
Final manuscript received September 8 1982
Reprint RE-27-6-12

to sense field crossover points and to provide signals for commutation of the current. Since the motor construction is ironless, there are no cogging torques and no hysteresis losses, and eddy-current losses are very low. These features make this motor design suitable for use in various high-performance systems. Much of the early development work on this type of motor was done by NASA for use in high-reliability space applications. Currently, such motors are extensively used in the United States and in Japan for consumer electronics appliances such as videotape recorders and record players.

The model

The first step in calculating the magnetic interactions of this motor is to study the interaction of one coil with one pole-pair of the rotor. The effects of the other coils and poles and the phasing of the drive current are discussed later. The fundamental torque equation is:

$$\vec{T} = \int_V [\vec{x} \times (\vec{J} \times \vec{B})] d^3x \quad (1)$$

where \vec{B} is the magnetic flux density, \vec{J} is the current density in the coil, and \vec{x} is the moment arm.

The shape of the coil is a smoothed wedge that approximately matches the distribution of field on a pole face. This wedge shape is approximated for computer input by listing 10 points each around the inner and outer peripheries of the coil. This outline is subdivided by the program into a finer grid of 48 elements (each 6×8). The thickness of the coil is represented by assuming there are four evenly spaced layers on this grid in the z-direction covering the $3/16$ -inch thickness. Thus, one coil is modeled by 1920 elements ($6 \times 8 \times 4 \times 10$). The fineness of this grid is less than $1/16$ inch in each dimension.

For approximation, equation (1) becomes:

$$T = \sum_{i \text{ elements}} (n_i I dl_i) B_i R_i \quad (2)$$

Here n_i is the number of turns through each element (this assumes a uniform winding n_i equal to $430/24$), I is the current, dl_i is the radial component of the current element length, B_i is the vertical component of the field at the center of the element, and R_i is the distance from the center of the element to the axis. If dl_i and R_i are in meters, I in amperes, and B_i in tesla, then T is in newton-meters. The torque

constant k_m of the motor is defined as the torque-per-unit-current in the coils:

$$k_m = T/I. \quad (3)$$

A detailed calculation of the magnetization of the rotor would require knowledge of the magnetizing apparatus. For the purpose of calculating torque in this model, the magnetic field at the face of the rotor is a fixed input. The field of the rotor was measured over the whole region in question. All three components of the field were mapped out over an approximate $1/8$ -inch fine grid over the face of the rotor. The fall-off of the field as the distance away from the rotor increased was also measured. This fall-off could be fit quite well into an equation of the form:

$$\vec{B} = \frac{\vec{C}(r,\theta)}{(a^2 + z^2)^{3/2}} \quad (4)$$

where $\vec{C}(r,\theta)$ is the field at the surface, z is the distance measured from the rotor surface facing the coils, and a is approximately 0.4 inch. The fit is shown in Fig. 2; within the range of interest, the fit is better than 4 percent. This equation reflects the z-dependence of the field of a magnetic pole of radius a .

The components of the field at the surface are input for each point on a grid covering every 5° azimuthally and every $1/8$ inch radially. To find the field at any given point, the program linearly interpolates on this grid. The z-dependence of the

field, as given in equation (4), is used to calculate the fall-off of the field away from the surface of the magnet.

Results of torque calculations

The program was written in FORTRAN and is implemented on CMS. A sample output plot of the torque constant of one coil as a function of the relative angle between coil and pole field is shown in Fig. 3. The curve plotted was calculated using as input parameters an air gap of 0.0625 inch and an inner radius of 0.65 inch. The inner radius parameter is the distance from the inner edge of the coil to the rotational axis. The torque constant is given in a practical unit of oz.in./A ($1 \text{ N}\cdot\text{m} = 141 \text{ oz}\cdot\text{in.}$). The usefulness of the model is shown in Figs. 4 and 5. By simply varying the input parameters of gap spacing or coil radial position, the model estimates the sensitivity to these changes of the torque constant.

An experimental check of these torque constant calculations for one set of parameters was made by taking back electromotive force (EMF) measurements on the coils. The back EMF (V_{emf}) is measured by recording the voltage across the coils with no drive current applied as the rotor is kept at a constant rotational speed by another motor. The back-EMF constant k_e is defined by $V_{emf} = k_e \omega$, where ω is the rotational speed. The back-EMF con-

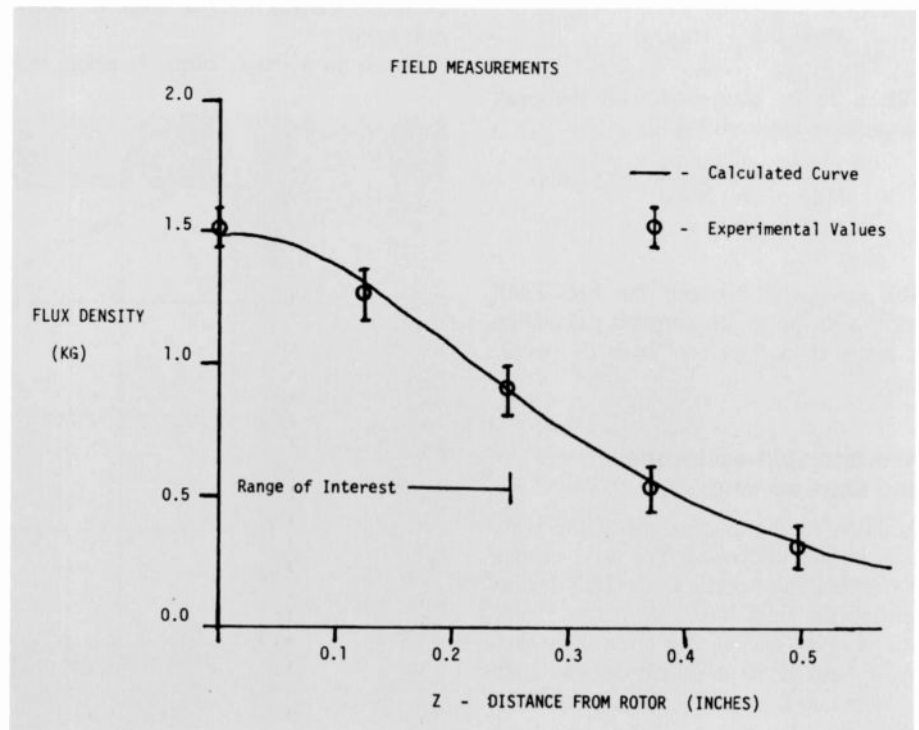


Fig. 2. Calculated and measured fall-off of rotor field away from the rotor surface.

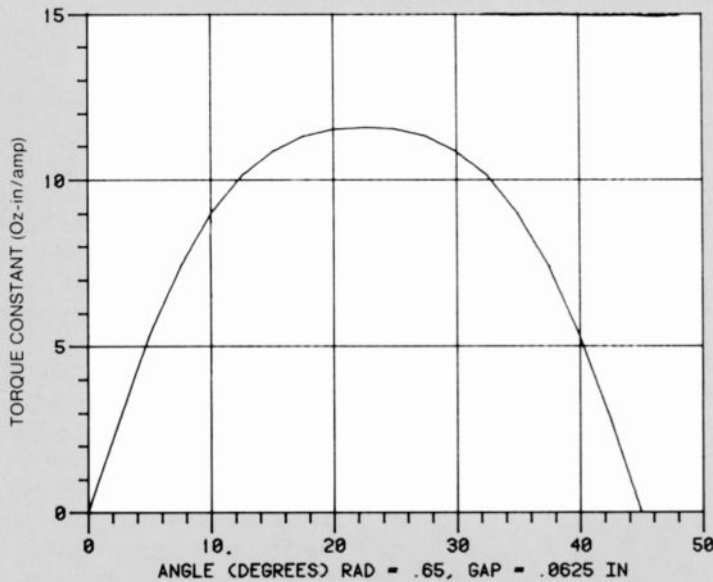


Fig. 3. Sample output plot of torque versus angle for one coil and one pole-pair.

stant is directly related to the torque constant; in fact, in MKS units, they are numerically equal ($1 \text{ N}\cdot\text{m}/\text{A} = 1 \text{ V}/(\text{rad}/\text{s})$). The back EMF measured for two coils in series was 7.8 V, at a speed of 7.5 revolutions per second and gap of 0.0625 inch. Thus, the back-EMF constant at the peak is:

$$k_e = \frac{7.8 \text{ V}}{2\pi (7.5 \text{ s})} = 0.165 \text{ V}/(\text{rad s})$$

This is to be compared with the peak torque constant from Fig. 3:

$$k_m = \frac{(11.03 \text{ oz}\cdot\text{in.}/\text{A})}{(141 \text{ oz}\cdot\text{in.}/\text{N}\cdot\text{m})} \times 2 \text{ coils} = 0.16 \text{ N}\cdot\text{m}/\text{A}$$

The agreement between the back-EMF curve and the torque-constant calculation is better than 5 percent over the whole curve.

Average start-up torque and start-up time

Addition of the interactions of the other coils is straightforward. The drive current is switched in response to the Hall devices sensing the field crossover points. There are two Hall devices, one controlling each phase, spaced 90 electrical degrees apart (which means the Hall spacing is 22.5°, physically). For maximum start-up torque, the Hall devices should be spaced electri-

cally 45° from the centers of the coils they drive. This corresponds to a physical separation of 56.25° from the Hall device to the center of the nearby coil (see Fig. 1). For other design reasons, this spacing is usually closer to 60°. A curve showing the calculated torque for both coils, assuming a current of 0.5 A, is shown in Fig. 6. The average torque is 10.5 oz-in. The effect upon average torque of changing the Hall position relative to the coils is easily calculated.

Given an average torque constant, the

time required to reach a given angular velocity can be estimated in the following manner. First, the relevant physical parameters of the motor are:

$$J_m = 0.0047 \text{ kg}\cdot\text{m}^2 \text{ (moment of inertia of motor and load)}$$

$$R_m = 40 \Omega \text{ (effective coil resistance)}$$

$$k_e = 0.16 \text{ V}/(\text{rad}/\text{s})$$

$$k_m = 0.16 \text{ N}\cdot\text{m}/\text{A} \text{ (motor constant calculated)}$$

The dynamic equation of the motor is (neglecting bearing friction):

$$T = J_m \frac{d\omega}{dt} \quad (5)$$

The relational equations are:

$$V_o = k_e \omega + IR_m$$

$$T = k_m I$$

with V_o being the maximum voltage applied across the coils. For maximum drive current of 0.5 ampere, V_o is 20 volts. Integration of equation (5) gives:

$$\omega = \frac{V_o}{k_e} (1 - e^{-t/\tau})$$

with

$$\tau = \frac{R_m J_m}{k_e k_m} = 7.3 \text{ s}$$

Based on equation (6), the time necessary to reach a given running speed of 7.5 revolutions per second is about 4 seconds.

Once the motor approaches this running speed, its mode of drive is changed such that, while running, only short current pulses are applied to maintain speed. Extensions of the model to simulate be-

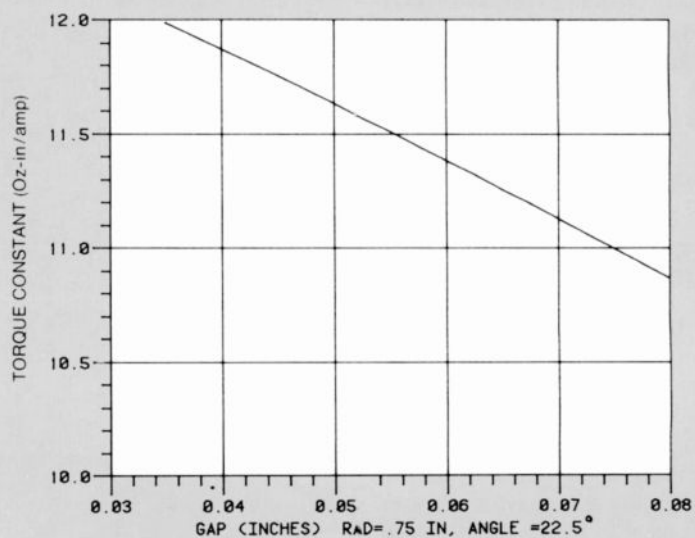


Fig. 4. Peak-torque constant as a function of rotor-to-coil-gap spacing variation.

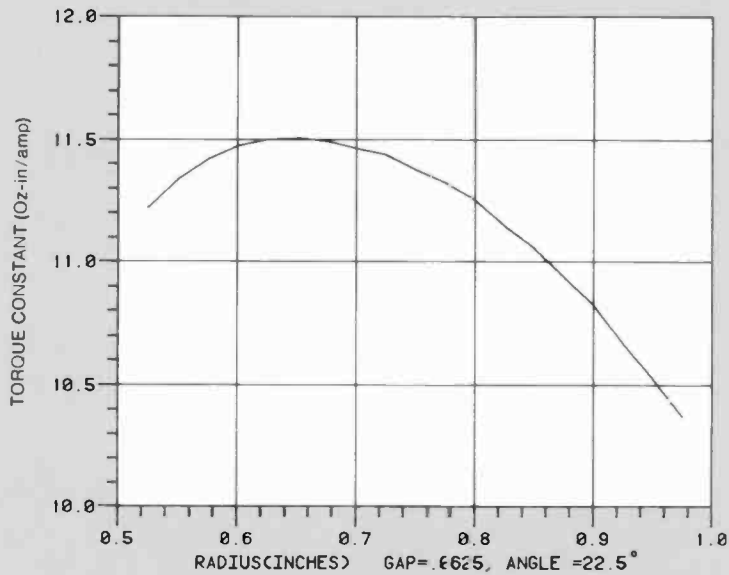


Fig. 5. Peak-torque constant as a function of relative coil-to-rotor lateral positioning.

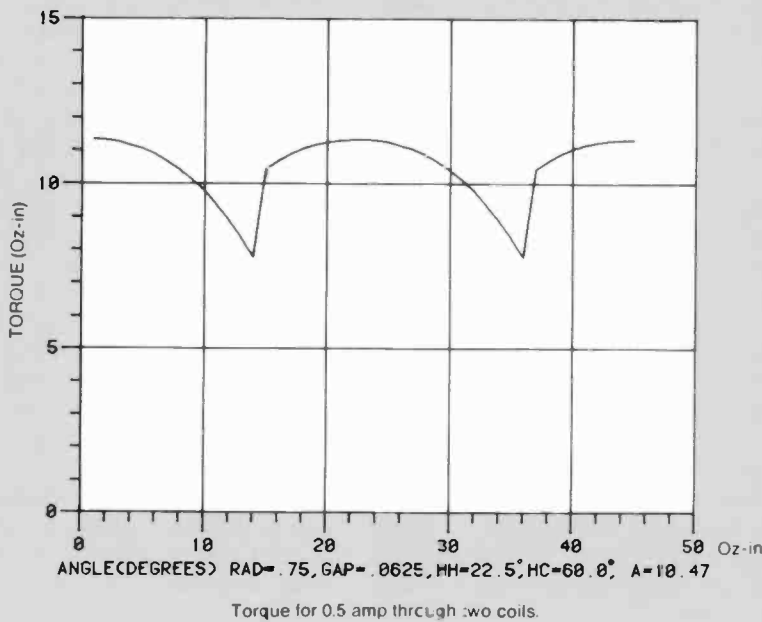
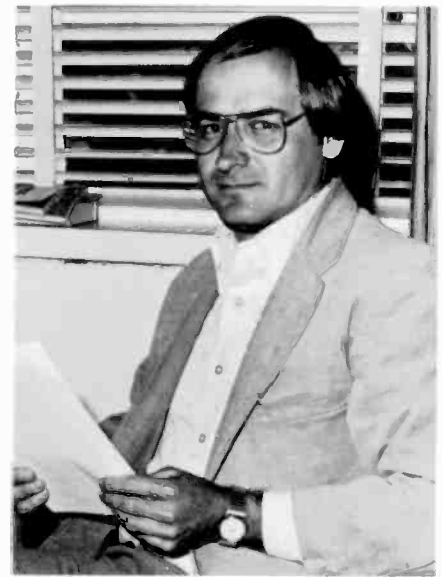


Fig. 6. Sample output torque curve for a motor with Hall sensors switching current through each pair of coils.

havior during the running operation of the motor, as well as estimates of stopping

time, were done in a fashion similar to modeling described here.



Robert Browne joined the Technical Staff in the Manufacturing Technology Research Laboratory at the David Sarnoff Research Center in late 1978. He participated in a variety of manufacturing systems research projects, some with Consumer Electronics and others related to Picture Tube Division work. Dr. Browne received his Ph.D. from Princeton University in 1979 and is a member of both the American Physical Society and the IEEE. Contact him at:
RCA Laboratories
Princeton, N.J.
TACNET: 226-2363

Summary

This paper has presented typical examples illustrating the usefulness of computer modeling in calculating start-up torque and start-up time as a function of input parameters. The model helps design engineers to set manufacturing tolerances by providing estimates of motor-performance variation from these various design parameters.

Acknowledgments

Useful discussions with W.G. McGuffin, T. Christopher, E.A. Goldberg, and K. Kelleher were held on motor design. R.W. Burgen provided the experimental back-EMF data.

Computer modeling in the RCA Satcom system

Different computer simulations are used for different types of services carried on the RCA Satcom system.

Abstract: *Each of the four RCA Satcom satellites now in orbit has 24 transponders that carry a wide variety of communications services such as television/frequency modulation (TV/FM), frequency-division multiplexing/frequency modulation (FDM/FM) voice, time-division multi-access (TDMA), and frequency-division multi-access (FDMA), with a variety of carriers. Each type of service is subject to different impairments from the transponder channel, and this has necessitated creation of a number of computer models that simulate performance. This paper presents some of these models.*

A transponder in the Satcom system may be assigned to carry one of a large number of possible services. Each service has its own modulation plan and system parameters. Each type of service is impacted in a different way by the transponder channel it passes through. This has resulted in different computer models or simulations for different types of services. These models are used by Americom as traffic assignment aids for scheduling which services are placed on which transponders and for planning accompanying ground systems. New services are being developed continuously, and computer models are typically used before physical simulation and over-the-air satellite tests.

The basic satellite power amplifier is usually modeled as a zero-memory or instantaneous nonlinearity. That is, the amplitude and phase of the radio-frequency (RF) signal out of the amplifier is a nonlinear function of the amplitude of the RF input,

but independent of past values of RF input. The signal arrives at the power amplifier after passing through a filter that separates the signal destined for this transponder from the signals destined for other transponders. Likewise, before transmission to earth, the output of the power amplifier is refiltered. This model of input filter, instantaneous nonlinearity, and output filter is the kernel of most Satcom computer models. Sometimes some elements of the ground system or other elements of the satellite must be included in a model, in other cases some parts of the kernel model may be eliminated, but the kernel remains the starting point. Because it is easiest to calculate the output of a filter from a frequency domain description of its input, and, likewise, to calculate the output of an instantaneous nonlinearity with a time-domain description of its input, it is necessary to flip back and forth between time and frequency domain descriptions of a signal as it transits the transponder. Hence, large fast Fourier transforms (FFTs) are used extensively in these models.

Even when it is clear that the simple kernel model of a transponder suffices, different computer models are needed for different types of signals sent through the transponder. To begin with, the information expected from the model is different for different types of signals.

If the signal is high-speed digital, the model should generate "eye patterns," pattern-dependent timing jitter, bit error rate, and so forth. If the signal is television/frequency modulation (TV/FM), the model should generate differential phase, differential gain, T-pulse response, and so forth. The computer models must be signal or service specific. Sometimes creating a com-

puter program to specifically analyze one type of service allows for simplification in the basic kernel model, either because some results can be calculated analytically and built into the model or because the signal structure allows for simplification. An example of the latter is the case of multicarrier frequency-division multiaccess (FDMA) when each of the individual carrier bandwidths is small (or equivalently, the carrier spectra do not get near the filter band edge). In this case, filter amplitude and delay are fairly flat across any one carrier and, hence, have little effect. The primary impairment is classical intermodulation distortion, and the kernel model reduces to the effect of the nonlinearity above. This simplification allows optimization of carrier levels and frequencies that would be impractical with the more general transponder model.

The following is a description of a few sample computer models created for use in the Satcom system. The emphasis is on what the models do, not how they do it.

Computer simulation and optimization of multicarrier transponder operation

To evaluate and compare various transmission arrangements for the many signals that go through the RCA satellite, a computer program was developed that simulates any given multicarrier arrangement with a transponder. To reduce the computer time needed for any one calculation, certain simplifications were employed. As a result, some special interference effects that occur in the actual satellite system do not show up in this particular computer model. The result is a computer program

that tells the user the carrier-to-noise (C/N) ratios achievable with a particular arrangement of carriers in one transponder. When the optimization feature is used, the model cycles through many possible carrier arrangements in a systematic manner, while moving toward the best arrangement in terms of C/N. It is important, however, for the user to know the limitations of the model before making a final decision.

A transmission system modeled by the computer program

The transmission system consists of a transmitting earth station, a 22,300-mile uplink path, a satellite traveling-wave tube (TWT) (linear and nonlinear) with one transponder, a 22,300-mile downlink path, and a receiving earth station (see Fig. 1). The input to this system is a set of two or more carriers that enter the uplink path from the transmitting earth station. In the uplink path, Gaussian thermal noise is added to the carriers. In the TWT, the carriers undergo gain changes, and intermodulation distortion carriers (nonlinear product terms) are added. In the downlink path, more Gaussian thermal noise and some cross-polarization noise, signals from adjacent cross-polarized transponders, are added to the carriers. In some cases, the input carriers originate from more than one earth station and may also terminate at more than one earth station. As a result, the uplink and downlink path losses for all the carriers may be unequal.

The five components of the transmission system noted above are modeled in the computer program by entering certain specific parameters of each component. Table I lists the parameters associated with each component. The following is a partial list of parameters not included in the model:

1. Satellite location (longitude)
2. Transmitting earth-station location (latitude, longitude)
3. Receiving earth-station location (latitude, longitude)
4. Rain data for each earth station

These parameters can be important for a few special cases.

Carrier types

At the present, satellite transmission of five types of carriers can be analyzed with the OPTX program:

- FDM/FM (voice/data channel carrier)

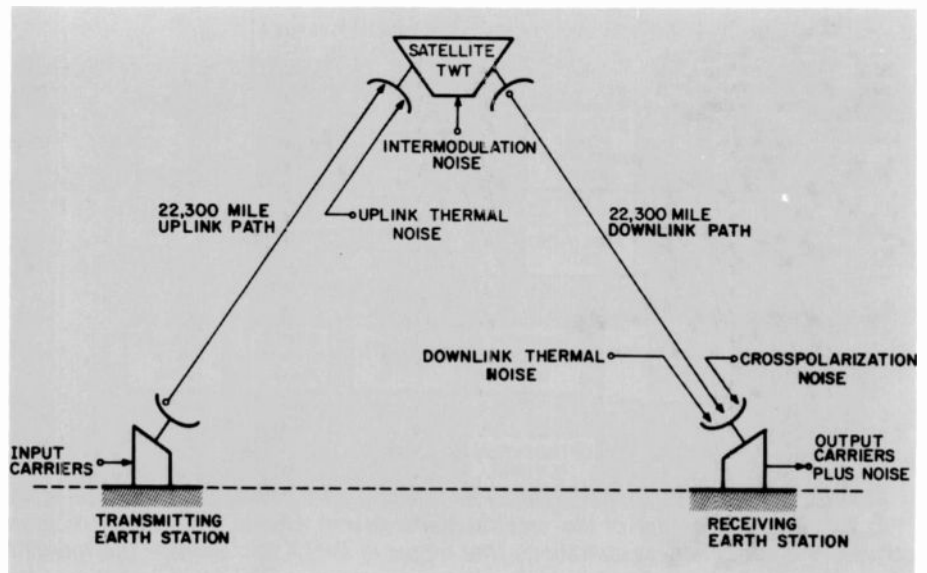


Fig. 1. Satellite transmission system. The diagram shows a typical path in a satellite transmission system, including all sources of interference (noise plus intermodulation distortion) to be considered in the optimization process.

- TV/FM (TV carrier)
- SCPC (single channel per carrier—many small carriers)
- BPSK (digital data carrier—2-phase)
- QPSK (digital data carrier—4-phase)

For each carrier type listed above, the user models the carriers by entering the following parameters:

- Power level
- Center frequency
- Signal bandwidth (for noise calculations)
- Allocated bandwidth (for frequency spacing)
- Desired carrier-to-noise ratio
- Deviation (FDM/FM and TV/FM carriers)

Computer model of the transmission system

Based on the actual transmission system shown in Fig. 1, a computer model of the transmission system, shown in Fig. 2, was created. The two most important blocks in the system are the computer models for the satellite power amplifier and the noise. Further details on modeling the satellite power amplifier, are provided in references 1 and 2. The noise model is based on a simple addition of the four noise sources in the system. With this simplification, the C/N value for each carrier is obtained by adding together the uplink thermal-noise power times carrier gain, the downlink thermal-noise power, the amplifier intermodulation power, and the cross-polarization noise power, then dividing the result into the output carrier power. In the optimization mode, the computer program tries to maximize the minimum margin for each carrier where

Table I. Parameters associated with each component.

Component	Parameters
1. Transmitting earth station	None
2. Uplink path	None
3a. Satellite linear devices	Noise (kTB) Uplink antenna G/T Saturation flux density Effective isotropic radiated power
3b. Satellite nonlinear device (power amplifier)	Amplifier data
4. Downlink path	Path loss Cross-polarization noise power
5. Receiving earth station	Antenna G/T

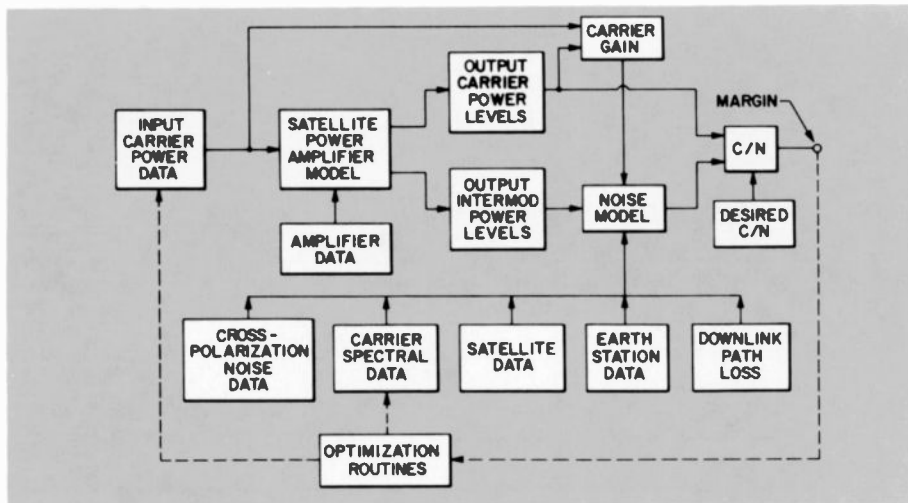


Fig. 2. Computer model of the satellite transmission system. This block diagram shows the sequence of operations that occur in OPTX to calculate the margins, given the input carrier data (power levels and spectrums). OPTX tries to optimize the margins by manipulating the power levels and center frequencies.

```

RUN OPTX
DHSL107401 EXECUTION BEGINS...
ENTER THE DATA FN FT (FM) [CAR3 DATA
CAR3 DATA FOR GLOBAL BEAM,3 CARRIERS ( FULL)
INTERMOD LINE DATA....
NO. OF LINES= 48 LOWEST LINE= -63 DB CUTOFF= -80
FIRST= 3 THIRD= 9 FIFTH= 15 SEVENTH= 21
CARRIER DATA....
MIN MAR= 2.70 MAX MAR= 4.49 TIBO= -5.00 PEAK V= 1.38
MARGIN= 2.70
CAPI= -9.77 -9.57 -9.97
MARG= 2.70 3.15 4.49
OPTIMIZE=1,OPTIMIZE(N)=2,SLIDE=3,PERMUTE=4,STOP=5,CHANGE(TIBO)=6
?
[1
MIN MAR= -1.84 MAX MAR= 5.25 TIBO= -4.53 PEAK V= 1.43
MIN MAR= 1.91 MAX MAR= 6.05 TIBO= -4.61 PEAK V= 1.43
MIN MAR= 2.65 MAX MAR= 4.72 TIBO= -5.24 PEAK V= 1.34
MIN MAR= 2.89 MAX MAR= 3.80 TIBO= -5.29 PEAK V= 1.32
MIN MAR= 0.79 MAX MAR= 7.78 TIBO= -2.39 PEAK V= 1.76
MIN MAR= 0.88 MAX MAR= 7.64 TIBO= -2.28 PEAK V= 1.80
MIN MAR= 0.54 MAX MAR= 7.53 TIBO= -2.25 PEAK V= 1.81
MIN MAR= 2.97 MAX MAR= 3.91 TIBO= -4.59 PEAK V= 1.44
MIN MAR= 1.20 MAX MAR= 6.44 TIBO= -2.59 PEAK V= 1.79
MIN MAR= 1.61 MAX MAR= 6.31 TIBO= -3.66 PEAK V= 1.59
MIN MAR= 1.87 MAX MAR= 5.13 TIBO= -3.32 PEAK V= 1.67
MIN MAR= 3.21 MAX MAR= 3.49 TIBO= -5.08 PEAK V= 1.36
MIN MAR= 3.21 MAX MAR= 3.31 TIBO= -4.48 PEAK V= 1.46
NO. OF OPTIMIZE RUNS= 1 MARG= 3.210 TIBO= -4.48 NCAL= 14
CONTINUE OPTIMIZATION=1,END OPTIMIZATION=0
?
[0
CARRIER DATA....
TIBO= -4.48 MARG= 3.21038
CAPI= -8.67 -8.90 -10.36
MARG= 3.21 3.23 3.31
OPTIMIZE=1,OPTIMIZE(N)=2,SLIDE=3,PERMUTE=4,STOP=5,CHANGE(TIBO)=6
?
[4
PERMUTE THE ORDER OF THE CARRIERS
...MAX MAR...AVE MAR...PERM NUM...CARRIER SEQUENCE
2.81073 3.53822 1 1 2 3
0.76188 4.43621 2 1 3 2
-0.98594 4.62566 3 2 1 3
OPTIMIZE=1,OPTIMIZE(N)=2,SLIDE=3,PERMUTE=4,STOP=5,CHANGE(TIBO)=6
?
[3
SLIDE(SUCCESS)...AVMARG(MIN),AVMARG(MAX)= 3.483 4.058
FREQ 5.000 19.893 30.000
MARG 2.399 4.578 4.815
OPTIMIZE=1,OPTIMIZE(N)=2,SLIDE=3,PERMUTE=4,STOP=5,CHANGE(TIBO)=6
?
[5
REAL CPU TIME(USEC)= 1354580 COST= 1.79
R:
[LOG
CONNECT= 00:02:38 VIRTCPU= 000:01:22 TOTCPU= 000:02:30
LOGOFF AT 10:00:57 EST TUESDAY 09/07/82

```

Fig. 3. Optimization with the OPTX program. In this sample run of the OPTX program, calls are made to the routines OPTIMIZE (adjust the carrier power levels to maximize the minimum margin), PERMUTE (rearrange the frequency order of the carriers), and SLIDE (shift the center frequencies of the carriers within the available frequency space) to try to maximize the minimum margin.

margin is defined as

$$\text{Margin} = C/N \text{ (dB)} - \text{desired } C/N \text{ (dB)}$$

Depending on the user's choice, this can be done by varying input carrier power levels, rearranging the spacing between carriers, or changing the order of the carriers in the frequency domain. A typical calculation using the OPTX program and a data file called CAR3 DATA is shown in Fig. 3.

Communication of television signals over satellite

Frequency modulation is usually employed to transmit TV signals over satellites. The signals are distorted by transmit and receive earth-station filters, satellite input and output filters, and the nonlinear behavior of the satellite power amplifier. The signal is also corrupted by noise received along with the desired signals.

Noise performance of FM systems can be accurately determined by using well-known mathematical models. However, no simple analytical model exists that can predict the distortion performance satisfactorily. Consequently, a computer simulation model was developed that consists of a test waveform as the baseband signal. Many types of test waveforms, such as a composite test signal, combination test signal, staircase signal, and color bars, are developed and standardized by the television industry. Figure 4 shows the composite test signal, a part of which is shown in Fig. 5 to an expanded scale. In the computer model, this waveform is generated by use of the mathematical functions that accurately define all the components. In Fig. 5, the waveform shows the trailing edge of the T-step or line bar, at 31.75 μs , the 2T-pulse, beginning at 35.0 μs , the chrominance pulse, beginning at about 36.5 μs , and the first part of a five-step staircase. These components of the composite signal, as well as other test waveforms, are designed so that the distortion obtained is representative of the distortion suffered by a real picture as it goes through the various parts of a communication link.

In computer simulation, two lines of TV picture carrying the test waveform are generated, including the chrominance signal over its entire period, which is two lines. The spectrum of this signal, after it is normalized to 1 V peak-to-peak, is shown in Fig. 6. The baseband signal is pre-emphasized at the modulator and is de-emphasized at the demodulator. These filtering actions result in nearly flat noise power at all frequency regions of the baseband. However, filtering creates distortion problems if

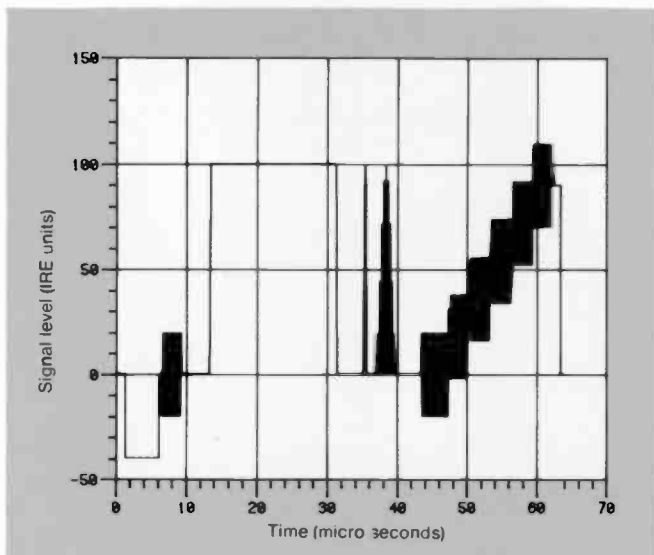


Fig. 4. Composite test signal. The components of the signal are designed to produce a kind of distortion that real pictures suffer when they go through a communication link.

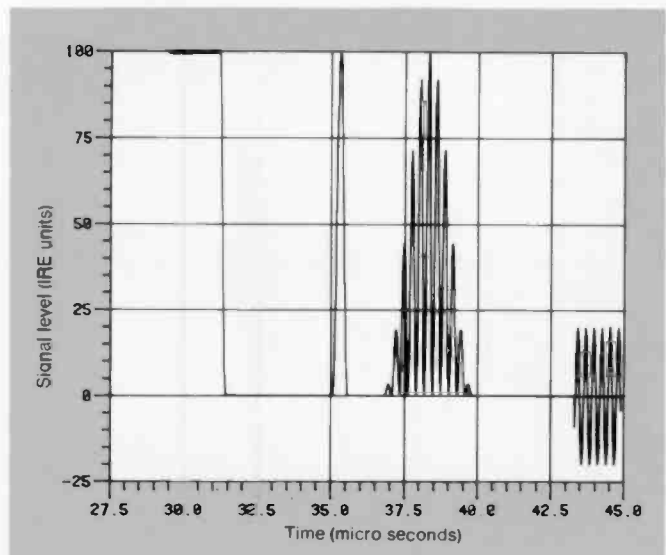


Fig. 5. A segment of the composite test signal.

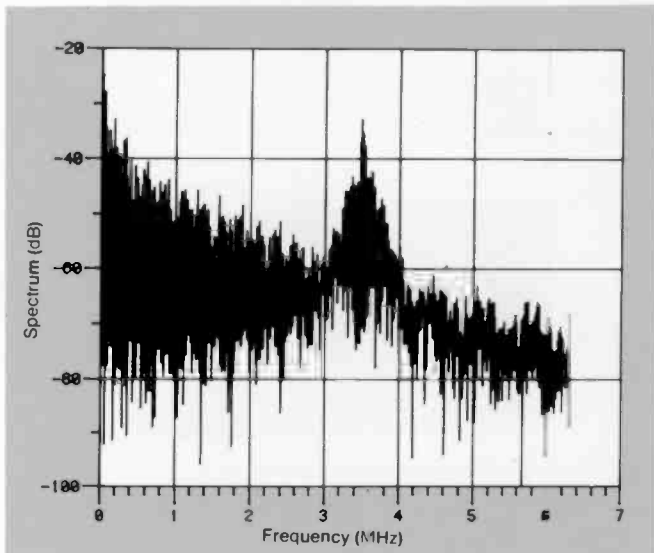


Fig. 6. Spectrum of the composite test signal. The discrete spectral lines arise because TV signals have periodic line structure.

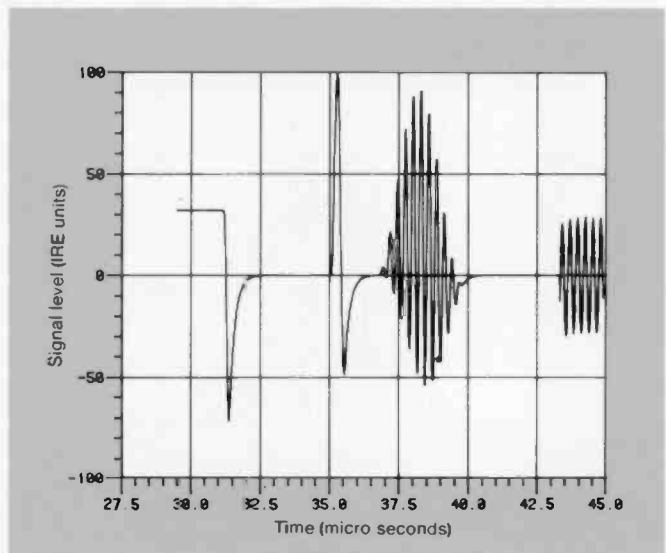


Fig. 7. Pre-emphasized composite test signal. The peak values of the transients are related to the pre-emphasis filter parameters.

the frequency deviation is excessive. Figure 7 shows the output of the pre-emphasis filter (CCIR type) when its input is the composite signal. Notice the sharp transients generated. Suppose such a signal is given a peak-to-peak deviation of 16 MHz, frequency modulated, and passed through a 17.5-MHz filter to limit the spectrum to an allocated bandwidth of 18.0 MHz. The filter output does not have a constant envelope. Figure 8 shows the envelope of the output. The envelope takes a sharp dip wherever the transients produced by the pre-emphasis filter dominate. In the regions of the TV picture where the FM signal envelope has a sharp reduction, the noise

dominates; the channel noise creates impulses or clicks that result in a visible degradation, often referred to as "tearing." Using the computer model, it is possible to determine the impulse rate and study its dependence on the type of pre-emphasis filter, the deviation given to the carrier, and the channel filter.

The filtered waveform passes through the satellite power amplifier, whose characteristics are nonlinear. To obtain maximum output power, the amplifier is operated near the saturation region. The result is that the amplifier works as a nonlinearity that gives varying amounts of gain as a function of its input power. Further, the commonly

used power amplifiers have the undesirable feature of introducing a phase component at the output, whose value fluctuates as a function of the input signal envelope. This effect, termed amplitude modulation-to-phase modulation (AM-to-PM) conversion is especially bothersome when a satellite transponder carries two TV-FM signals. As shown in Figs. 7 and 8, the envelope of the output of the channel filter is a function of the baseband signal. When two carriers are given as input to the filter, the fluctuation of the envelope of the combined signal at the filter output is a function of the baseband signals of both the carriers. Through the AM-to-PM conver-

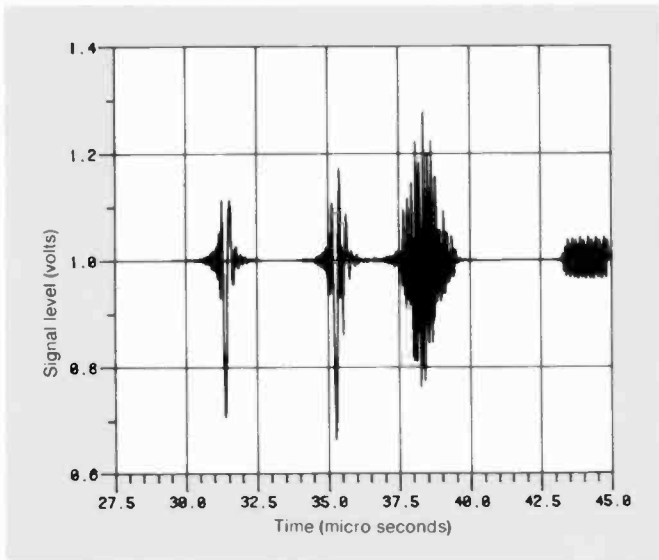


Fig. 8. Envelope of the filter output when its input is the FM signal modulated by the composite test signal.

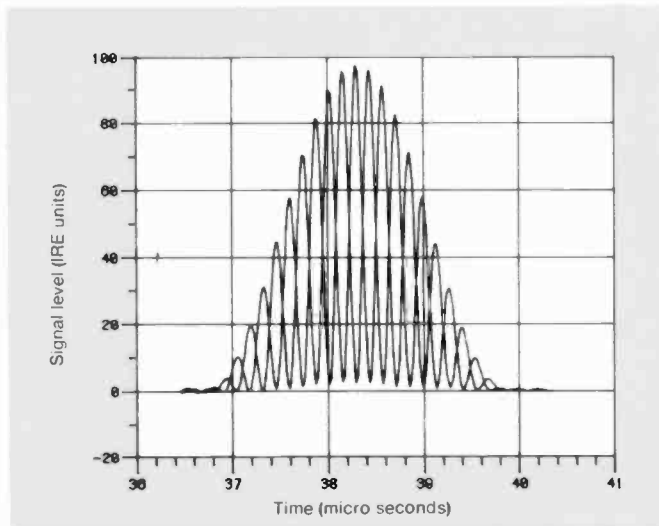


Fig. 10. Demodulated chrominance pulse. The maximum value and the envelope of the minimum values are used in computing chrominance distortions.

sion. the envelope fluctuations are translated into the phase components of each of the carriers. Thus, the phase of each of the carriers has a component that depends on the baseband of the other carrier. The result is that, after demodulation, the cross-talk component of one picture appears as a background signal in the other. The visible portion of the crosstalk appears as a slow color fluctuation (breathing of color). These nonlinear cross-talk problems were analyzed using computer models.

The filtering action by the channel filters can not only introduce click noise problems, but also lead to excessive distortions in the baseband signal. Figure 9 shows the leading edge of the T-step after the received FM carrier is demodulated; ringing of the

waveform is seen. The "short-time distortion" can be computed analytically, or, as shown in Fig. 9, a computer-generated graticule can be used to obtain a quick estimate. In Fig. 10 the chrominance pulse (also referred to as 12.5 T-modulated pulse) is shown. The shown response is that of two TV lines, superimposed on each other. Notice the peak, smaller than 100 IRE, and the envelope of the bottom part, which is not a constant. Using this waveform, the "relative chrominance level" and the "relative chrominance time" may be determined.

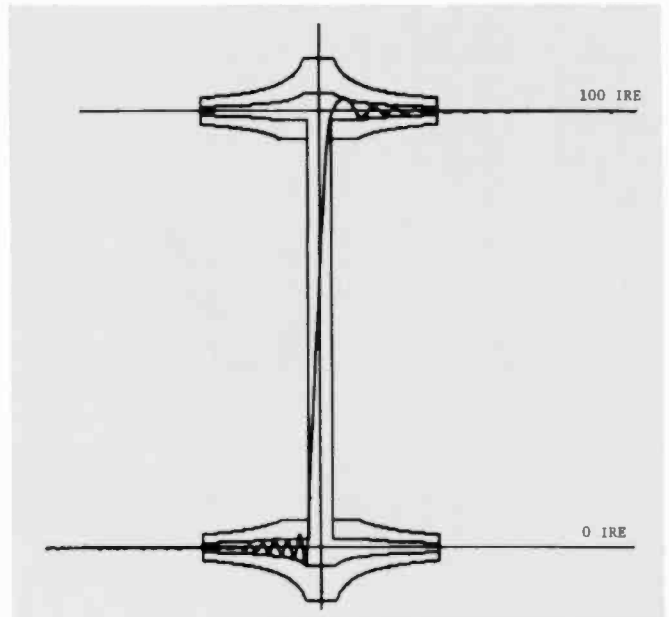


Fig. 9. Demodulated T-step superimposed on a graticule. The outer graticule corresponds to 3-percent distortion, and the inner graticule corresponds to a lower value of distortion.

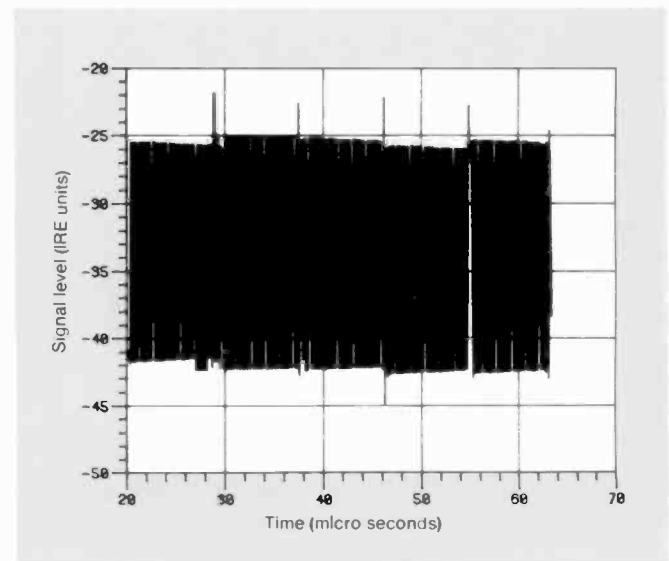


Fig. 11. Demodulated staircase signal (luminance pedestals are removed after demodulation). The five bursts are delineated by spikes.

Satellite communication links generate other types of distortions, most of which can be predicted by using suitable test waveforms and processing them on the computer. A staircase signal can be used to estimate, for instance, "differential gain and phase" generated by the link. The response to the staircase signal is shown in Fig. 11, with the luminance component removed. The input to the modulator consists of five chrominance steps, each 18-IRE peak-to-peak and about 9 μ s wide, with different values of luminance. The luminance variations induce

```

PSK2
SPECIFY PSK TYPE: BPSK=1,QPSK=2,8-PSK=3
?
2
OFFSET MODULATION? YES=1,NO=0
?
0
SPECIFY SYSTEM STRUCTURE
1 = MODULATOR - FILTER1 - RECEIVER
2 = MODULATOR-FILTER1-TWT-FILTER2-RECEIVER
3 = GENERAL STRUCTURE ( TO BE SPECIFIED )
?
2
SUPPLY THE TWT DATA FILE NAME IN INU COMMAS
?
'RCATWT'
SUPPLY THE TWT INPUT BACKOFF IN DB (POS NO )
?
0 0
SPECIFY FILTER TYPE
1 = INTERNAL IDEAL FILTER
2 = USER SUPPLIED FILTER DATA
?
SUPPLY THE SYMBOL RATE IN M-SYM/SEC
?
30.0
SUPPLY THE FILTER1 DATA FILE NAME IN INU. COMMAS
?
'ELLIPLAB'
SUPPLY THE FILTER2 DATA FILE NAME IN INU. COMMAS
?
'INTELSAT'

```

Fig. 12. Typical execution sequence for PSK. PSK has been designed to execute with a simple set of commands and data. As shown above for a typical run, the user needs to specify the modulation type, system structure, data file names of system elements, data rate, and TWT backoff.

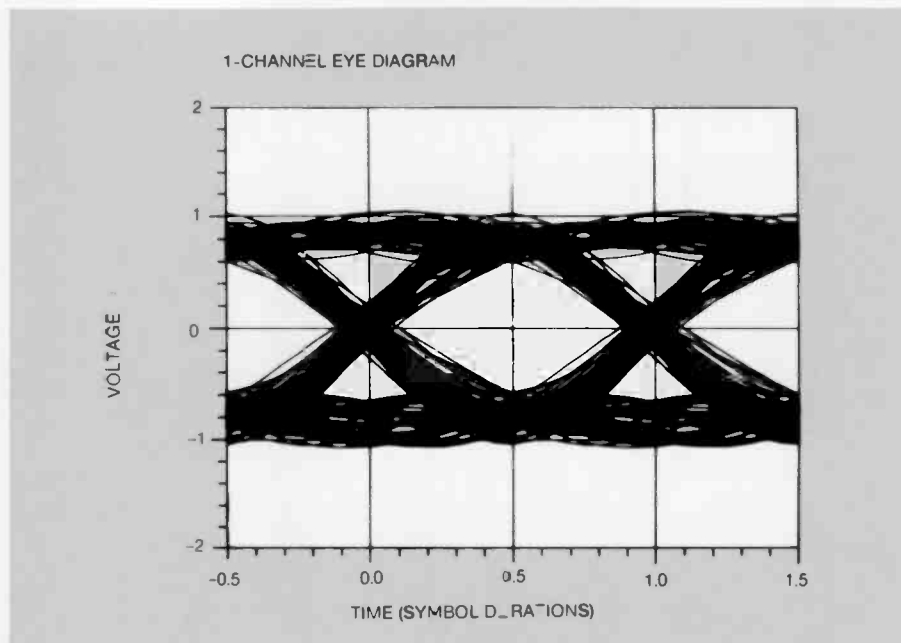


Fig. 13. Eye pattern output from PSK for the exemplified link. The eye pattern, which is a superposition of successive two-bit intervals of the demodulated data waveform, is a commonly used qualitative indicator for overall link performance.

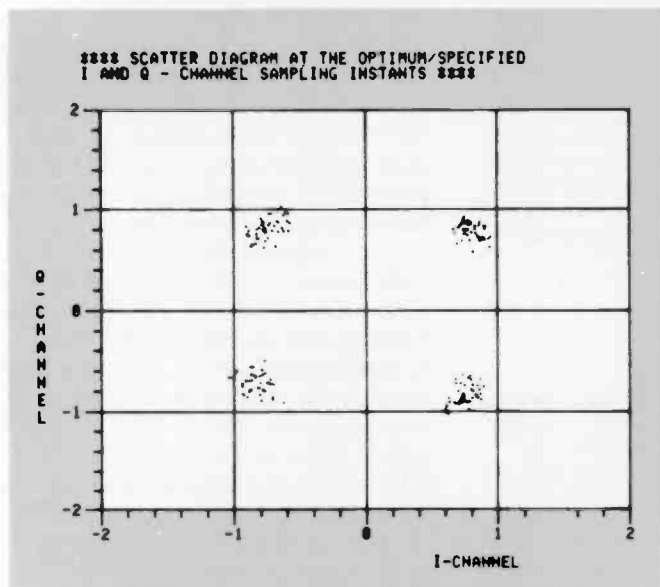


Fig. 14. Scatter diagram for the exemplified link. The scatter diagram is a plot that shows the ensemble I and Q channel values at the detector's sampling instant. Increased dispersion of the points from their nominal values (± 0.7 , ± 0.7 for QPSK) is an indicator of greater link degradation.

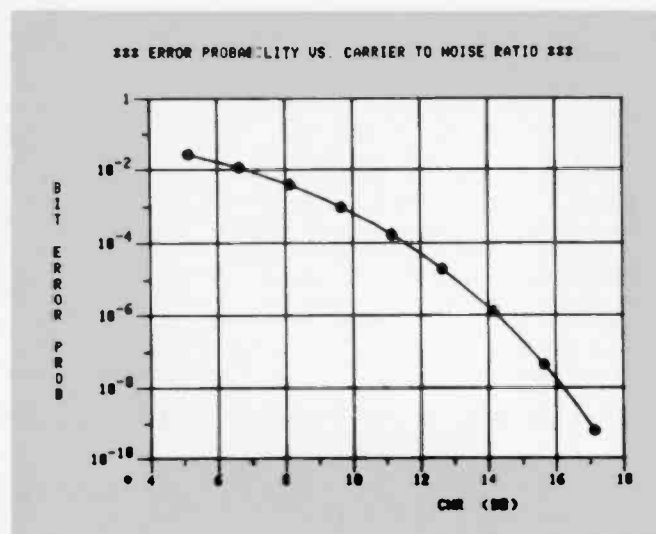


Fig. 15. Error probability versus CNR curve for the exemplified link. The error probability curve is the final and main result of the PSK program. Such curves form the basis for designing digital satellite systems.

varying amounts of gain and phase to the color steps. Figure 11 shows that the peak-to-peak values of the five steps are different. By noting these values, the differential gain from the communication link can be computed. Similarly, the "zero crossing" in-

formation of the sinusoids can be used to estimate the differential phase. The computer models are useful in analyzing the effects of different deviation parameters, channel filters, and satellite amplifiers, on the performance of TV-FM.

PSK—a flexible simulation/analysis program for digital satellite links

PSK is a hybrid, simulation-analysis program that can provide various qualitative and quantitative performance measures for digital communication systems. The program was written for ease of use and can be operated with a minimum of prior knowledge. While the present version of the program is intended for evaluating phase-shift



Authors (left to right) Raychaudhuri, Guida, Jonnalagadda, and Schiff.

Krish Jonnalagadda, Member of Technical Staff, RCA Laboratories, joined RCA in 1978. His activities include analysis and design of satellite communication systems and signal processing methods in Video-Disc and tape recorders. In 1980, he received the RCA Laboratories Outstanding Achievement Award for analysis of nonlinear crosstalk effects in satellites. In 1981, he received the David Sarnoff Award for Outstanding Technical Achievement for work that led to a significant increase in the capacity of RCA's domestic satellite system.

Contact him at:
RCA Laboratories
Princeton, N.J.
TACNET: 226-2025

Dipankar Raychaudhuri received the Bachelor's degree in Electronics and Communication Engineering from the Indian Institute of Technology, Kharagpur, in 1976, and the MS and PhD degrees from the State University of New York at Stony Brook in 1978. Since 1979, he has been with RCA Laboratories, where he is involved in the analysis of satellite communication systems. In 1981, he was a recipient of the RCA Laboratories Outstanding Achievement Award. His primary interests are in the areas of satellite multiple access, computer communications, and queueing theory. Dr. Raychaudhuri is a member of the IEEE and Sigma Xi and has served as an Associate Editor of the *IEEE Communications Magazine* since 1980.

Contact him at:
RCA Laboratories
Princeton, N.J.
TACNET: 226-2311

Leonard Schiff is Head of Communication Analysis Research. He joined RCA Laboratories in 1967 and worked in a number of communications areas such as cellular radio, magnetic recording, video processing, data transmission, and satellite systems. Since 1978, his work has centered on modulation and transmission techniques for use in satellite systems for the transmission of voice, video, and data. In 1981, he received the David Sarnoff Award for Outstanding Technical Achievement for achieving dramatic increases in the capacity of the RCA domestic satellite system.

Contact him at:
RCA Laboratories
Princeton, N.J.
TACNET: 226-2170

Allan Guida received a BS degree from the City College of New York in 1957, and MS and PhD degrees from the Polytechnic Institute of Brooklyn, New York, in 1961 and 1968, respectively, all in electrical engineering. He joined RCA Astro-Electronics Division in 1967 and transferred to the RCA David Sarnoff Research Center in 1968. In 1971, Dr. Guida received an RCA Laboratories Outstanding Achievement Award for work done in the area of digital magnetic recording systems. He received a second RCA Laboratories Outstanding Achievement Award in 1982 for creating computer programs to optimize traffic flow in RCA Americom communication satellites. He is presently working on new techniques for calculating intermodulation distortion in TWTs and SSPAs.

Contact him at:
RCA Laboratories
Princeton, N.J.
TACNET: 226-2689

keyed systems such as BPSK, QPSK, and 8-PSK, it can also accommodate other modulation techniques with minor modifications. The basic performance measures of interest in a digital satellite link are the eye pattern and scatter diagrams (qualitative) and error probability as a function of receive-earth-station carrier-to-noise ratio (quantitative). The eye pattern is a superposition of all possible detected binary baseband waveforms, and is widely used by engineers to size up a digital link broadly. The scatter diagram, of particular interest for QPSK and other higher-level modulation, is a polar plot of the I and Q voltages at the specified sampling instant. The most important result is the quantitative evaluation of link performance, for example, error probability as a function of carrier-to-noise ratio.

Principles

PSK uses a combination of simulation and analysis to obtain these performance characterizations. Simulation must be used because there is no simple analytical approach for a realistic channel with filters and nonlinearities. The program first models the satellite channel as a finite memory device, and obtains what can be thought of as a noise-free, input-output function. This is done by applying a data sequence that contains all possible K -bit-long subsequences to the link. The passage of the signal through the channel is simulated by appropriate transformations, using FFTs where appropriate, corresponding to the filtering and nonlinearities encountered. After the noise-free channel behavior is obtained, analysis is used to obtain error probability results. The assumption required is that downlink noise dominates so that noise can be superimposed linearly on the received signal. If this assumption does not hold, other techniques must be used to convert uplink noise to an equivalent downlink quantity. The program makes certain assumptions about the nature of the detector. The current version of PSK can incorporate carrier recovery effects in the error probability calculation. A simpler version of the program assumes ideal synchronization at the receive end.

Using PSK

PSK has been used extensively by RCA Americom and RCA Astro-Electronics for evaluating high-speed QPSK satellite links. The program is easy to use for such applications. What is needed is a numerical specification of the actual filter and ampli-

fier elements in the link. These numerical specifications are stored in data files with unique names and are accessed by the program. Generally, the important elements of the satellite link are the satellite input filter, the satellite amplifier, TWT, and the receive earth-station filter. Figure 12 shows the execution sequence for evaluation of a typical 60-Mbps RCA Satcom link. The names ELLIPLAB, RCATWT, and INTELSAT correspond to the data file names of the satellite input filter, the TWTA, and the earth-station receive filter respectively. After all the required transmission parameters are supplied, the program provides the desired outputs one by one, at the option of the

user. The first output is the *I*-channel eye diagram, shown in Fig. 13. A similar diagram can be obtained for the *Q*-channel. The next output is the scatter diagram, shown in Fig. 14. Finally, the main result showing bit-error probability as a function of receive-station carrier-to-noise ratio is shown in Fig. 15. Such a simulation tells the system designer what the required carrier-to-noise ratio (CNR) at the receive earth station must be to maintain a desired error probability level. The program is a valuable tool for studying various trade-offs in the link design, making it possible to answer frequently asked questions, such as: What is the effect of equalizing the satellite

filter or replacing the TWTA with a solid-state amplifier? In addition to its primary use for satellite PSK links, simple modifications of PSK have been used for studying teletext systems, digital transmission over cables, and so forth.

References

1. J. Fuenzalida, O. Shimbo, and W. Cook, "Time Domain Analysis of Intermodulation Effects Caused by Nonlinear Amplifiers," *Comsat Tech. Rev.*, Vol. 3, No. 1, pp. 89-143 (Spring 1973).
2. R. Lyons, "A Stochastic Analysis of Signal Sharing in a Bandpass Nonlinearity," *IEEE Trans.*, COM-22, pp. 1778-1788 (November 1974).

Cumulative Index

available at no charge

According to the RCA Engineering Information Survey conducted in 1977, the *RCA Engineer* is the second most important source of technical information about RCA (the most important information source is the engineer's associates). The back issues of the *Engineer*—150 of them—provide a record of RCA's progress in invention, development, and manufacturing. To make this wealth of technical information accessible to the engineers, a 25-Year *Index to the RCA Engineer* has been published.

The *Index* can help you find specific information that is needed in your work.

Or the *Index* might provide a vital contact in another RCA business, someone who has related experience and who would be willing to consult with you. The *Index* gives you the opportunity to profit from RCA's technical heritage—to reuse knowledge, to build on past accomplishments.

The 25-Year *Index to the RCA Engineer* is available in all RCA Libraries. Recipients of the *RCA Engineer* can obtain their personal copies by writing to:

RCA Engineer
 Building 204-2
 Cherry Hill, N.J.

Patents

Consumer Electronics

Carlson, D.J. | Tsou, S.H.
Multi-band antenna coupling network—4352111

Gries, R.J. | Conn, C.E. | Miko, S.
Television receiver high frequency regulated power supply including a low voltage ferroresonant transformer coupled to a step-up high voltage transformer—4345188

Harlan, W.E.
Self-limiting video signal peaking circuit—4350995

Harlan, W.E.
Automatic video signal peaking control—4351003

Hicks, J.E.
Television receiver high voltage generator protection circuit—4343028

Lagoni, W.A.
Apparatus for reducing the effect of co-channel interference on synchronizing pulses—4343019

Speer, W.F.
Rotary tuning mechanism—4347628

Waybright, G.C.
High voltage protection circuit for a television receiver—4345275

West, C.E. | Rampacher, R.J.
Transistor heat sink assembly—4344106

Wilmarth, P.C.
Method for making printed circuit boards with connector terminals—4343084

Government Communications Systems

Caracappa, M.G.
System and method for frequency discrimination—4352194

Corsover, S.L. | Dobbins, L.W. | Pierson, P.B.
Variable-velocity film exposing and developing apparatus—4344088

Crowley, A.T.
Precise digitally programmed frequency source—4349887

Laboratories

Aschwanden, F.
Comparison arrangement for a digital tuning system—4352206

Bleazey, J.C. | Guarracini, J.
Driver arrangement for stylus lifting/lowering apparatus—4344166

Botez, D.
Single filament semiconductor laser with large emitting area—4347486

Catanese, C.A. | Bloom, S.
Multicolor cathode-ray tube with quadrupolar focusing color-selection structure—4350922

Duffy, M.T. | Zanzucchi, P.J.
Method and apparatus for determining the quality of a semiconductor surface—4352016

Duffy, M.T. | Corboy, J.F. | Zanzucchi, P.J.
Apparatus for determining the quality of a semiconductor surface—4352017

Faith, Jr., T.J.
Monitor for oxygen concentration in aluminum-based films—4348886

Flatley, D.W. | Hsu, S.T.
Process for tapering openings in ternary glass coatings—4349584

Goodman, A.M. | Tarng, M.L.
Method of passivating a semiconductor device with a multi-layer passivant system by thermally growing a layer of oxide on an oxygen doped polycrystalline silicon layer—4344985

Henderson, J.G.
Apparatus for automatically steering an electrically steerable television antenna—4349840

Jastrzebski, L.L. | Levine, P.A.
Semiconductor imagers—4348690

Johnston, L.B.
System for compensating for transfer characteristic variations of electron guns—4344021

Okamoto, F. | Kato, K.
Method for preparing inorganic sulfides—4348299

Phillips, W. | Neil, C.C. | Hammer, J.M.
Method for making planar optical wave-

guide comprising thin metal oxide film incorporating a relief phase grating—4343890

Reitmeier, G.A. | Dischert, R.A.
Adaptive composite-component transcoding hierarchy for digital video—4352122

Salt, Jr., W.W.
Retainer ring for securing substrates in a vacuum deposition system—4344383

Southgate, P.D. | Beltz, J.P.
Inspection system for detecting defects in regular patterns—4349880

Subbarao, S.N. | Huang, H.
Method for fabricating via holes in a semiconductor wafer—4348253

Tarng, M.L.
Etching a semiconductor material and automatically stopping same—4343676

Tarng, M.L. | Hicinbothem, Jr., W.A.
Method of depositing a refractory metal on a semiconductor substrate—4349408

Toda, M. | Osaka, S.
Fluid flow velocity sensor using a piezoelectric element—4351192

Valachovic, J. | Alphonse, G.A. | Reisner, J.H. | Etzold, K.F.
Piezoelectric transducer for recording video information—4349902

Wang, C.C. | Ekstrom, L. | Lausman, T.C. | Wielicki, H.
Video disc lubricants—4342659

Woodward, O.M. | Henderson, J.G.
Loop antenna arrangements for inclusion in a television receiver—4342999

Missile & Surface Radar

Bull, J.F.
Actuation rate limiter—4349754

Landry, N.R.
Coax to rectangular waveguide coupler—4349790

Picture Tube Division

Hertzler, M.E.
System for applying a liquid to the studs of

a color kinescope faceplate panel—4351265

Hughes, R.H.

Electron gun with balanced lens lips to reduce astigmatism—4350923

Rarig, L.L. |Alleman, R.A. |Miller, D.L.

Apparatus for sensing bare metal on a moving strip of insulatively coated conductive material—4351263

Wardell, Jr., M.H.

Electron tube base with flow channels therein—4345812

"SelectaVision"

VideoDisc Operations

Crooks, H.N.

Video disc player having record side identifying apparatus—4352175

Elliott, C.A.

Video disc player having carriage detent mechanism—4351046

Taylor, B.K.

Removable protective cover for a video disc stylus cartridge—4342394

Solid State Division

Atherton, J.H. |Jindra, C.P.

Signal comparison circuit—4348596

Benner, T.E.

Mesh assembly having reduced microphonics for a pick-up tube—4347459

Caprari, F.

Radiation shadow projection exposure system—4348105

Gillberg, J.E.

Circuit with dual-purpose terminal—4350906

Gubitose, N.F. |Schuler, M.R.

Patterson, D.L.

Crystal seed holder assembly—4348365

Harford, J.R.

Variable load impedance gain-controlled amplifier—4344043

Harford, J.R.

Gain-controlled amplifier utilizing variable emitter degeneration and collector load impedance—4344044

Harford, J.R.

Variable emitter degeneration gain-controlled amplifier—4345214

Harmon, J.W. |Atherton, J.H.

Low power voltage multiplier circuit—4344003

Holbrook, M.D. |Knapp, W.K.

Precharge circuit—4352031

Marschka, F.D.

Screen contact means for a cathode ray tube—4344015

Marschka, F.D.

Main lens assembly for an electron gun—4350925

Rudy, J.E.

Timing circuit for the digital generation of

composite luminance and chrominance video signal for non-interlaced television raster scan-line pattern—4344075

Schade, Jr., O.H.

Differential-input amplifier circuitry with increased common-mode voltage range—4345213

Schade, Jr., O.H.

Compensation of base-current-related error in current mirror amplifier circuitry—4345216

Stewart, R.G.

Power gated decoding—4344005

Tomasetti, C.M. |Ulaky, J.A.

Photomultiplier tube having a gain modifying nichrome dynode—4347458

Special Contract Inventors

Berry, D.A. |Preston, J.R. |Hillenbrand, L.J.

High density information disc lubricants—4342660

Berry, D.A.

High density information disc lubricants—4351048

Hillenbrand, L.J. |Preston, J.R. |Berry, D.A.

High density information disc—4346469

Preston, J.R. |Hillenbrand, L.J. |Berry, D.A.

High density information disc—4346468

Pen and Podium

Recent RCA technical papers and presentations

To obtain copies of papers, check your library or contact the author or his divisional Technical Publications Administrator (listed on back cover) for a reprint.

Advanced Technology Laboratories

A. Feller

Automated Layout Techniques for Custom VLSI—Presented at the 19th Design Automation Conference, Las Vegas, Nev., and published in *Proceedings* (6/19/82)

W. Heagerty |W. Gehweiler
G. Caracciolo |G. Brucker (Labs)

Design and Performance of Two 1K CMOS/SOS Hardened RAMs—Presented at the Nuclear & Space Radiation Effects Conference, Las Vegas, Nev. (6/19/82)

P.T. Parrish |T.G. Sollner (U. of Mass.)
R.H. Matthews (U. of Mass.) |H. Fetterman (Lincoln Labs)

Printed Dipole-Schottky-Diode Millimeter Wave Antenna Array—Presented at the SPIE Technical Symposium East '82, Arlington, Va., and published in the *Proceedings* (5/2/82)

P. Parrish |K. Yngvesson (U. of Mass.)
K. Korzenioski (U. of Mass.) |R. Matthews (U. of Mass.)

Planar Millimeter Wave Antennas With Application to Monolithic Receivers—Presented at the SPIE Technical Sympo-

sium East '82, Arlington, Va., and published in the *Proceedings* (5/2/82)

R. Putatunda

A Delay Calculation Program for Custom Generated LSI/VLSI Chips—Presented at the Custom Integrated Circuit Conference, Rochester, N.Y., and published in the *Proceedings* (6/19/82)

D. Rea (ATL) |H. Urkowitz (MSR)

Sensor Design Considerations for an Anti-Ship Cruise Missile—Presented at the 1982 Tri-Service Workshop on Missile

Targeting, and published in *Proceedings* (May/June)

R. Putatunda

Auto-Delay: A Program for Automatic Delay Calculation for LSI/VLSI Chips—Presented at the 19th Design Automation Conference, Las Vegas, Nev., and published in the *Proceedings* (6/19/82)

W. Schaming

An Adaptive Gate Multifeature Bayesian Statistical Tracker—Presented at the SPIE 26th Annual International Technical Symposium & Instrument Display, San Diego, Calif., and published in *Proceedings* (8/21-27/82)

D. Shazeer

Performance Measures for Statistical Segmentation—Presented at the SPIE 26th Annual International Technical Symposium & Instrument Display, San Diego, Calif., and published in *Proceedings* (8/21-27/82)

D.C. Smith | B.S. Wagner

A Low Cost, Transportable, Data Management System for R&D Oriented LSI/VLSI Design—Presented at the 19th Design Automation Conference, Las Vegas, Nev., and published in the *Proceedings* (6/19/82)

J.R. Tower | H. Elabd (Labs) | T. Villani (Labs)

High Density Schottky-Barrier IRCCD Sensors for SWIR Applications at Intermediate Temperature—Presented at the SPIE Technical Symposium East '82, Arlington, Va., and published in *Proceedings* (5/2/82)

Astro-Electronics

W. Altman

A Simplified Derivation of Geometrical Dynamic Range Compression—*Optical Engineering Journal* (7-8/82)

C.H. An

Design of Lumped Element 20-GHz FET Amplifier—Proposal for MS Thesis, Mass. Institute of Technology (8/82)

K. Budlong

Testing Large Spacecraft Deployables—7th Annual Testing Seminar, Los Angeles, Calif. (10/13/82)

R. Buntschuh

NOVA Disturbance Control (DISCOS) Testing—Aerospace Testing Seminar, San Diego, Calif. (10/13/82)

J. Chang

Gyroless Attitude Determination & Control System for Advanced Environmental Satellites—AIAA Guidance & Control Conference, San Diego, Calif. (8/9/82)

F. Chu | B. Wang

On Changing Boundary Conditions in Structural Dynamics—AIAA 23rd Structural

Materials Conference, New Orleans, La. (5/10/82)

M. Feyerherm

Reliability of Radiation Hardened MOS RAMs in S/C Memory Application—GOMAC/82, Orlando, Fla. (11/2/82)

L. Freedman

Space Shuttle Closed Circuit TV System—National Telesystems Conference, Galveston, Tex. (11/10/82)

W. Fuldner

Integration & Test of Explorer Class Scientific S/C Dynamics Explorer A and B—NIA - ATG Meeting, San Diego, Calif. (6/23/82)

F. Gargione

Use of 8236 Plotter with 430 Offline Plotter—Fall Technical Mtg. Applicon Users Group—(11/2/82)

M. Goldberger

Switched Mode of DC/DC Power Converter—BS Thesis, MIT (5/82)

L. Gomberg

Presentation/Discussion on the DMSP Spacecraft—National Security Industrial Association, San Diego, Calif. (6/23/82)

J. Kara

Dual Beam Networks for Communication Satellite Antennas—Ben Franklin Symposium, Philadelphia, Pa. (5/15/82)

J. Keigler

K-Band Spacecraft Technology—4th Annual Satellite Users Conference, Denver, Col. (8/12/82)

J.N. LaPrade

Measurement of AM-to-PM Effects in a GaAs FET Power Amplifier—Thesis, Drexel University Library, Philadelphia, Pa. (6/82)

K. Muller

Space Shuttle's Impact on Future RCA Spacecraft—*RCA TREND* (11/82)

W. Nunan

Satellite Power System Optimized for Larger Load—Proposal for BS/MS Thesis, MIT (8/82)

C. Profera, et al.

Appl. Method of Steepest Descent Opt. Des. of Shaped Beam Antennas—1982 Joint Int'l. IEEE/APS Symposium, Univ. of New Mexico, Albuquerque, New Mexico (5/24/82)

C. Profera | E. Ngai

Distortion Analysis for Satellite Reflector Antennas—1982 Joint Int'l. IEEE/APS Symposium, Univ. of New Mexico, Albuquerque, New Mexico (5/24/82)

R. Ritter

Thermal Radiation Characteristics of 30 Amp-Hr Ni-H₂ Battery Cell—17th Interso-

ciety Energy Conversion Engineering Conference, Los Angeles, Calif. (8/8/82)

A. Rosenberg

Remote Laser Measurement Temperature Humidity Using Differential Absorption in Atmospheric Water Vapor—II International Laser Radar Conference, Madison, Wis. (6/21/82)

T. Truong (co-op student)

Des. Shaped Beam Pattern Using Phase Excitation of Antenna Array—BS Thesis, MIT (5/82)

S. Seehra | W. Slusark

The Effect of Operating Conditions on Radiation Resistance of VDMOS Power FETs—IEEE Conference, Nuclear & Space Rad. Effects, Las Vegas, Nev. (7/20/82)

Automated Systems

M.J. Cantella (Automated Systems)

H. Elabd | W.F. Kosonocky (Labs)

Solid State Infrared Imagers—*Microstructure Science and Engineering*, Vol. 5

M.J. Cantella | J.J. Klein (Automated Systems)

H. Elabd | W.F. Kosonocky (Labs)

A New Solid State Infrared Sensor for Military Applications—*Military Electronics/Countermeasures* (9/82)

W.F. Kosonocky (Labs)

F.F. Martin (Automated Systems)

Status of IR Schottky-Barrier Image Technology—SPIE 26th Annual International Symposium, San Diego, Calif. (8/82)

J.D. Rickman

Designing with the Intel One-Megabit Bubble Memory—*EDN Magazine* (9/82)

Commercial Communications Systems Division

J.F. McCoy

A Photoconductive Telecine Camera with Automatic Setup—Presented at the IEEE Broadcast Symposium, in Washington, D.C. (9/16/82)

J.F. McCoy

Automatic Burst Phase Matching Arrangement for Color Television Camera Systems—RCA Technical Note, Princeton Docket No. 77060 (1982)

Government Communications Systems

H.R. Barton, Jr.

User Guide-RCA Unit Production Cost Tracking Model UPCT5—EIA G-47 Committee Mtg., Washington, D.C., and published in *EIA Engineering Design Integration Bulletin*, No. 1 (10/15/82)

R.R. Bigler | J.P. Heenen

Method for Attaching Edge Terminals—RCA Technical Note, Disclosure 76,931 (10/82)

R.R. Bigler | T.G. Butt

System for Optically Aligning a Screen Printer—RCA Technical Note, Disclosure 76,503 (10/82)

T.T.N. Bucher

Spectrum Occupancy of Pulsed FSK—MILCON '82, Boston, Mass., published in the Conference Record (10/17-20/82)

A. Garcia

Cleaning Audio Records—RCA Technical Note, Disclosure 74,911 (10/82)

J.L. Lynerd

Tactical Military Equipment Reliability & Maintainability Demo. Programs, Planning, Demo. Test & Analysis of Results—17th Int'l. Logistics Symposium, Boston, Mass. (8/82)

D. McClure

Keying Improvements to the ICOM IC-730—QST, Vol. LXVI, No. 7 (7/82)

E.J. Nossen

Integrated Radar Communications—1982 IEEE Military Communications Conference, Boston, Mass., published in the Conference Record (10/82)

M. Packer

Touch-Up Ink for Photoemulsion Artwork—RCA Technical Note (Domestic & Foreign Distribution)

P.T. Patterson

E-COM—Christ Episcopal Church Men's Club, Riverton, N.J. (9/26/82)

K. Weir | J.J. Cohen | W. Rizzo

Operation & Maintenance Trainers for TRIDENT Integrated Radio Room—Int'l. Conf. on Simulators, Univ. of Sussex, Brighton, U.K., published in the *Proceedings* (9/26-30/82)

D.J. Webster

Software Management Experience in Distributed C³I System Development—AF-CEA, Ft. Monmouth Chapter Symposium (9/21-22/82)

Government Systems Division

J. Hayman

Design & Simulation of An Intelligent Missile Seeker—AGARD - A North Atlantic Treaty Organization Guidance & Control Symposium, Lisbon, Portugal, published in *Proceedings* (10/12-14/82)

J. Hilibrand

Some Recent Perspectives in Microelectronics—IEEE Philadelphia Section Meeting (9/21/82)

Laboratories

D.P. Barton

VDTIS: A VideoDisc Testing Information System—ORSA/TIMS, San Diego Joint National Meeting (10/26/82)

D. Botez | D.J. Channin | M. Ettenberg

High Power Single-Mode AlGaAs Laser Diodes—*Proceedings*, SPIE International Society for Optical Engineering, Vol. 321, Los Angeles, Calif. (1/28-29/82)

D. Botez | J.C. Connolly

Terraced-Heterostructure Large-Optical Cavity AlGaAs Diode Laser: A New Type of High-Power cw Single-Mode Device—*Appl. Phys Lett.*, Vol. 41, No. 4 (8/15/82)

A. Catalano | R.V. D'Aiello | J. Dresner

B. Faughnan | A. Firester | J. Kane
H. Schade | Z.E. Smith | G. Swartz | A. Triano
Attainment of 10% Conversion Efficiency in Amorphous Silicon Solar Cells—Presented at IEEE PV Specialists Conference, San Diego, Calif. (9/27-30/82)

A.H. Firester

Amorphous Silicon Module—*Photovoltaic-The Solar Energy Magazine*—(8-9/82)

L.P. Fox

Rheology of Carbon-Polymer Composites—*Carbon Black-Polymer Composites, The Physics of Electrically Conducting Composites*, ed. by Enid Keil Sichel, Marcel Dekker, Inc.

B. Goldstein | J. Dresner | D.J. Szostak

The Diffusion of Holes in Undoped Amorphous Si:H—*Philosophical Magazine B*, Vol. 46, No. 1, pp. 63-70 (1982)

J.M. Hammer

In-Line Anamorphic Beam Expanders—*Applied Optics*, Vol. 21, p. 2861 (8/1/82)

L. Jastrzebski, P. Zanzucchi

D. Thebault | J. Lagowski

Method to Measure the Precipitated and Total Oxygen Concentration in Silicon—*Journal of the Electrochemical Society*, Vol. 129, No. 7 (7/82)

M. Kumar | S.N. Subbarao

R.J. Menna | H. Huang

Monolithic GaAs Interdigitated 90° Hybrids with 50- and 25-ohm Impedances—IEEE Microwave and Millimeter-Wave Monolithic Circuits Symposium (5/82)

A. Okada | M. Toda

Influence of Silicone Contamination on Brush-Commutator Contacts in Small-Size DC Motors—*IEEE Transactions on Components, Hybrids, and Manufacturing Technology*, Vol. CHMT-5, No. 2 (6/82)

D. Raychaudhuri

Utilizing TDMA Idle Periods for Random Access Transmission—IEEE International Conference on Communications, ICC '82, Philadelphia, Pa. (6/13-17/82)

P.H. Robinson | R.V. D'Aiello (Labs)

C.P. Khattak | F. Schmid (Crystal Systems, Inc.)

Thin-Film Epitaxial Solar Cells on Substrates Made From MG Silicon by the HEM Process—Presented at IEEE PV Specialists Conference, San Diego, Calif. (9/27-30/82)

A. Rosen | M. Caulton

P. Stabile | A. Gombar

W. Janton | C.P. Wu | C.W. Magee

Silicon Technology Applicable to Monolithic Millimeter Wave Sources—*SPIE, Integrated Optics and Millimeter and Microwave Integrated Circuits*, Vol. 317 (1981)

J.R. Sandercock

Trends in Brillouin Scattering: Studies of Opaque Materials, Supported Films, and Central Modes—*Topics in Applied Physics, Vol. 51: Light Scattering in Solids III*

D.L. Staebler

Stability of Amorphous Silicon Solar Cells—*IEEE Transactions on Reliability*, Vol. R-31, No. 3 (8/82)

J.H. Thompson III | S. Hofmann (visiting Scientist at RCA Labs from Germany)

The Use of Plasmon-Loss Peaks in Studying the Epitaxial Silicon on Alumina Interface—*Surface and Interface Analysis*, Vol. 4, No. 4 (1982)

R. Williams

The Relation Between Contact Charge Transfer and Chemical Donor Properties—*Journal of Colloid and Interface Science*, Vol. 88, No. 2 (8/82)

R. Williams | P.J. Wojtowicz

A Simple Model for Droplet Size Distribution in Atmospheric Clouds—*Journal of Applied Meteorology*, Vol. 12, No. 7 (7/82)

Missile & Surface Radar

K. Abend | H. Urkowitz

Some Sensor Design Considerations for an Anti-Ship Cruise Missile—1982 Tri-Service Workshop on Missile Ship Targeting Naval Research Laboratory, Washington, D.C., Workshop *Proceedings* (8/10-12/82)

J.A. Bauer

Leadless Chip Carrier Packaging—SEMICON Southwest (Part of presentation on VLSI assembly, reliability, and testing), Dallas, Tex. (10/14/82)

R. Blasewitz (co-author)

Microcomputer Systems Hardware/Software Design—Published by Hayden Book Co., Rochelle Park, N.J., 550 pages (1982)

M.E. Breese

A Planar Phased Array Antenna Having Increased Scan Coverage—Technical Note (8/31/82)

J.J. Campbell | R.S. Johnson

A New Integrated Radiating Element for

Phased Array—*IEEE Transactions on Antennas and Propagation* (7/82)

R.I. Creedon

Support Systems—Electrical, and Support Systems—Mechanical Room Arrangements—Summer Course (Guest Lecturer): Combat Systems Engineering and Ship Design, MIT, Cambridge, Mass. (8/82)

M.L. Dorman, Jr.

Missiles From the Deep—*Sea Classics*, Vol. 15, No. 6, pp. 18-27, Part 1 of 3 parts (11/82)

R.C. Durham

Radar Design for Electromagnetic Compatibility—IEEE EMC International Symposium, Santa Clara, Calif. (9/8-10/82)

R.F. Kolc

VLSI Packaging Techniques at RCA Moorestown—IEEE VLSI Packaging Workshop, Gaithersburg, Md. (9/14/82)

S. Gaskell

A Fixed-Beam Multilateration Radar System for Weapon Impact Scoring—Int'l. Conference - Radar '82, London, England, Conference *Proceedings* (10/18-20/82)

L.J. Grantner

Anti-Submarine Warfare: Detect, Control, Engage; and Anti-Submarine Warfare: Ship Impacts—Summer Course (Guest Lecturer): Combat Systems Engineering and Ship Design, MIT, Cambridge, Mass. (8/82)

W.C. Grubb, Jr.

Minicomputers and Microcomputers for Non-Electrical Engineers—George Washington University, Presented at Naval Air Test Center, Patuxent, Md. (8/20/82)

J. Haness

How to Critique A Document—1982 Professional Communications Society (IEEE), Boston, Mass., *Proceedings* (10/13-15/82)

M. Kant

Applying EMC Technology to the Next Generation of Navy Ships—1982 IEEE International Symposium on Electromagnetic Compatibility, Santa Clara, Calif., Symposium *Proceedings* (9/8-10/82)

M.H. Plofker

Combat System Availability—Summer

Course (Guest Lecturer): Combat Systems Engineering and Ship Design, MIT, Cambridge, Mass. (8/82)

R.J. Renfrow

Topside Design—Radar; and Topside Design—Weapons—Summer Course (Guest Lecturer): Combat Systems Engineering and Ship Design, MIT, Cambridge, Mass. (8/82)

E.E. Roberts, Jr.

Error Budgeting Alignment and Ships' Flexure—Summer Course (Guest Lecturer): Combat Systems Engineering and Ship Design, MIT, Cambridge, Mass. (8/82)

P.S. Sawkar | T.J. Forquer

E.J. Scherneck | H. Li

A Multi-Port Memory Organization for Use in Distributed Computing Systems—Int'l. Conference on Distributed Computing Systems, Ft. Lauderdale, Fla. (10/18/82)

R.L. Schelhorn

Universal Test Fixture for Testing Chip Carriers—Technical Note (10/12/82)

R.L. Schelhorn

Test Fixture for Testing Chip Carrier Devices Assembled in Larger Circuits—Technical Note (10/12/82)

R.L. Schelhorn

High Density Metal Core Substrate for Chip Carrier Circuits—IEEE Computer Packaging Conference, New York, N.Y. (9/9/82)

S.A. Steele

System Software Design Trade-Offs for Real-Time Data Measurement and Control Systems—*International Journal of Mini and Microcomputers*, Vol. 4, No. 2 (1982)

J.T. Threston

System Functional Analysis and Functional Allocation; Performance Tradeoff Analysis; Anti-Air Warfare: Detect, Control, Engage; Computers/Digital Technology; and Contemporary Combat System Designs—Summer Course (Guest Lecturer): Combat Systems Engineering and Ship Design, MIT, Cambridge, Mass. (8/82)

H. Urkowitz | K. Abend

Some Sensor Design Considerations for an Anti-Ship Cruise Missile—*Proceedings of the 1982 Tri-Service Workshop on Mis-*

sile Ship Targeting, Naval Research Laboratory, Washington, D.C. (8/10-12/82)

H. Urkowitz (MSR) | M.M. Rea (ATL)

Some Sensor Design Considerations for an Anti-Ship Cruise Missile—1982 Tri-Service Workshop on Missile Ship Targeting, Naval Research Laboratory, Washington, D.C. (8/10-12/82)

National Broadcasting Company (NBC)

C.E. Spicer

NTSC Color Field Identification—*SMPTE Journal*, Vol. 91, No. 7 (July, 1982); presented at the SMPTE 122nd Technical Conference, New York, N.Y. (11/14/82)

RCA Ltd.

P.P. Webb (Electro-Optics, RCA Inc., Montreal) | G.H. Olsen (Labs)

Large Area and Visible Response VPE InGaAs Photodiodes—IEEE Specialist Conference on LEDs and Photoconductors (9/15-16/82)

RCA Service Company

A.B. Jones

Computers Are Their Thing—Apple Users' Educational Software Convention (10/27/82)

J.C. Phillips

Responding to Competition—1982 IEEE Conference of Professional Communication Society, Boston, Mass. (10/14/82)

Solid State Division

H. Veloric | R. Denning

Reliability of Radiation-Hardened CMOS/SOS RAMs in Spacecraft Applications—GOMAC/82, Orlando, Fla. (11/2/82)

H. Veloric | R. Denning | G. Schnable | J. Yeh

Reliability of Silicon-on-Sapphire ICs—1982 SOS/SOI Technology Workshop, Provincetown, Mass. (10/5-7/82)

Engineering News and Highlights

Staff announcements

Thornton F. Bradshaw, Chairman of the Board and Chief Executive Officer, announced that RCA Corporation elected **Robert R. Frederick**, President and Chief Operating Officer. Mr. Frederick will have responsibility for all Divisions and Subsidiary Companies of the Corporation except the National Broadcasting Company, Inc., which will continue to report to the Chairman of the Board and Chief Executive Officer. Messrs. **William C. Hittinger**, **Frank A. Olson**, **Roy H. Pollack**, and **Herbert S. Schlosser** will report to Mr. Frederick. RCA Staff executives **Eugene E. Beyer, Jr.**, **Kenneth W. Bilby**, **George H. Fuchs**, **Rocco M. Laginestra**, **Richard W. Miller**, and **Thomas B. Ross** will continue to report to the Chairman of the Board and Chief Executive Officer.

Laboratories

Emil V. Fitzke, Head, Technological Services, announces his organization as follows: **Austin J. Kelley, Jr.**, Manager, Technical Support Services; **Jack F. Otto**, Manager, Device Technology; **William J. Schnell**, Administrator, Display Device Development; and **Donald J. Tamutus**, Manager, Process Technology.

Carmen A. Catanese, Director, Picture Tube Systems Research Laboratory, announces the appointment of **Harry E. McCandless** as Manager, Advanced Development—Electron Guns, Transfer Technology Laboratories.

National Broadcasting Company (NBC)

Jeffrey P. Meadows, Vice-President, Engineering and Technical Services, Operations and Technical Services, announces the appointment of **Donald R. Musson** as Director, Technical Development, Operations and Technical Services, NBC, and the appointment of **Steven Bonica** as Director, Broadcast Systems, Engineering, NBC.

Patents

John V. Regan, Vice-President, Patent Operations, announces the appointment of **Joseph S. Tripoli** as Director, Patents—Electronic Systems.

Solid State Division

Stephen L. Pletcher, Division Vice-President, Marketing, announces the appointment of **Michel Musso** as Director of Marketing, Europe.

Erich Burlefinger, Division Vice-President, Electro-Optics and Power Devices, announces the appointment of **S. Paul Davis** as Director, Power Operations.

Carl R. Turner, Division Vice-President, Product Assurance and Planning, announces the appointment of **John E. Mainzer** as Director, Division Planning and Operations Support.

David S. Jacobson, Director, Custom Large Scale Integration, announces the appointment of **Peter Ferlita** as Manager, Custom LSI Production and Production Control.

James W. Hively, Director, Semicustom Device Operations, Integrated Circuits, an-

nounces the appointment of **Henry S. Müller** as Manager, Design Systems Engineering, and **Walter Clauhs** as Manager, Product Engineering, Semicustom Device Operations.

RCA Cylinx Communications Network, Inc.

Eugene F. Murphy, Chairman of the Board, RCA Cylinx Communications Network, Inc., announces the organization as follows: **James C. Ziegler**, Vice-Chairman; **Ralph R. Johnson**, President and Chief Executive Officer. The organization of the President and Chief Executive Officer will be as follows: **Bryan M. Eagle**, Vice-President, Finance and Administration; **Richard C. Furnival**, Vice-President, Operations; **Floyd H. Jean**, Vice-President, Engineering Development; and **Ronald L. Young**, Vice-President, Marketing.

Professional activities

A tribute to Otto Schade

Otto Schade, Sr., devoted most of his professional career to research on television and the image sciences at RCA. Perhaps more than anyone else, he was responsible for unifying our understanding of the evaluation of optical, photographic, and electronic imaging systems, as well as the human visual system. In honor of his numerous contributions to the imaging sciences, the Optical Society of America held a Symposium in Tribute to Otto Schade at its Annual Meeting in Tucson, Arizona, on October 21, 1982. The Symposium began with three invited papers that reviewed Schade's contributions.

Dr. Albert Rose, retired Fellow at RCA Laboratories, presented a paper entitled: "Otto Schade: A Personal Retrospective." Prof. John Robson of Cambridge University (U.K.) then gave a paper summarizing Schade's contributions to the visual sciences, followed by a paper by Dean Brian



Otto Schade, Sr.

Thompson, of the University of Rochester, which reviewed Schade's research on image quality and evaluation. Other papers, on related topics, were given by **Ted Adelson**, **Jim Bergen**, and **Albert Pica**. These scientists are all members of the Image Quality and Human Perception group at RCA Laboratories. **Curtis Carlson**, also of RCA Laboratories, presided at the Symposium.

Dr. Woll honored by University of Pennsylvania

Dr. Harry J. Woll, Staff Vice-President and Chief Engineer of RCA Electronic Products, Systems and Services, has received the 1982 Yarnall Award from the University of Pennsylvania's Engineering Alumni Society. The award is given annually to a graduate of the School for outstanding contributions.

Dr. Woll received his Ph.D. degree from the University of Pennsylvania in 1953. On the 50th anniversary of the University's Moore School of Electrical Engineering in 1973, he was awarded the School's Gold Medal as a distinguished alumnus. Dr. Woll currently serves as Chairman of the Trustees for the Moore School and is a member of the Board of Overseers for the School of Engineering and Applied Science.

During his 41-year career with RCA, Dr. Woll has advanced through a number of engineering and management positions. Prior to being named to his current post in 1981, he was Division Vice-President and General Manager, RCA Automated Systems, located in Burlington, Mass.

Dr. Woll holds 20 patents in various fields of electronics. His activities and responsibilities at RCA have included the development of circuitry, micro-electronics, lasers, computers, electro-optics, automatic test equipment and air traffic control systems. In addition, he has been responsible for the design of the rendezvous radar, attitude control electronics, and descent engine control electronics for the Apollo Lunar Module spacecraft.

New TIMS President-Elect

Dr. H. Newton Garber, Director of Operations Research for the RCA Corporation, has become President-Elect of the Institute of Management Sciences (TIMS). His term as President of TIMS will begin in September, 1983. The organization's goals are to identify, extend and unify scientific knowledge pertaining to management, through publication of journals and through local, regional, national and international meetings.

Astro scientist cited at Computer Society conference

Kamal N. Karna, Astro-Electronics, served as the tutorial chairman and an executive committee member for The CompCon Fall 1982 conference held in Washington, D.C., in September, 1982. As a tutorial chairman, he organized four tutorials: Integrated voice and data PBXs; Data Communications: Techniques and Approaches; Local Networks; Introduction and Equipment; and Computer Communications—Protocols.

RCA Labs celebrates its 40th Anniversary



Aerial view of RCA Laboratories in Princeton, N.J. Established in 1942, the Princeton facility was 40 years old on September 27, 1982. In 1951, the facility was dedicated as the David Sarnoff Research Center.

RCA Laboratories formally opened on September 27, 1942. Research accomplishments during the past 40 years have been many and versatile. RCA scientists have contributed importantly to the fields of optics, acoustics, and communications and have developed valuable tools and systems for our national defense.

Dr. William M. Webster, Vice-President of the Laboratories, in a message to employees said, "We are a little more than midway between our 25th and 50th anniversaries, so we might take time to look back to the 60s and 70s and ahead to the next decade. We have learned that our strengths lie in our traditional businesses—communications, electronics, and entertainment.

"We can take pride in an impressive list of achievements over the years; perhaps the most notable one was the development of the all-electronic color televi-

sion system in use today. And a year ago, we introduced our new capacitance electronic disc VideoDisc system. Ours is an industry in which our eyes are usually on the future, but occasionally it is pleasant to look back on the past."

RCA Laboratories has carried out pioneering work in computer memories and systems, high-fidelity stereo recording, lasers, solid-state materials and devices, satellite communications, and numerous other achievements covering the entire electronics spectrum. (See box, opposite.)

"Ten years from now, on our 50th birthday, our research projects will be at least as different as today's are from 1972," Dr. Webster predicted. "RCA Laboratories has been outstanding in developing and applying technology throughout its history. By the diligence, dedication, and creativity from all of us, let's prove that life begins at 40."

Mr. Karna was given a special citation for his contribution to the success of the conference.

Degrees awarded

Two individuals at SSD, Somerville, recently completed their undergraduate education. Alan S. Gutwillig received his Bachelor of Science degree in Electrical Engineering from Rutgers University. Louis Pennisi received his degree in Electrical Engineering from Fairleigh Dickinson University.

New IEEE Senior Member

Richard M. Dombrosky, RCA Service Company, Cherry Hill, has been elected a senior member of the Institute of Electrical & Electronics Engineers. Senior member, the highest professional grade for which application may be made, requires experience reflecting professional maturity.

Licensed engineer

"SelectaVision"
VideoDisc Operations:

T.J. Dudziak, IN 19887

Some milestones in Laboratories research

1942 Dedication of RCA Laboratories, on September 27. The technical staff in Princeton numbered 125 scientists and engineers.

1943 Development of the Image Orthicon with sensitivity 1,000 times greater than that of the Iconoscope. For postwar television, it provided flexible operation in the studio or in the field.

1946 All-electronic color television system demonstrated publicly. . . . Development of aluminized picture tube which doubled brightness with no increase in power.

1949 Development of Vidicon, a miniature pickup tube with a photoconductive surface; important for closed-circuit TV in industrial and educational applications.

1950 Development and demonstration to the FCC of three-gun shadow-mask tube—the tricolor kinescope that became standard in the industry.

1953 Magnetic tape recording system for both color and black-and-white TV programs developed and demonstrated.

1954 "Electrofax," a high-speed electrostatic printing process developed; later licensed to photocopier manufacturers.

1955 Electronic music synthesizer, first of two models, built. . . . Alloy-junction "drift" transistor developed.

1958 Intensifier Orthicon camera tube, which could "see" in surroundings completely dark to human eye, developed.

1959 Direct-coupled-unipolar-transistor-logic circuit developed.

1960 *N-on-P* radiation-resistant solar cells developed for U.S. Signal Corps.

1961 Cadmium-sulfide thin-film transistor, made entirely by evaporation technique.

1962 First sun-pumped laser developed.

1963 Development of the metal oxide semiconductor (MOS) transistor.

1966 First practical-technology, vapor-phase growth process developed for using gallium arsenide in high-performance electronic devices.

1967 Silicon-on-sapphire fabrication technique developed for producing large arrays of silicon field-effect transistors. . . . Development of an experimental system

(Homefax) for broadcasting printed copy into the home along with standard TV programming.

1968 Liquid crystal technology providing new type of electronic display for print, pictures and moving images; read by reflected light.

1973 First linear CMOS circuits introduced.

1974 Development of solid-state image sensor (CCD) containing more than 120,000 electronic elements on a silicon sensor chip the size of a nickel—the forerunner of the CCD camera.

1975 Introduction of first COS/MOS microprocessor.

1976 Development of microwave hyperthermia units for treatment of deep-seated tumors.

1977 First SOS memory introduced.

1979 Development of solid-state laser for high-bit-rate fiber optic communications.

1980 Completion of 15-year development of "SelectaVision" Video-Disc system. . . . Demonstration of concept for a 50-inch, flat-panel color TV display for wall mounting.

Technician awards at Lancaster plant

Each year outstanding technicians and draftsmen at Lancaster are chosen for Technician Recognition awards to recognize the very important contributions made by them.

The Picture Tube Division recipients of the 1981 Technician of the Year award are as follows:

C. Gerald Berrier—for outstanding contributions in picture tube life test expansion and modernization.

Robert P. Bitzer—for outstanding contributions in picture tube electron gun shunt and enhancer modifications.

David E. Booth—for outstanding contributions in PTD and SSD process equipment mechanical coordination and redesign.



PTD's 1981 Technician of the Year award recipients, left to right: R. William Collins, William H. Shelton, Gerald R. Long, Robert P. Bitzer, Richard E. Roland, Kevin M. Rapp, James W. Hauer, C. Gerald Berrier, Dennis J. Urban, and Dennis L. Miller. (Missing from the photo are David E. Booth, Glenn W. Brunner, and John H. Ries.)



SSD's 1981 Technician of the Year award recipients, left to right: Scott K. Kurtz, Thadeus J. Jaworski, James P. Irvin, Kenneth J. Altmanshofer, Mark W. Howard, James E. Horst, Galen E. Shaud, Jr., Mary F. Kross, and Robert A. Barnes. (Missing from the photo is John S. Ritchey.)

Glenn W. Brunner—for outstanding contributions in color display tube pilot production matrix screening.

R. William Collins—for outstanding contributions in the picture tube high-voltage stability computer-controlled data acquisition systems.

James W. Hauer—for outstanding contributions in high-resolution color display tube quality standards and product demonstrations.

Gerald R. Long—for outstanding contributions in picture tube process-equipment mechanical design, development and manufacturing start-up.

Dennis L. Miller—for outstanding contributions in picture tube process-equipment computer-aided design systems.

Kevin M. Rapp—for outstanding contributions in high-resolution color-display-tube

shadow-mask materials and etching developments.

John H. Ries—for outstanding contributions in the study of picture tube deflection component relationship on beam register.

Richard E. Roland—for outstanding contributions in start-up of the Defect Analysis Center.

William H. Shelton—for outstanding contributions in the elevation of PQT to a high level of competence and respect.

Dennis J. Urban—for outstanding contributions in the detection and analysis of plant waste water effluents.

The Solid State Division recipients of the 1981 Technician of the Year awards are as follows:

Kenneth J. Altmanshofer—for outstanding

contributions in neutral beam source and power tube product improvements.

Robert A. Barnes—for outstanding contributions in solid-state systems products, 9-inch black-and-white monitor development.

James E. Horst—for outstanding contributions in CCD imager design, layout and testing.

Mark W. Howard—for outstanding contributions in closed-circuit video equipment development utilizing computer-aided design techniques.

James P. Irvin—for outstanding contributions in vistacon yield and process-control improvement.

Thadeus J. Jaworski—for outstanding contributions in conversion tube SIT and vidicon exhaust processing improvements.

Mary F. Kross—for outstanding contributions in silicon wafer processing efficiency and yield improvements.

Scott K. Kurtz—for outstanding contributions in gallium arsenide material and laser fabrication yield and process-control improvements.

John S. Ritchey—for outstanding contributions in small power and pencil-tube process-control development.

Galen E. Shaud, Jr.—for outstanding contributions in closed-circuit video equipment, quality and reliability yield improvements.

Technical excellence



Frank Denny, Chairman of the new Technical Excellence Committee, addressing Americom's engineers and engineering managers. To the left is John Christopher, Vice-President of Technical Operations, Americom. TEC members at the right are Carlton Barnes, Jim Colonna, Len Derkach, Fred Hoedl, and Doreen Jakubcak.

Americom launches its TEC

RCA American Communications formally introduced a Technical Excellence program to its engineers and engineering management on October 6, in a meeting at the Hilton Conference Center in Princeton.

The meeting began with brief statements by Americom Vice Presidents **John Christopher** and **Allen Cook** and by Americom's President, **Andrew F. Inglis**, in which they voiced their support of the Technical Excellence Program. The chairman of Americom's Technical Excellence Committee, **Frank Denny**, introduced the committee members and spoke about the purpose of the program.

A social hour after the meeting provided engineers, managers, and committee members with an excellent opportunity to exchange ideas regarding the technical excellence program.

Five receive Consumer Electronics Division quarterly awards



Gobush



Lord



McVety



Nortrup



Price

The Consumer Electronics Division TEC has selected their second quarter 1982 Technical Excellence Award winners. Based on

managers' recommendations, the recipients' work was researched by the Technical Excellence Committee. The nominating managers were then interviewed by the committee.

The award winners listed below will receive a plaque and a reference book of their choice. They are also eligible to receive an annual award for their work.

Raymond Gobush—for the development and implementation of electrical, mechanical, and plumbing plans to convert the printed circuit board etching process from using ferric chloride to cupric chloride, resulting in considerable monetary savings.

Jill Lord—for the development and implementation of chemical processes and safety procedures to convert the printed circuit board etching process from using ferric chloride to cupric chloride, resulting in considerable monetary savings.

Ronald McVety—for the invention of a chip (leadless resistor or capacitor) removal tool, and for the factory implementation of the method which prevents damaging printed circuit boards.

Kevin Nortrup—for significant personal dedication for the use of innovative techniques to maximize feature content and cost effectiveness in J-Line (1983) remote control TV systems.

Tim Price—for significant contributions to the area of computer assisted engineering characterization of radio frequency (RF) devices and systems.

Custom LSI Symposium held at Princeton

The second corporate technical symposium on custom LSI circuits was held on November 18 at the David Sarnoff Research Center, with over 60 in attendance. According to **Jack Hilibrand**, GSD Engineering, who served as chairman and organizer, the objective of the symposium program was "to encourage the use of custom and semi-custom LSIs within RCA where that use is advantageous to the RCA product being built." The morning session focused on tools available in RCA, while the afternoon was devoted to case studies of programs now underway.

The speakers and their topics are listed below. Copies of the viewgraphs used in the presentations are available at RCA technical libraries. For more information on a specific talk, contact the respective author. The Custom LSI Symposium was videotaped and tapes will be available from the Corporate Engineering Education videotape library by January 1983. To borrow this tape (at no charge), call Margaret Gilfillan at TACNET 222-5255. Order Tape No. 440. Available in the 3/4-inch U-Matic and the 1/2-inch VHS formats.

Opening Remarks, H.J. Woll, Staff Vice-President and Chief Engineer, RCA Electronic Products, Systems and Services.

"Why Custom Designs Now—A Current Perspective," J. Hively, Solid State Division.

"A System for the Automated Design of Complex Integrated Circuits," R.P. Lydick, Solid State Division.

"Custom VLSI Design for GSD, by GSD," A. Feller, Advanced Technology Laboratories.

"How to Use CAD Tools to be Sure Your Custom LSI Part Will Work the First Time," L. Rosenberg, Solid State Technology Center.

"What is Involved in Building a Custom LSI Skill Group to Support Your Requirements," F.H. Tillwick, Missile and Surface Radar.

Panel Discussion: What Tools/Techniques/Technology Are We Missing? Strengths and Weaknesses?

"The Military Computer Family—An Application of Custom VLSI and Standard Parts," S.E. Ozga, Missile and Surface Radar.

"Planning A Chip Set for Digital Video," I.H. Kalish, RCA Laboratories.

"Planning Custom LSI Development in Consumer Electronics," H. Scaff, Consumer Electronics.

"Obstacles to the Use of Custom LSI in Low-Volume Systems—Two Broadcast Camera LSI Circuits," T.R. Smith, RCA Laboratories, and A.H. Lind, Commercial Communications Systems Division.

Second-quarter 1982 MSR award-winners announced



Matulis



Matthews

Bernie Matulis, Chief Engineer, Missile and Surface Radar, announced that the following award-winners will receive a commemorative desk plaque and a current text or reference book, and will be honored at a function next year.

D.L. Matthews—for system configuration design and the development of prototype hard-

ware and unique printed circuit designs for the RCA Control Processor Microcomputer. Largely as a result of Mr. Matthews' innovative approach, the prototype designs produced have met all microcomputer system requirements with an accuracy that allowed debugging to be accomplished in less than one month.

D. Shaw—for developing the basic computer architecture for the RCA Control Processor Microcomputer. In particular, his approach to coding led to the microcoding of more than 200 instructions in 13 weeks instead of the anticipated 40 weeks. Mr. Shaw's architecture, developed in what was considered by many to be an unworkably short schedule, has been proved by the performance of the microcomputer tested with an Air Force acceptance program.

Index to Volume 27

Subject Index

In this Subject Index, we asked the authors to classify their own articles under three principal subject headings. Under these headings you will find appropriate article titles, each followed by author name(s), volume and issue numbers, issue date, and initial page number.

Algorithms

Mechanically scanned radar systems, dynamic analysis and simulation of. Liston, J. and Sparks, G. M., v27n6, Nov/Dec 1982, p24.

Amplifiers

GaAs microwave monolithic integrated circuits, a review of. Huang, H. C., Upadhyayula, L. C. and Kumar, M., v27n5, Sept/Oct 1982, p58.
Solid-state power amplifier replacing TWTs in C-band satellites. Wolkstein, H. J. and LaPrade, J. N., v27n5, Sept/Oct 1982, p7.

Analog-to-digital converters

GaAs microwave monolithic integrated circuits, a review of. Huang, H. C., Upadhyayula, L. C. and Kumar, M., v27n5, Sept/Oct 1982, p58.

Analytical chemistry

Chemical and Physical Laboratory supports VideoDisc. Hakala, D. F., v27n1, Jan/Feb 1982, p39.

Antennas

Low-sidelobe antennas for tactical phased-array radars. Patton, W. T., v27n5, Sept/Oct 1982, p31.

Astronomy

Making telescopes is my hobby. Schneider, W., v27n2, Mar/Apr 1982, p75.

Automated design

Computer design and testing of a microwave antenna-feed manifold. Bolger, G. P. and Holaday, V. D., v27n5, Sept/Oct 1982, p87.
MIMIC logic simulator. Ashkinazy, A., v27n6, Nov/Dec 1982, p10.

Automated testing

ATE, distributed system architectures for. Fay, J. E., v27n4, July/Aug 1982, p53.
Automated measurement of transistor I-V characteristics. Snowden, M. P. and Amantea, R., v27n2, Mar/Apr 1982, p69.
Automatic test equipment for VideoDisc and stylus. Kowalchik, J. J. and Selwa, A. P., v27n1, Jan/Feb 1982, p30.
Large system development, digital interface simulation for. Suhy, G. W., v27n6, Nov/Dec 1982, p39.

Automation

Assembly mechanization program at RCA Solid State (RAMP). Koskulitz, J. and Rosenfield, M., v27n4, July/Aug 1982, p57.
Automated assembly of lumped-element GaAs FET power amplifiers. Klatskin, J. B., Haggis, D., Camisa, R. L. and Joyce, B. T., v27n5, Sept/Oct 1982, p64.

Awards

David Sarnoff Awards for Outstanding Technical Achievement (1982). *RCA ENGINEER* Staff, v27n4, July/Aug 1982, p4.
"SelectaVision" VideoDisc Awards. *RCA ENGINEER* Staff, v27n1, Jan/Feb 1982, p4.

Broadcasting

Direct Broadcasting Satellite: Black hole or bonanza? Clark, J. F., v27n4, July/Aug 1982, p82.

Business operations

Strategic framework to strengthen RCA. Bradshaw, T. F., v27n4, July/Aug 1982, p1.

Charge coupled devices (CCDs)

An intelligent missile seeker, design and simulation of. Hayman, J., v27n6, Nov/Dec 1982, p43.
Infrared sensor systems, design and performance prediction of. Cantella, M. J., v27n3, May/June 1982, p67.
Infrared-camera system developed to use the Schottky-barrier IR-CCD array. Klein, J. J., Roberts, N. L. and Chin, G. D., v27n3, May/June 1982, p60.

Circuit analysis

MIMIC logic simulator. Ashkinazy, A., v27n6, Nov/Dec 1982, p10.

Circuit boards

Parylene-coating process at MSR. Philip, G. O., v27n2, Mar/Apr 1982, p56.

Circuit design

ANA radio frequency circuit simulation and analysis. Perlow, S. M., v27n6, Nov/Dec 1982, p46.

Circuit devices

Active and passive microwave components. Denlinger, E. J., v27n5, Sept/Oct 1982, p50.

Command and control systems

Large system development, digital interface simulation for. Suhy, G. W., v27n6, Nov/Dec 1982, p39.

Communication components

Linear integrated circuits are going digital. Wittlinger, H. A., v27n1, Jan/Feb 1982, p58.

Communication satellites

RCA Satcom system, computer modeling in the. Guida, A. A., Jonnalagadda, K., Raychaudhuri, D. and Schiff, L., v27n6, Nov/Dec 1982, p84.
Receivers, wideband, for communications satellites. Goldberg, H., v27n5, Sept/Oct 1982, p37.

Communication systems

Microwave communications system for RCA Globcom. Solomon, S. M., v27n4, July/Aug 1982, p75.

Compounds

Material compounding of VideoDiscs demands the right chemistry. Whipple, B. and Dunn, V. S., v27n1, Jan/Feb 1982, p16.

Computer applications

Automated measurement of transistor I-V characteristics. Snowden, M. P. and Amantea, R., v27n2, Mar/Apr 1982, p69.
Computer music, an illustrated history of. Mercuri, R. T., v27n4, July/Aug 1982, p65.
Computer programming and systems analysis in the rapidly changing VideoDisc environment (application of FOCUS). Myers, W. W., v27n4, July/Aug 1982, p48.
Engineering environment, simulation in an. Pitts, K. A. and Barton, R. R., v27n6, Nov/Dec 1982, p4.

Computer graphics

Engineering Form and Function: Windows on RCA Technology. *RCA ENGINEER* Staff, v27n4, July/Aug 1982, p33.

Computer programming

Complex weapon systems, discrete-event simulations of. Golub, J., v27n6, Nov/Dec 1982, p32.
Computer programming and systems analysis in the rapidly changing VideoDisc environment (application of FOCUS). Myers, W. W., v27n4, July/Aug 1982, p48.
Software reliability, discovering how to ensure. Trachtenberg, M., v27n1, Jan/Feb 1982, p53.

Computer programs

Computer design and testing of a microwave antenna-feed manifold. Bolger, G. P. and Holaday, V. D., v27n5, Sept/Oct 1982, p87.

Computer simulation

- An intelligent missile seeker, design and simulation of. Hayman, J., v27n6, Nov/Dec 1982, p43.
- Business modeling and the engineer: An Astro-Electronics application. Nigam, A. K., Hong, S. and Spence, S. R., v27n6, Nov/Dec 1982, p65.
- Complex weapon systems, discrete-event simulations of. Golub, J., v27n6, Nov/Dec 1982, p32.
- Computer-aided design of metal-forming processes. Chen, C. C., v27n2, Mar/Apr 1982, p45.
- Electromechanical motor simulation. Browne, R. G., v27n6, Nov/Dec 1982, p80.
- Engineering environment, simulation in an. Pitts, K. A. and Barton, R. R., v27n6, Nov/Dec 1982, p4.
- HF modem simulation. DeMaria, P. A. and Bodzioch, K. J., v27n6, Nov/Dec 1982, p18.
- Infrared sensor systems, design and performance prediction of. Cantella, M. J., v27n3, May/June 1982, p67.
- Large system development, digital interface simulation for. Suhy, G. W., v27n6, Nov/Dec 1982, p39.
- Mechanically scanned radar systems, dynamic analysis and simulation of. Liston, J. and Sparks, G. M., v27n6, Nov/Dec 1982, p24.
- MIMIC logic simulator. Ashkinazy, A., v27n6, Nov/Dec 1982, p10.
- Modeling and simulation: Tools for the 80s. Teger, A. H., v27n6, Nov/Dec 1982, p1.
- RCA Satcom system, computer modeling in the. Guida, A. A., Jonnalagadda, K., Raychaudhuri, D. and Schiff, L., v27n6, Nov/Dec 1982, p84.

Computer storage

- Data recording on optical discs at 300 Mb/s. Ammon, G. J. and Reno, C. W., v27n3, May/June 1982, p36.

Computer systems

- ATE, distributed system architectures for. Fay, J. E., v27n4, July/Aug 1982, p53.

Computer terminals

- Color-data-display CRT: A product whose time has come. Barbin, R. L., Simpson, T. F. and Marks, B. G., v27n4, July/Aug 1982, p23.

Computer-aided analysis

- ANA radio frequency circuit simulation and analysis. Perlow, S. M., v27n6, Nov/Dec 1982, p46.
- Automated assembly of lumped-element GaAs FET power amplifiers. Klatskin, J. B., Haggis, D., Camisa, R. L. and Joyce, B. T., v27n5, Sept/Oct 1982, p64.
- Mechanical and thermal design, modeling and simulation in. Enstrom, R. E., v27n6, Nov/Dec 1982, p71.

Computer-aided design (CAD)

- Computer-aided design and testing of microwave circuits. Perlman, B. S., Rhodes, D. L. and Schepps, J. L., v27n5, Sept/Oct 1982, p76.
- Computer-aided design of metal-forming processes. Chen, C. C., v27n2, Mar/Apr 1982, p45.
- MIMIC logic simulator. Ashkinazy, A., v27n6, Nov/Dec 1982, p10.

Computer-aided manufacturing (CAM)

- Numerical control: The cornerstone of computers in manufacturing. Young, C., v27n2, Mar/Apr 1982, p41.

Computer-aided testing (CAT)

- Computer design and testing of a microwave antenna-feed manifold. Bolger, G. P. and Holaday, V. D., v27n5, Sept/Oct 1982, p87.
- Computer-aided design and testing of microwave circuits. Perlman, B. S., Rhodes, D. L. and Schepps, J. L., v27n5, Sept/Oct 1982, p76.

Computers, home

- Computer music, an illustrated history of. Mercuri, R. T., v27n4, July/Aug 1982, p65.

Computers, manufacturing

- Computer-aided manufacture of precision microwave components for phased-array radar GaAs MESFET power amplifiers. Breese, M. E. and Mason, R. J., v27n5, Sept/Oct 1982, p71.

Data communications

- HF modem simulation. DeMaria, P. A. and Bodzioch, K. J., v27n6, Nov/Dec 1982, p18.

Data processing

- Computer programming and systems analysis in the rapidly changing VideoDisc environment (application of FOCUS). Myers, W. W., v27n4, July/Aug 1982, p48.

Design

- Engineering Form and Function: Windows on RCA Technology. *RCA ENGINEER Staff*, v27n4, July/Aug 1982, p33.

Digital electronics

- Linear integrated circuits are going digital. Wittlinger, H. A., v27n1, Jan/Feb 1982, p58.

Direct broadcasting satellites (DBS)

- Direct Broadcasting Satellite: Black hole or bonanza? Clark, J. F., v27n4, July/Aug 1982, p82.

Display systems

- Color-data-display CRT: A product whose time has come. Barbin, R. L., Simpson, T. F. and Marks, B. G., v27n4, July/Aug 1982, p23.

Editorials

- Editorial input: Two new editorial features. King, T. E., v27n5, Sept/Oct 1982, p30.

Education

- Continuing education for manufacturing engineers. *RCA Corporate Engineering Education*, v27n2, Mar/Apr 1982, p38.

Electro-optics, lasers

- Long-wavelength semiconductor diode lasers for optical communications. Olsen, G. H. and Ettenberg, M., v27n4, July/Aug 1982, p38.
- Space applications of lidar. Altman, W., Hogan, D. B., Hutter, E. C. and Rosenberg, A., v27n3, May/June 1982, p44.

Electro-optics, systems and techniques

- Data recording on optical discs at 300 Mb/s. Ammon, G. J. and Reno, C. W., v27n3, May/June 1982, p36.

- Electro-Optics: Insight to the future. Decker, C. D., v27n3, May/June 1982, p1.
- Silicon avalanche photodiodes, recent developments in. Webb, P. P. and McIntyre, R. J., v27n3, May/June 1982, p96.
- Space applications for RCA infrared technology. Warren, F. B., Tower, J. R., Gandolfo, D. A., Elabd, H. A. and Villani, T. S., v27n3, May/June 1982, p76.
- TV camera for target-acquisition and laser-designator systems, high performance. Arlan, L., v27n3, May/June 1982, p87.

Electrochemical energy storage

- Coal, upgrading, for more efficient electric-power generation. Williams, R., v27n4, July/Aug 1982, p45.

Energy conversion

- Coal, upgrading, for more efficient electric-power generation. Williams, R., v27n4, July/Aug 1982, p45.

Engineering tools and techniques

- Engineering environment, simulation in an. Pitts, K. A. and Barton, R. R., v27n6, Nov/Dec 1982, p4.

Fiber optics

- Fiber-optic communications systems, design, development and installation of. Ainsbury, D. C., v27n3, May/June 1982, p28.

Finite element analysis

- Mechanical and thermal design, modeling and simulation in. Enstrom, R. E., v27n6, Nov/Dec 1982, p71.

Heat transfer

- Mechanical and thermal design, modeling and simulation in. Enstrom, R. E., v27n6, Nov/Dec 1982, p71.

Image encoding

- Human visual system, modeling of the. Adelson, E. H., Pica, A. P. and Carlson, C. R., v27n6, Nov/Dec 1982, p56.

Imaging systems

- Infrared-camera system developed to use the Schottky-barrier IR-CCD array. Klein, J. J., Roberts, N. L. and Chin, G. D., v27n3, May/June 1982, p60.
- Schottky-barrier infrared image sensors. Kosonocky, W.F., Elabd, H.A., Erhardt, H.G., Shallcross, F.V., Meray, G.M., Miller, R., Villani, T.S., Groppe, J.V., Frantz, V.L., and Tams, F.J., v27n3, May/June 1982, p49.
- Space applications for RCA infrared technology. Warren, F. B., Tower, J. R., Gandolfo, D. A., Elabd, H. A. and Villani, T. S., v27n3, May/June 1982, p76.
- TV camera for target-acquisition and laser-designator systems, high performance. Arlan, L., v27n3, May/June 1982, p87.

Industrial engineering

- Mirror Fusion Test Facility, producing neutral beam ion sources for the. Lynch, W. S. and Reed, R. E., v27n2, Mar/Apr 1982, p62.

Information management

Computer programming and systems analysis in the rapidly changing VideoDisc environment (application of FOCUS). Myers, W. W., v27n4, July/Aug 1982, p48.

Technical abstracts database (TAD): RCA database now an on-line system. Technical Information Systems, v27n2, Mar/Apr 1982, p22.

Information sciences

Technical abstracts database (TAD): RCA database now an on-line system. Technical Information Systems, v27n2, Mar/Apr 1982, p22.

Infrared equipment

Infrared sensor systems, design and performance prediction of. Cantella, M. J., v27n3, May/June 1982, p67.

Infrared-camera system developed to use the Schottky-barrier IR-CCD array. Klein, J. J., Roberts, N. L. and Chin, G. D., v27n3, May/June 1982, p60.

Schottky-barrier infrared image sensors. Kosonocky, W.F., Elabd, H.A., Erhardt, H.G., Shallcross, F.V., Meray, G.M., Miller, R., Villani, T.S., Groppe, J.V., Frantz, V.L., and Tams, F.J., v27n3, May/June 1982, p49.

Integrated circuits

Assembly mechanization program at RCA Solid State (RAMP). Koskultiz, J. and Rosenfield, M., v27n4, July/Aug 1982, p57.

Schottky-barrier infrared image sensors. Kosonocky, W.F., Elabd, H.A., Erhardt, H.G., Shallcross, F.V., Meray, G.M., Miller, R., Villani, T.S., Groppe, J.V., Frantz, V.L., and Tams, F.J., v27n3, May/June 1982, p49.

Introductions (to issues)

Electro-Optics: Insight to the future. Decker, C. D., v27n3, May/June 1982, p1.

Manufacturing programs at Consumer Electronics. Borman, B. L., v27n2, Mar/Apr 1982, p1.

Microwave technology at RCA. Sterzer, F., v27n5, Sept/Oct 1982, p1.

Modeling and simulation: Tools for the 80s. Teger, A. H., v27n6, Nov/Dec 1982, p1.

Quality plus diversity plus availability equals success. Schlosser, H. S., v27n1, Jan/Feb 1982, p1.

Strategic framework to strengthen RCA. Bradshaw, T. F., v27n4, July/Aug 1982, p1.

Laboratory equipment and techniques

Automated measurement of transistor I-V characteristics. Snowden, M. P. and Amantea, R., v27n2, Mar/Apr 1982, p69.

Laser applications

Long-wavelength semiconductor diode lasers for optical communications. Olsen, G. H. and Ettenberg, M., v27n4, July/Aug 1982, p38.

Space applications of lidar. Altman, W., Hogan, D. B., Hutter, E. C. and Rosenberg, A., v27n3, May/June 1982, p44.

Laser tracking

Space applications of lidar. Altman, W., Hogan, D. B., Hutter, E. C. and Rosenberg, A., v27n3, May/June 1982, p44.

Lasers, injection

High-density optical recording using laser diodes. Bartolini, R. A., v27n3, May/June 1982, p20.

Single-mode diode lasers for systems-oriented applications. Botez, D., v27n3, May/June 1982, p8.

Lenses

Making telescopes is my hobby. Schneider, W., v27n2, Mar/Apr 1982, p75.

Management

Strategic framework to strengthen RCA. Bradshaw, T. F., v27n4, July/Aug 1982, p1.

Manufacturing

Computer-aided design of metal-forming processes. Chen, C. C., v27n2, Mar/Apr 1982, p45.

Equipment decisions for VLSI-circuit manufacture. Blumenfeld, M. A. and Shambelan, R. C., v27n2, Mar/Apr 1982, p35.

Manufacturing the VideoDiscs: An overview. Weisberg, H., v27n1, Jan/Feb 1982, p6.

Manufacturing. Custom and Quantity Manufacturing: An Engineering Comparison. D'Arcy, J. A. and Miller, R., v27n2, Mar/Apr 1982, p4.

Mastering VideoDiscs: The software to hardware conversion. Kell, F. D., John, G. and Stevens, J., v27n1, Jan/Feb 1982, p11.

Player Technology Center: Key to innovation. Mishra, D., v27n2, Mar/Apr 1982, p24.

Manufacturing engineering

Continuing education for manufacturing engineers. RCA Corporate Engineering Education, v27n2, Mar/Apr 1982, p38.

Equipment decisions for VLSI-circuit manufacture. Blumenfeld, M. A. and Shambelan, R. C., v27n2, Mar/Apr 1982, p35.

Manufacturing programs at Consumer Electronics. Borman, B. L., v27n2, Mar/Apr 1982, p1.

Manufacturing. Custom and Quantity Manufacturing: An Engineering Comparison. D'Arcy, J. A. and Miller, R., v27n2, Mar/Apr 1982, p4.

Mirror Fusion Test Facility, producing neutral beam ion sources for the. Lynch, W. S. and Reed, R. E., v27n2, Mar/Apr 1982, p62.

Numerical control: The cornerstone of computers in manufacturing. Young, C., v27n2, Mar/Apr 1982, p41.

Player Technology Center: Key to innovation. Mishra, D., v27n2, Mar/Apr 1982, p24.

Manufacturing equipment

Equipment decisions for VLSI-circuit manufacture. Blumenfeld, M. A. and Shambelan, R. C., v27n2, Mar/Apr 1982, p35.

Manufacturing. Custom and Quantity Manufacturing: An Engineering Comparison. D'Arcy, J. A. and Miller, R., v27n2, Mar/Apr 1982, p4.

Numerical control: The cornerstone of computers in manufacturing. Young, C., v27n2, Mar/Apr 1982, p41.

Materials

Chemical and Physical Laboratory supports VideoDisc. Hakala, D. F., v27n1, Jan/Feb 1982, p39.

Medical electronics

Localized hyperthermia treatment of cancer. Sterzer, F., v27n1, Jan/Feb 1982, p43.

Medical applications of microwave energy. Paglione, R. W., v27n5, Sept/Oct 1982, p17.

Microelectronics

Parylene-coating process at MSR. Philip, G. O., v27n2, Mar/Apr 1982, p56.

Microwave antennas

Low-sidelobe antennas for tactical phased-array radars. Patton, W. T., v27n5, Sept/Oct 1982, p31.

Medical applications of microwave energy. Paglione, R. W., v27n5, Sept/Oct 1982, p17.

Shaped-beam reflector antennas for communications satellites. Profera, C. E., Rosol, G. L., Soule, H. H. and Kara, J., v27n5, Sept/Oct 1982, p43.

Microwave relay systems

Microwave communications system for RCA Globcom. Solomon, S. M., v27n4, July/Aug 1982, p75.

Microwave technology

Active and passive microwave components. Denlinger, E. J., v27n5, Sept/Oct 1982, p50.

ANA radio frequency circuit simulation and analysis. Perlow, S. M., v27n6, Nov/Dec 1982, p46.

Automated assembly of lumped-element GaAs FET power amplifiers. Klatskin, J. B., Haggis, D., Camisa, R. L. and Joyce, B. T., v27n5, Sept/Oct 1982, p64.

Computer design and testing of a microwave antenna-feed manifold. Bolger, G. P. and Holaday, V. D., v27n5, Sept/Oct 1982, p87.

Computer-aided design and testing of microwave circuits. Perlman, B. S., Rhodes, D. L. and Schepps, J. L., v27n5, Sept/Oct 1982, p76.

Computer-aided manufacture of precision microwave components for phased-array radar GaAs MESFET power amplifiers. Breese, M. E. and Mason, R. J., v27n5, Sept/Oct 1982, p71.

Localized hyperthermia treatment of cancer. Sterzer, F., v27n1, Jan/Feb 1982, p43.

Medical applications of microwave energy. Paglione, R. W., v27n5, Sept/Oct 1982, p17.

Microwave components research at RCA. Nowogrodzki, M., v27n5, Sept/Oct 1982, p4.

Microwave technology at RCA. Sterzer, F., v27n5, Sept/Oct 1982, p1.

Radar instruments: Sensors for industrial applications. Nowogrodzki, M., Mawhinney, D. D. and Kipp, R. W., v27n5, Sept/Oct 1982, p23.

Receivers, wideband, for communications satellites. Goldberg, H., v27n5, Sept/Oct 1982, p37.

Solid-state power amplifier replacing TWTs in C-band satellites. Wolkstein, H. J. and LaPrade, J. N., v27n5, Sept/Oct 1982, p7.

Microwaves

GaAs microwave monolithic integrated circuits, a review of. Huang, H. C., Upadhyayula, L. C. and Kumar, M., v27n5, Sept/Oct 1982, p58.

Microwave communications system for RCA Globcom. Solomon, S. M., v27n4, July/Aug 1982, p75.

Shaped-beam reflector antennas for communications satellites. Profera, C. E., Rosol, G. L., Soule, H. H. and Kara, J., v27n5, Sept/Oct 1982, p43.

Military communications

Pin diode, high-power, the Engineer's Notebook. Stabile, P. J., v27n5, Sept/Oct 1982, p21.

Missile systems

An intelligent missile seeker, design and simulation of. Hayman, J., v27n6, Nov/Dec 1982, p43.

Molding, phonograph records

Micro-molding is a VideoDisc requirement.

McNeely, M. and Bock, M., v27n1, Jan/Feb 1982, p19.

Motors

Electromechanical motor simulation. Browne, R. G., v27n6, Nov/Dec 1982, p80.

Music

Computer music, an illustrated history of. Mercuri, R. T., v27n4, July/Aug 1982, p65.

Navigation satellites

The second-generation Navy Navigation Satellite, NOVA-1, expectations achieved. Staniszewski, J. R., v27n4, July/Aug 1982, p89.

Nuclear energy

Mirror Fusion Test Facility, producing neutral beam ion sources for the. Lynch, W. S. and Reed, R. E., v27n2, Mar/Apr 1982, p62.

On the job/off the job

Making telescopes is my hobby. Schneider, W., v27n2, Mar/Apr 1982, p75.

Operations research

Business modeling and the engineer: An Astro-Electronics application. Nigam, A. K., Hong, S. and Spence, S. R., v27n6, Nov/Dec 1982, p65.

Optical communications

Electro-Optics: Insight to the future. Decker, C. D., v27n3, May/June 1982, p1.

Fiber-optic communications systems, design, development and installation of. Ainsbury, D. C., v27n3, May/June 1982, p28.

Long-wavelength semiconductor diode lasers for optical communications. Olsen, G. H. and Ettenberg, M., v27n4, July/Aug 1982, p38.

Optoelectronic systems, some of the new systems. Ettenberg, M., v27n3, May/June 1982, p4.

Silicon avalanche photodiodes, recent developments in. Webb, P. P. and McIntyre, R. J., v27n3, May/June 1982, p96.

Single-mode diode lasers for systems-oriented applications. Botez, D., v27n3, May/June 1982, p8.

Optical systems

High-density optical recording using laser diodes. Bartolini, R. A., v27n3, May/June 1982, p20.

Optoelectronic systems, some of the new systems. Ettenberg, M., v27n3, May/June 1982, p4.

Package engineering

Package engineering for the Picture Tube Division. Haggerty, G. L., v27n2, Mar/Apr 1982, p50.

Photoconductivity

Saticon photoconductor: The latest in color-camera-tube photoconductors. Neuhauser, R. G., v27n3, May/June 1982, p81.

Photodiodes

Silicon avalanche photodiodes, recent developments in. Webb, P. P. and McIntyre, R. J., v27n3, May/June 1982, p96.

Physical chemistry

Coal, upgrading, for more efficient electric-power generation. Williams, R., v27n4, July/Aug 1982, p45.

Picture tubes

Color-data-display CRT: A product whose time has come. Barbin, R. L., Simpson, T. F. and Marks, B. G., v27n4, July/Aug 1982, p23.

Package engineering for the Picture Tube Division. Haggerty, G. L., v27n2, Mar/Apr 1982, p50.

Plastics

Caddy design and manufacturing of the VideoDisc caddy. Torrington, L. A., v27n1, Jan/Feb 1982, p23.

Material compounding of VideoDiscs demands the right chemistry. Whipple, B. and Dunn, V. S., v27n1, Jan/Feb 1982, p16.

Printed circuit boards

Parylene-coating process at MSR. Philip, G. O., v27n2, Mar/Apr 1982, p56.

Process control

Statistics applications in manufacturing. Gunter, B. H. and Rayl, M., v27n2, Mar/Apr 1982, p14.

Productivity

Quality Circles at RCA Scranton. Mecca, S. J., v27n2, Mar/Apr 1982, p30.

Propulsion, electronic and ionic

The second-generation Navy Navigation Satellite, NOVA-1, expectations achieved. Staniszewski, J. R., v27n4, July/Aug 1982, p89.

Publishing

Editorial input: Two new editorial features. King, T. E., v27n5, Sept/Oct 1982, p30.

Editorial Representatives, meet your. *RCA ENGINEER* Staff, v27n1, Jan/Feb 1982, p35.

Technical abstracts database (TAD): RCA database now an on-line system. Technical Information Systems, v27n2, Mar/Apr 1982, p22.

Quality control

Product Assurance of VideoDisc: VideoDisc performance in the real world. Huck, R. H., v27n1, Jan/Feb 1982, p27.

Quality Circles at RCA Scranton. Mecca, S. J., v27n2, Mar/Apr 1982, p30.

Statistics applications in manufacturing. Gunter, B. H. and Rayl, M., v27n2, Mar/Apr 1982, p14.

Radar antennas

Low-sidelobe antennas for tactical phased-array radars. Patton, W. T., v27n5, Sept/Oct 1982, p31.

Radar applications

Radar instruments: Sensors for industrial applications. Nowogrodzki, M., Mawhinney, D. D. and Kipp, R. W., v27n5, Sept/Oct 1982, p23.

Radar systems

Mechanically scanned radar systems, dynamic analysis and simulation of. Liston, J. and Sparks, G. M., v27n6, Nov/Dec 1982, p24.

Radar, Doppler

Radar instruments: Sensors for industrial applications. Nowogrodzki, M., Mawhinney, D. D. and Kipp, R. W., v27n5, Sept/Oct 1982, p23.

Radar, phased arrays

Computer-aided manufacture of precision microwave components for phased-array radar GaAs MESFET power amplifiers. Breese, M. E. and Mason, R. J., v27n5, Sept/Oct 1982, p71.

Radiometers

Medical applications of microwave energy. Paglione, R. W., v27n5, Sept/Oct 1982, p17.

RCA Astro-Electronics

Business modeling and the engineer: An Astro-Electronics application. Nigam, A. K., Hong, S. and Spence, S. R., v27n6, Nov/Dec 1982, p65.

RCA Consumer Electronics

Manufacturing programs at Consumer Electronics. Borman, B. L., v27n2, Mar/Apr 1982, p1.

RCA Electron Tube Division

Microwave components research at RCA. Nowogrodzki, M., v27n5, Sept/Oct 1982, p4.

RCA ENGINEER

Editorial Representatives, meet your. *RCA ENGINEER* Staff, v27n1, Jan/Feb 1982, p35.

RCA Laboratories

Microwave components research at RCA. Nowogrodzki, M., v27n5, Sept/Oct 1982, p4.

RCA Picture Tube Division

Package engineering for the Picture Tube Division. Haggerty, G. L., v27n2, Mar/Apr 1982, p50. Quality Circles at RCA Scranton. Mecca, S. J., v27n2, Mar/Apr 1982, p30.

RCA "SelectaVision" VideoDisc Operations

Automatic test equipment for VideoDisc and stylus. Kowalchik, J. J. and Selwa, A. P., v27n1, Jan/Feb 1982, p30.

Caddy design and manufacturing of the VideoDisc caddy. Torrington, L. A., v27n1, Jan/Feb 1982, p23.

Manufacturing the VideoDiscs: An overview. Weisberg, H., v27n1, Jan/Feb 1982, p6.

Micro-molding is a VideoDisc requirement. McNeely, M. and Bock, M., v27n1, Jan/Feb 1982, p19.

Product Assurance of VideoDisc: VideoDisc performance in the real world. Huck, R. H., v27n1, Jan/Feb 1982, p27.

RCA Solid State Division

Linear integrated circuits are going digital. Wittlinger, H. A., v27n1, Jan/Feb 1982, p58.

Recording systems, laser

- Data recording on optical discs at 300 Mb/s. Ammon, G. J. and Reno, C. W., v27n3, May/June 1982, p36.
- High-density optical recording using laser diodes. Bartolini, R. A., v27n3, May/June 1982, p20.
- Optoelectronic systems, some of the new systems. Ettenberg, M., v27n3, May/June 1982, p4.
- Single-mode diode lasers for systems-oriented applications. Botez, D., v27n3, May/June 1982, p8.

Reliability

- Software reliability, discovering how to ensure. Trachtenberg, M., v27n1, Jan/Feb 1982, p53.

Satellite communication

- Direct Broadcasting Satellite: Black hole or bonanza? Clark, J. F., v27n4, July/Aug 1982, p82.
- RCA Satcom system, computer modeling in the. Guida, A. A., Jonnalagadda, K., Raychaudhuri, D. and Schiff, L., v27n6, Nov/Dec 1982, p84.
- Receivers, wideband, for communications satellites. Goldberg, H., v27n5, Sept/Oct 1982, p37.
- Shaped-beam reflector antennas for communications satellites. Profera, C. E., Rosol, G. L., Soule, H. H. and Kara, J., v27n5, Sept/Oct 1982, p43.
- Solid-state power amplifier replacing TWTs in C-band satellites. Wolkstein, H. J. and LaPrade, J. N., v27n5, Sept/Oct 1982, p7.

Satellite technology

- The second-generation Navy Navigation Satellite, NOVA-1, expectations achieved. Staniszewski, J. R., v27n4, July/Aug 1982, p89.

Signal processing

- Automatic test equipment for VideoDisc and stylus. Kowalchik, J. J. and Selwa, A. P., v27n1, Jan/Feb 1982, p30.

Solid state devices

- Active and passive microwave components. Denlinger, E. J., v27n5, Sept/Oct 1982, p50.
- Pin diode, high-power, the Engineer's Notebook. Stabile, P. J., v27n5, Sept/Oct 1982, p21.

Solid state materials

- Space applications for RCA infrared technology. Warren, F. B., Tower, J. R., Gandolfo, D. A., Elabd, H. A. and Villani, T. S., v27n3, May/June 1982, p76.

Solid state processing

- Assembly mechanization program at RCA Solid State (RAMP). Koskulitz, J. and Rosenfield, M., v27n4, July/Aug 1982, p57.

Statistics

- Statistics applications in manufacturing. Gunter, B. H. and Rayl, M., v27n2, Mar/Apr 1982, p14.

Stereophonic systems

- Stereo CED VideoDisc system. Freeman, E. J., Mehrotra, G. N. and Repka, C. P., v27n4, July/Aug 1982, p12.

Switching circuits

- Pin diode, high-power, the Engineer's Notebook. Stabile, P. J., v27n5, Sept/Oct 1982, p21.

Systems engineering

- ATE, distributed system architectures for. Fay, J. E., v27n4, July/Aug 1982, p53.
- Fiber-optic communications systems, design, development and installation of. Ainsbury, D. C., v27n3, May/June 1982, p28.
- HF modem simulation. DeMaria, P. A. and Bodzioch, K. J., v27n6, Nov/Dec 1982, p18.

Tape recording

- Hawkeye camera. Bendell, S. L., Bazin, L. J. and Clarke, J. J., v27n4, July/Aug 1982, p18.

Television cameras

- Hawkeye camera. Bendell, S. L., Bazin, L. J. and Clarke, J. J., v27n4, July/Aug 1982, p18.
- Saticon photoconductor: The latest in color-camera-tube photoconductors. Neuhauser, R. G., v27n3, May/June 1982, p81.
- TV camera for target-acquisition and laser-designator systems, high performance. Arlan, L., v27n3, May/June 1982, p87.

Television display systems

- Human visual system, modeling of the. Adelson, E. H., Pica, A. P. and Carlson, C. R., v27n6, Nov/Dec 1982, p56.

Television, audio

- Stereo CED VideoDisc system. Freeman, E. J., Mehrotra, G. N. and Repka, C. P., v27n4, July/Aug 1982, p12.

Television, mobile units

- Hawkeye camera. Bendell, S. L., Bazin, L. J. and Clarke, J. J., v27n4, July/Aug 1982, p18.

Testing

- Computer-aided design and testing of microwave circuits. Perlman, B. S., Rhodes, D. L. and

- Schepps, J. L., v27n5, Sept/Oct 1982, p76.
- Software reliability, discovering how to ensure. Trachtenberg, M., v27n1, Jan/Feb 1982, p53.

Typesetting

- Editorial input: Two new editorial features. King, T. E., v27n5, Sept/Oct 1982, p30.

Value engineering

- Mirror Fusion Test Facility, producing neutral beam ion sources for the. Lynch, W. S. and Reed, R. E., v27n2, Mar/Apr 1982, p62.

VideoDisc, Capacitance electronic disc system

- Caddy design and manufacturing of the VideoDisc caddy. Torrington, L. A., v27n1, Jan/Feb 1982, p23.
- Chemical and Physical Laboratory supports VideoDisc. Hakala, D. F., v27n1, Jan/Feb 1982, p39.
- Manufacturing the VideoDiscs: An overview. Weisberg, H., v27n1, Jan/Feb 1982, p6.
- Mastering VideoDiscs: The software to hardware conversion. Kell, F. D., John, G. and Stevens, J., v27n1, Jan/Feb 1982, p11.
- Material compounding of VideoDiscs demands the right chemistry. Whipple, B. and Dunn, V. S., v27n1, Jan/Feb 1982, p16.
- Micro-molding is a VideoDisc requirement. McNeely, M. and Bock, M., v27n1, Jan/Feb 1982, p19.
- Player Technology Center: Key to innovation. Mishra, D., v27n2, Mar/Apr 1982, p24.
- Product Assurance of VideoDisc: VideoDisc performance in the real world. Huck, R. H., v27n1, Jan/Feb 1982, p27.
- Quality plus diversity plus availability equals success. Schlosser, H. S., v27n1, Jan/Feb 1982, p1.
- "SelectaVision" VideoDisc Awards. RCA ENGINEER Staff, v27n1, Jan/Feb 1982, p4.
- Stereo CED VideoDisc system. Freeman, E. J., Mehrotra, G. N. and Repka, C. P., v27n4, July/Aug 1982, p12.

Vidicons

- Saticon photoconductor: The latest in color-camera-tube photoconductors. Neuhauser, R. G., v27n3, May/June 1982, p81.

Vision

- Human visual system, modeling of the. Adelson, E. H., Pica, A. P. and Carlson, C. R., v27n6, Nov/Dec 1982, p56.

Weapon systems

- Complex weapon systems, discrete-event simulations of. Golub, J., v27n6, Nov/Dec 1982, p32.

Author Index

- Adelson, E. H., Pica, A. P. and Carlson, C. R., Human visual system, modeling of the. v27n6, Nov/Dec 1982, p56.
- Ainsbury, D. C., Fiber-optic communications systems, design, development and installation of. v27n3, May/June 1982, p28.
- Altman, W., Hogan, D. B., Hutter, E. C. and Rosenberg, A., Space applications of lidar. v27n3, May/June 1982, p44.
- Amantea, R. with Snowden, M. P., Automated measurement of transistor I-V characteristics. v27n2, Mar/Apr 1982, p69.
- Ammon, G. J. and Reno, C. W., Data recording on optical discs at 300 Mb/s. v27n3, May/June 1982, p36.
- Arian, L., TV camera for target-acquisition and laser-designator systems, high performance. v27n3, May/June 1982, p87.
- Ashkinazy, A., MIMIC logic simulator. v27n6, Nov/Dec 1982, p10.
- Barbin, R. L., Simpson, T. F. and Marks, B. G., Color-data-display CRT: A product whose time has come. v27n4, July/Aug 1982, p23.
- Bartolini, R. A., High-density optical recording using laser diodes. v27n3, May/June 1982, p20.
- Barton, R. R. with Pitts, K. A., Engineering environment, simulation in an. v27n6, Nov/Dec 1982, p4.
- Bazin, L. J. with Bendell, S. L. et al., Hawkeye camera. v27n4, July/Aug 1982, p18.
- Bendell, S. L., Bazin, L. J. and Clarke, J. J., Hawkeye camera. v27n4, July/Aug 1982, p18.
- Blumenfeld, M. A. and Shambelan, R. C., Equipment decisions for VLSI-circuit manufacture. v27n2, Mar/Apr 1982, p35.
- Bock, M. with McNeely, M., Micro-molding is a VideoDisc requirement. v27n1, Jan/Feb 1982, p19.
- Bodzioch, K. J. with DeMaria, P. A., HF modem simulation. v27n6, Nov/Dec 1982, p18.
- Bolger, G. P. and Holaday, V. D., Computer design and testing of a microwave antenna-feed manifold. v27n5, Sept/Oct 1982, p87.
- Borman, B. L., Manufacturing programs at Consumer Electronics. v27n2, Mar/Apr 1982, p1.
- Botez, D., Single-mode diode lasers for systems-oriented applications. v27n3, May/June 1982, p8.
- Bradshaw, T. F., Strategic framework to strengthen RCA. v27n4, July/Aug 1982, p1.
- Breese, M. E. and Mason, R. J., Computer-aided manufacture of precision microwave components for phased-array radar GaAs MESFET power amplifiers. v27n5, Sept/Oct 1982, p71.
- Browne, R. G., Electromechanical motor simulation. v27n6, Nov/Dec 1982, p80.
- Camisa, R. L. with Klatskin, J. B. et al., Automated assembly of lumped-element GaAs FET power amplifiers. v27n5, Sept/Oct 1982, p64.
- Cantella, M. J., Infrared sensor systems, design and performance prediction of. v27n3, May/June 1982, p67.
- Carlson, C. R. with Adelson, E. H. et al., Human visual system, modeling of the. v27n6, Nov/Dec 1982, p56.
- Chen, C. C., Computer-aided design of metal-forming processes. v27n2, Mar/Apr 1982, p45.
- Chin, G. D. with Klein, J. J. et al., Infrared-camera system developed to use the Schottky-barrier IR-CCD array. v27n3, May/June 1982, p60.
- Clark, J. F., Direct Broadcasting Satellite: Black hole or bonanza? v27n4, July/Aug 1982, p82.
- Clarke, J. J. with Bendell, S. L. et al., Hawkeye camera. v27n4, July/Aug 1982, p18.
- D'Arcy, J. A. and Miller, R., Manufacturing, Custom and Quantity Manufacturing: An Engineering Comparison. v27n2, Mar/Apr 1982, p4.
- Decker, C. D., Electro-Optics: Insight to the future. v27n3, May/June 1982, p1.
- DeMaria, P. A. and Bodzioch, K. J., HF modem simulation. v27n6, Nov/Dec 1982, p18.
- Denlinger, E. J., Active and passive microwave components. v27n5, Sept/Oct 1982, p50.
- Dunn, V. S. with Whipple, B., Material compounding of VideoDiscs demands the right chemistry. v27n1, Jan/Feb 1982, p16.
- Elabd, H. A. with Kosonocky, W. F. et al., Schottky-barrier infrared image sensors. v27n3, May/June 1982, p49.
- with Warren, F. B. et al., Space applications for RCA infrared technology. v27n3, May/June 1982, p76.
- Enstrom, R. E., Mechanical and thermal design, modeling and simulation in. v27n6, Nov/Dec 1982, p71.
- Erhardt, H. G. with Kosonocky, W. F. et al., Schottky-barrier infrared image sensors. v27n3, May/June 1982, p49.
- Ettenberg, M., Optoelectronic systems, some of the new systems. v27n3, May/June 1982, p4.
- with Olsen, G. H., Long-wavelength semiconductor diode lasers for optical communications. v27n4, July/Aug 1982, p38.
- Fay, J. E., ATE, distributed system architectures for. v27n4, July/Aug 1982, p53.
- Frantz, V. L., et al., Schottky-barrier infrared image sensors. v27n3, May/June 1982, p49.
- Freeman, E. J., Mehrotra, G. N. and Repka, C. P., Stereo CED VideoDisc system. v27n4, July/Aug 1982, p12.
- Gandolfo, D. A. with Warren, F. B. et al., Space applications for RCA infrared technology. v27n3, May/June 1982, p76.
- Goldberg, H., Receivers, wideband, for communications satellites. v27n5, Sept/Oct 1982, p37.
- Golub, J., Complex weapon systems, discrete-event simulations of. v27n6, Nov/Dec 1982, p32.
- Groppe, J. V. with Kosonocky, W. F. et al., Schottky-barrier infrared image sensors. v27n3, May/June 1982, p49.
- Guida, A. A., Jonnalagadda, K., Raychaudhuri, D. and Schiff, L., RCA Satcom system, computer modeling in the. v27n6, Nov/Dec 1982, p84.
- Gunter, B. H. and Rayl, M., Statistics applications in manufacturing. v27n2, Mar/Apr 1982, p14.
- Haggerty, G. L., Package engineering for the Picture Tube Division. v27n2, Mar/Apr 1982, p50.
- Haggis, D. with Klatskin, J. B. et al., Automated assembly of lumped-element GaAs FET power amplifiers. v27n5, Sept/Oct 1982, p64.
- Hakala, D. F., Chemical and Physical Laboratory supports VideoDisc. v27n1, Jan/Feb 1982, p39.
- Hayman, J., An intelligent missile seeker, design and simulation of. v27n6, Nov/Dec 1982, p43.
- Hogan, D. B. with Altman, W. et al., Space applications of lidar. v27n3, May/June 1982, p44.
- Holaday, V. D. with Bolger, G. P., Computer design and testing of a microwave antenna-feed manifold. v27n5, Sept/Oct 1982, p87.
- Hong, S. with Nigam, A. K. et al., Business modeling and the engineer: An Astro-Electronics application. v27n6, Nov/Dec 1982, p65.
- Huang, H. C., Upadhyayula, L. C. and Kumar, M., GaAs microwave monolithic integrated circuits, a review of. v27n5, Sept/Oct 1982, p58.
- Huck, R. H., Product Assurance of VideoDisc: VideoDisc performance in the real world. v27n1, Jan/Feb 1982, p27.
- Hutter, E. C. with Altman, W. et al., Space applications of lidar. v27n3, May/June 1982, p44.
- John, G. with Kell, F. D. et al., Mastering VideoDiscs: The software to hardware conversion. v27n1, Jan/Feb 1982, p11.
- Jonnalagadda, K. with Guida, A. A. et al., RCA Satcom system, computer modeling in the. v27n6, Nov/Dec 1982, p84.
- Joyce, B. T. with Klatskin, J. B. et al., Automated assembly of lumped-element GaAs FET power amplifiers. v27n5, Sept/Oct 1982, p64.
- Kara, J. with Profera, C. E. et al., Shaped-beam reflector antennas for communications satellites. v27n5, Sept/Oct 1982, p43.
- Kell, F. D., John, G. and Stevens, J., Mastering VideoDiscs: The software to hardware conversion. v27n1, Jan/Feb 1982, p11.
- King, T. E., Editorial input: Two new editorial features. v27n5, Sept/Oct 1982, p30.
- Kipp, R. W. with Nowogrodzki, M. et al., Radar instruments: Sensors for industrial applications. v27n5, Sept/Oct 1982, p23.
- Klatskin, J. B., Haggis, D., Camisa, R. L. and Joyce, B. T., Automated assembly of lumped-element GaAs FET power amplifiers. v27n5, Sept/Oct 1982, p64.
- Klein, J. J., Roberts, N. L. and Chin, G. D., Infrared-camera system developed to use the Schottky-barrier IR-CCD array. v27n3, May/June 1982, p60.
- Koskultz, J. and Rosenfield, M., Assembly mechanization program at RCA Solid State (RAMP). v27n4, July/Aug 1982, p57.
- Kosonocky, W. F., Elabd, H. A., Erhardt, H. G., Shallcross, F. V., Meray, G. M., Miller, R., Villani, T. S., Frantz, V. L., and Tams, F. J., Schottky-barrier infrared image sensors. v27n3, May/June 1982, p49.
- Kowalchik, J. J. and Selwa, A. P., Automatic test equipment for VideoDisc and stylus. v27n1, Jan/Feb 1982, p30.
- Kumar, M. with Huang, H. C. et al., GaAs microwave monolithic integrated circuits, a review of. v27n5, Sept/Oct 1982, p58.
- LaPrade, J. N. with Wolkstein, H. J., Solid-state power amplifier replacing TWTs in C-band satellites. v27n5, Sept/Oct 1982, p7.
- Liston, J. and Sparks, G. M., Mechanically scanned radar systems, dynamic analysis and simulation of. v27n6, Nov/Dec 1982, p24.
- Lynch, W. S. and Reed, R. E., Mirror Fusion Test Facility, producing neutral beam ion sources for the. v27n2, Mar/Apr 1982, p62.
- Marks, B. G. with Barbin, R. L. et al., Color-data-display CRT: A product whose time has come. v27n4, July/Aug 1982, p23.
- Mason, R. J. with Breese, M. E., Computer-aid-

- ed manufacture of precision microwave components for phased-array radar GaAs MESFET power amplifiers. v27n5, Sept/Oct 1982, p71.
- Mawhinney, D. D. with Nowogrodzki, M. et al.**, Radar instruments: Sensors for industrial applications. v27n5, Sept/Oct 1982, p23.
- McIntyre, R. J. with Webb, P. P.**, Silicon avalanche photodiodes, recent developments in. v27n3, May/June 1982, p96.
- McNeely, M. and Bock, M.**, Micro-molding is a VideoDisc requirement. v27n1, Jan/Feb 1982, p19.
- Mecca, S. J.**, Quality Circles at RCA Scranton. v27n2, Mar/Apr 1982, p30.
- Mehrotra, G. N. with Freeman, E. J. et al.**, Stereo CED VideoDisc system. v27n4, July/Aug 1982, p12.
- Meray, G. M. with Kosonocky, W. F. et al.**, Schottky-barrier infrared image sensors. v27n3, May/June 1982, p49.
- Mercuri, R. T.**, Computer music, an illustrated history of. v27n4, July/Aug 1982, p65.
- Miller, R. with D'Arcy, J. A.**, Manufacturing, Custom and Quantity Manufacturing: An Engineering Comparison. v27n2, Mar/Apr 1982, p4.
- with **Kosonocky, W. F. et al.**, Schottky-barrier infrared image sensors. v27n3, May/June 1982, p49.
- Mishra, D.**, Player Technology Center: Key to innovation. v27n2, Mar/Apr 1982, p24.
- Myers, W. W.**, Computer programming and systems analysis in the rapidly changing VideoDisc environment (application of FOCUS). v27n4, July/Aug 1982, p48.
- Neuhauser, R. G.**, Saticon photoconductor: The latest in color-camera-tube photoconductors. v27n3, May/June 1982, p81.
- Nigam, A. K., Hong, S. and Spence, S. R.**, Business modeling and the engineer: An Astro-Electronics application. v27n6, Nov/Dec 1982, p65.
- Nowogrodzki, M.**, Microwave components research at RCA. v27n5, Sept/Oct 1982, p4.
- , **Mawhinney, D. D. and Kipp, R. W.**, Radar instruments: Sensors for industrial applications. v27n5, Sept/Oct 1982, p23.
- Olsen, G. H. and Ettenberg, M.**, Long-wavelength semiconductor diode lasers for optical communications. v27n4, July/Aug 1982, p38.
- Paglione, R. W.**, Medical applications of microwave energy. v27n5, Sept/Oct 1982, p17.
- Patton, W. T.**, Low-sidelobe antennas for tactical phased-array radars. v27n5, Sept/Oct 1982, p31.
- Periman, B. S., Rhodes, D. L. and Schepps, J. L.**, Computer-aided design and testing of microwave circuits. v27n5, Sept/Oct 1982, p76.
- Perlow, S. M.**, ANA radio frequency circuit simulation and analysis. v27n6, Nov/Dec 1982, p46.
- Phillip, G. O.**, Parylene-coating process at MSR. v27n2, Mar/Apr 1982, p56.
- Pica, A. P. with Adelson, E. H. et al.**, Human visual system, modeling of the. v27n6, Nov/Dec 1982, p56.
- Pitts, K. A. and Barton, R. R.**, Engineering environment, simulation in an. v27n6, Nov/Dec 1982, p4.
- Profera, C. E., Rosol, G. L., Soule, H. H. and Kara, J.**, Shaped-beam reflector antennas for communications satellites. v27n5, Sept/Oct 1982, p43.
- Raychaudhuri, D. with Guida, A. A. et al.**, RCA Satcom system, computer modeling in the. v27n6, Nov/Dec 1982, p84.
- Rayl, M. with Gunter, B. H.**, Statistics applications in manufacturing. v27n2, Mar/Apr 1982, p14.
- RCA Corporate Engineering Education**, Continuing education for manufacturing engineers. v27n2, Mar/Apr 1982, p38.
- RCA ENGINEER Staff**, David Sarnoff Awards for Outstanding Technical Achievement (1982). v27n4, July/Aug 1982, p4.
- Editorial Representatives, meet your. v27n1, Jan/Feb 1982, p35.
- Engineering Form and Function: Windows on RCA Technology. v27n4, July/Aug 1982, p33.
- "SelectaVision" VideoDisc Awards. v27n1, Jan/Feb 1982, p4.
- Reed, R. E. with Lynch, W. S.**, Mirror Fusion Test Facility, producing neutral beam ion sources for the. v27n2, Mar/Apr 1982, p62.
- Reno, C. W. with Ammon, G. J.**, Data recording on optical discs at 300 Mb/s. v27n3, May/June 1982, p36.
- Repka, C. P. with Freeman, E. J. et al.**, Stereo CED VideoDisc system. v27n4, July/Aug 1982, p12.
- Rhodes, D. L. with Periman, B. S. et al.**, Computer-aided design and testing of microwave circuits. v27n5, Sept/Oct 1982, p76.
- Roberts, N. L. with Klein, J. J. et al.**, Infrared-camera system developed to use the Schottky-barrier IR-CCD array. v27n3, May/June 1982, p60.
- Rosenberg, A. with Altman, W. et al.**, Space applications of lidar. v27n3, May/June 1982, p44.
- Rosenfield, M. with Koskultz, J.**, Assembly mechanization program at RCA Solid State (RAMP). v27n4, July/Aug 1982, p57.
- Rosol, G. L. with Profera, C. E. et al.**, Shaped-beam reflector antennas for communications satellites. v27n5, Sept/Oct 1982, p43.
- Schepps, J. L. with Periman, B. S. et al.**, Computer-aided design and testing of microwave circuits. v27n5, Sept/Oct 1982, p76.
- Schiff, L. with Guida, A. A. et al.**, RCA Satcom system, computer modeling in the. v27n6, Nov/Dec 1982, p84.
- Schlosser, H. S.**, Quality plus diversity plus availability equals success. v27n1, Jan/Feb 1982, p1.
- Schneider, W.**, Making telescopes is my hobby. v27n2, Mar/Apr 1982, p75.
- Selwa, A. P. with Kowalchik, J. J.**, Automatic test equipment for VideoDisc and stylus. v27n1, Jan/Feb 1982, p30.
- Shallcross, F. V. with Kosonocky, W. F. et al.**, Schottky-barrier infrared image sensors. v27n3, May/June 1982, p49.
- Shambelan, R. C. with Blumenfeld, M. A.**, Equipment decisions for VLSI-circuit manufacture. v27n2, Mar/Apr 1982, p35.
- Simpson, T. F. with Barbin, R. L. et al.**, Color-data-display CRT: A product whose time has come. v27n4, July/Aug 1982, p23.
- Snowden, M. P. and Amantea, R.**, Automated measurement of transistor I-V characteristics. v27n2, Mar/Apr 1982, p69.
- Solomon, S. M.**, Microwave communications system for RCA Globcom. v27n4, July/Aug 1982, p75.
- Soule, H. H. with Profera, C. E. et al.**, Shaped-beam reflector antennas for communications satellites. v27n5, Sept/Oct 1982, p43.
- Sparks, G. M. with Liston, J.**, Mechanically scanned radar systems, dynamic analysis and simulation of. v27n6, Nov/Dec 1982, p24.
- Spence, S. R. with Nigam, A. K. et al.**, Business modeling and the engineer: An Astro-Electronics application. v27n6, Nov/Dec 1982, p65.
- Stabile, P. J.**, Pin diode, high-power, the Engineer's Notebook. v27n5, Sept/Oct 1982, p21.
- Staniszewski, J. R.**, The second-generation Navy Navigation Satellite, NOVA-1, expectations achieved. v27n4, July/Aug 1982, p89.
- Sterzer, F.**, Localized hyperthermia treatment of cancer. v27n1, Jan/Feb 1982, p43.
- Microwave technology at RCA. v27n5, Sept/Oct 1982, p1.
- Stevens, J. with Kell, F. D. et al.**, Mastering VideoDiscs: The software to hardware conversion. v27n1, Jan/Feb 1982, p11.
- Suh, G. W.**, Large system development, digital interface simulation for. v27n6, Nov/Dec 1982, p39.
- Tams, F. J., et al.**, Schottky-barrier infrared image sensors. v27n3, May/June 1982, p50.
- Technical Information Systems**, Technical abstracts database (TAD): RCA database now an on-line system. v27n2, Mar/Apr 1982, p22.
- Teger, A. H.**, Modeling and simulation: Tools for the 80s. v27n6, Nov/Dec 1982, p1.
- Torrington, L. A.**, Caddy design and manufacturing of the VideoDisc caddy. v27n1, Jan/Feb 1982, p23.
- Tower, J. R. with Warren, F. B. et al.**, Space applications for RCA infrared technology. v27n3, May/June 1982, p76.
- Trachtenberg, M.**, Software reliability, discovering how to ensure. v27n1, Jan/Feb 1982, p53.
- Upadhyayula, L. C. with Huang, H. C. et al.**, GaAs microwave monolithic integrated circuits, a review of. v27n5, Sept/Oct 1982, p58.
- Villani, T. S. with Kosonocky, W. F. et al.**, Schottky-barrier infrared image sensors. v27n3, May/June 1982, p49.
- with **Warren, F. B. et al.**, Space applications for RCA infrared technology. v27n3, May/June 1982, p76.
- Warren, F. B., Tower, J. R., Gandolfo, D. A., Elabd, H. A. and Villani, T. S.**, Space applications for RCA infrared technology. v27n3, May/June 1982, p76.
- Webb, P. P. and McIntyre, R. J.**, Silicon avalanche photodiodes, recent developments in. v27n3, May/June 1982, p96.
- Weisberg, H.**, Manufacturing the VideoDiscs: An overview. v27n1, Jan/Feb 1982, p6.
- Whipple, B. and Dunn, V. S.**, Material compounding of VideoDiscs demands the right chemistry. v27n1, Jan/Feb 1982, p16.
- Williams, R.**, Coal, upgrading, for more efficient electric-power generation. v27n4, July/Aug 1982, p45.
- Wittlinger, H. A.**, Linear integrated circuits are going digital. v27n1, Jan/Feb 1982, p58.
- Wolkstein, H. J. and LaPrade, J. N.**, Solid-state power amplifier replacing TWTs in C-band satellites. v27n5, Sept/Oct 1982, p7.
- Young, C.**, Numerical control: The cornerstone of computers in manufacturing. v27n2, Mar/Apr 1982, p41.

Editorial Representatives

Contact your Editorial Representative at the TACNET numbers listed here to schedule technical papers and announce your professional activities.

Cablevision Systems

*John Ovnick Van Nuys, California 534-3011

Commercial Communications Systems Division (CCSD)

*Bill Sepich Camden, New Jersey 222-2156
Clinton Glenn Meadowlands, Pennsylvania 228-6231

Consumer Electronics (CE)

*Eugene Janson Indianapolis, Indiana 422-5208
Francis Holt Indianapolis, Indiana 422-5217
Chuck Limberg Indianapolis, Indiana 422-5117
Don Willis Indianapolis, Indiana 422-5883
Byron Taylor Indianapolis, Indiana 426-3247

Government Systems Division (GSD)

Advanced Technology Laboratories

*Merle Pietz Camden, New Jersey 222-2161
Ed Master Camden, New Jersey 222-2731

Astro-Electronics

*Frank Yannotti Princeton, New Jersey 229-2544
Carol Klarmann Princeton, New Jersey 229-2919

Automated Systems

*Paul Seeley Burlington, Massachusetts 326-3095
Dale Sherman Burlington, Massachusetts 326-2985

Government Communications Systems

*Dan Tannenbaum Camden, New Jersey 222-3081
Harry Ketcham Camden, New Jersey 222-3913

GSD Staff

*Ed Moore Cherry Hill, New Jersey 222-5833

Missile and Surface Radar

*Don Higgs Moorestown, New Jersey 224-2836
Jack Friedman Moorestown, New Jersey 224-2112
Graham Boose Moorestown, New Jersey 224-3680

National Broadcasting Company (NBC)

*Bob Mausler New York, New York 324-4385

Patent Operations

George Haas Princeton, New Jersey 226-2491

Picture Tube Division (PTD)

*Ed Madenford Lancaster, Pennsylvania 227-3657
Nick Meena Circleville, Ohio 432-1228
Jack Nubani Scranton, Pennsylvania 329-1499
J.R. Reece Marion, Indiana 427-5566

TACNET

RCA Communications

TACNET

American Communications

*Murray Rosenthal Princeton, New Jersey 258-4192
Carolyn Powell Princeton, New Jersey 258-4194

Global Communications

*Dorothy Unger New York, New York 323-7348

RCA Limited (Canada)

Bob McIntyre Ste Anne de Bellevue 514-457-9000

RCA Records

*Greg Bogantz Indianapolis, Indiana 424-6141

RCA Service Company

*Joe Steoger Cherry Hill, New Jersey 222-5547
Ray MacWilliams Cherry Hill, New Jersey 222-5986
Dick Dombrosky Cherry Hill, New Jersey 222-4414

Research and Engineering

Corporate Engineering

*Hans Jenny Cherry Hill, New Jersey 222-4251

Laboratories

Eva Dukes Princeton, New Jersey 226-2882

"SelectaVision" VideoDisc Operations

*Nelson Crooks Indianapolis, Indiana 426-3164

Solid State Division (SSD)

*John Schoen Somerville, New Jersey 325-6467

Power Devices

Harold Ronan Mountaintop, Pennsylvania 327-1633
or 327-1827

Integrated Circuits

Dick Morey Palm Beach Gardens, Florida 722-1262
Sy Silverstein Somerville, New Jersey 325-6168
John Young Findlay, Ohio 425-1307

Electro-Optics and Power Devices

John Grosh Lancaster, Pennsylvania 227-2077

Solid State Technology Center

Judy Yeast Somerville, New Jersey 325-6248

*Technical Publications Administrators, responsible for review and approval of papers and presentations, are indicated here with asterisks before their names.

RCA Engineer

A technical journal published by
Corporate Research and Engineering
"by and for the RCA engineer"

Bldg 204-2, Cherry Hill, NJ 08358

Forwarding and return postage guaranteed

BULK RATE
US Postage

PAID

Phila., Pa.
Permit No. 2906

EM MUSSELMANN
PO BOX 9
STRASBURG
PA 17579

LCTT